AFFDL-TR-78-194
Part III

LEVEL II

TRANSONIC WIND TUNNEL TESTS ON AN OSCILLATING WING WITH EXTERNAL STORES

PART III. The Wing With Tip Store

NATIONAL AEROSPACE LABORATORY
THE NETHERLANDS

MAY 1979

TECHNICAL REPORT AFFDL-TR-78-194
Final Report for the Period February 1977 through May 1979

AIR FORCE FLIGHT DYNAMICS LABORATORY
AIR FORCE WRIGHT AERONAUTICAL LABORATORIES
AIR FORCE SYSTEMS COMMAND
WRIGHT-PATTERSON AIR FORCE BASE, OHIO 45433

Report III of IV Parts

NOTICE

When Government drawings, specifications, or other data are used for any purpose other than in connection with a definitely related Government procurement operation, the United States Government thereby incurs no responsibility nor any obligation whatsoever; and the fact that the government may have formulated, furnished, or in any way supplied the said drawings, specifications, or other data, is not to be regarded by implication or otherwise as in any manner licensing the holder or any other person or corporation, or conveying any rights or permission to manufacture, use, or sell any patented invention that may in any way be related thereto.

This report has been reviewed by the Information Office (OI) and is releasable to the National Technical Information Service (NTIS). At NTIS, it will be available to the general public, including foreign nations.

This technical report has been reviewed and is approved for publication.

JAMES J. OLSEN
Principal Scientist
Analysis & Optimization Branch

HARTLEY M. CALDWELL, III, Capt, USAF
Acting Chief
Analysis & Optimization Branch

FOR THE COMMANDER

RALPH L. KUSTER, JR., Col, USAF
Chief, Structures & Dynamics Division

"If your address has changed, if you wish to be removed from our mailing list, or if the addressee is no longer employed by your organization please notify AFFDL/FBE, WPAFB, OH 45433 to help us maintain a current mailing list."

Copies of this report should not be returned unless return is required by security considerations, contractual obligations, or notice on a specific document.

AIR FORCE/56780/11 September 1979 — 160

UNCLASSIFIED

SECURITY CLASSIFICATION OF THIS PAGE (When Data Entered)

TR-78-194-PT-3

REPORT DOCUMENTATION PAGE

READ INSTRUCTIONS BEFORE COMPLETING FORM

1. REPORT NUMBER: AFFDL-TR-78-134, Part III	2. GOVT ACCESSION NO.
3. RECIPIENT'S CATALOG NUMBER	
4. TITLE (and Subtitle): Transonic Wind Tunnel Tests on an Oscillating Wing with External Stores, Part III. The Wing With Tip Store	5. TYPE OF REPORT & PERIOD COVERED: Final Report. Feb 77 - May 79
6. PERFORMING ORG. REPORT NUMBER: NLR-TR-78106-U-PT-3	
7. AUTHOR(s): H. Tijdeman, J. W. G. van Nunen, A. N. Kraan, A. J. Persoon, R. Poestkoke, P. Schippers, O. M. Siebert	8. CONTRACT OR GRANT NUMBER(s): AFOSR Grant 77-3233
9. PERFORMING ORGANIZATION NAME AND ADDRESS: National Aerospace Laboratory, Anthony Fokkerweg 2, Amsterdam, The Netherlands	10. PROGRAM ELEMENT, PROJECT, TASK AREA & WORK UNIT NUMBERS: [redacted] 2307 [redacted] N5
11. CONTROLLING OFFICE NAME AND ADDRESS: Air Force Flight Dynamics Laboratory, Structures and Dynamics Division, W-P AFB, Ohio 45433	12. REPORT DATE: May 79
	13. NUMBER OF PAGES: 246
14. MONITORING AGENCY NAME & ADDRESS (if different from Controlling Office)	15. SECURITY CLASS. (of this report): Unclassified
	15a. DECLASSIFICATION/DOWNGRADING SCHEDULE

16. DISTRIBUTION STATEMENT (of this Report)

Approved for Public Release: Distribution Unlimited

AFOSR-77-3233

17. DISTRIBUTION STATEMENT (of the abstract entered in Block 20, if different from Report)

Approved for Public Release; Distribution Unlimited

18. SUPPLEMENTARY NOTES

19. KEY WORDS (Continue on reverse side if necessary and identify by block number)

Transonic
Unsteady Aerodynamics
Experiments
External Stores
Flutter

20. ABSTRACT (Continue on reverse side if necessary and identify by block number)

A wind-tunnel investigation was carried out on an oscillating model of the F-5 wing with and without an external store (AIM-9J missile). The store was mounted at the wing tip as well as at a pylon underneath the wing. Detailed steady and unsteady pressure distributions were measured over the wing, while on the store aerodynamic loads were obtained. In addition, wind-tunnel wall pressures were recorded.

The tests covered the Mach number range between Ma = .6 and 1.35, and frequencies up to 40 Hz.

DD FORM 1 JAN 73 1473 EDITION OF 1 NOV 65 IS OBSOLETE

UNCLASSIFIED

SECURITY CLASSIFICATION OF THIS PAGE (When Data Entered)

405 964

This report (Part III) gives an analysis of the results of the configuration with the store mounted at the wing tip. Emphasis is put on the influence of the store on the wing loading and further on the store loads. A comparison is presented of experimental data and theoretical results obtained with the unsteady NLRI and Doublet Lattice methods.

FOREWORD

This report was prepared by the National Aerospace Laboratory (NLR of Amsterdam, the Netherlands. The sponsors were the Air Force Armament Test Laboratory (AFATL/DLJ) of Eglin Air Force Base, Florida and the Air Force Flight Dynamics Laboratory (AFFDL/FBR and AFFDL/FBE) of Wright-Patterson Air Force Base, Ohio. The sponsorship was performed through AFOSR Grant 77-3233, administered by Captain D. Wilkins of the Air Force Office of Scientific Research (AFOSR/TKN) of Bolling Air Force Base, Washington D.C.

The report consists of four parts. Part I contains the general description; Part II discusses the steady and unsteady aerodynamic tests of the clean F-5 wing; Part III discusses the tests for the wing with tip-mounted stores; and Part IV discusses the tests for the wing with under-wing stores.

The principal investigators were Dr. H. Tijdeman and Mr. J. W. G. van Nunen of NLR. They were assisted by A. N. Kraan, A. J. Persoon, R. Poestkoke, Dr R. Roos, P. Schippers and C. M. Siebert of NLR.

Within the United States Air Force, this program was initiated by Lovic Thomas of the AFATL. It would not have been possible without the expert assistance of Richard Wallace (Lt Colonel, USAF, Retired), and Lt Colonel Daniel Seger and Major Robert Powell of the European Office of Aerospace Research Development (EOARD).

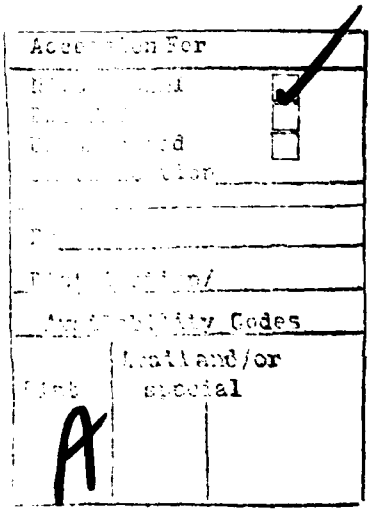

CONTENTS

LIST OF SYMBOLS

a_{mn}	coefficient in the approximation of the vibration modes	
C	chord	(m)
$\bar{C}$	mean geometric chord; $\bar{C}$ = .4183	(m)
C_M	pitch moment coefficient for the store	
C_m	sectional pitch moment coefficient	
C_p	pressure coefficient	
C_r	root chord; C_r = 0.6396	(m)
C_Z	normal force coefficient for the store	
C_z	sectional normal force coefficient	
F	frequency of oscillation	(Hz)
K	reduced frequency; $K = \frac{\pi F C_r}{V}$	
M	pitching moment	(Nm)
Ma	free-stream Mach number	
P	free-stream static pressure	(Pa)
P_i	unsteady pressure at model surface	(Pa)
P_{loc}	local static pressure	(Pa)
P_o	stagnation pressure	(Pa)
Q	dynamic pressure	(Pa)
S	semi span; S = 0.6226	(m)
V	free-stream velocity	(m/s)
w	modal displacement	(m)

LIST OF SYMBOLS (Cont'd)

x	coordinate in free-stream direction	(m)
y	coordinate in spanwise direction	(m)
Z	normal force	(N)
α	incidence; positive nose up	(degrees)
θ	amplitude of oscillation in the section of accelerometers 1 and 2; positive nose up	(rad)
ω	angular velocity; $= 2\pi F$	(rad/s)

SUBSCRIPTS

i	referring to unsteady quantities
q	referring to quasi-steady quantities
st	referring to the store
tip	referring to the wing tip

SUFFICES

+	denotes upper surface
-	denotes lower surface

1 INTRODUCTION

In order to determine the unsteady airloads on a representative fighter-type wing at transonic and supersonic speeds, wind-tunnel tests were carried out on an oscillating model of the F-5 wing with and without external store. If present, this external store (AIM-9J missile + launcher) was mounted either at the tip or under the wing.

The wing model was oscillated in pitch about a 50 per cent root-chord axis at frequencies varying up to 40 Hz (for dimensions see Fig. 1a). The Mach number ranged between 0.6 and 1.35. Detailed pressure distributions, both steady and unsteady, were measured over the wing, while on the store the total aerodynamic loads were obtained. A description of the experimental test set-up and the test program is given in part I of this report (Ref. 1). The results are published in a data report (Ref. 2), while for easy data handling they are available also on magnetic tape.

To assist in the evaluation of the data, reference 1 is supplemented by three additional parts, covering successively the clean wing, the wing with tipstore and the wing with underwing store. Each part contains plots of the steady and unsteady pressure distributions and gives a brief analysis of some selected results.

The present report (part III) focusses on the configuration of the wing with tipstore. Figure 1b shows the model of this configuration mounted on the HST wind-tunnel wall, while the location of the pressure orifices is given in figure 1c. The report considers in particular the influence of the tipstore on the wing loading and on the loads, experienced by the store itself. For the wing this analysis concerns a comparison with the clean wing configuration results of which are taken from part II (Ref. 3), where the behaviour of the unsteady pressures and integrated loads with frequency and Mach number for the clean wing is analyzed in detail. For the store the successive contributions of the launcher, missile body, aft wings and canard fins are considered.

For subsonic flow the experimental data are supplemented with theoretical results obtained with the NLRI-method for wing-body configurations (Ref. 4). Further, since the NLRI-method is rather expensive in terms of computer costs, a successful attempt has been made to devise a panel distribution , which will lead to comparative results when applied in a Doublet Lattice calculation.

2 STEADY RESULTS

2.1 General

During the wind-tunnel experiment steady pressures were measured over the wing at incidences of -0.5, 0 and 0.5 degrees. For all tip-store configurations a listing of the test variables as well as a complete set of plots of the resulting steady pressure distributions in the eight measuring sections is gathered in Appendix III.B. In addition to the pressures on the wing also the normal load and pitching moment experienced by the store were measured for the same incidences. The results of these measurements are given in Appendix III.D.

For the limiting case of zero frequency so-called "quasi-steady" results can be obtained by considering the steady results for small incidences around a certain mid-position. In the present investigation "quasi-steady" loads for a mid-position of zero degrees were obtained from the steady data taken at incidences of -0.5 and 0.5 degrees. The definitions are given in Appendix III.A.

The steady and quasi-steady load distributions presented in the following part of this chapter, were obtained from the measured pressure distributions. In this respect, it is noted that for the integration, in section 3 and 5 the faulty value, found on the upperside near the leading edge, was replaced by a new value obtained by interpolation between the sections 2, 4 and 6.

2.2 Steady and quasi-steady loads on the wing

In order to better understand the influence the tipstore has on the quasi-steady and unsteady spanwise load distributions, it is useful to investigate first its effect on the steady load distribution. Figures 2a through 2c show these distributions for subsonic (Ma = 0.6), transonic (Ma = 0.9) and supersonic (Ma = 1.35) flow conditions. For incidences of -0.5, 0 and 0.5 degrees, each figure gives a comparison of the steady load distributions for the configuration with the complete tipstore and for the clean wing.

At Ma = 0.6 (Fig. 2a) the store affects the normal load on the outer two-thirds of the wing. As expected, at a positive incidence the store causes the normal force to increase to higher values, while for negative incidences the loading becomes more negative. The maximal influence is found in the vicinity of the store. At $\alpha \sim 0^0$ the normal load on the

wing varies around zero and in that case the store does not produce any marked influence.

When the Mach number is increased to Ma = 0.9 (Fig. 2b) the behaviour is similar except that now the influence of the store is felt over the complete span of the wing. Further, the presence of the store induces a slightly stronger shock on the upperside of the wing, which in turn results in an increased interference effect near the store. Again at $\alpha \sim 0^0$ the influence is minimal.

Under supersonic conditions (Ma = 1.35) the clean wing experiences a negative steady normal load for all three incidences considered (Fig. 2c). Consequently the store raises the magnitude of this negative loading even further, be it that for positive incidence the difference is less than for negative incidences. Contrary to the subsonic and transsonic cases, the area of the wing influenced is limited to the outer 30 per cent of the span. The interference is maximal near the wing tip and gradually reduces to zero near measuring section 5. This behaviour corresponds well with the supersonic zone of influence which at Ma = 1.35 can be thought to originate from the forward wing-tip corner.

In general one can conclude that for all Mach numbers the store acts as an endplate, increasing the circulation about the wing.

The quasi-steady spanwise load distributions derived from the steady distributions, are presented in figures 3a to 3c. As can be expected, they show qualitatively the same interference effects, i.e. the interference is maximal near the tip and diminishes towards the root.

This behaviour is found also in figure 4, in which the quasi-steady normal loads in section 2, 5 and 8 are plotted against Mach number. In section 2 the only noticeable influence of the tipstore is found in the transonic range. Section 5 is influenced at Mach numbers below 1.2, while in section 8 the presence of the tipstore is felt at all Mach numbers.

At Ma = 1.1 the configuration with tipstore was tested for two different stagnation pressures $P_o = 0.7 \times 10^5$ Pa and $P_o = 1.0 \times 10^5$ Pa. The results in figure 4 indicate that a decrease in the stagnation pressure results in an increase of C_{zq}, especially over the outer part of the span. From the steady pressure distributions (Figs. III.B. 55 to 60) it can be concluded that this decrease is mainly due to variations in the pressures on the lower side of the wing in the recompression region behind the leading edge. This may be caused by the change in Reynolds number from 6×10^6 to 4.3×10^6 or by a change of the local incidence due to

torsional deformation of the model. Since the loading on the outer part of the wing and on the store acts at a position behind the pitch axis (50 % root chord), this deformation tends to diminish the local indidence with increasing stagnation pressure.

Most probably, the same effect is present also for the clean wing configuration, which means that in sections 5 and 8 the values for Ma = 1.2 and 1.35 are slightly too high when compared to the results found for the lower Mach numbers.

2.3 Steady and quasi-steady loads on the store

The present tests were carried out with the store in various stages of completeness, making it possible to investigate the aerodynamic contribution of specific parts of the store. For the different configurations tested the steady normal force and pitching moment acting on the store were measured by a strain gage balance located at the interface of the wingtip and the launcher. The measured results are presented in figures 5a and 5b. For the three test incidences of -0.5, 0, 0.5 degrees the normal force and pitching moment coefficients are plotted versus Mach number for four configurations, i.e. the wing to which consecutively the launcher, the missile body, the aft wing and the canard fins are added.

For all configurations the normal force and even more the pitching moment do show qualitatively the same behaviour with Mach number. Adding one by one the different parts of the store results in general in an increase of the normal force. For $\alpha = 0.5^0$ and -0.5^0 the missile body and the aft wings roughly give a doubling of the normal force, when compared to the preceding case. The canard fins, with their small physical dimensions, are responsible for only a very small increase. For $\alpha = 0^0$ the influence of the completeness of the store is most effective at Ma = 1.35.

On the pitching moment the effect of the various parts is quite different. Here the aft wings and the canard fins generate counteracting contributions caused by their positioning relative to the balance centre (see Fig. 1a). For $\alpha = 0.5^0$ and -0.5^0 the aft wings produce a stabilizing moment, while the moment due to the canard fins tends to increase the incidence. Further, because the canard fins are located at a large distance from the balance centre, their contribution to the pitching moment is relatively large, even though they produce only a very small normal force.

The quasi-steady normal force and pitching moment extracted from these steady data are presented in figure 6. The general trends found for the steady coefficients, are visible here too. Missile body and aft wings each double the normal load with respect to the preceding case, while the effect of the canard fins is negligible. For the pitching moment, the aft wings completely nullify the contribution of the missile body and at the higher Mach numbers also of the launcher. The canard fins restore the pitching moment to and even above the level of the configuration with missile body and launcher present.

3 UNSTEADY RESULTS

3.1 Vibration modes

To monitor the vibration modes of the wing and store during the tests, the model was equipped with 10 accelerometers, eight in the wing and two in the launcher (for exact locations see Fig. 1a). As was done for the clean wing configuration (see Ref. 3), also for the configuration with the complete tipstore the readings of these accelerometers were used to make analytical approximations of the vibration modes for the 20 Hz testruns. The polynomial expression used for these approximations is:

$$w(x,y) = \sum a_{mn} x^n y^m \quad \begin{matrix} \text{(wing : } m = 0, 1, 2;\ n = 0, 1\text{)} \\ \text{(store: } m = 0;\ n = 0, 1\text{)} \end{matrix}$$

This expression assumes no deformation in chordwise direction and a parabolic deformation in spanwise direction. In using the measured values, for a few testruns the readings of accelerometers 5 and 7 were carefully weighted to ensure a realistic development of the torsion angle along the span. Taking this into account, the difference between the analytically approximated displacements and the experimental readings remains within 2 per cent of the maximal displacement. Table 1 presents the numerical values of the coefficients a_{mn} for the analyzed vibration modes. The normalization is carried out such that at the wing section of accelerometer 2 the tangent of the angle of oscillation equals one.

To obtain insight into the effect of the tipstore on the vibration modes of the wing, the nodal lines as found for the clean wing (for the approximation see Ref. 3) and the wing with complete tipstore are presented in figures 7a and 7b. The figures show that for 20 Hz the wing with tipstore possesses a nodal line which compared to the clean wing is bent

more backwards, especially over the outer part of the wing. The development with Mach number is similar to that of the clean wing i.e.: in the subsonic and transonic regime the nodal line bends to the rear, while in the supersonic range the nodal line tends to return to its original position. The local torsion angle was found to remain almost constant over the wing. The store itself follows the motion of the wingtip very well except for Ma = 0.9 and 1.1 in which case deviations of 5 and 7 per cent are present.

Changing the stagnation pressure from 1.0×10^5 Pa to 0.7×10^5 Pa has a marked effect on the position of the nodal line. The decreased aerodynamic load on the wing causes the nodal line to move forward to the 50 % rootchord pitch axis. The small difference between the torsion angles of the wingtip and of the store is not affected by this change in stagnation pressure.

No approximations were made for the 40 Hz testruns of the wing with tipstore. However, a preliminary analysis of the data indicates that for this frequency at several Mach numbers the vibration mode becomes complex, i.e. during an oscillation cycle the nodal line does not remain at the same position, but moves back and forth over the wing. Also, the discrepancy between the motion of the wingtip and of the store increases.

3.2 Unsteady loads

3.2.1 General

For all tipstore configurations the unsteady pressure distributions, measured over the wing, are tabulated in reference 2 and plotted in the present report. These plots and a list of the relevant test variables are given in Appendix III.C. For a better comparison the values on the upperside are shown with a reversed sign.

In the present experiment the unsteady normal load and pitching moment acting on the tipstore were measured by the same strain-gage balance with which the steady data were obtained (for details see Ref. 1 and 5). Plots of these quantities versus Mach number are presented in Appendix III.D. For test cases above 30 Hz, in part I (Ref. 1) doubts have been expressed concerning the store loads. For that reason all 40 Hz cases were omitted from this Appendix as well as from the tabulated data (Ref. 2).

3.2.2 Unsteady loads on the wing

The development of the unsteady normal force*) versus Mach number in the sections 2, 5 and 8 is given in figure 8. For a frequency of 20 Hz this figure presents a comparison between the results of the clean wing and the wing with complete tipstore.

As can be expected the influence of the tipstore is similar to that found for the quasi-steady sectional normal load distributions (Fig. 4). In section 2 the presence of the store is hardly felt, and in section 5 up to Ma = 1.1 some influence is visible only in the real part of the unsteady normal force. Finally, close to the tip in section 8 a considerable effect is found for the real part, while the imaginary part is affected only slightly. Apart form the interference of the store both configurations do show a similar behaviour with Mach number.

Like the quasi-steady loads, also the unsteady loads are affected by a change in stagnation pressure. Figure 8 indicates, that at Ma = 1.1 a drop in the stagnation pressure leads to a significant increase in the real part of the normal force in all three sections, while in the imaginary part some influence can be observed also. The unsteady pressure distributions (Figs. III.C.49 and III.C.53) show this effect to be localized around the recompression region on the lower side behind the leading edge. As to the cause for this dependency on stagnation pressure two possibilities may be mentioned: the change in Reynolds number and the change in vibration mode (see chapter 3.1).

To get a feeling for the way in which the tipstore interference spreads over the wing, in figures 9 to 11 the spanwise distributions of the normal load and pitching moment for the configurations with and without store are compared for Ma = 0.6, 0.9, 1.35 and a frequency of 20 Hz.

For the normal load distributions it can be expected that the real part is very similar to the quasi-steady distributions in figures 3a to 3c. At Ma = 0.6 (figures 9a and 9b) the unsteady interference extends up to section 1, which is slightly further than in the quasi-steady case. The imaginary part hardly shows any interference except near the tip. Both the normal force and the pitching moment show a maximal interference

*) For the integration of the unsteady pressure distributions in sections 3 and 5 the zero value, wrongly measured on the upperside near the leading edge was replaced by a new value, obtained by spanwise interpolation between sections 2, 4 and 6.

in the vicinity of the store.

At transonic conditions (Ma = 0.9, figures 10a and 10b) the effect of the store is present over all of the span, with again a maximum near the tip. Both the normal force and pitching moment exhibit a dip in the vicinity of section 5, which was not found in the quasi-steady load distributions. In the analysis of the clean wing (Ref. 3) this dip or the bulge near the tip was explained as partly due to an insufficient resolution necessary to integrate over the peaks generated by the shock moving over the outer part of the wing.

As the Mach number is increased to Ma = 1.35 the concept of a supersonic zone of influence already brought up in the discussion on the quasi-steady loading on the wing, does explain the unsteady tipstore interference also. Inboard of section 5 both configurations possess the same load and moment distributions. From thereon the interference grows towards the tip.

3.2.3 Unsteady loads on the store

The unsteady loads on the store measured by the balance between wingtip and launcher are shown in figure 12. In this figure the unsteady normal force and pitching moment for a frequency of 20 Hz are plotted versus Mach number for the various store configurations. As in the steady and quasi-steady case, the configuration is made more complex by starting with the launcher and adding consecutively the missile body, the aft wings and the canard fins.

The behaviour of the real part of the normal force and the pitching moment are very similar to the quasi-steady situation (Fig. 6). This holds for the development with Mach number as well as for the variation of store configuration. Concerning the normal force, the missile body and the aft wings each double the preceding case, while the canard fins hardly contribute to the normal force. This contribution is so small not only because of the relatively small physical dimensions of the canard fins, but also due to the fact that their motion consist of mainly a heave. For the pitching moment the picture is completely different. As in the quasi-steady case, the missile body indeed gives an increase, but the aft wings produce a significant reduction of the pitching moment, which at supersonic Mach numbers changes from nose up to nose down (negative). This means that the addition of the aft wings causes the centre of force to move backwards even past the balance centre. Completing the configu-

ration with the canard fins, the pitching moment returns to a level above that of the configuration with the launcher and missile body. For the imaginary parts of normal force and pitching moment, figure 12 shows that this part of the unsteady aerodynamic load remains rather small and that the various components of the store have only little influence. This last point is not surprising since the reduced frequency, based on the dimensions of the aft wings or canard fins, is very small.

4 COMPARISON WITH THEORY

4.1 The NLRI-method

Next to the Doublet Lattice method the NLR possesses a theoretical method for the calculation of the unsteady aerodynamic forces on a wing-body configuration oscillating in subsonic flow. This so-called "NLRI-method" is a panel-type method based on the potential flow approximation. For the bodies, such as fuselage and stores, use is made of a representation in terms of unsteady source panels distributed over the contour of the body, while for the lifting surfaces, which are taken to be infinitely thin, the Doublet Lattice approach is used. A detailed description of the method is given in reference 4.

As part of the present investigation the NLRI-method was applied to the configuration with the complete tipstore at Ma = 0.6 and a frequency of 20 Hz. The panel distribution used in this calculation is shown in figure 13. The wing, the canard fins and the aft wings are represented as thin lifting surfaces, while the launcher and missile body are combined to one long body with an open rear end. As vibration mode the approximation of run 350 (see table 1) was used. In figure 13 the theoretical pressure distributions in three sections of the wing are compared with the experimental data*). The theoretical lines represent the calculated pressure jump across the wing divided by two. In section 2 and 5 the agreement between theory and experiment is very good. The same holds for the unsteady pressures on the lower side in section 8. However, on the upper side of section 8 the experimental pressure distribution shows a dip which for this specific Mach number was found also in the clean wing

*) Note that for the purpose of comparison the unsteady pressures measured on the upperside are plotted with a reversed sign.

configuration (see Ref. 3). This dip is not predicted theoretically, nor is a physical explanation readily available.

A comparison of the corresponding theoretical and experimental unsteady spanwise normal load distributions for both the clean wing and the wing with tipstore is given in figure 15. The theoretical results for the wing with tipstore were computed with the NLRI-method, while for the clean wing the Doublet Lattice method was used (Ref. 3).

As found for the clean wing, also for the wing with tipstore the real part of the calculated unsteady loading, as normal, is larger than the experimental value, be it that in the present case the difference is somewhat extraordinary. The main reason herefore is that from section 4 to 8 irregularities in one or more points of the measured pressure distributions (see Fig. III.C.32 of Appendix C) affect the accuracy of the integration. However, since these differences are similar for both configurations conclusions concerning interference effects should remain valid.

The theoretical calculations predict a tipstore interference which qualitatively agrees very well with what was found experimentally. The presence of the store results in an increase of the real part of the unsteady normal load. This increase is maximal near the tip and becomes smaller towards the wingroot. The imaginary part is hardly affected.

In table 2 the experimental unsteady normal force and pitching moment acting on the complete tipstore are compared with the values obtained with the NLRI-method. The agreement is satisfactory. The magnitude of the store load is of the order of 7.5 per cent of the total wing load. However, compared to the normal load acting on a strip of the wing near the tip, having the same width as the store, the store load amounts to about 125 per cent.

In the calculations with the NLRI-method the unsteady store loads could be divided in the contributions due to the individual components of the tipstore. This made it possible to compute also the normal force and pitching moment for the other configurations measured. In doing so, it should be realized that the interference effects due to the deleted parts remain present. Therefore, a comparison with experimental data for these different configurations gives only qualitative information. Nevertheless, such a comparison is attempted in table 3. The results indicate that the real part of the normal force increases with the complexity of the store, while the imaginary part, although predicted with the wrong

sign, remains small. For the real part of the pitching moment the aft wings give a reduction and the canard fins an increase. The imaginary part of the moment is almost zero for all configurations.

4.2 The Doublet Lattice method

The calculations described above have the disadvantage, that compared to the Doublet Lattice (DL) method, the NLRI-methode uses 2 to 3 times more computer time. This makes the computation of unsteady aerodynamic force coefficients for flutter certification very expensive and impractical if carried out solely with the NLRI-method. Therefore, in reference 4 it was proposed already to use the NLRI-method as a datum, against which results of a cheaper method such as the DL-method can be checked.

In this investigation it is tried to devise a panel distribution for the Doublet Lattice method, in which the store is represented as additional thin lifting surface parts. These additional lifting surfaces have to fulfil two roles. They should lead to a good prediction of the interference on the wing and at the same time give reliable values for the store loads. The panel distribution, which turned out to satisfy these criteria sufficiently well, is shown in figure 16. The launcher and missile body are represented by a long tip extension in the plane of the wing. The canard fins and aft wings are kept in their original configuration except that they extend towards the missile centre line.

The unsteady pressure distributions computed with this DL panel layout for Ma = 0.6 and F = 20 Hz are presented in figure 17. The agreement with the experimental results is good, while a comparison with figure 14 indicates that only in section 8 a minimal difference between DL and NLRI results exists. This difference is visible also in the unsteady spanwise normal force distribution shown in figure 18. The store loads computed with this panel layout are given in table 4a. As can be noticed, they compare reasonably well with both the NLRI results and the experimental data.

To check if this DL panel layout made for Ma = 0.6, would give satisfactory results also for other Mach numbers, it was applied for Ma = 0.8 (Run 358) as well. In figure 19 the resulting unsteady pressure distributions are compared with the measured ones. All three sections show a very good agreement. Also for the store loads presented in table 4b the agreement is as good as for Ma = 0.6.

5 CONCLUSIONS

A wind-tunnel investigation was carried out on a harmonically oscillating model of the F-5 wing with and without external store. As part of the test program steady and unsteady measurements were performed on the configuration with the store mounted at the wingtip. These measurements concerned pressures on the wing and aerodynamic loads on the store. The present report gives a brief analysis of the results for this configuration. This analysis concerns:

- the interference of the tipstore on the steady, quasi-steady and unsteady wing loading indicating that the tipstore acts as an endplate, thus increasing the load on the wing
- the behaviour of this interference with Mach number showing an increase as the flow becomes transonic, but a reduction for supersonic flow
- the influence of the various parts of the store on the store loads which for the normal force grows consistenly with complexity of the store, but which for the pitching moment depends on the location of the added part with respect to the balance centre
- a description in terms of polynomials of the in-wind vibration modes for 20 Hz
- a comparison of these vibration modes with those of the clean wing indicating that the tipstore causes the nodal line tc move backwards
- the influence of the stagnation pressure on the vibration modes and the quasi-steady and unsteady sectional loads
- a comparison of unsteady experimental data for Ma = 0.6 with the results obtained with the NLRI-method, showing a good agreement
- the development of a panel distribution which in Doublet Lattice calculations gives similar results as the NLRI-method and shows good agreement with the experiment.

6 REFERENCES

1 Tijdeman, H. et al.
Transonic wind-tunnel tests on an oscillating wing with external store.
Part I: General Description
NLR TR 78106 U Part I (1978)

2
Results of transonic wind-tunnel measurements on an oscillating wing with external store.
NLR TR 78030 U (1978)

3 Tijdeman, H. et al.
Transonic wind-tunnel tests on an oscillating wing with external store.
Part II: The clean wing
NLR TR 78106 U Part II (1978)

4 Roos, R.
Bennekers, B. and Zwaan, R.J.
Calculation of unsteady subsonic flow about harmonically oscillating wing/body configurations.
J. of Aircraft, Vol.14, No.5, pp 447-454, 1977

5 Persoon, A.J.
Measuring unsteady aerodynamic loads on wing-mounted stores.
NLR TR 79013 U (1979)

6
AGARD Manual on Aeroelasticity.
Vol. VI (1968)

TABLE 1

Coefficients a_{mn} for the approximation of the in-wind vibration modes of the wing with complete tipstore at an oscillation frequency of 20 Hz

Run	Ma	$P_o \times 10^{-5}$ (Pa)	F (Hz)	K	WING						TIPSTORE	
					a_{00}	a_{01}	a_{10}	a_{11}	a_{20}	a_{21}	a_{00}	a_{01}
350	0.6	1.0	20	0.200	-0.336	0.997	0.045	0.032	-0.141	-0.001	-0.389	1.022
344	0.6			0.200	-0.336	1.000	0.074	-0.032	-0.304	0.304	-0.276	1.095
337	0.7			0.173	-0.346	1.020	0.127	-0.260	-0.400	0.596	-0.450	1.099
358	0.8			0.153	-0.351	1.022	0.162	-0.296	-0.531	0.677	-0.459	1.075
353	0.9			0.138	-0.349	1.016	0.082	-0.209	-0.442	0.424	-0.513	1.098
316	1.10	1.0		0.116	-0.362	1.035	0.161	-0.431	-0.597	0.696	-0.555	1.110
309	1.10	0.7		0.117	-0.347	1.005	0.071	-0.057	-0.339	0.095	-0.343	1.083
300	1.35	0.7	20	0.101	-0.351	1.023	0.145	-0.285	-0.402	0.506	-0.440	1.047

TABLE 2

Comparison of theoretical and experimental unsteady loads on the tipstore

Conf. 4: Wing with complete tipstore

Ma = 0.6 F = 20 Hz	EXPERIMENT	THEORY NLRI
Re C_Z	0.082	0.087
Im C_Z	0.017	-0.009
Re C_M	0.046	0.039
Im C_M	-0.003	-0.004

TABLE 3

Comparison of theoretical and experimental unsteady loads on different tipstore configurations

Ma = 0.6 F = 20 Hz		Re C_Z	Im C_Z	Re C_M	Im C_M
Conf. 2: Tiplauncher + Missile Body	EXP.	0.041	0.008	0.030	0.012
	NLRI	0.067	-0.014	0.023	0.003
Conf. 3: Tiplauncher + Missile Body + Aft Wings	EXP.	0.079	0.008	0.009	0
	NLRI	0.076	-0.006	0.018	0
Conf. 4: Complete Store	EXP.	0.082	0.017	0.046	-0.003
	NLRI	0.087	-0.009	0.039	-0.004

TABLE 4

Comparison of theoretical and experimental unsteady loads on the tipstore

Conf. 4: Wing with complete tipstore

(a)

Ma = 0.6 F = 20 Hz	THEORY D.L.	EXPERIMENT	THEORY NLRI
Re C_Z	0.083	0.082	0.087
Im C_Z	0.008	0.017	-0.009
Re C_M	0.032	0.046	0.039
Im C_M	-0.008	-0.003	-0.004

(b)

Ma = 0.8 F = 20 Hz	THEORY D.L.	EXPERIMENT
Re C_Z	0.094	0.097
Im C_Z	0.002	0.016
Re C_M	0.032	0.045
Im C_M	-0.009	-0.006

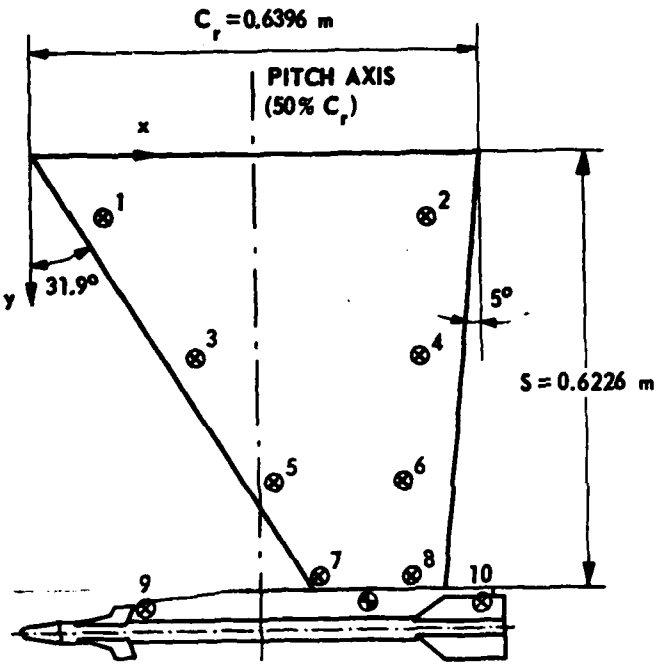

⊗ ACCELEROMETERS		
NR	x (m)	y (m)
1	0.1087	0.0957
2	0.5648	0.0977
3	0.2309	0.2971
4	0.5475	0.2991
5	0.3422	0.4772
6	0.5270	0.4772
7	0.4070	0.6176
8	0.5390	0.6176
9	0.1300	0.6350
10	0.6393	0.6350

⊕ BALANCE CENTRE
x = 0.480 ; y = 0.635

Fig. 1a Dimensions of the wing model

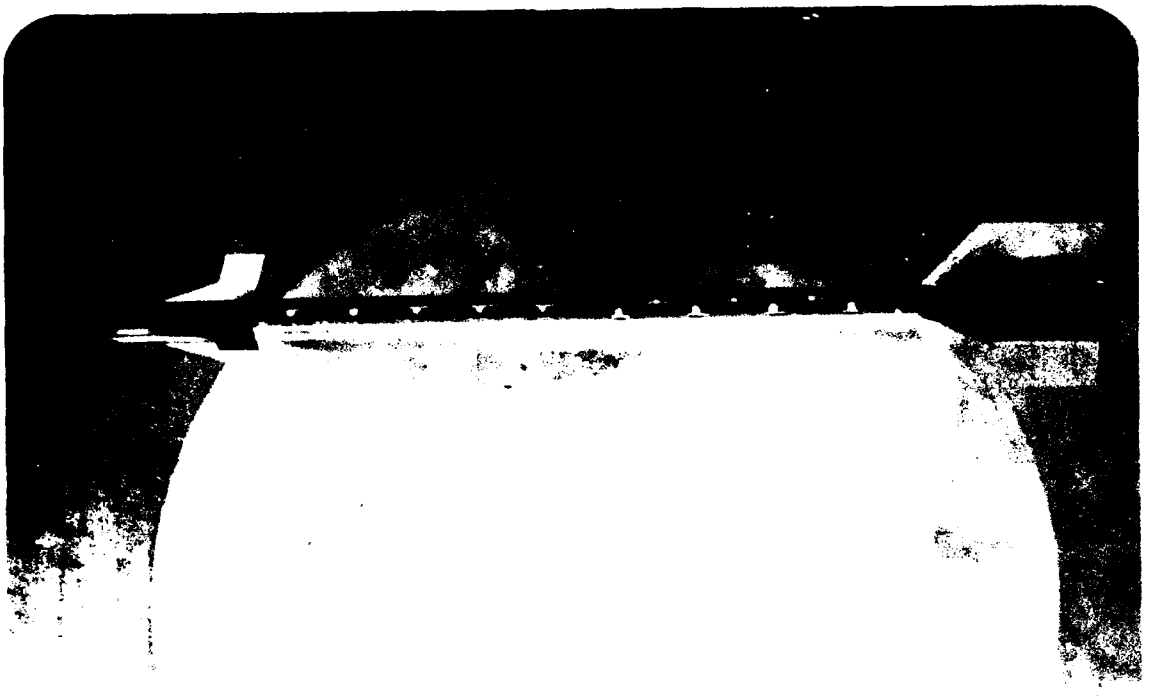

Fig. 1b Model of wing with tipstore mounted in the wind tunnel

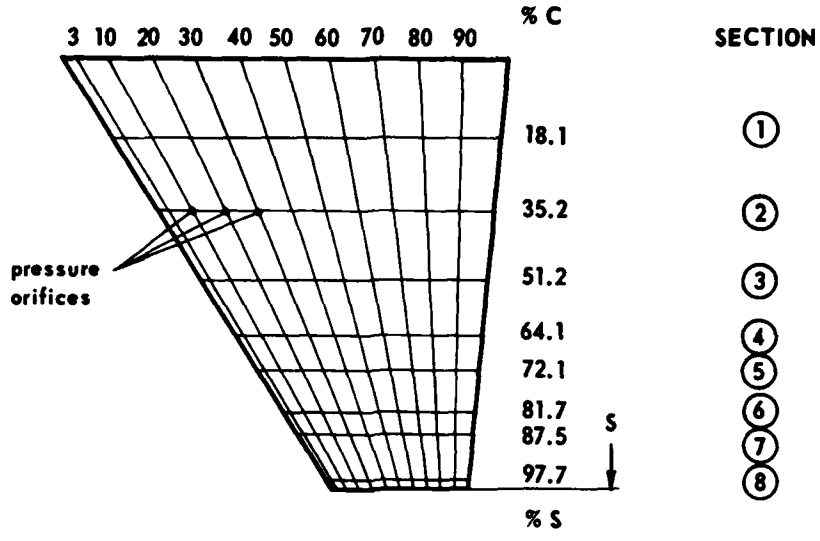

Fig. 1c Location of the pressure orifices

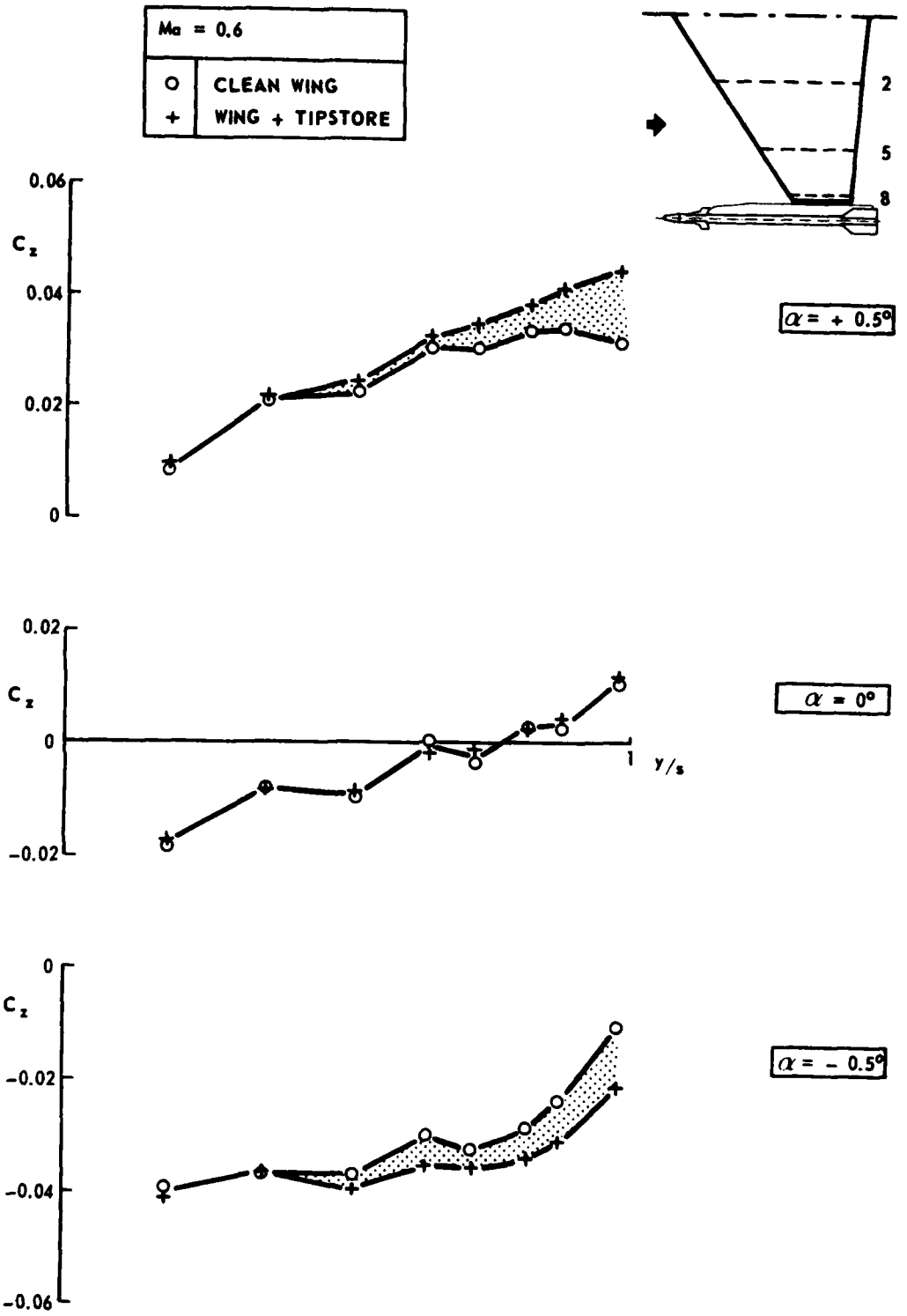

Fig. 2a Steady spanwise normal load distributions on the clean wing and on the wing with complete tipstore at Ma = 0.6

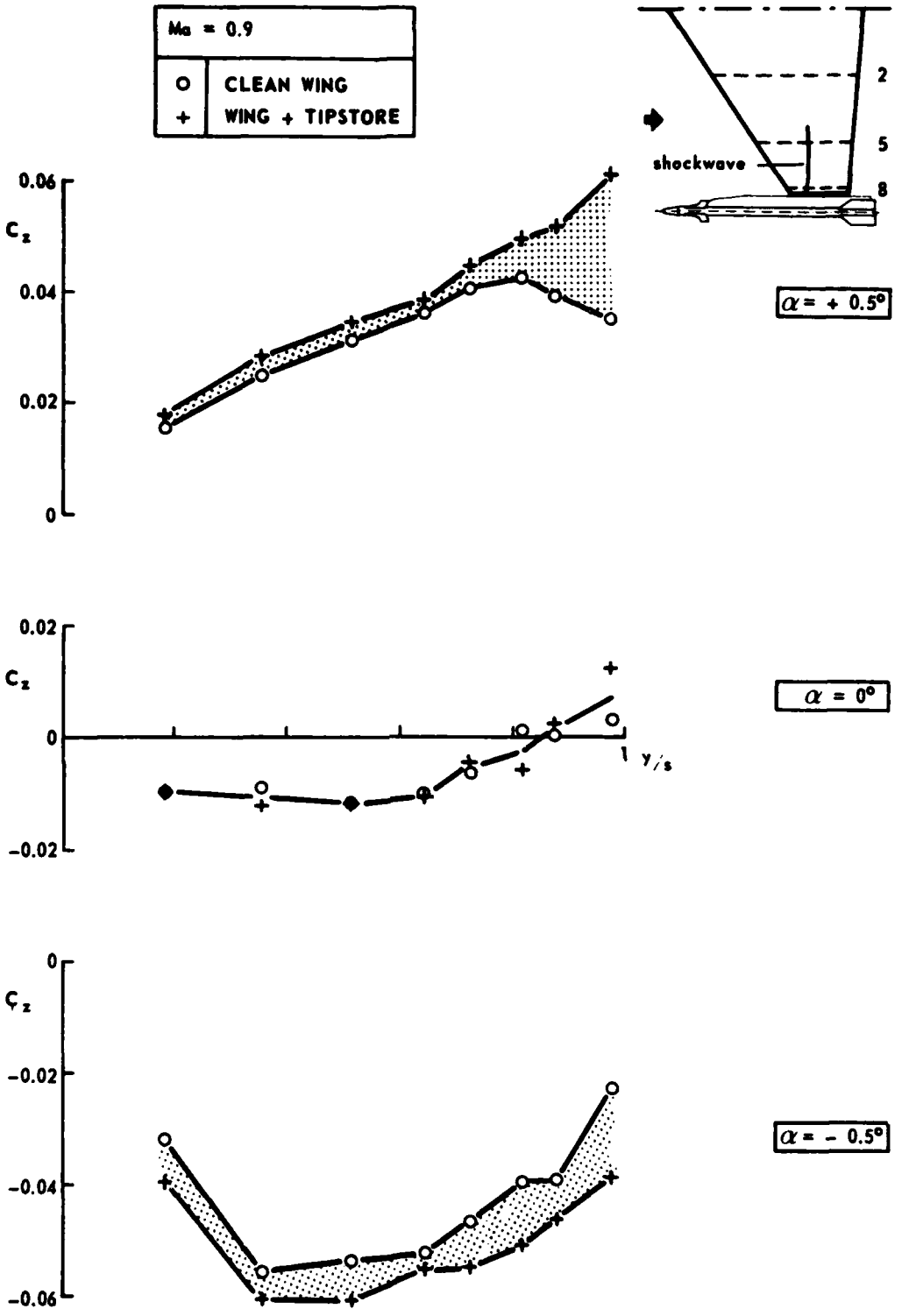

Fig. 2b Steady spanwise normal load distributions on the clean wing and on the wing with complete tipstore at Ma = 0.9

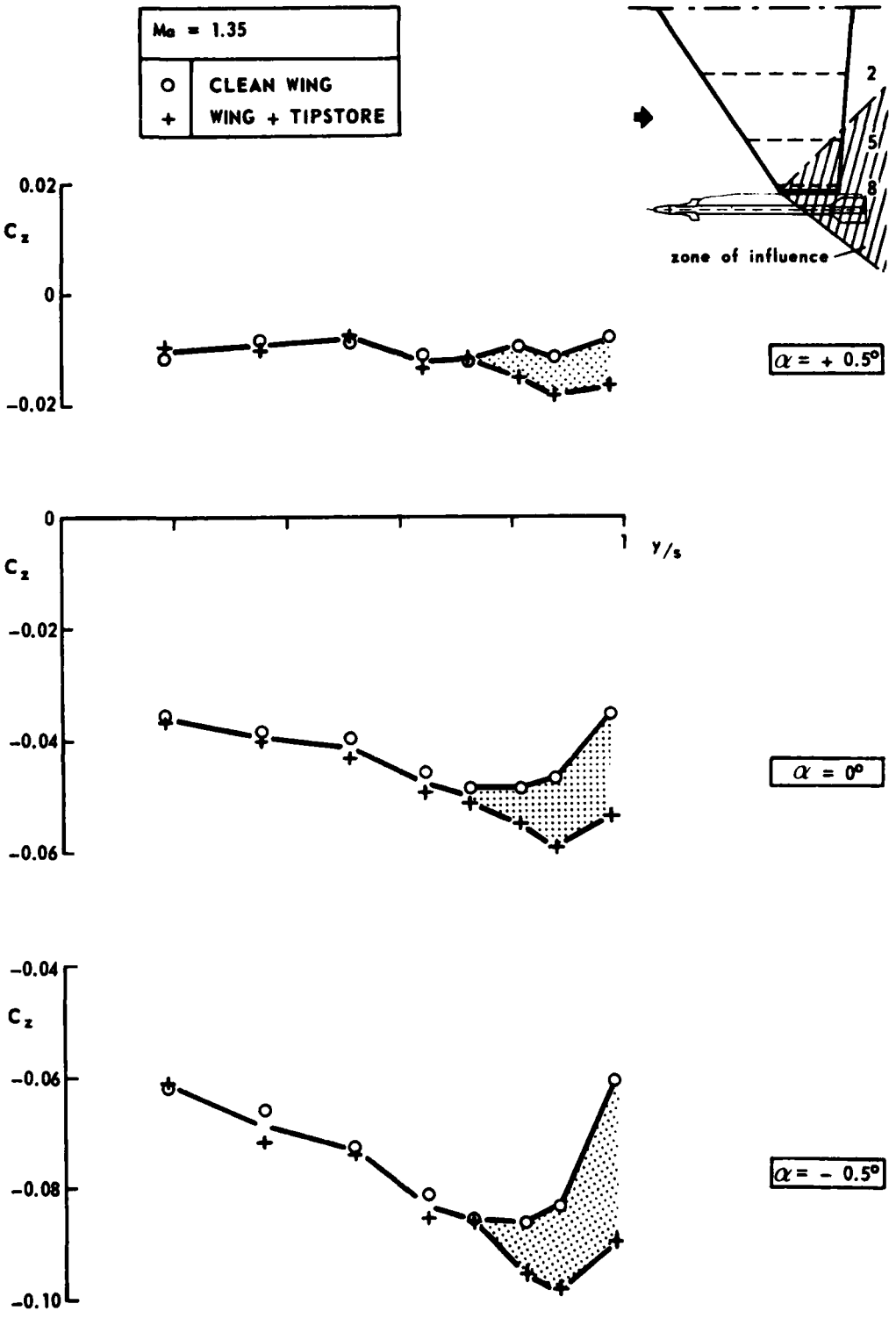

Fig. 2c Steady spanwise normal load distributions on the clean wing and on the wing with complete tipstore at Ma = 1.35

Ma = 0.6	EXP.	RUN	CONFIGURATION
F = 0 Hz	○	137	CLEAN WING
	+	341	WING + TIPSTORE

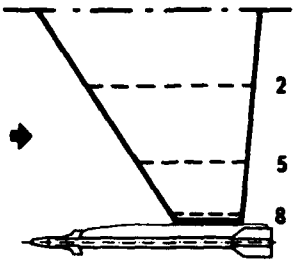

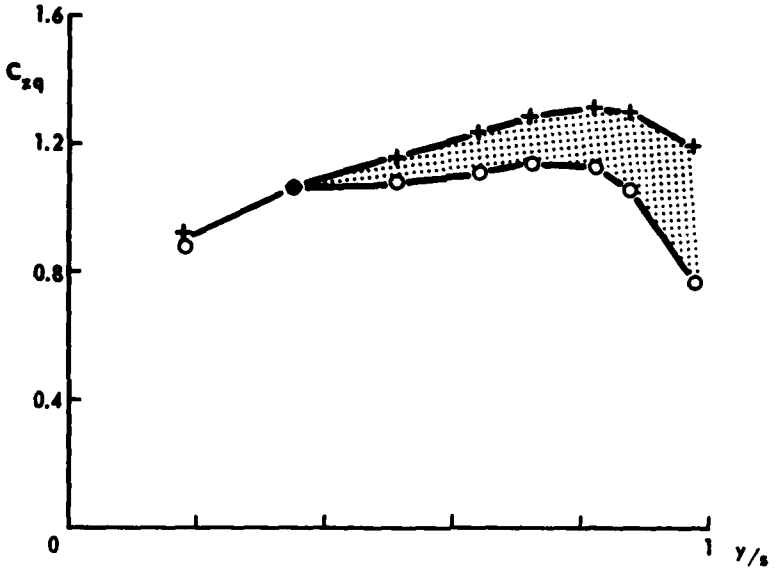

Fig. 3a Quasi-steady spanwise normal load distributions on the clean wing and on the wing with complete tipstore at Ma = 0.6

Ma = 0.9	EXP.	RUN	CONFIGURATION
F = 0 Hz	○	151	CLEAN WING
	+	320	WING + TIPSTORE

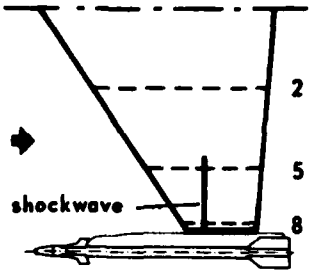

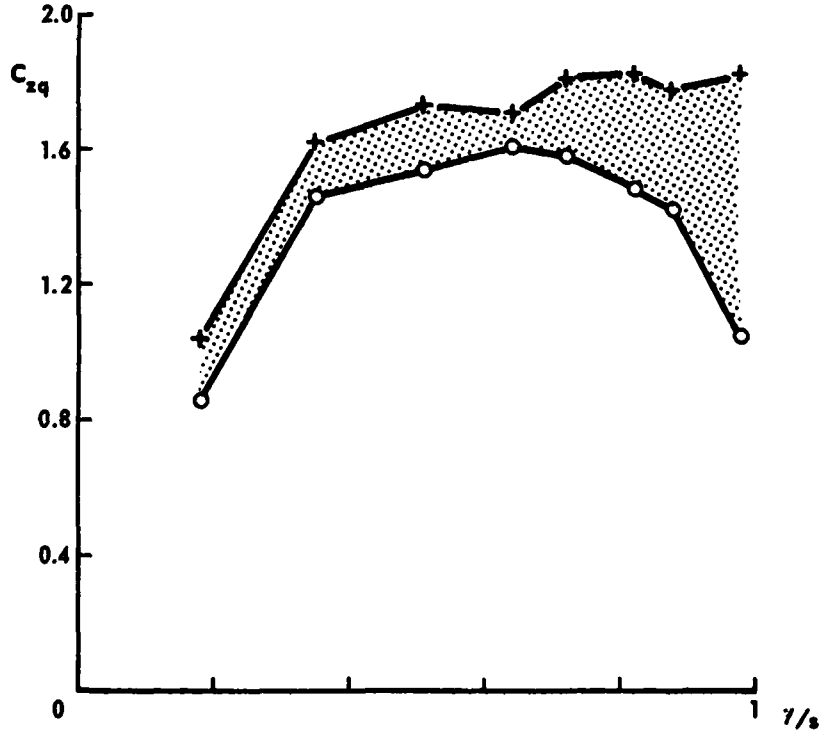

Fig. 3b Quasi-steady spanwise normal load distributions on the clean wing and on the wing with complete tipstore at Ma = 0.9

Ma = 1.35	EXP.	RUN	CONFIGURATION
F = 0 Hz	○	190	CLEAN WING
	+	297	WING + TIPSTORE

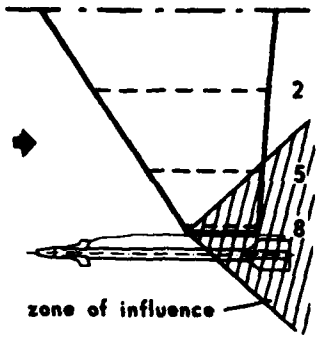

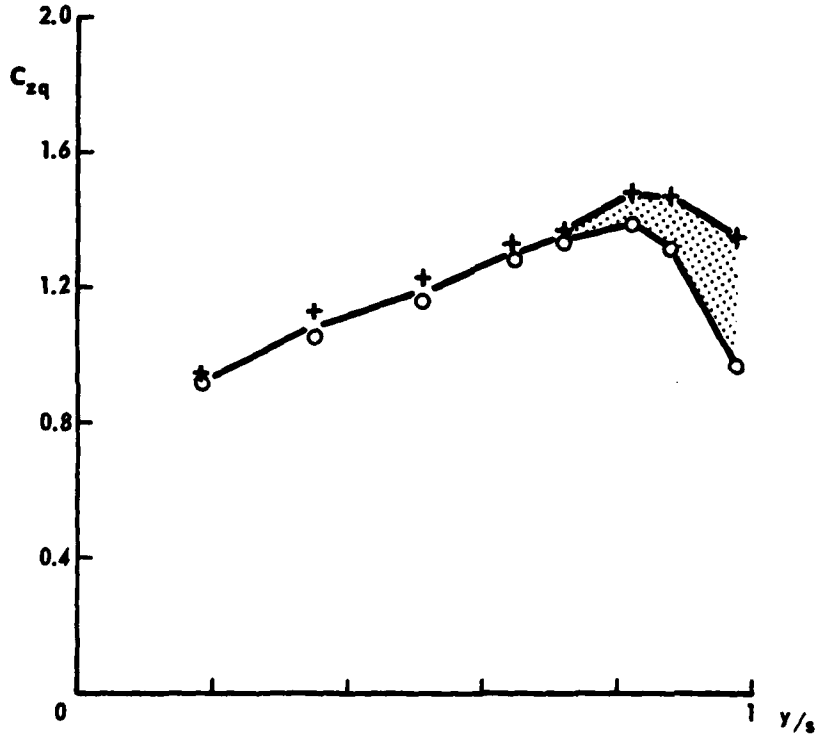

Fig. 3c Quasi-steady spanwise normal load distributions on the clean wing and on the wing with complete tipstore at Ma = 1.35

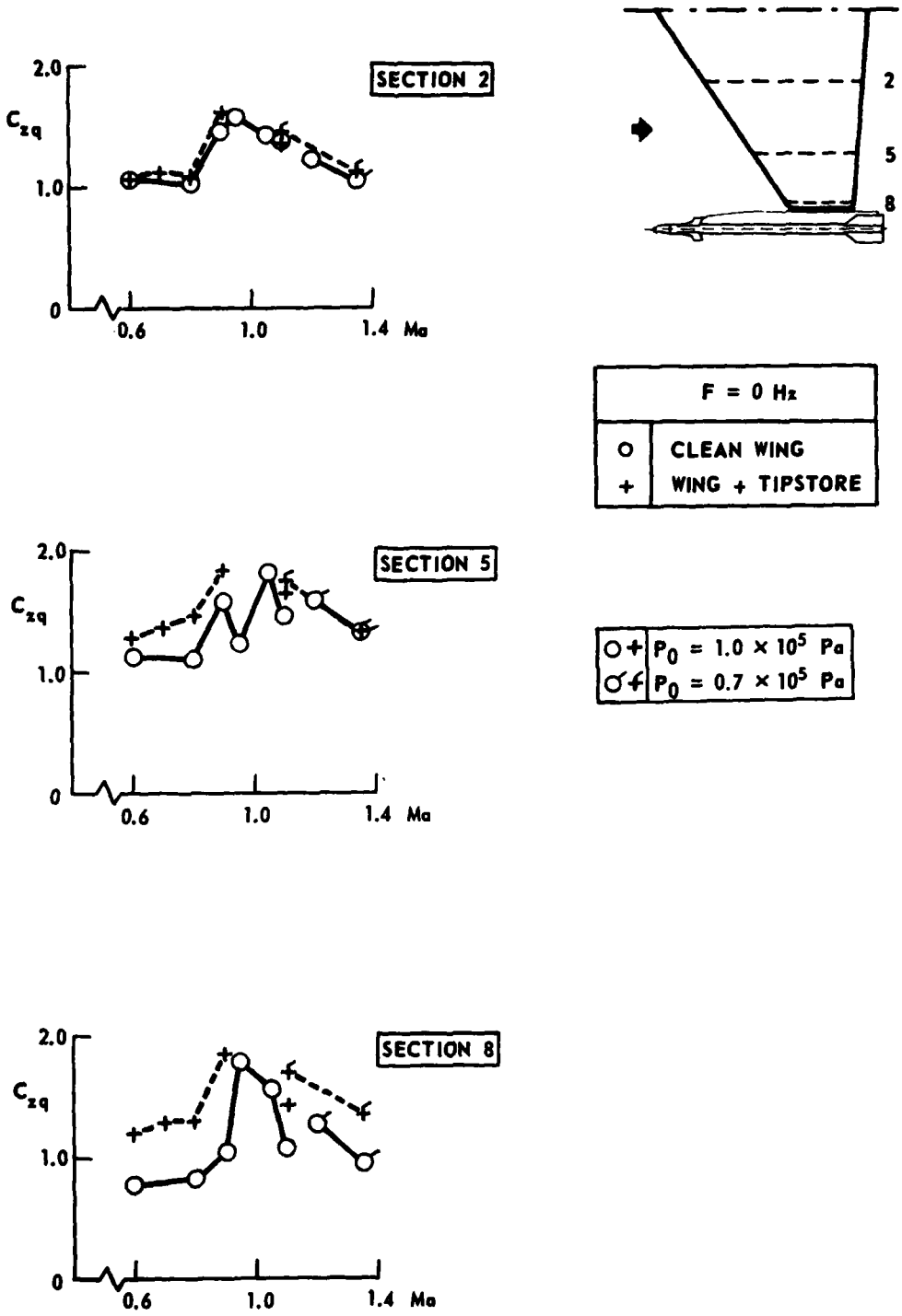

Fig. 4 Sectional quasi-steady normal load distribution on the clean wing and the wing with complete tipstore versus Mach number

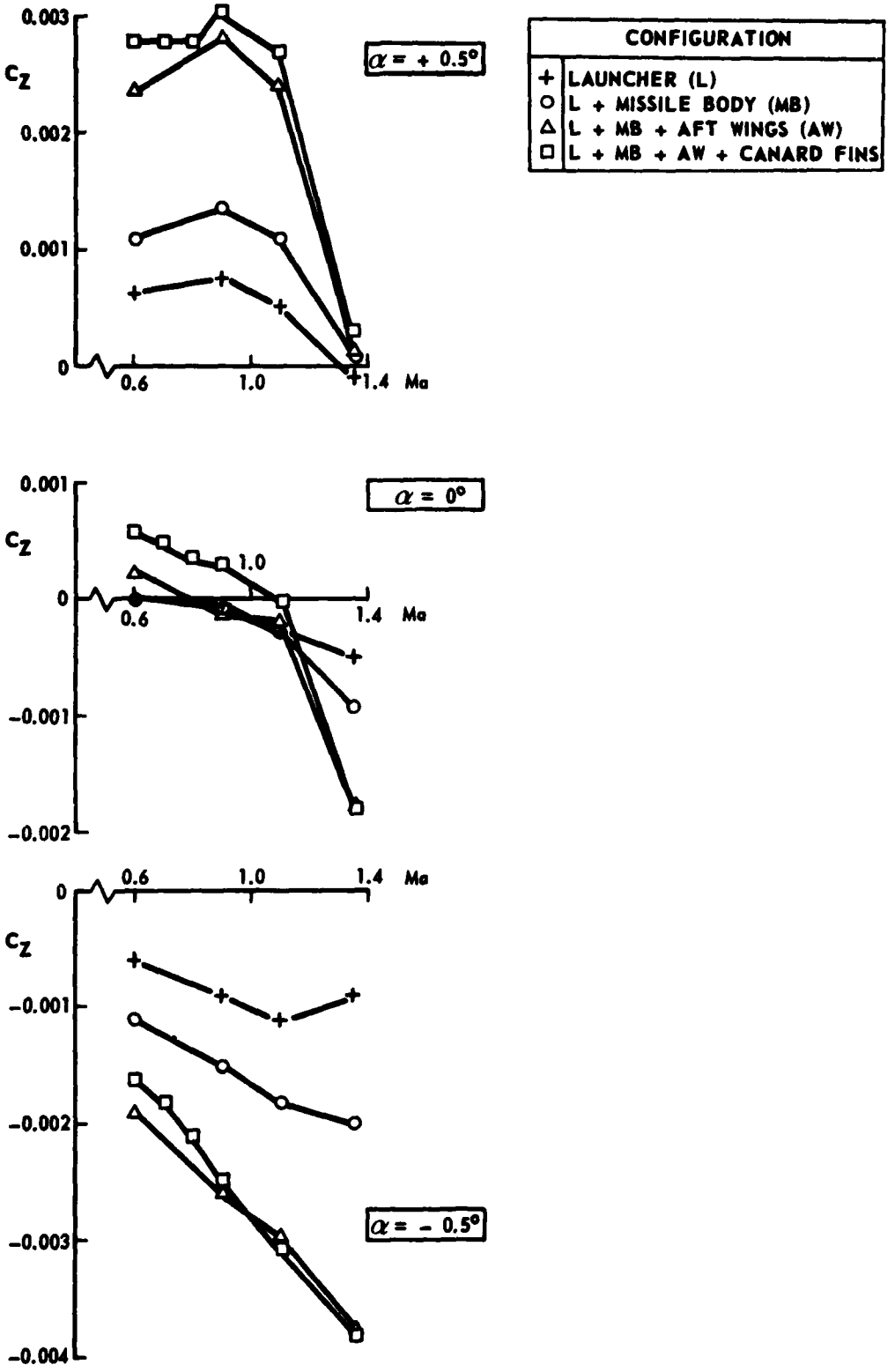

Fig. 5a Steady normal force on various tipstore configurations versus Mach number

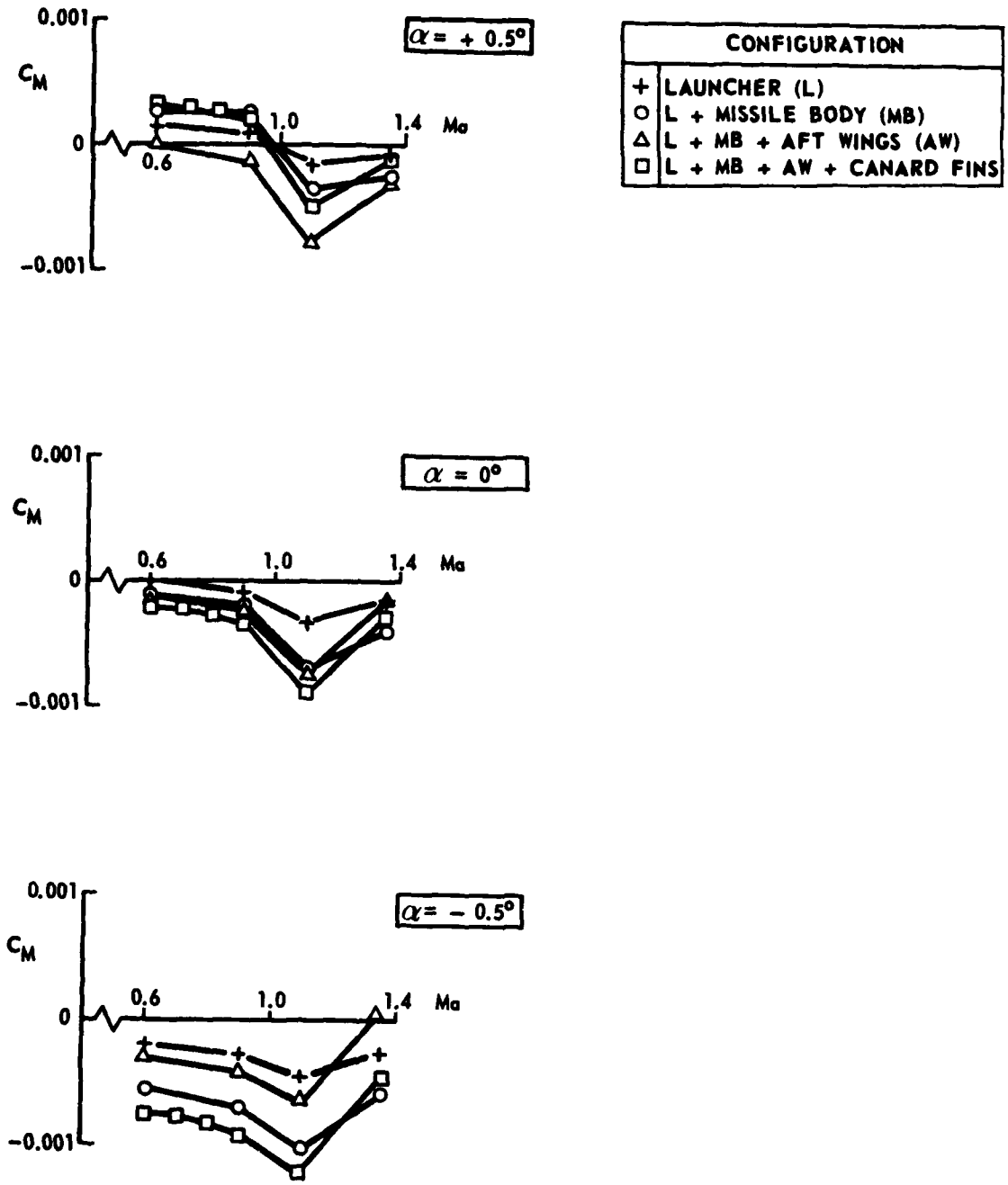

Fig. 5b Steady pitching moment on various tipstore configurations versus Mach number

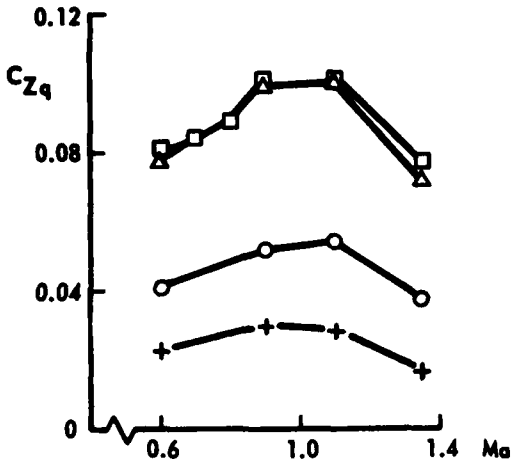

F = 0 Hz	
CONFIGURATION	
+	LAUNCHER (L)
○	L + MISSILE BODY (MB)
△	L + MB + AFT WINGS (AW)
□	L + MB + AW + CANARD FINS

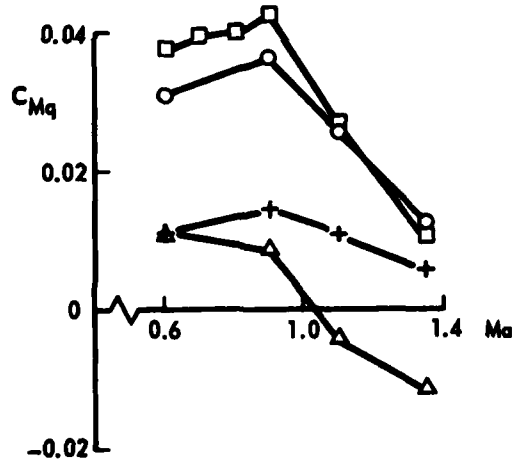

Fig. 6 Quasi-steady normal force and pitching moment on various tipstore configurations versus Mach number

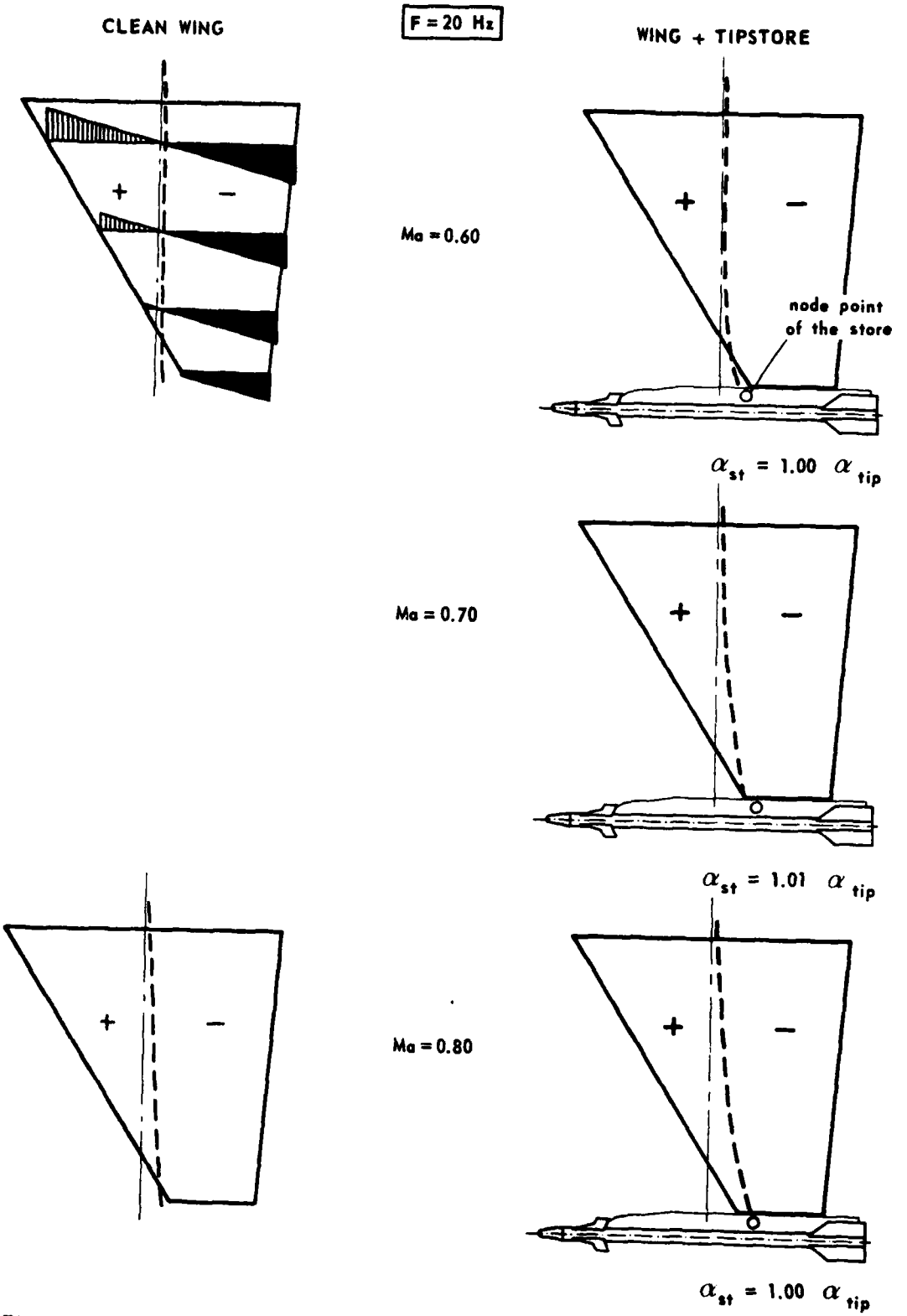

Fig. 7a In-wind vibration modes of the clean wing and the wing with complete tipstore

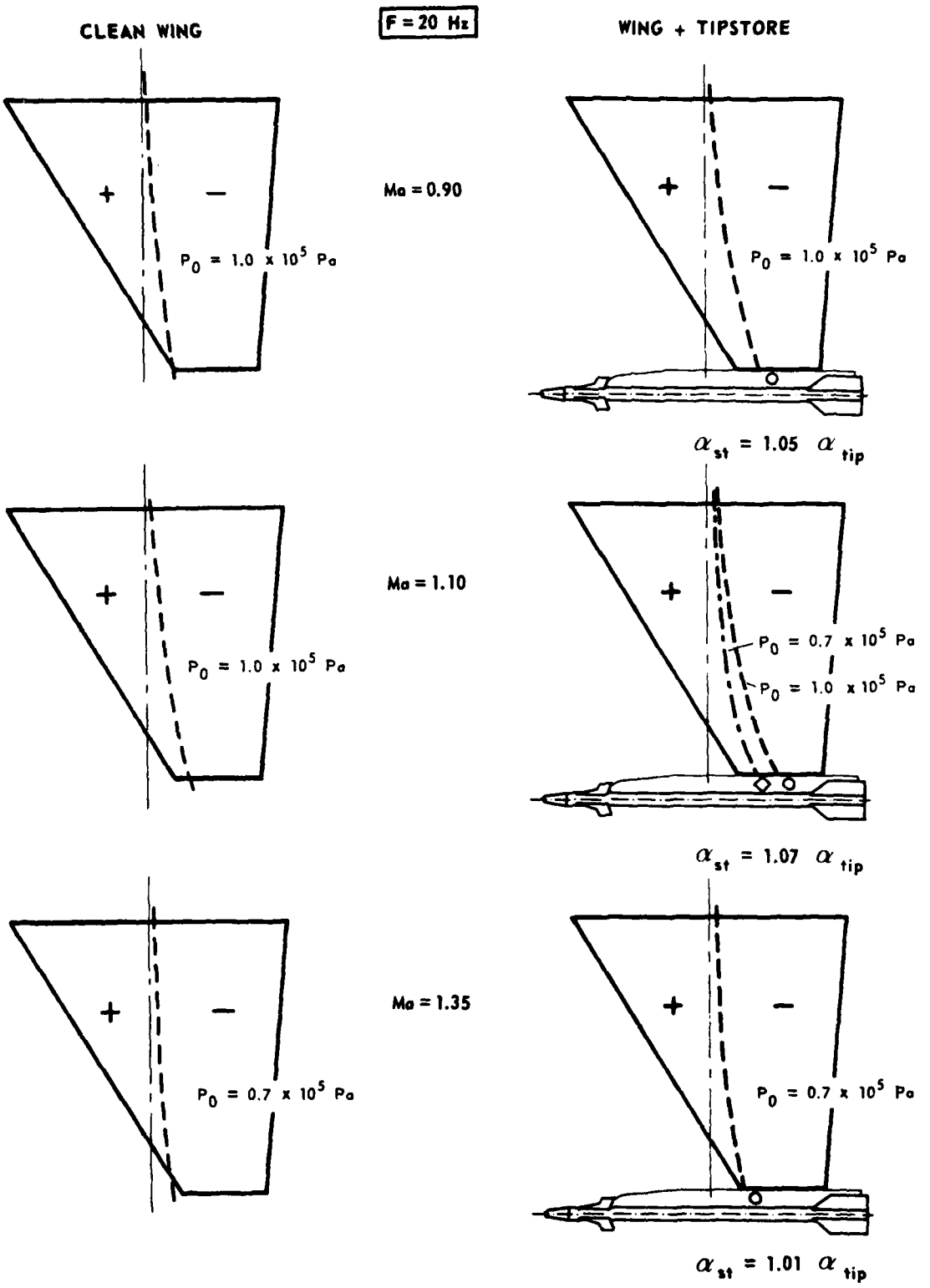

Fig. 7b In-wind vibration modes of the clean wing and the wing with complete tipstore

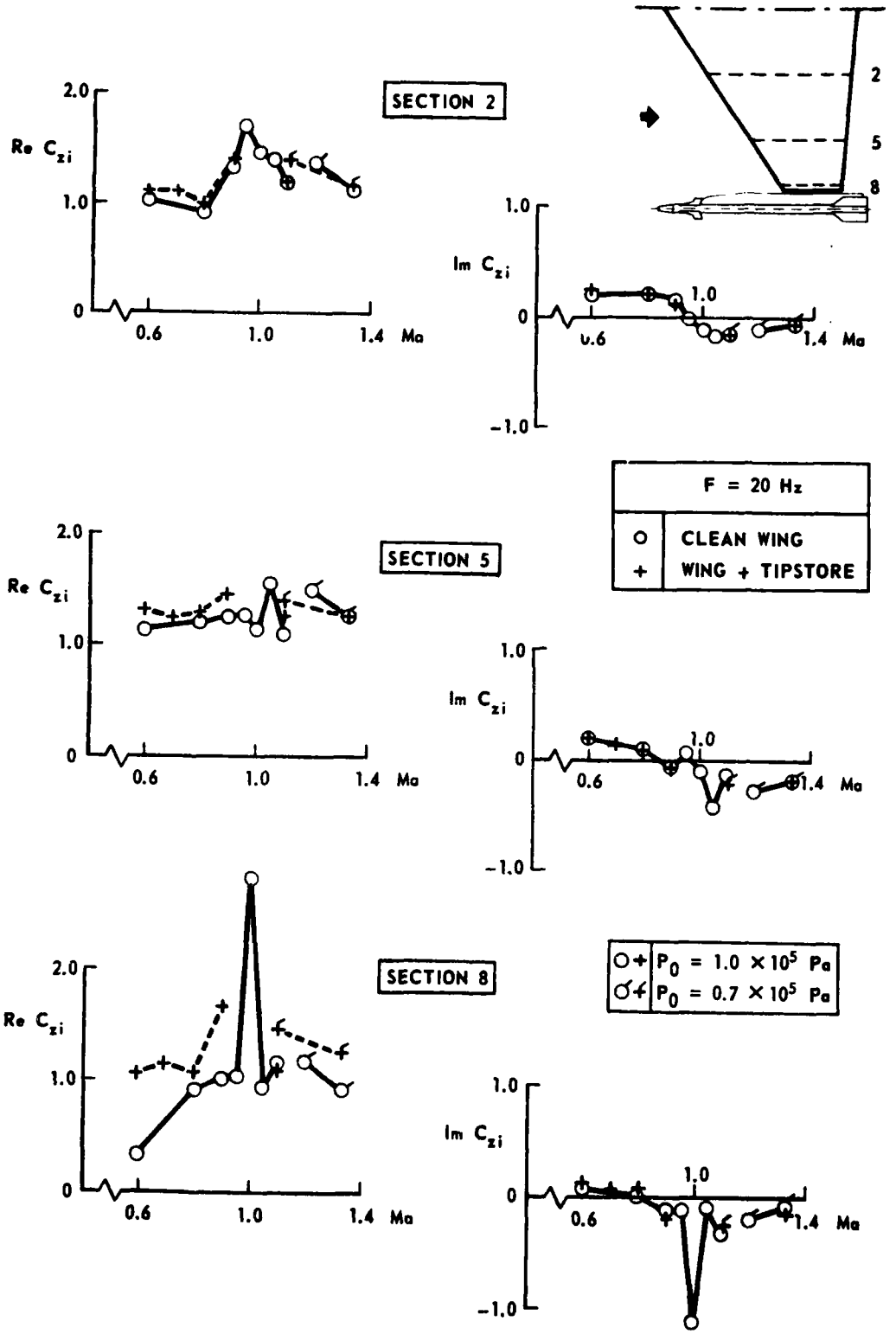

Fig. 8 Sectional unsteady normal load distribution on the clean wing and the wing with complete tipstore versus Mach number

Ma = 0.6	EXP.	RUN	CONFIGURATION
F = 20 Hz	○	382	CLEAN WING
K = 0.2	+	350	WING + TIPSTORE

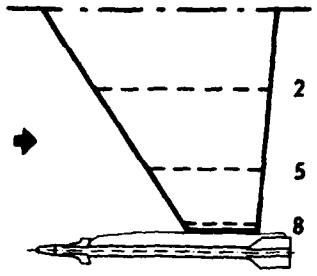

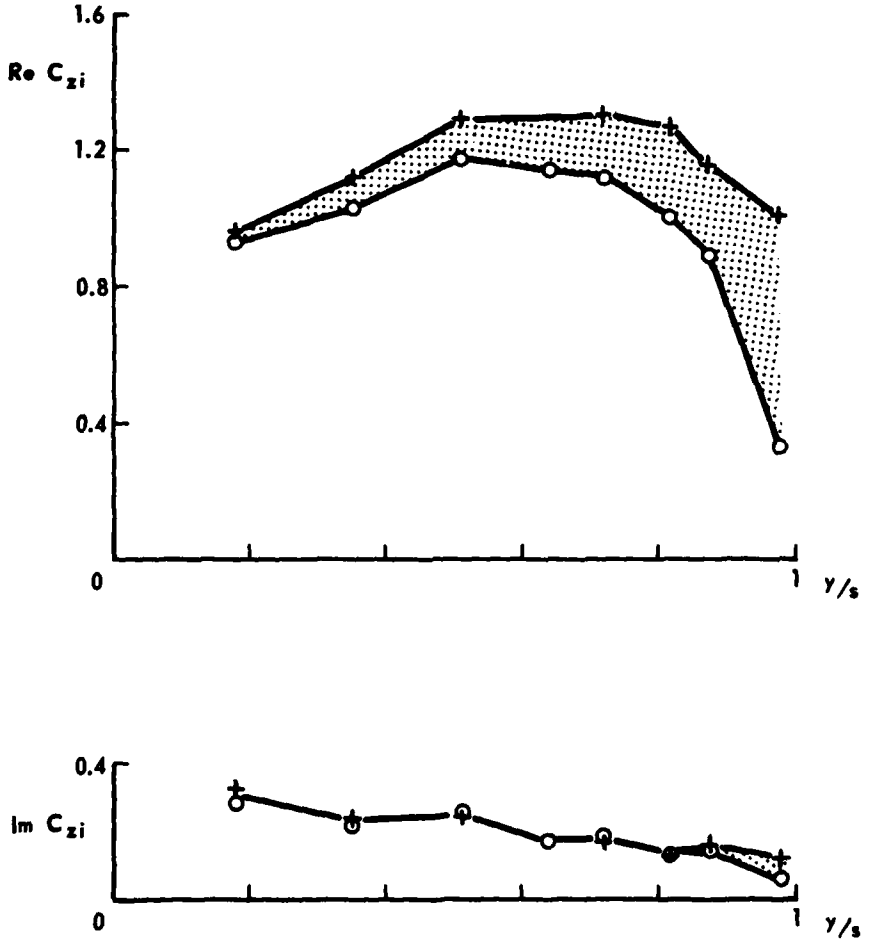

Fig. 9a Unsteady spanwise normal load distributions on the clean wing and on the wing with complete tipstore at Ma = 0.6

Ma = 0.6	EXP.	RUN	CONFIGURATION
F = 20 Hz	○	382	CLEAN WING
K = 0.2	+	350	WING + TIPSTORE

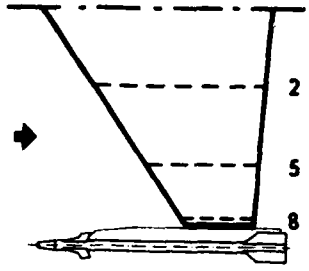

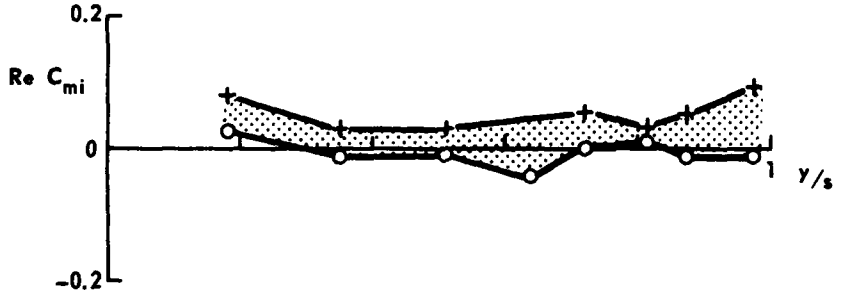

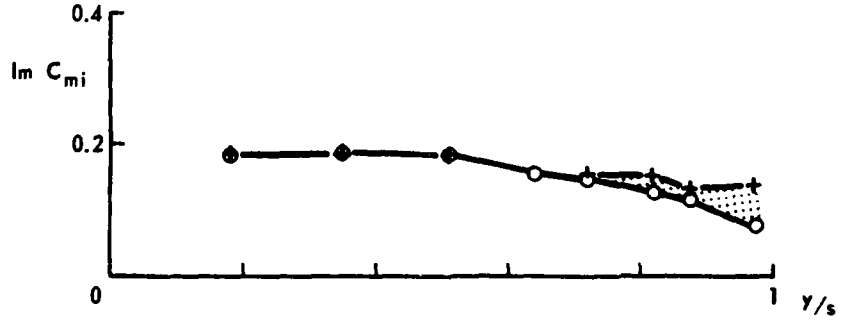

Fig. 9b Unsteady spanwise pitching moment distributions on the clean wing and on the wing with complete tipstore at Ma = 0.6

Ma = 0.9	EXP.	RUN	CONFIGURATION
F = 20 Hz	○	369	CLEAN WING
K = 0.14	+	353	WING + TIPSTORE

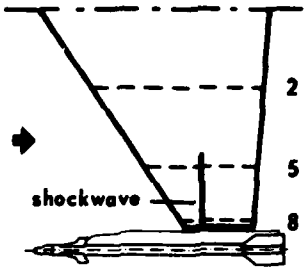

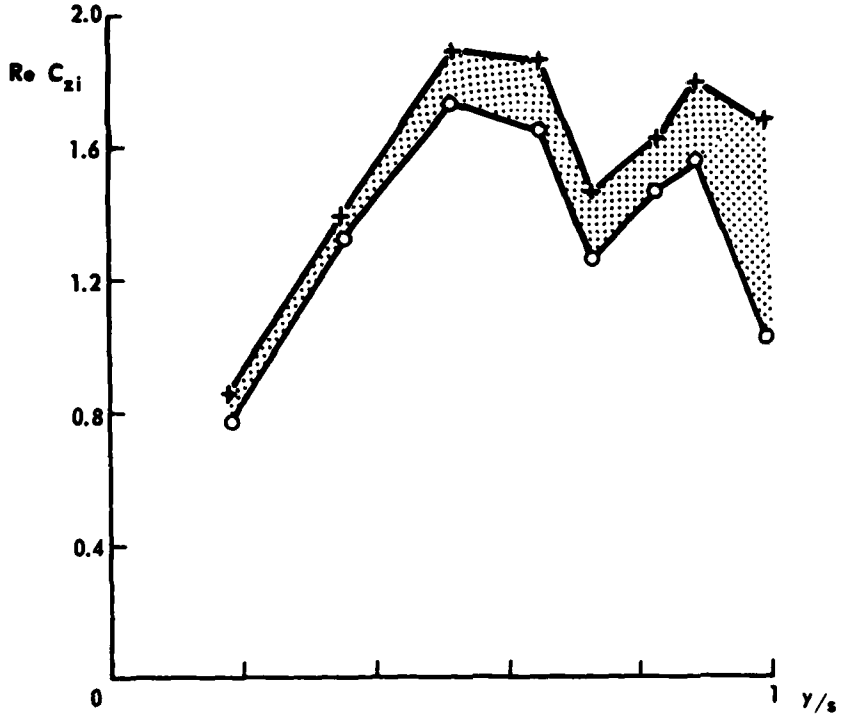

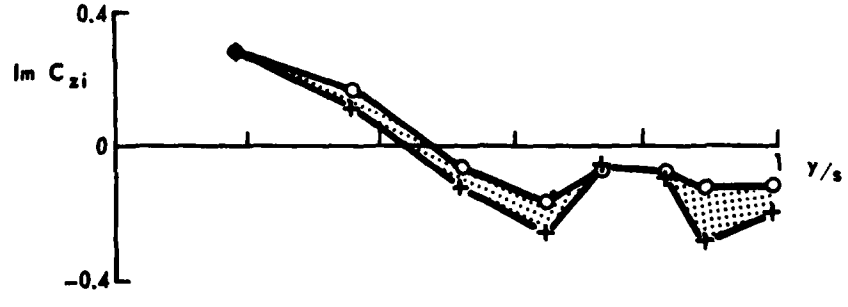

Fig. 10a Unsteady spanwise normal load distributions on the clean wing and on the wing with complete tipstore at Ma = 0.9

Ma = 0.9	EXP.	RUN	CONFIGURATION
F = 20 Hz	○	369	CLEAN WING
K = 0.14	+	353	WING + TIPSTORE

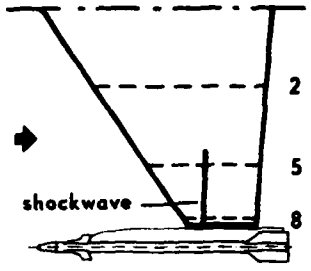

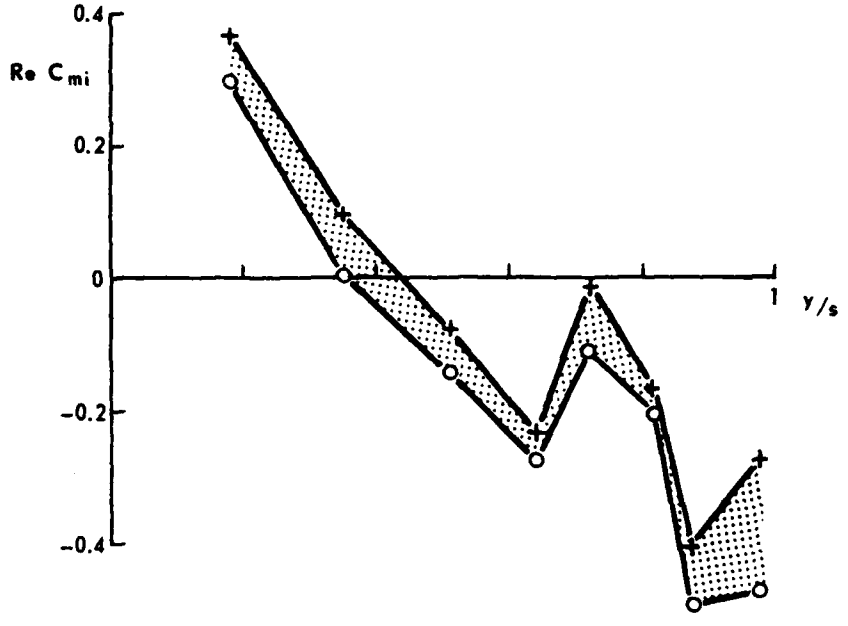

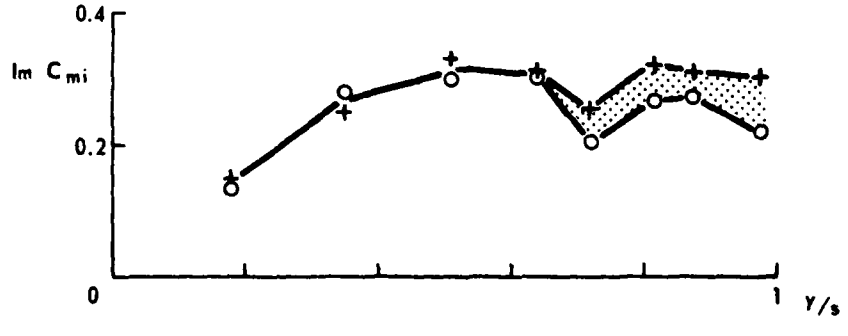

Fig. 10b Unsteady spanwise pitching moment distributions on the clean wing and on the wing with complete tipstore at Ma = 0.9

Ma = 1.35	EXP.	RUN	CONFIGURATION
F = 20 Hz	○	192	CLEAN WING
K = 0.1	+	300	WING + TIPSTORE

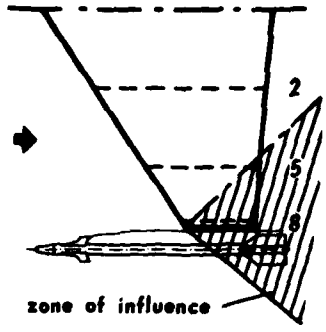

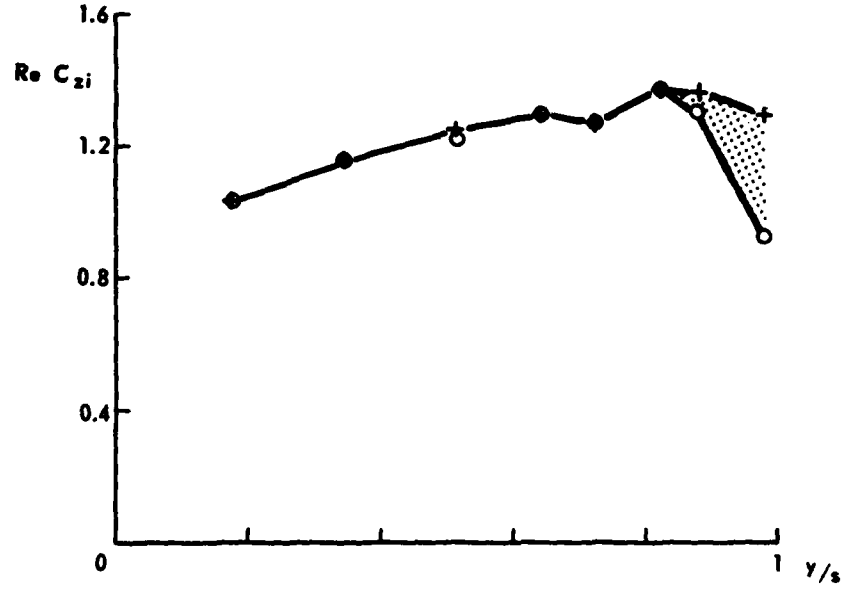

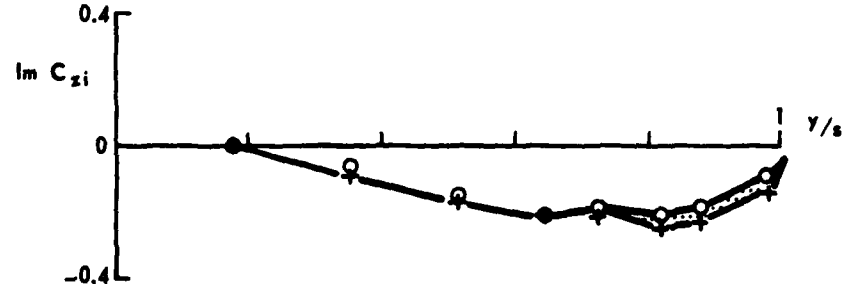

Fig. 11a Unsteady spanwise normal load distributions on the clean wing and on the wing with complete tipstore at Ma = 1.35

Ma = 1.35	EXP.	RUN	CONFIGURATION
F = 20 Hz	o	192	CLEAN WING
K = 0.1	+	300	WING + TIPSTORE

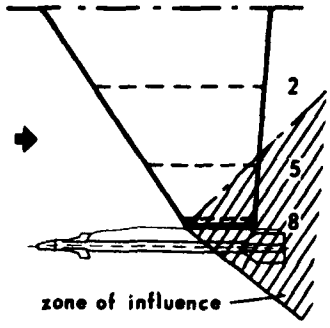

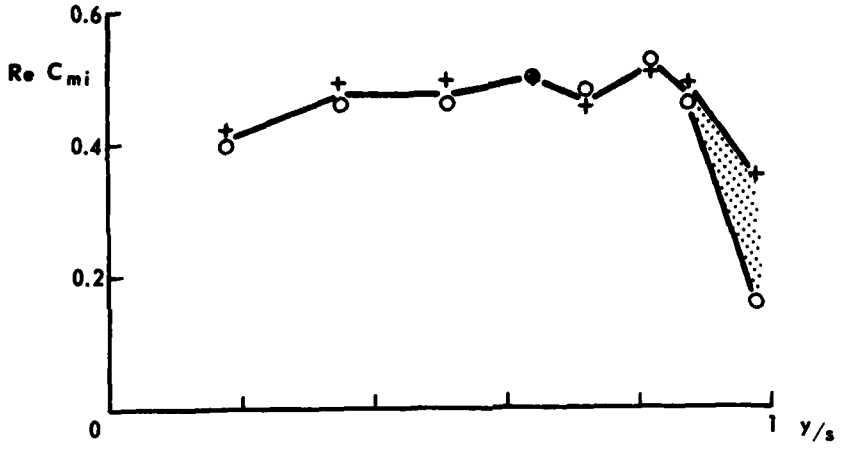

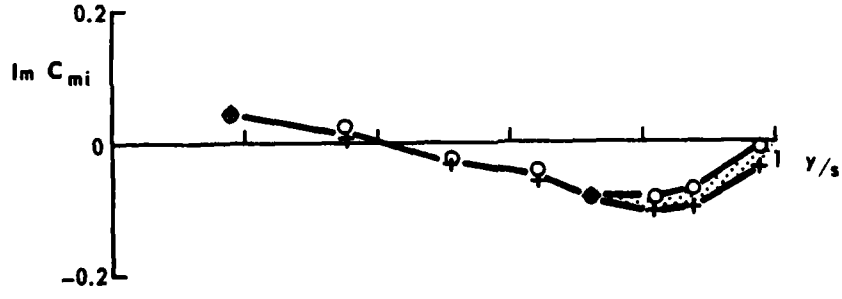

Fig. 11b Unsteady spanwise pitching moment distributions on the clean wing and on the wing with complete tipstore at Ma = 1.35

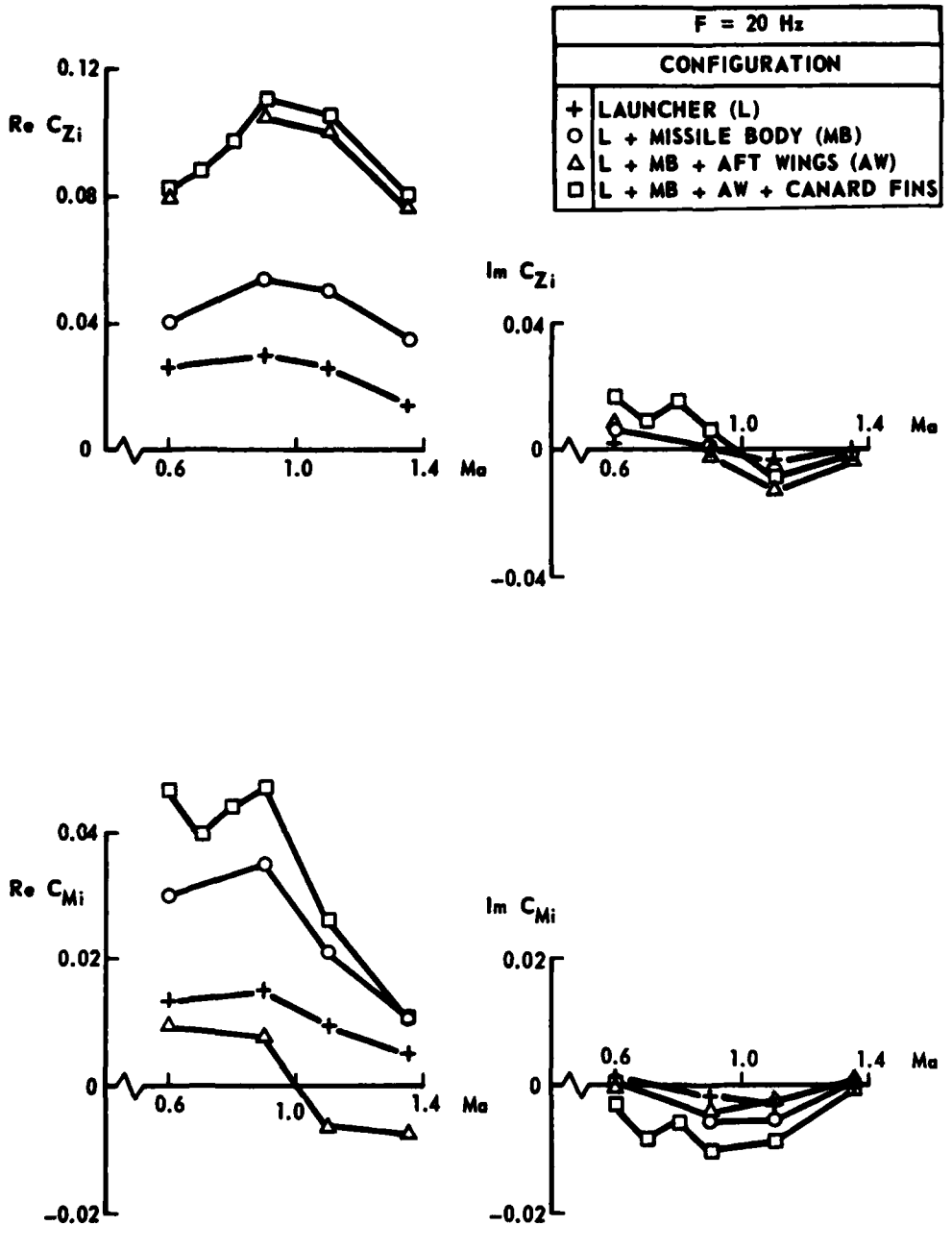

Fig. 12 Unsteady normal force and pitching moment on the various tipstore configurations versus Mach number

NUMBER OF PANELS	
WING	117
CANARD FINS	16
AFT WINGS	60
LAUNCHER - MISSILE BODY	294
TOTAL	487

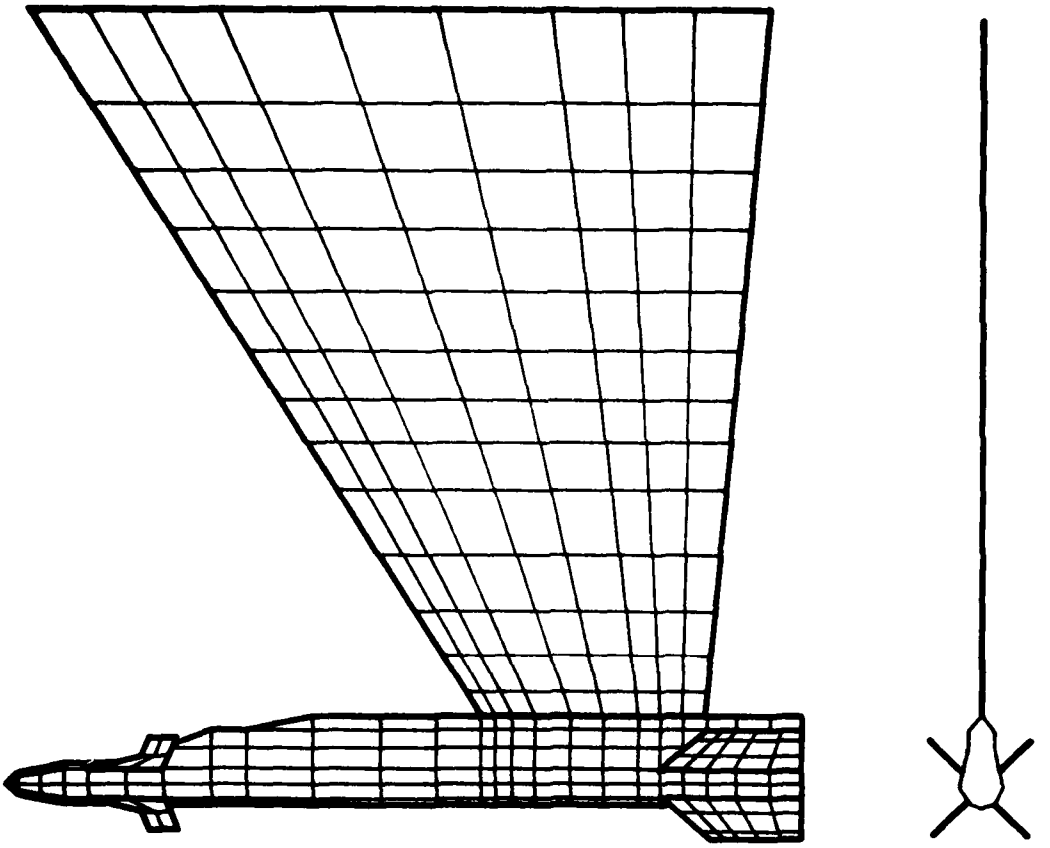

Fig. 13 Panel distribution used in calculations with the NLRI-method

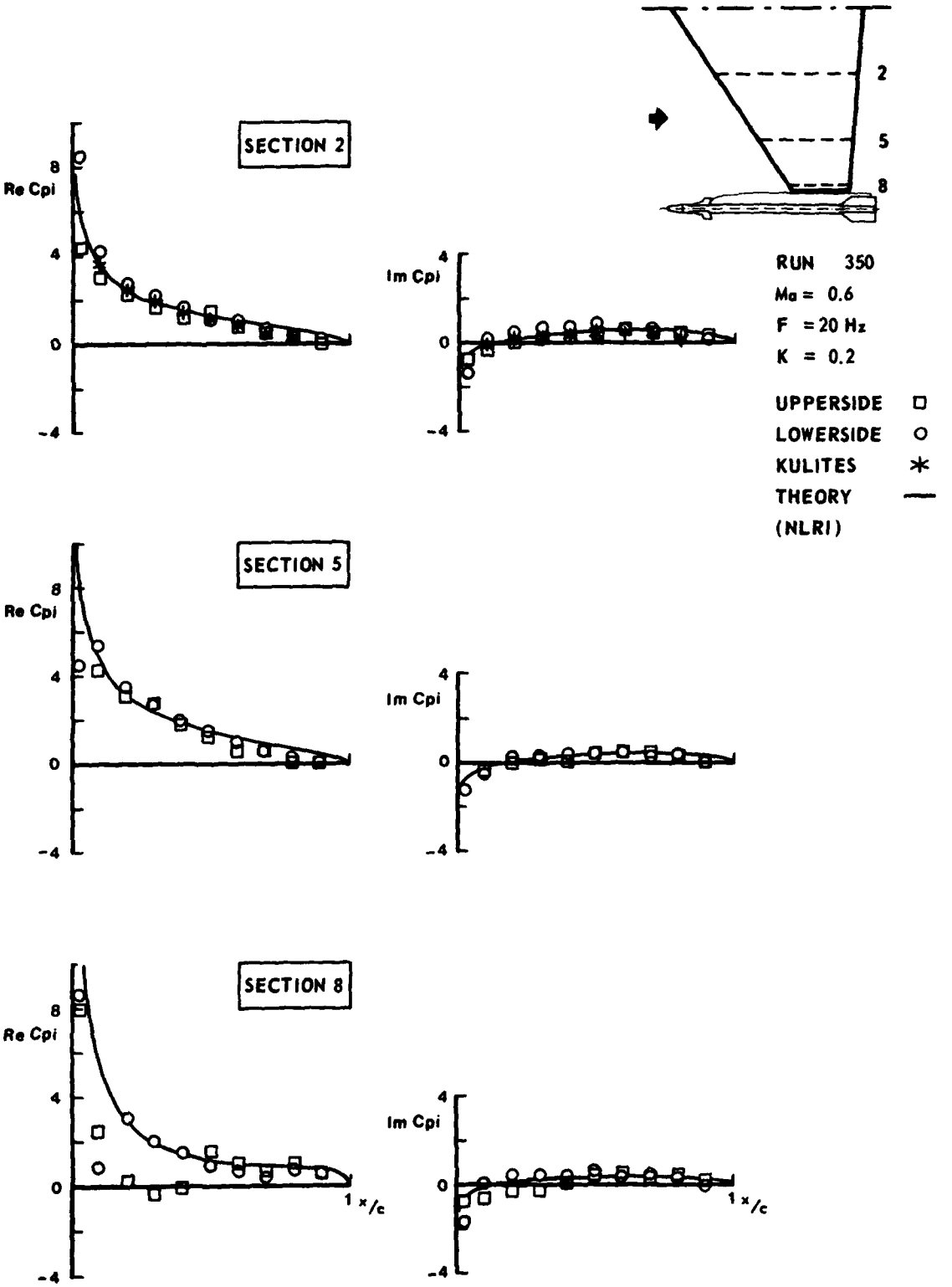

Fig. 14 Comparison of experimental and theoretical (NLRI-method) unsteady pressure distributions on the wing with complete tipstore at Ma = 0.6

M_∞ = 0.4	EXP.	THEORY	CONFIGURATION
F = 20 Hz	○	—— DL	CLEAN WING
K = 0.2	+	---NLR1	WING + TIPSTORE

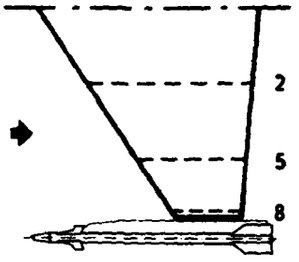

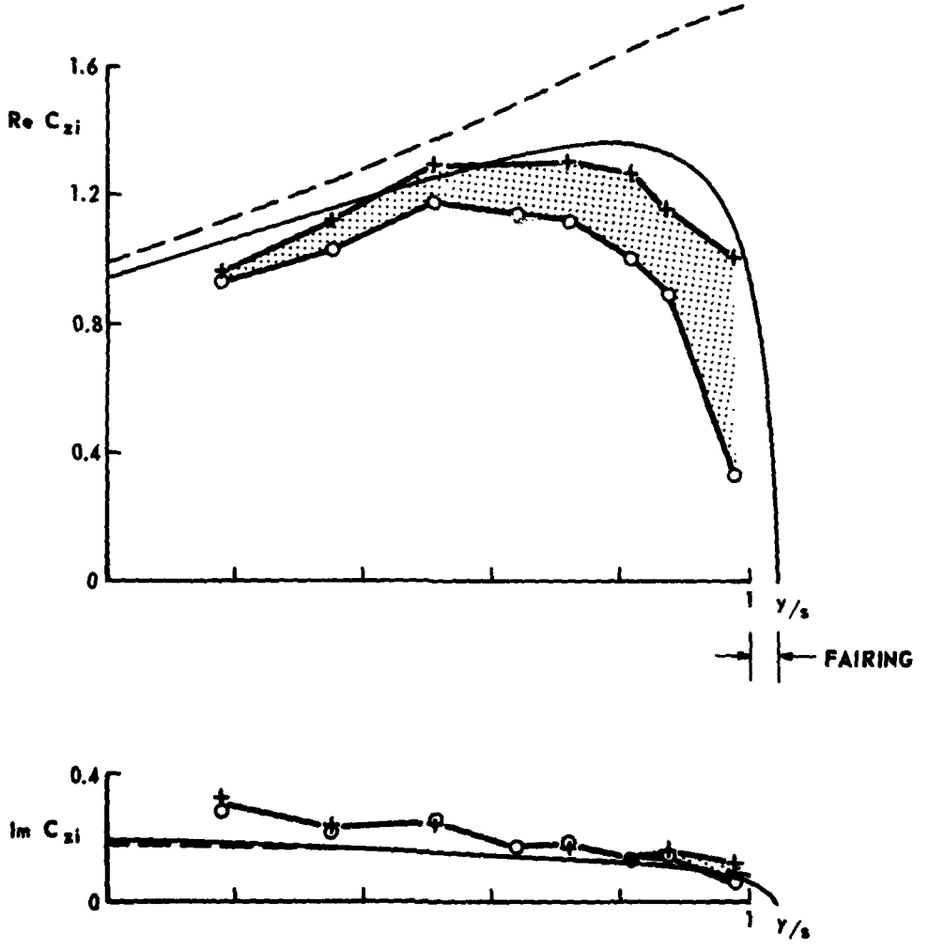

Fig. 15 Comparison of experimental and theoretical unsteady spanwise normal load distributions for the clean wing and the wing with complete tipstore at Ma = 0.6

NUMBER OF PANELS	
WING	117
CANARD FINS	24
AFT WINGS	80
LAUNCHER - MISSILE BODY	34
TOTAL	255

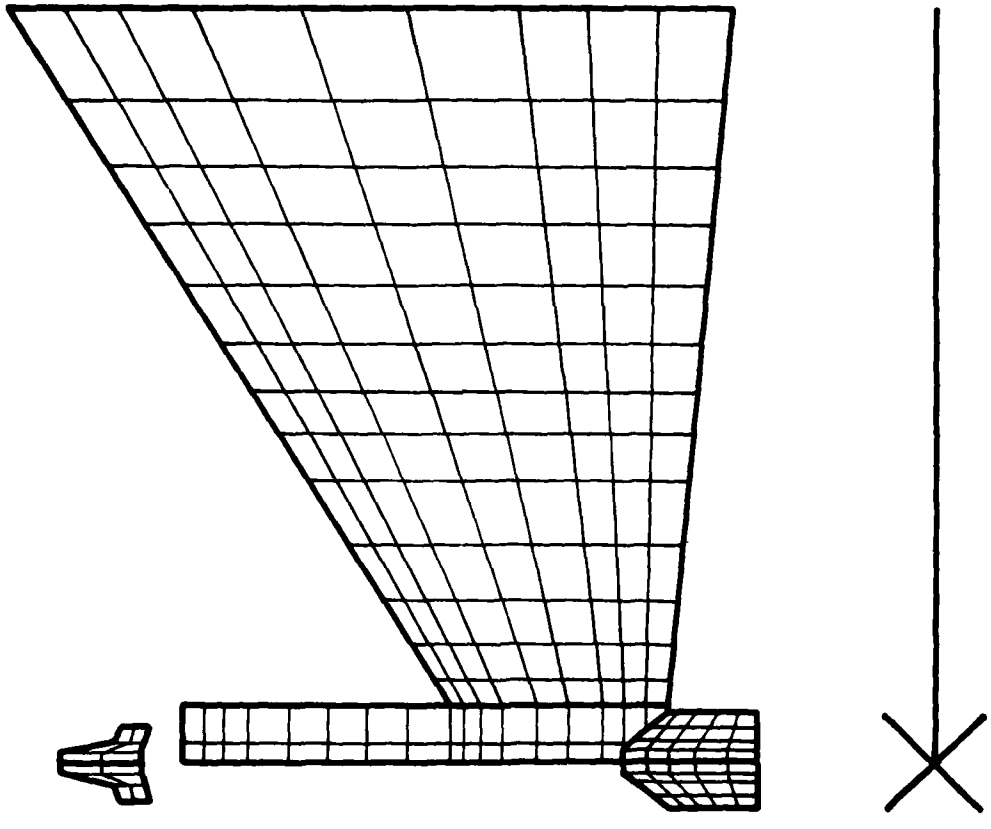

Fig. 16 Panel distribution used in calculations with the Doublet Lattice Method

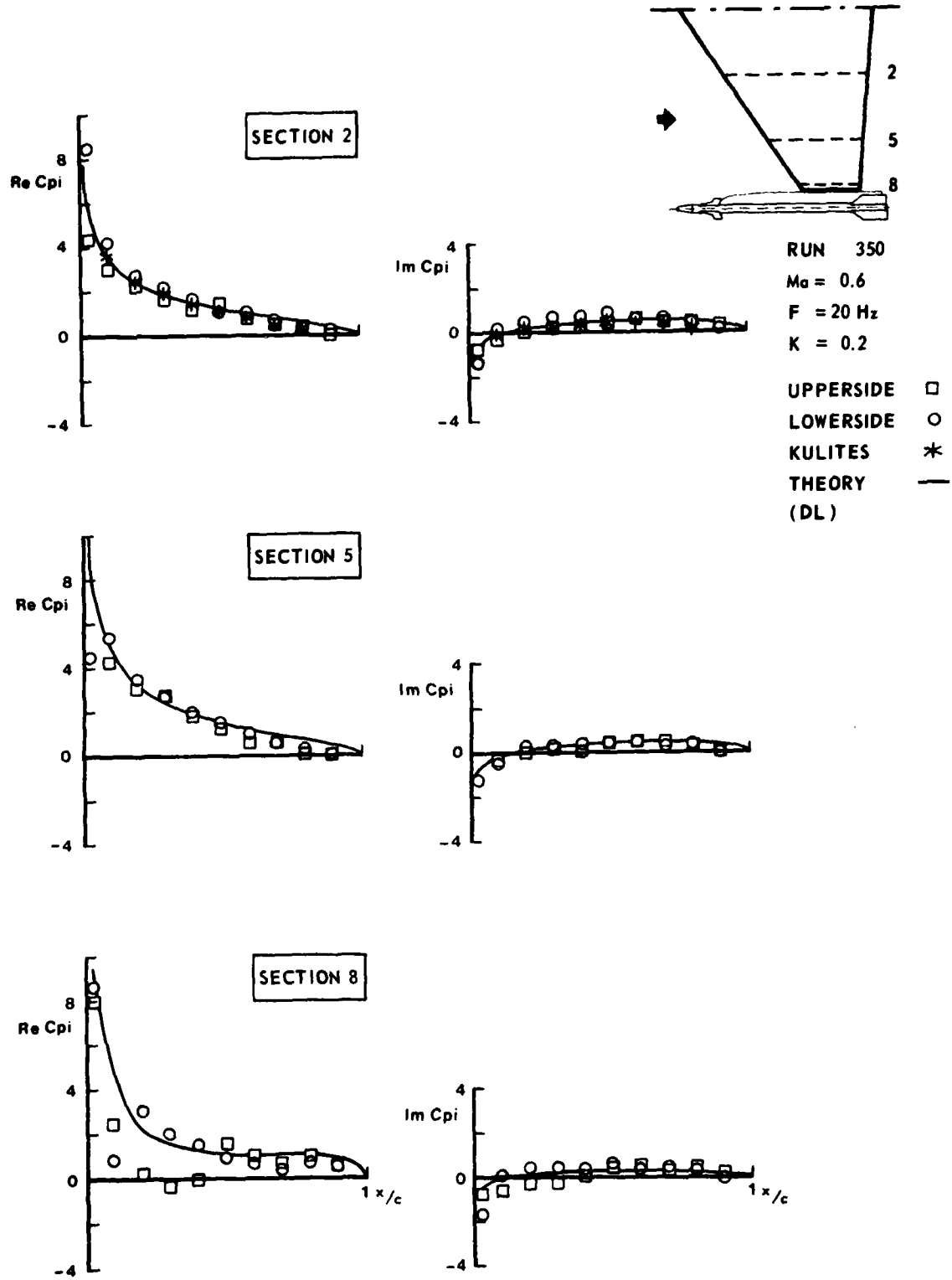

Fig. 17 Comparsion of experimental and theoretical (D.L. method) unsteady pressure distributions on the wing with complete tipstore at Ma = 0.6

Ma = 0.6	EXP.	THEORY	CONFIGURATION
F = 20 Hz	○	—— DL	CLEAN WING
K = 0.2	+	- - - NLR1 -·- DL	WING + TIPSTORE

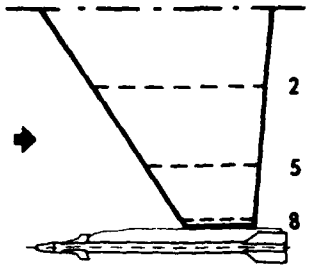

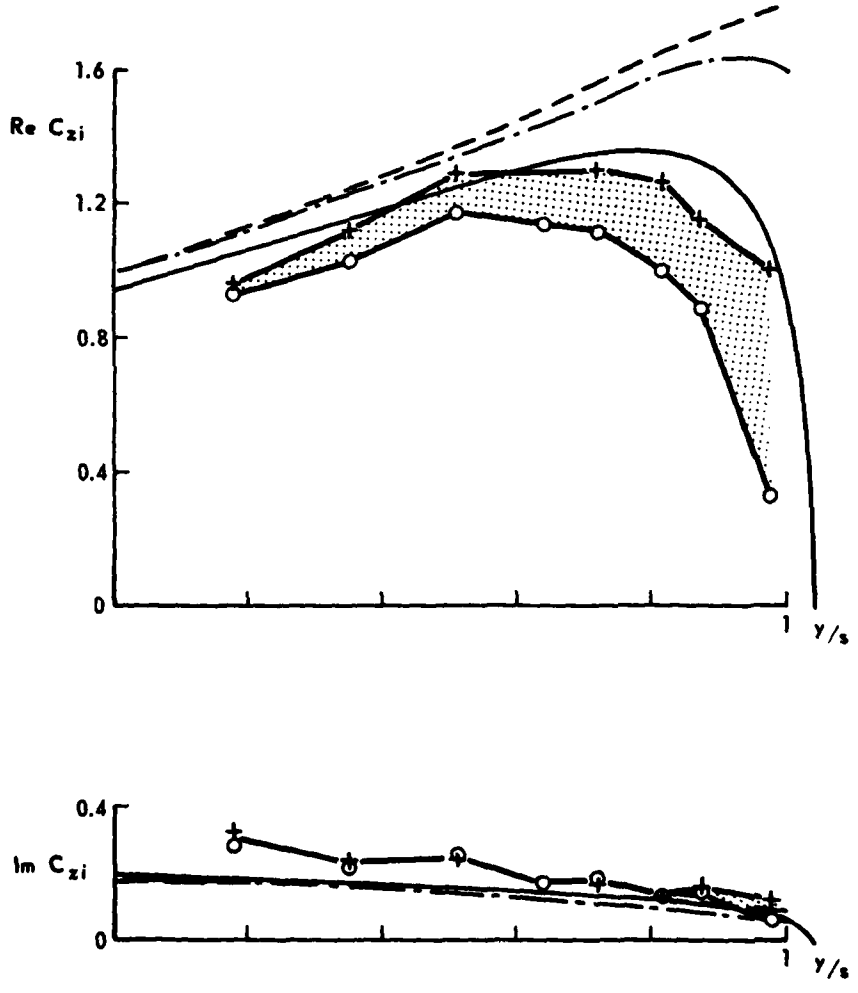

Fig. 18 Comparison of experimental and theoretical unsteady spanwise normal load distributions for the clean wing and the wing with complete tipstore at Ma = 0.6

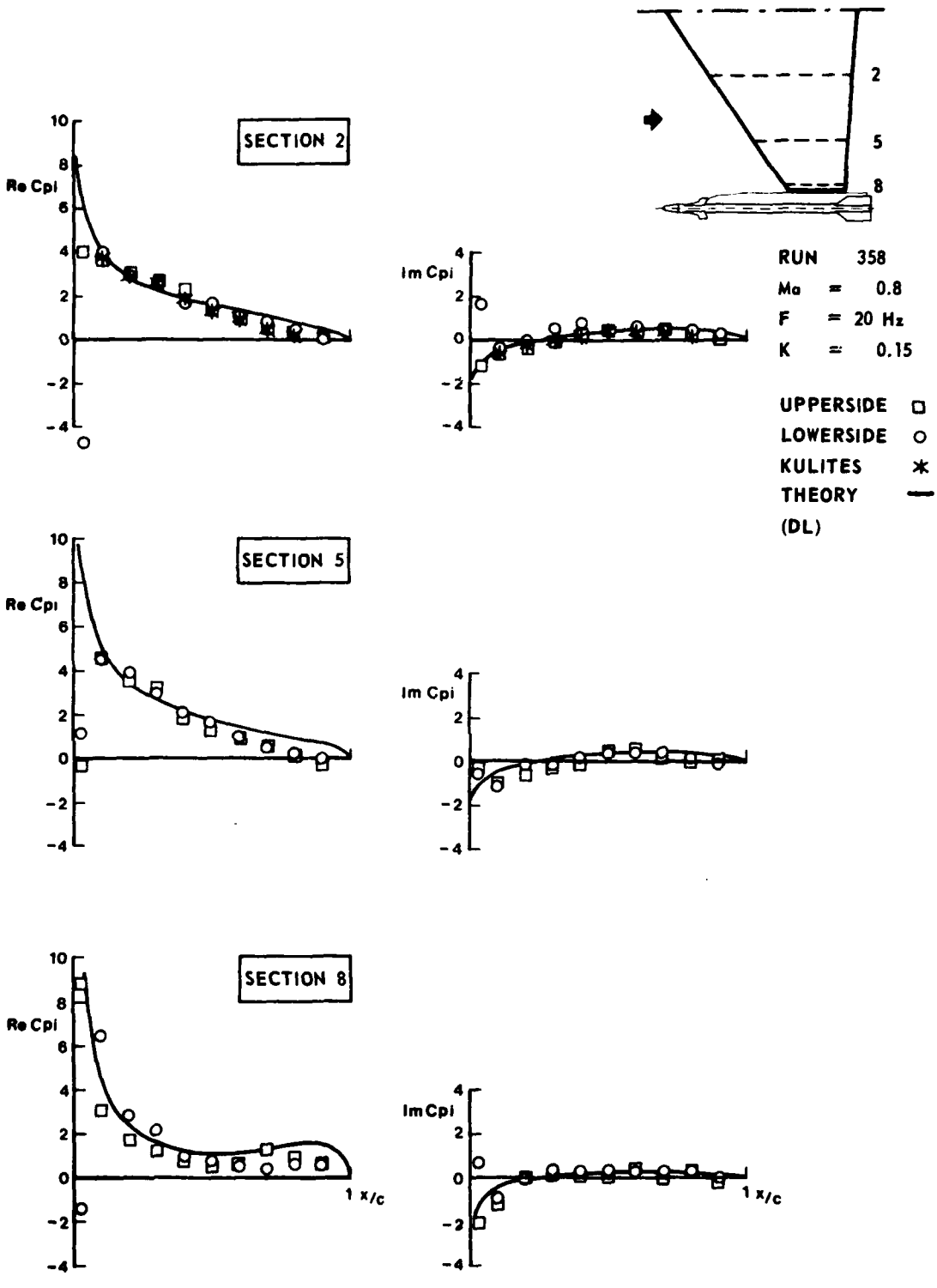

Fig. 19 Comparison of experimental and theoretical (D.L. method) unsteady pressure distributions on the wing with complete tipstore at Ma = 0.8

APPENDIX III.A

Definitions of Steady and Unsteady Aerodynamic Quantities*)

THE WING

Steady

Pressure coefficient C_p:

$$C_p = (P_{loc} - P)/Q \ .$$

Sectional normal force:

$$Z = C_z QC \ , \ C_z = - \int_0^1 (C_{p+} - C_{p-}) \ d(x/C) \ .$$

Sectional pitching moment about quarter chord point (positive nose down):

$$M = C_m QC^2 \ , \ C_m = - \int_0^1 (C_{p+} - C_{p-}) \ (x/C - 0.25) \ d(x/C) \ .$$

Quasi-steady at zero incidence ($\omega = 0$; $\alpha_o = 0^0$)

Pressure coefficient C_{pq}:

$$C_{pq} = \Delta C_p/\Delta\alpha = \frac{C_p \ (\alpha_o + \Delta\alpha_1) - C_p(\alpha_o - \Delta\alpha_2)}{\Delta\alpha_1 + \Delta\alpha_2} \ .$$

Sectional normal force:

$$Z_q = \pi QCC_{zq}\theta e^{i\omega t} \ , \ C_{zq} = \frac{1}{\pi} \Delta C_z/\Delta\alpha = \frac{1}{\pi} \frac{C_z \ (\alpha_o + \Delta\alpha_1) - C_z \ (\alpha_o - \Delta\alpha_2)}{\Delta\alpha_1 + \Delta\alpha_2} \ .$$

Sectional pitching moment (positive nose down):

$$M_q = \frac{\pi}{2} QC^2 C_{mq}\theta e^{i\omega t} \ , \ C_{mq} = \frac{2}{\pi} \Delta C_m/\Delta\alpha = \frac{2}{\pi} \frac{C_m(\alpha_o + \Delta\alpha_1) - C_m(\alpha_o - \Delta\alpha_2)}{\Delta\alpha_1 + \Delta\alpha_2} \ .$$

---

*)The definitions for the unsteady aerodynamic quantities are according to the AGARD Manual on Aeroelasticity Vol. VI (Ref. 6).

Unsteady

Pressure coefficient C_{pi}:

$$C_{pi} = ReC_{pi} + iImC_{pi} = P_i/Q\theta \ .$$

Sectional normal force:

$$Z_i = \pi QCC_{zi}\theta e^{i\omega t} \ , \ C_{zi} = ReC_{zi} + iImC_{zi} = -\frac{1}{\pi}\int_o^1 (C_{pi+} - C_{pi-})\, d(x/C) \ .$$

Sectional pitching moment about quarter chord point (positive nose down):

$$M_i = \frac{\pi}{2} QC^2 C_{mi}\theta e^{i\omega t} \ ,$$

$$C_{mi} = ReC_{mi} + iImC_{mi} = -\frac{2}{\pi}\int_o^1 (C_{pi+} - C_{pi-})\,(x/C - 0.25)\, d(x/C) \ .$$

THE STORE

Steady

Normal force:

$$Z = C_Z Q\bar{C}S \ .$$

Pitching moment about balance centre (positive nose up):

$$M = C_M Q\bar{C}^2 S \ .$$

Quasi-steady at zero incidence ($\omega = 0$; $\alpha_o = 0^0$)

Normal force:

$$Z_q = \pi Q\bar{C}SC_{Zq}\theta e^{i\omega t} \ ,$$

$$C_{Zq} = \frac{1}{\pi}\Delta C_Z/\Delta\alpha = \frac{1}{\pi}\frac{C_Z(\alpha_o + \Delta\alpha_1) - C_Z(\alpha_o - \Delta\alpha_2)}{\Delta\alpha_1 + \Delta\alpha_2} \ .$$

Pitching moment about balance centre (positive nose up):

$$M_q = \frac{\pi}{2} Q\bar{C}^2 SC_{Mq}\theta e^{i\omega t}$$

$$C_{Mq} = \frac{2}{\pi}\Delta C_M/\Delta\alpha = \frac{2}{\pi}\frac{C_M(\alpha_o + \Delta\alpha_1) - C_M(\alpha_o - \Delta\alpha_2)}{\Delta\alpha_1 + \Delta\alpha_2} \ .$$

Unsteady

Normal force:

$$Z_i = \pi Q \bar{C} S C_{Zi} \theta e^{i\omega t} \quad , \quad C_{Zi} = ReC_{Zi} + iImC_{Zi} \ .$$

Pitching moment about balance centre (positive nose up):

$$M_i = \frac{\pi}{2} Q \bar{C}^2 S C_{Mi} \theta e^{i\omega t} \quad , \quad C_{Mi} = ReC_{Mi} = iImC_{Mi} \ .$$

APPENDIX III.B

Steady Pressure Distributions*)

Wing + Tiplauncher (Conf. 1)

Run No.	Nominal Ma	Nominal α (degrees)	Nominal $P_o \times 10^{-5}$ (Pa)	Fig. No.
197	0.6	-0.5	1.0	III.B. 1
198		0		2
199		+0.5		3
206	0.9	-0.5		III.B. 4
208		0		5
209		+0.5		6
212	1.10	-0.5		III.B. 7
213		0		8
214		+0.5	1.0	9
223	1.10	-0.5	0.7	III.B.10
224		0		11
225		+0.5		12
217	1.35	-0.5		III.B.13
218		0		14
220		+0.5	0.7	15

*) Note that in sections 3 and 5 the first point on the upperside showing a zero value is a faulty pressure point, which should not be considered in any evaluation.

Wing + Tiplauncher + Missile Body (Conf. 2)

Run No.	Nominal Ma	Nominal α (degrees)	Nominal P_o x 10^{-5} (Pa)	Fig. No.
255	0.6	-0.5	1.0	III.B.16
256		0		17
257		+0.5		18
249	0.9	-0.5		III.B.19
251		0		20
252		+0.5		21
244	1.10	-0.5		III.B.22
245		0		23
246		+0.5	1.0	24
233	1.35	-0.5	0.7	III.B.25
234		0	0.7	26
235		+0.5	0.7	27

Wing + Tiplauncher + Missile Body + Aft Wings (Conf. 3)

Run No.	Nominal Ma	Nominal α (degrees)	Nominal P_o x 10^{-5} (Pa)	Fig. No.
285	0.6	-0.5	1.0	III.B.28
286		0		29
287		+0.5		30
280	0.9	-0.5		III.B.31
281		0		32
282		+0.5		33
274	1.10	-0.5		III.B.34
275		0		35
276		+0.5	1.0	36
269	1.10	-0.5	0.7	III.B.37
270		0		38
271		+0.5		39
264	1.35	-0.5		III.B.40
265		0		41
266		+0.5	0.7	42

Wing + Tiplauncher + Complete Missile (Conf. 4)

Run No.	Nominal Ma	Nominal α (degrees)	Nominal $P_o \times 10^{-5}$ (Pa)	Fig. No.
340	0.6	-0.5	1.0	III.B.43
341		0		44
342		+0.5		45
333	0.7	-0.5		III.B.46
334		0		47
335		+0.5		48
326	0.8	-0.5		III.B.49
327		0		50
328		+0.5		51
319	0.9	-0.5		III.B.52
320		0		53
321		+0.5		54
312	1.10	-0.5		III.B.55
313		0		56
314		+0.5	1.0	57
303	1.10	-0.5	0.7	III.B.58
306		0		59
307		+0.5		60
295	1.35	-0.5		III.B.61
297		0		62
298		+0.5	0.7	63

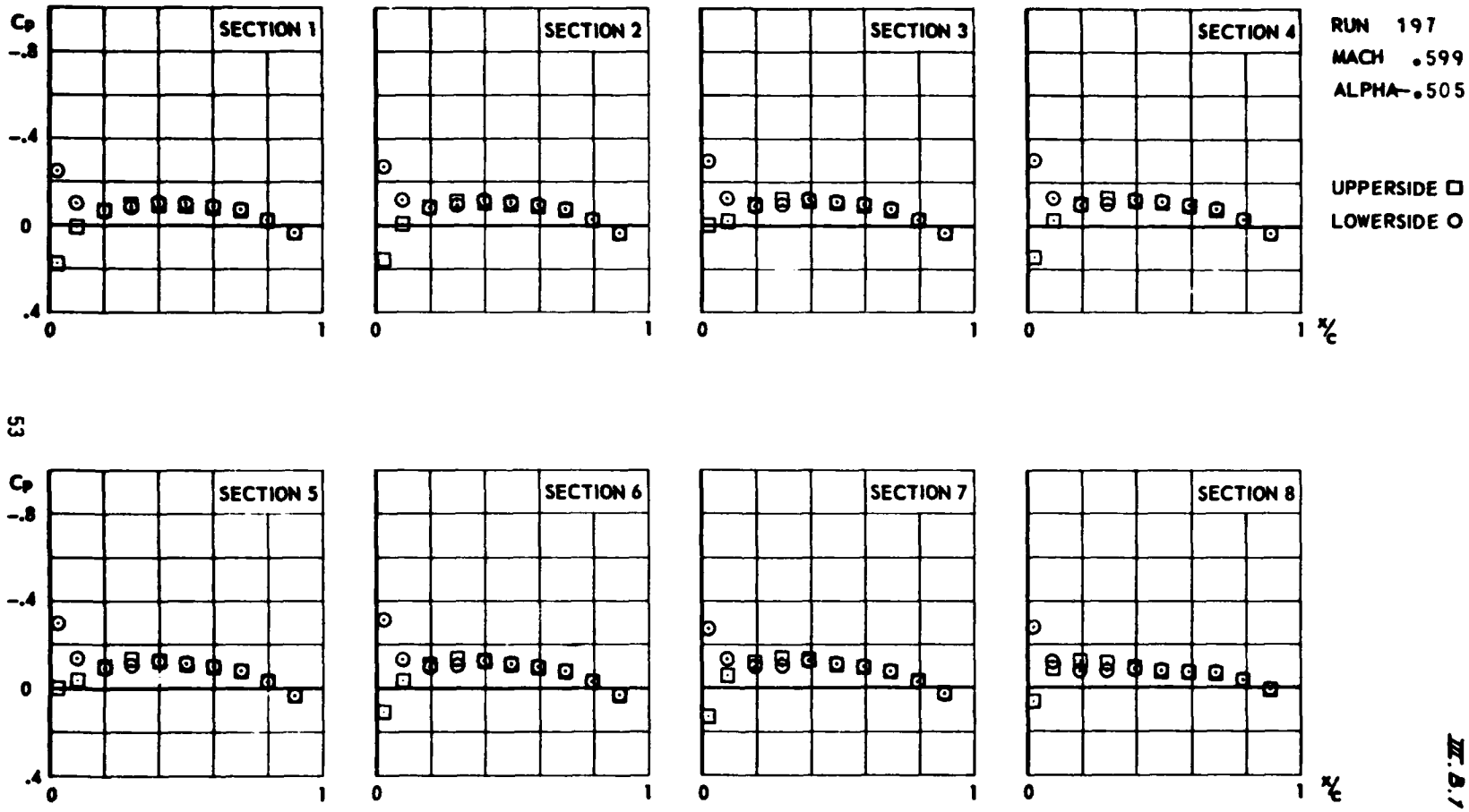

CONF.1 (WING + TIPLAUNCHER)

FIG. III.B.1

53

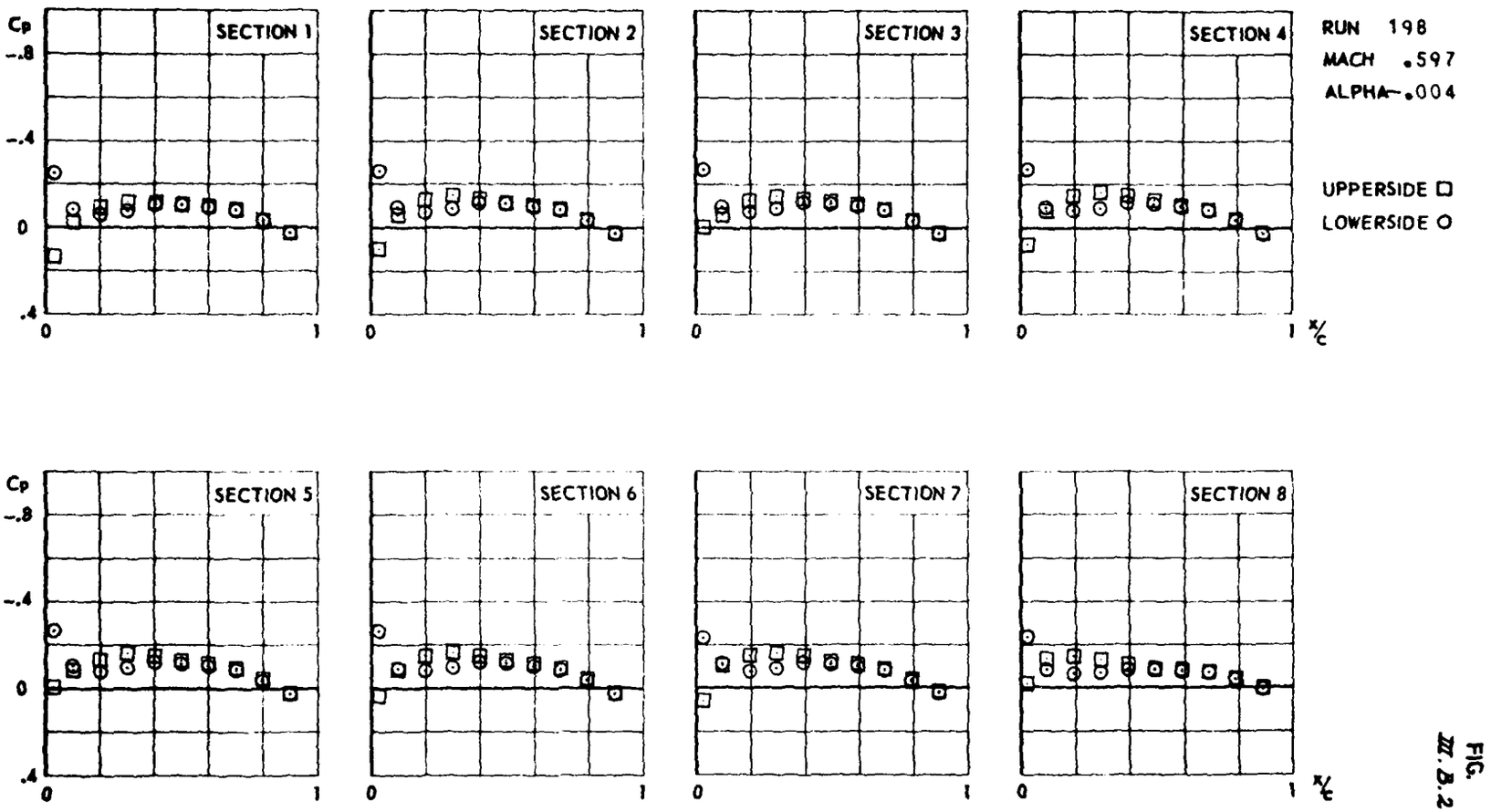

CONF.1 (WING + TIPLAUNCHER)

FIG. III.B.2

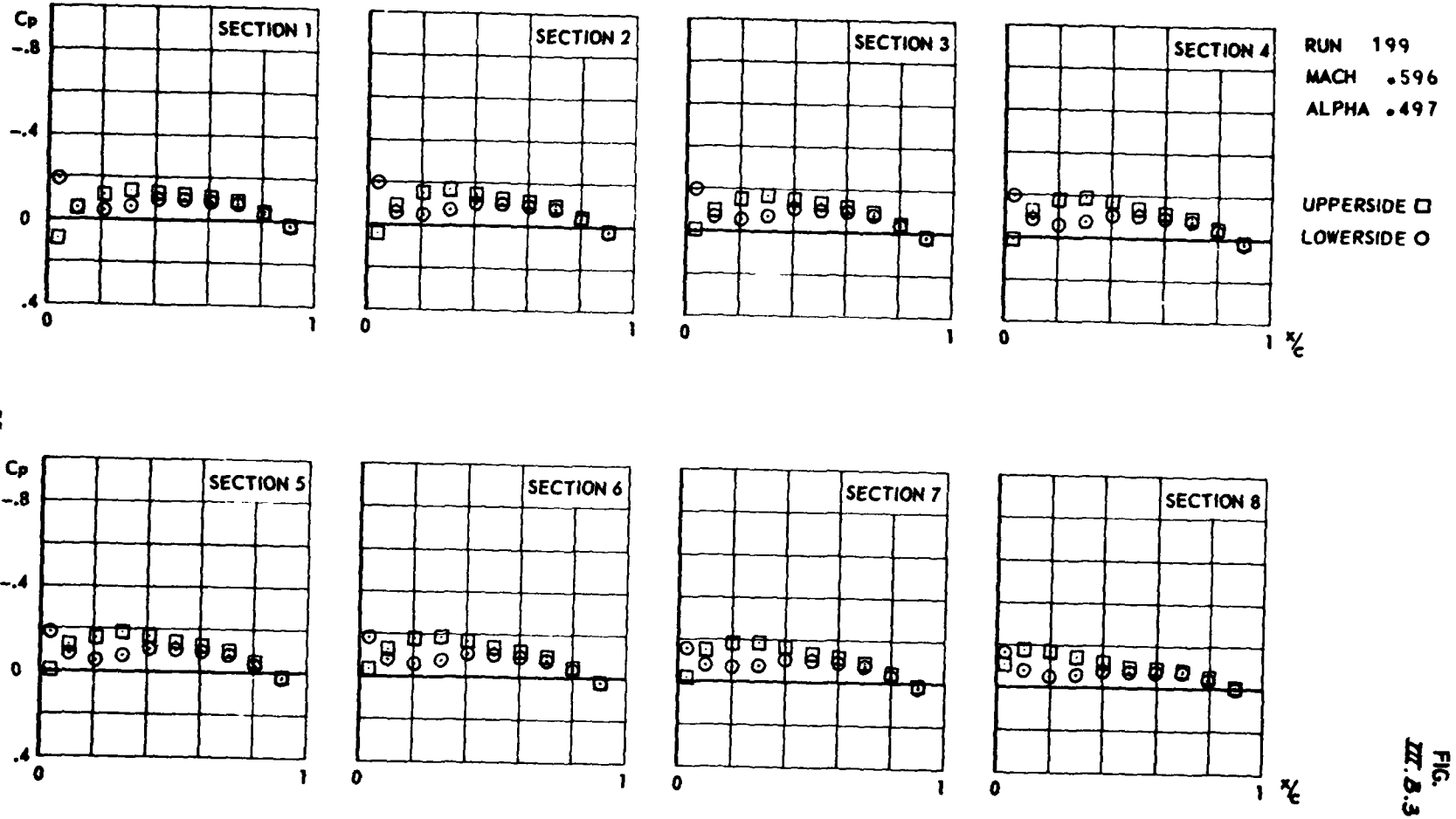

CONF.1 (WING + TIPLAUNCHER)

FIG. III.B.3

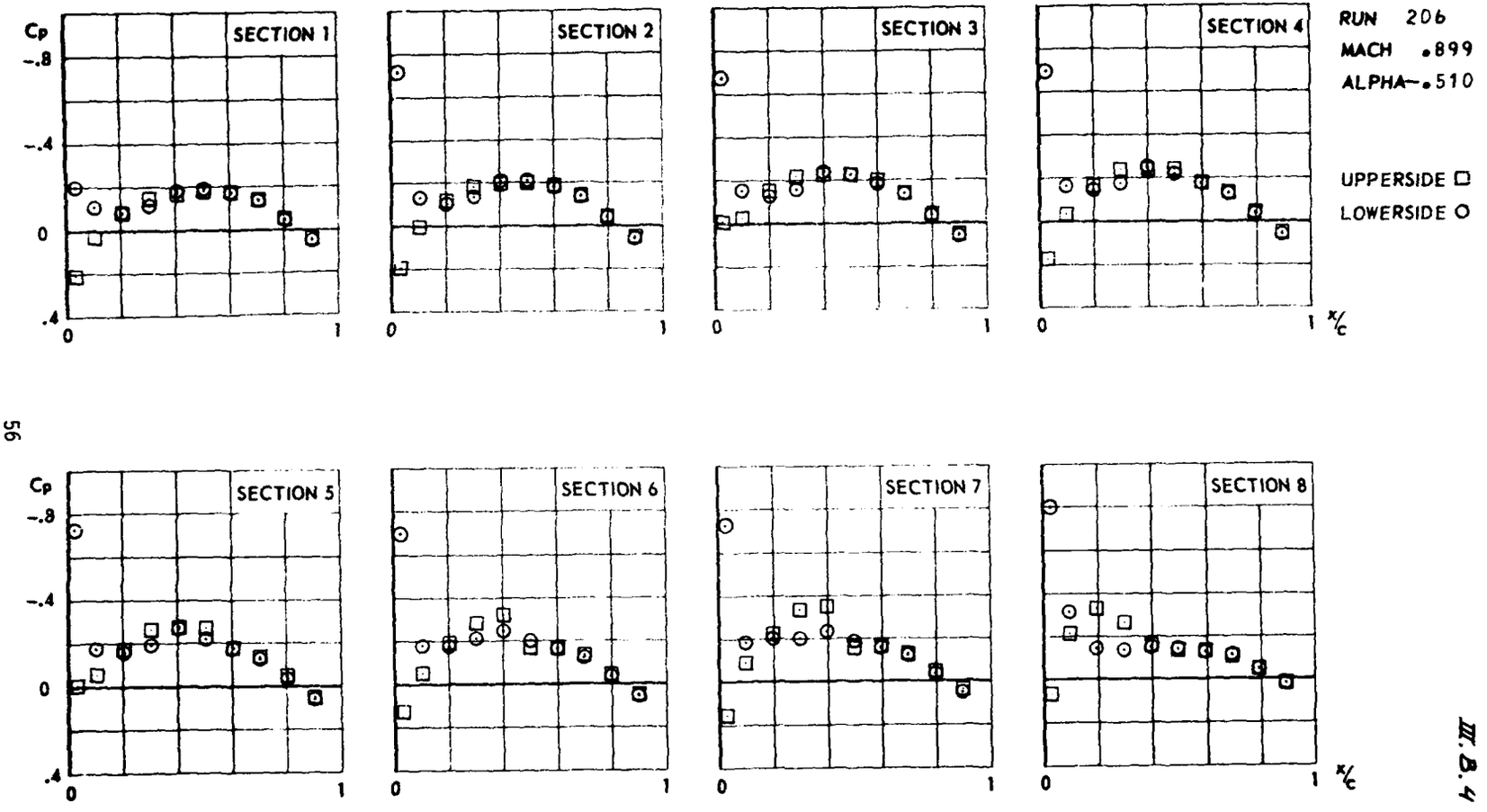

CONF.1 (WING + TIPLAUNCHER)

FIG. III.B.4

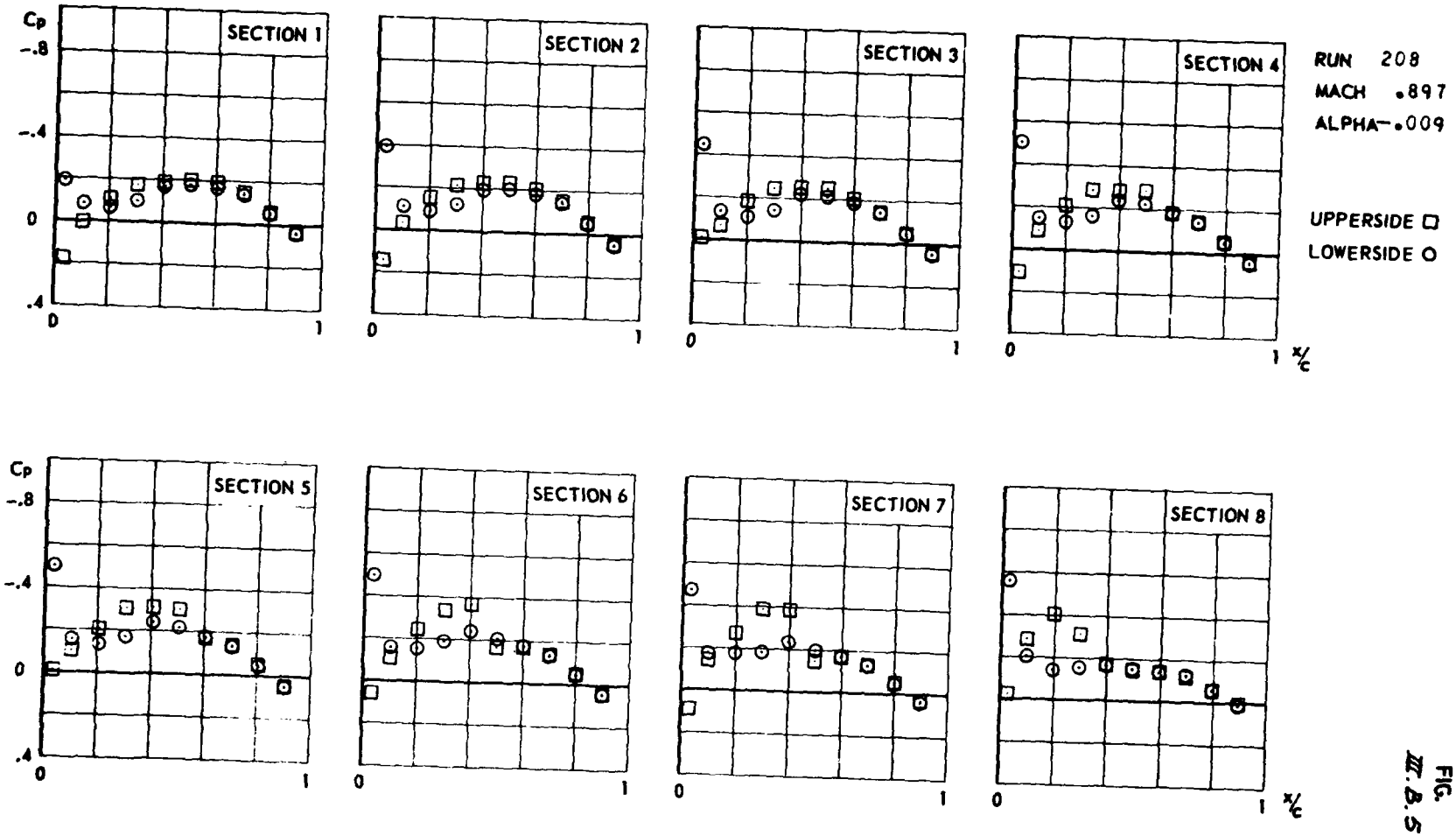

CONF.1 (WING + TIPLAUNCHER)

FIG. III.B.5

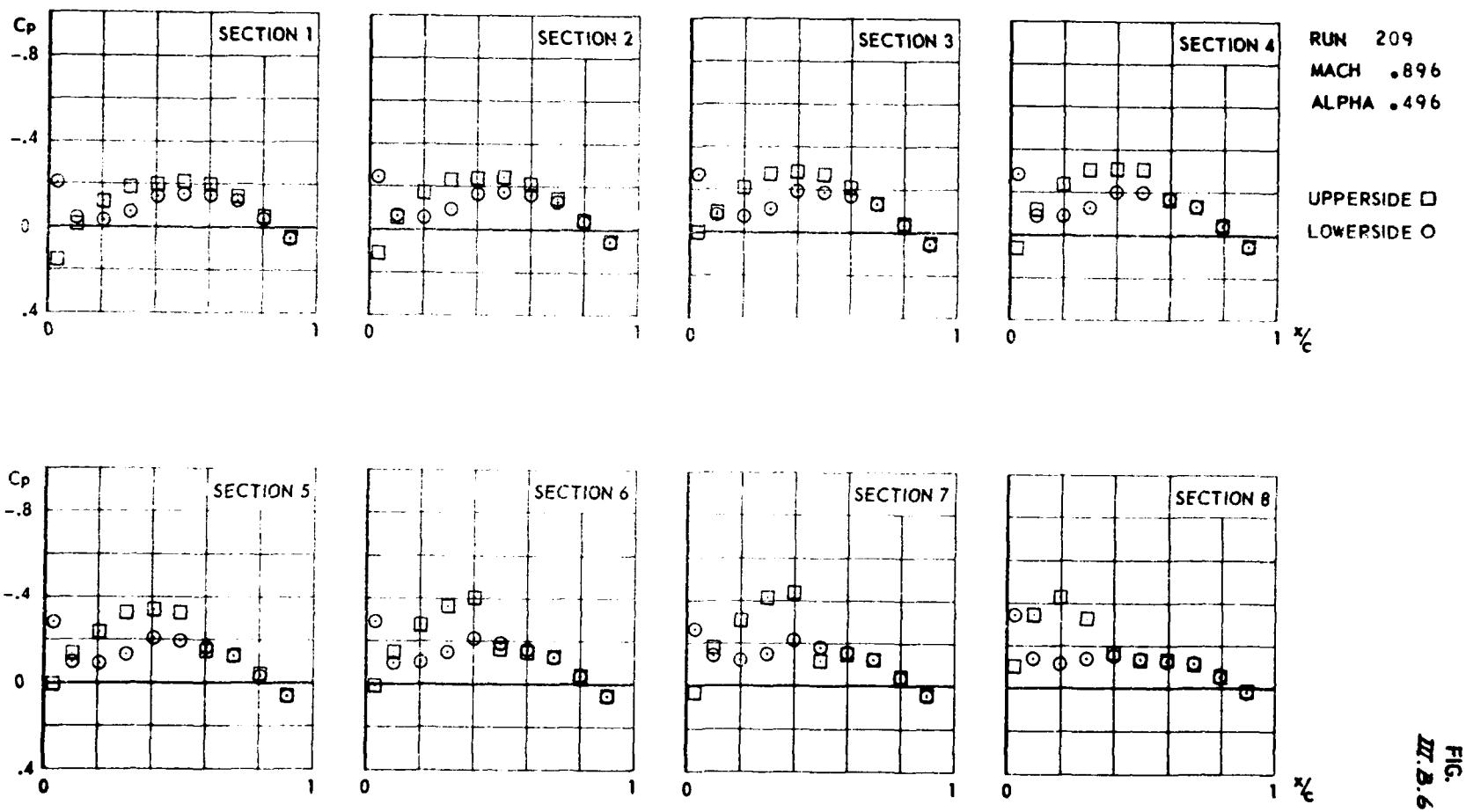

CONF.1 (WING + TIPLAUNCHER)

FIG. III.B.6

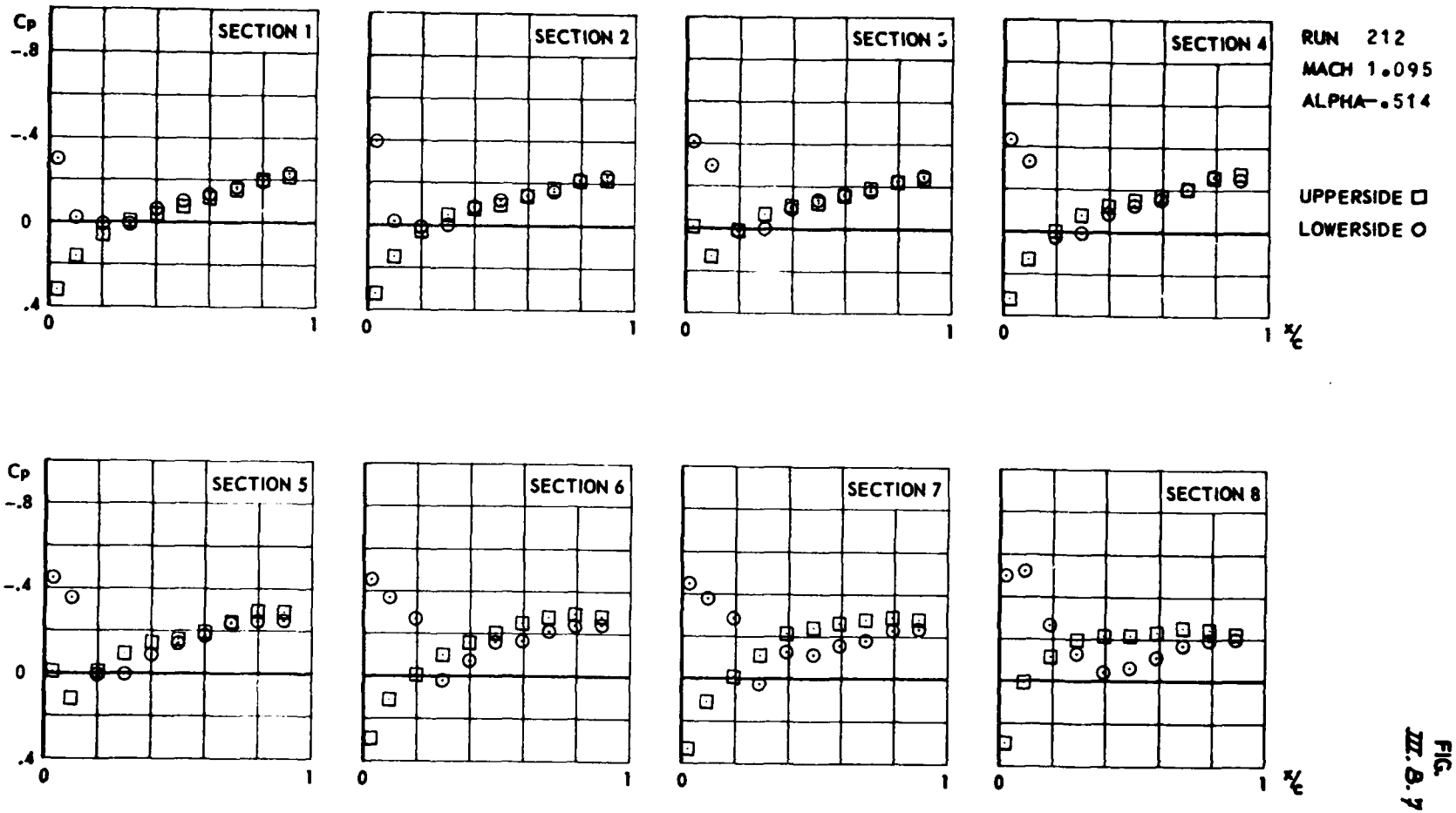

CONF.1 (WING + TIPLAUNCHER)

FIG. III.B.7

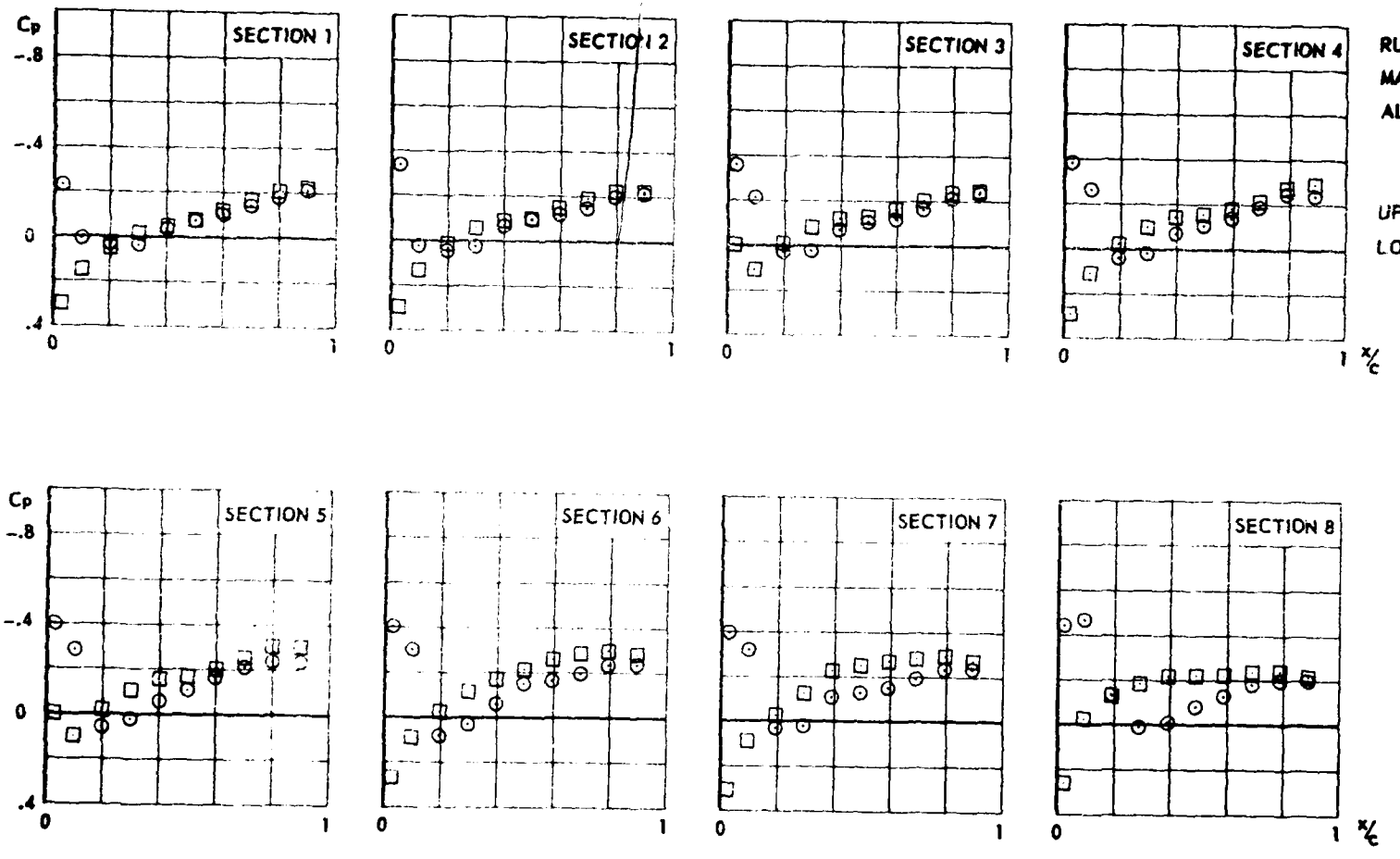

CONF.1 (WING + TIPLAUNCHER)

FIG. III.B.8

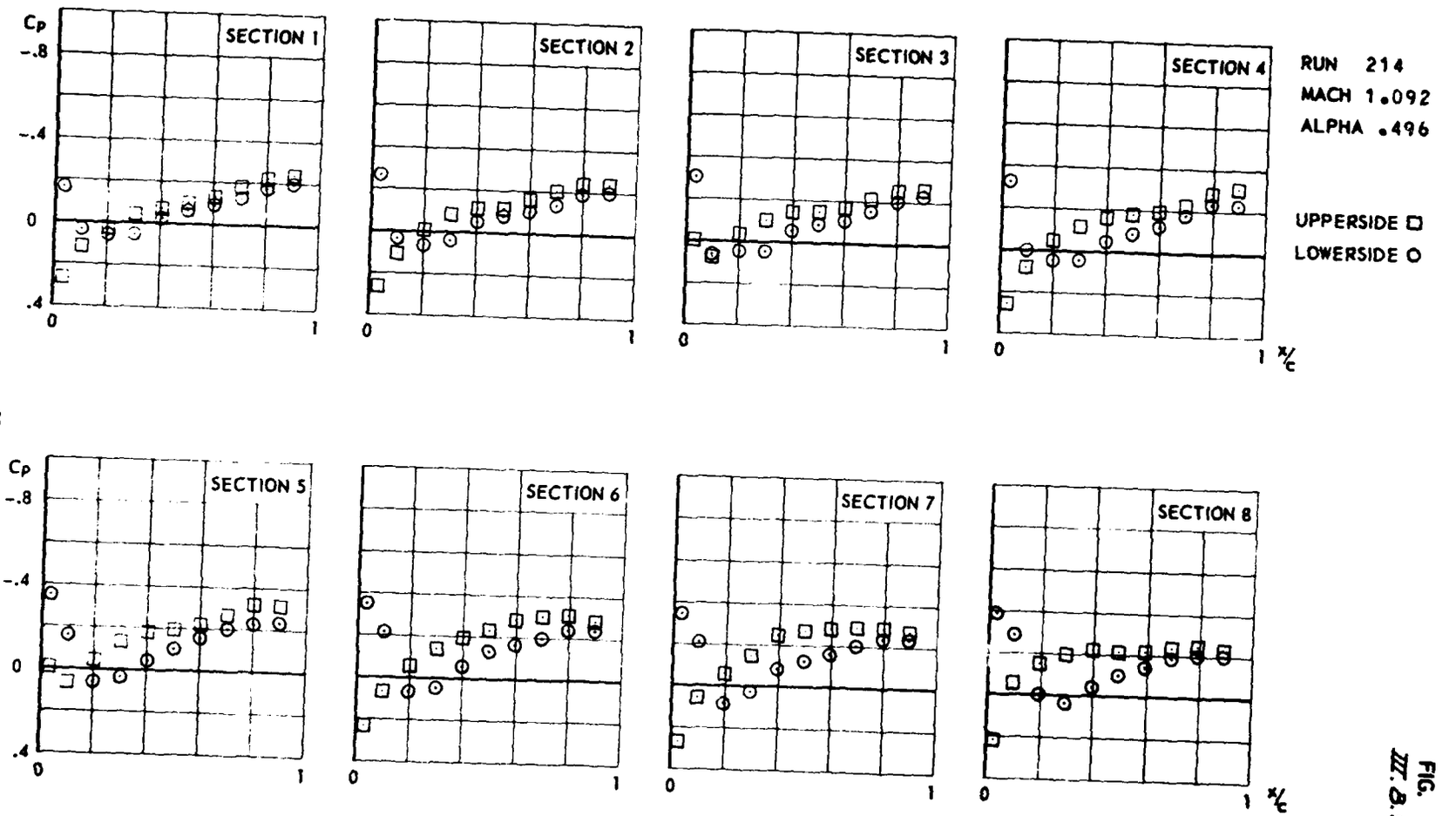

CONF.1 (WING + TIPLAUNCHER)

FIG. III.B.9

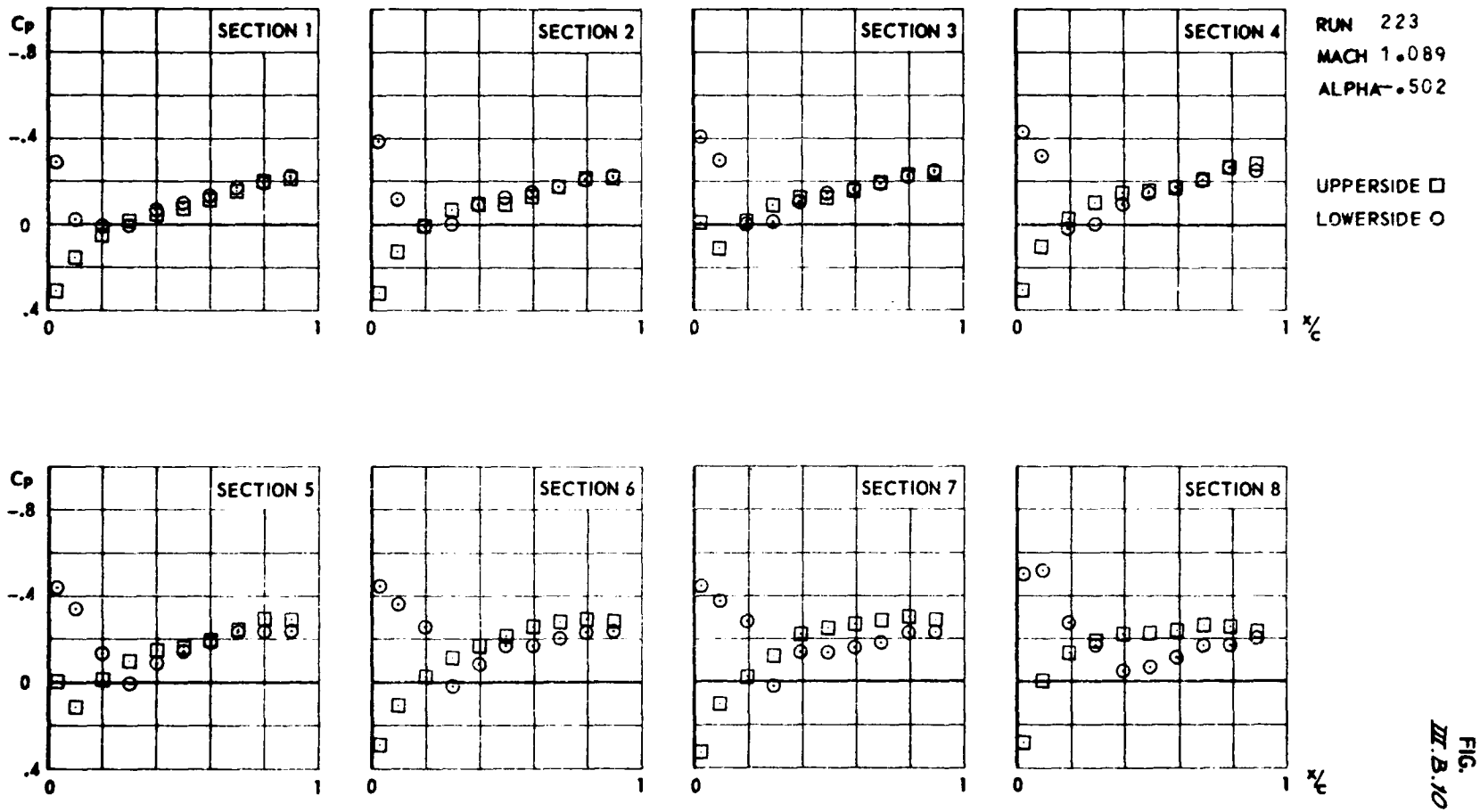

CONF.1 (WING + TIPLAUNCHER)

FIG. III.B.10

FIG.
III.B.11

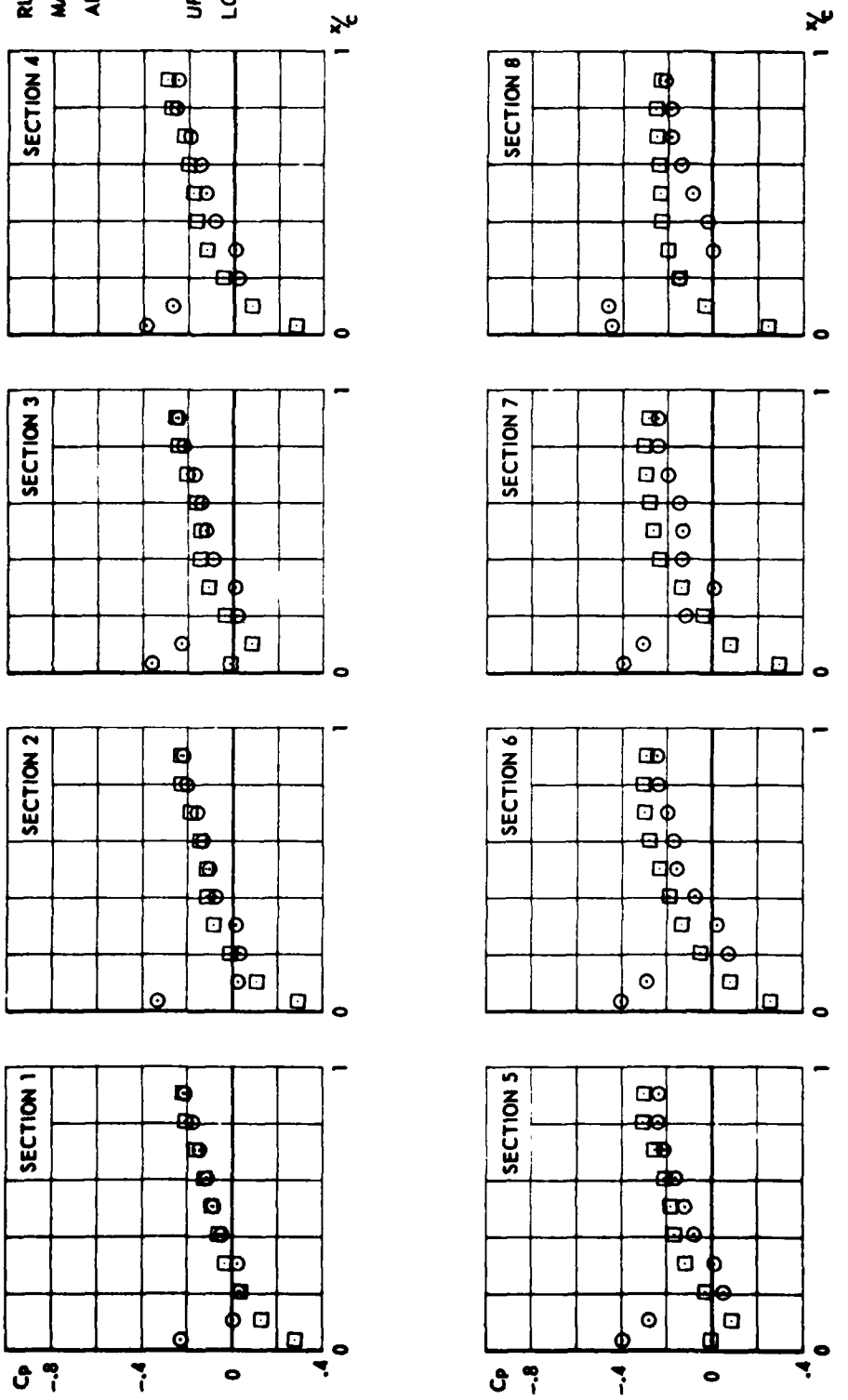

CONF.1 (WING + TIPLAUNCHER)

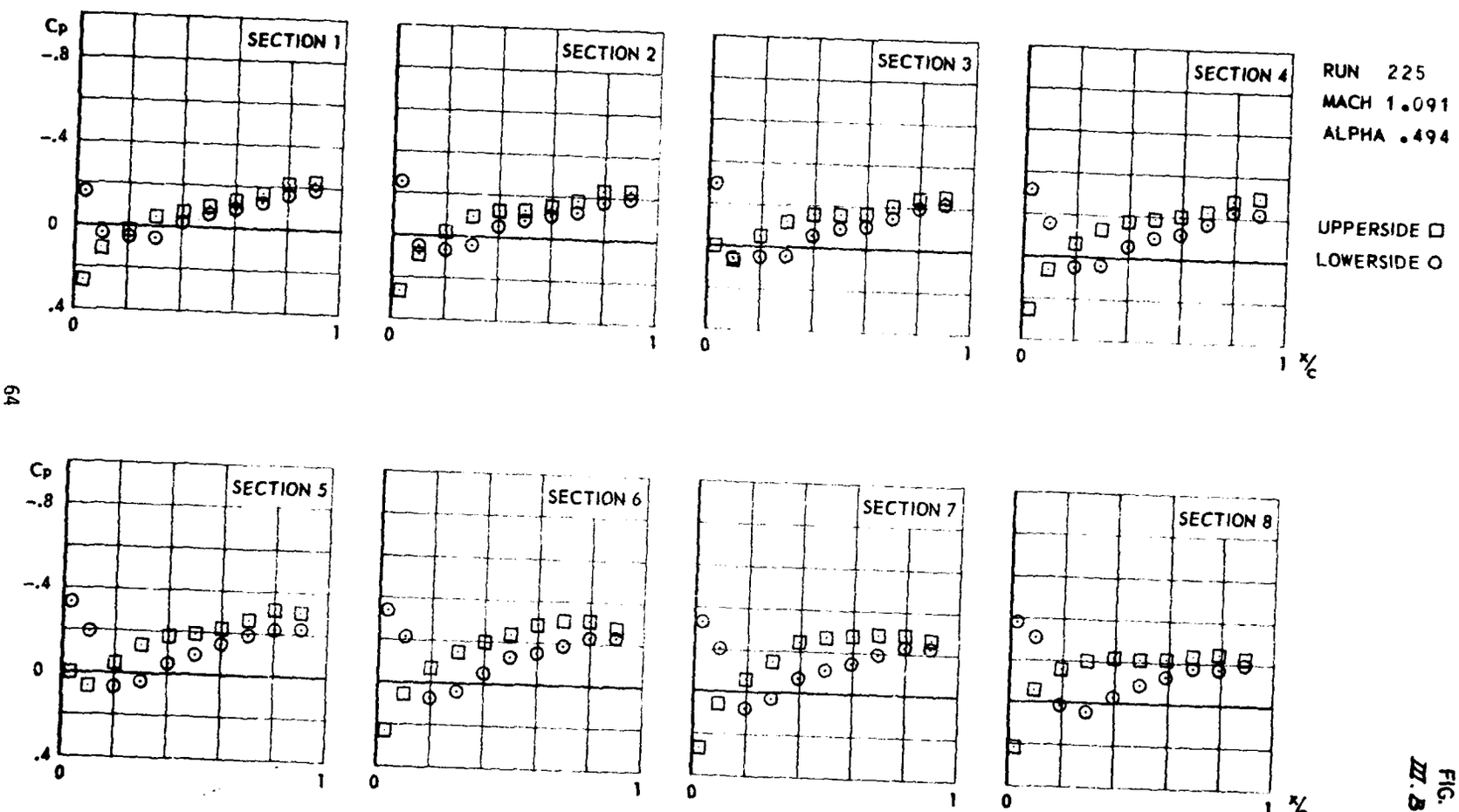

CONF.1 (WING + TIPLAUNCHER)

FIG. 77.B.12

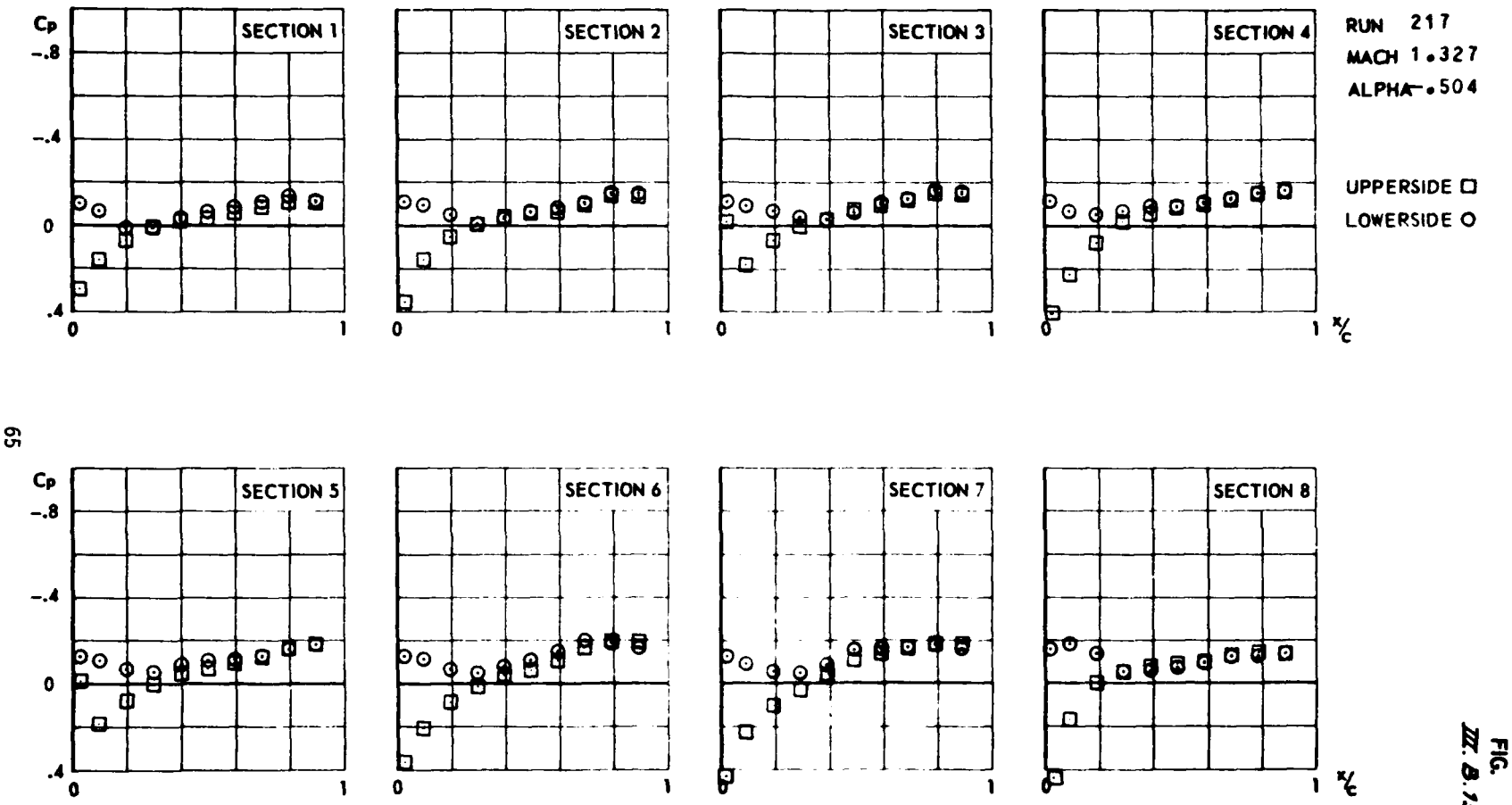

CONF.1 (WING + TIPLAUNCHER)

FIG. ZZ.8.13

FIG.
III.B.14

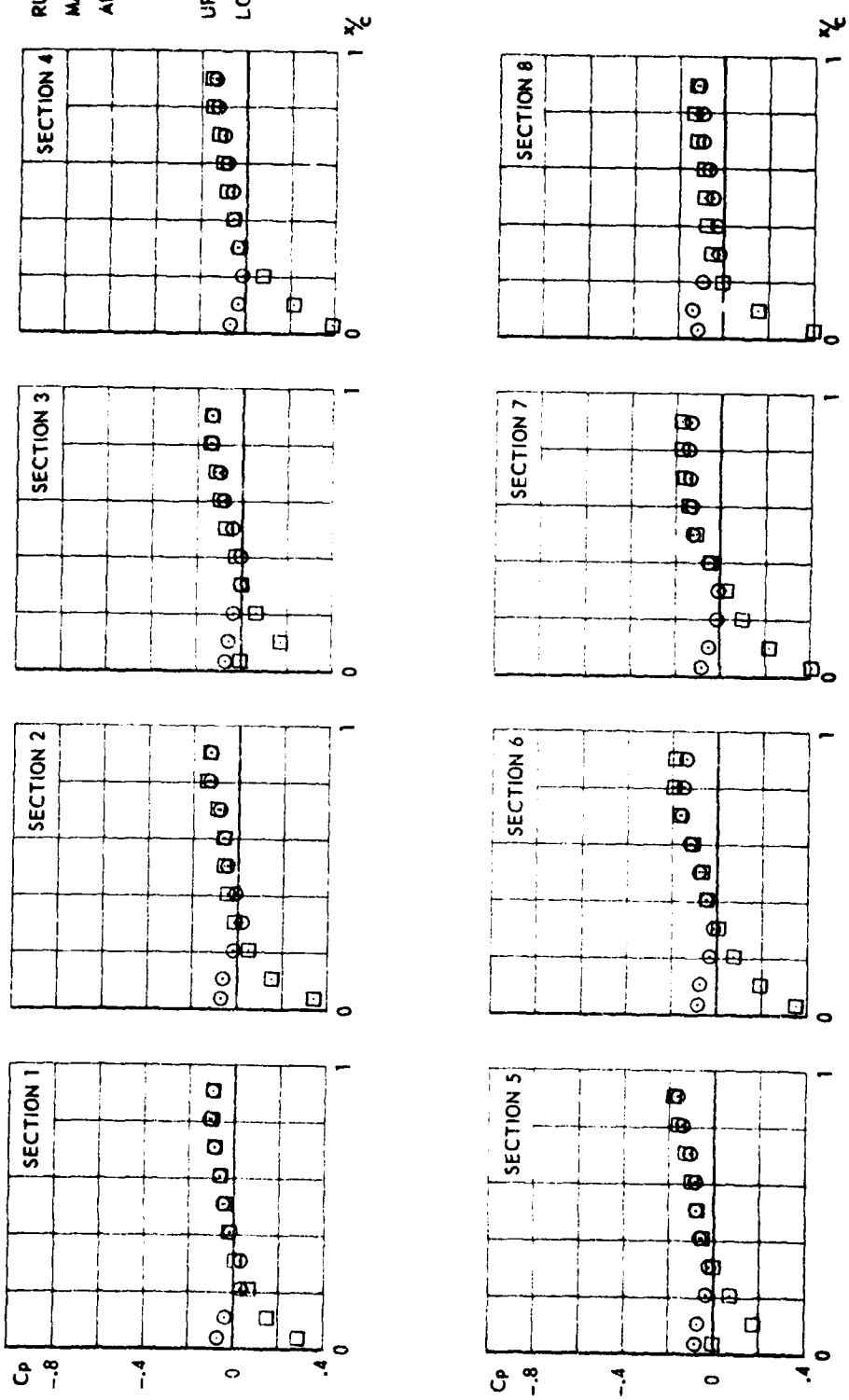

CONF.1 (WING + TIPLAUNCHER)

FIG.
III.B.15

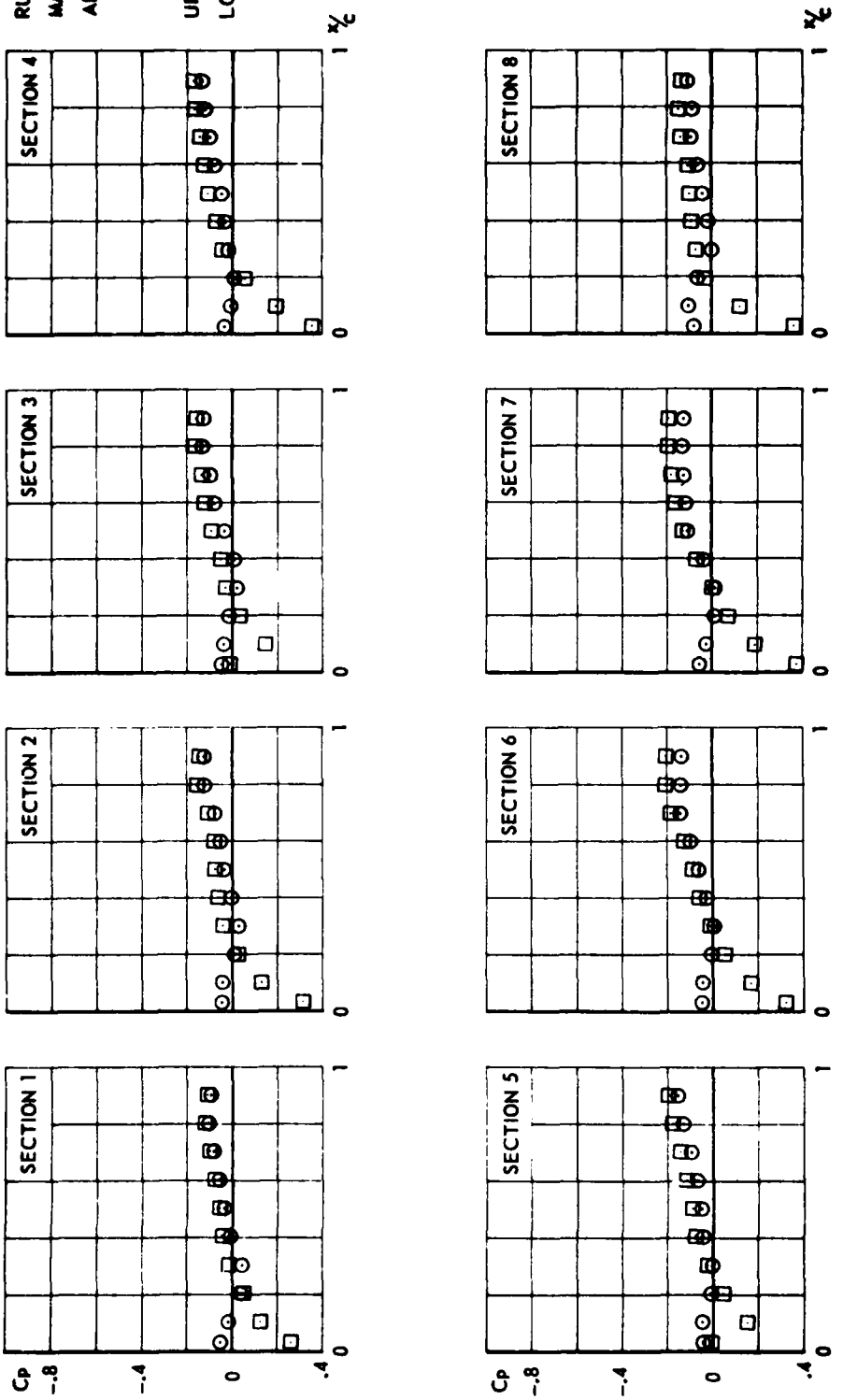

CONF.1 (WING + TIPLAUNCHER)

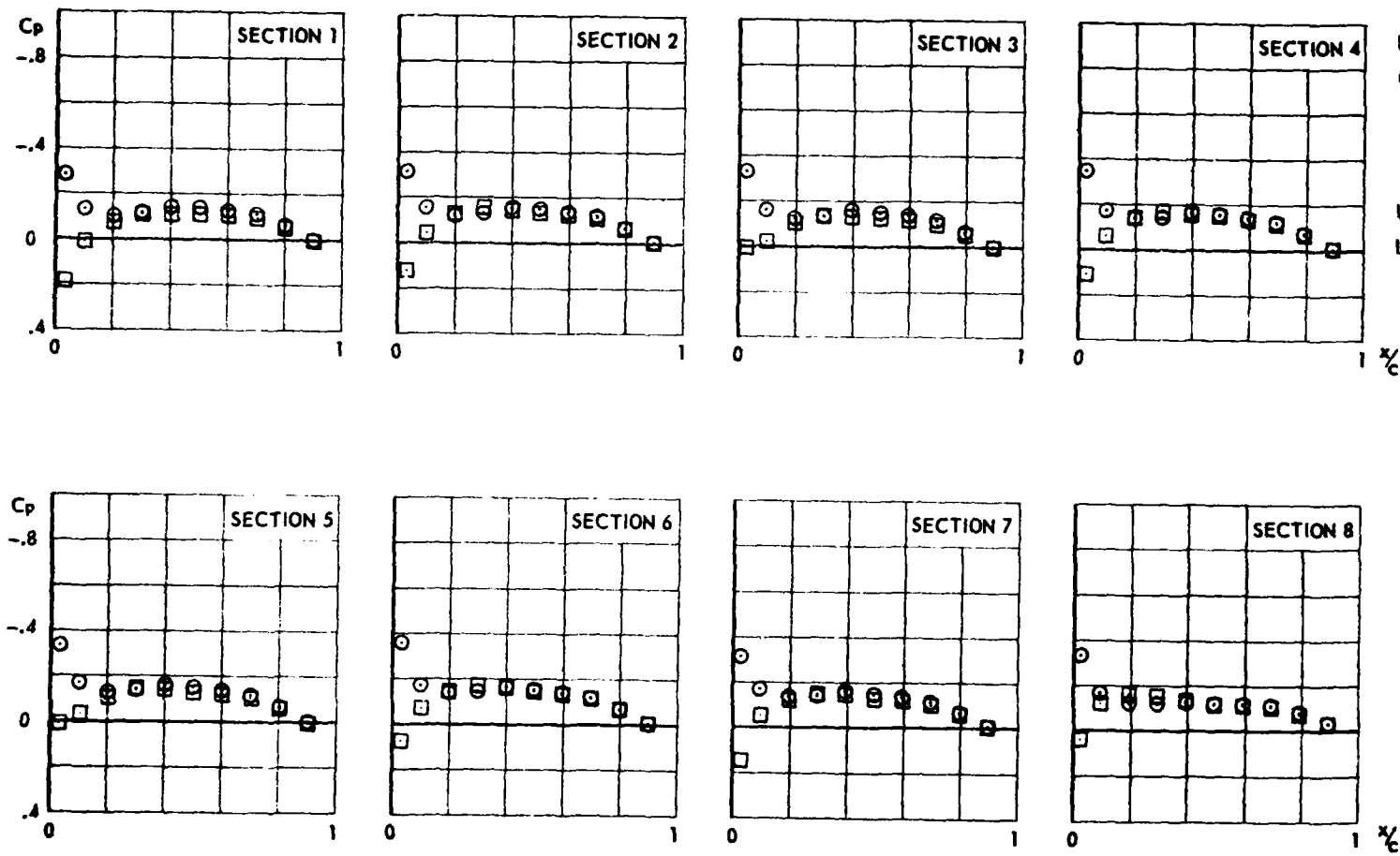

CONF.2 (WING + TIPLAUNCHER + MISSILEBODY)

FIG. III.B.16

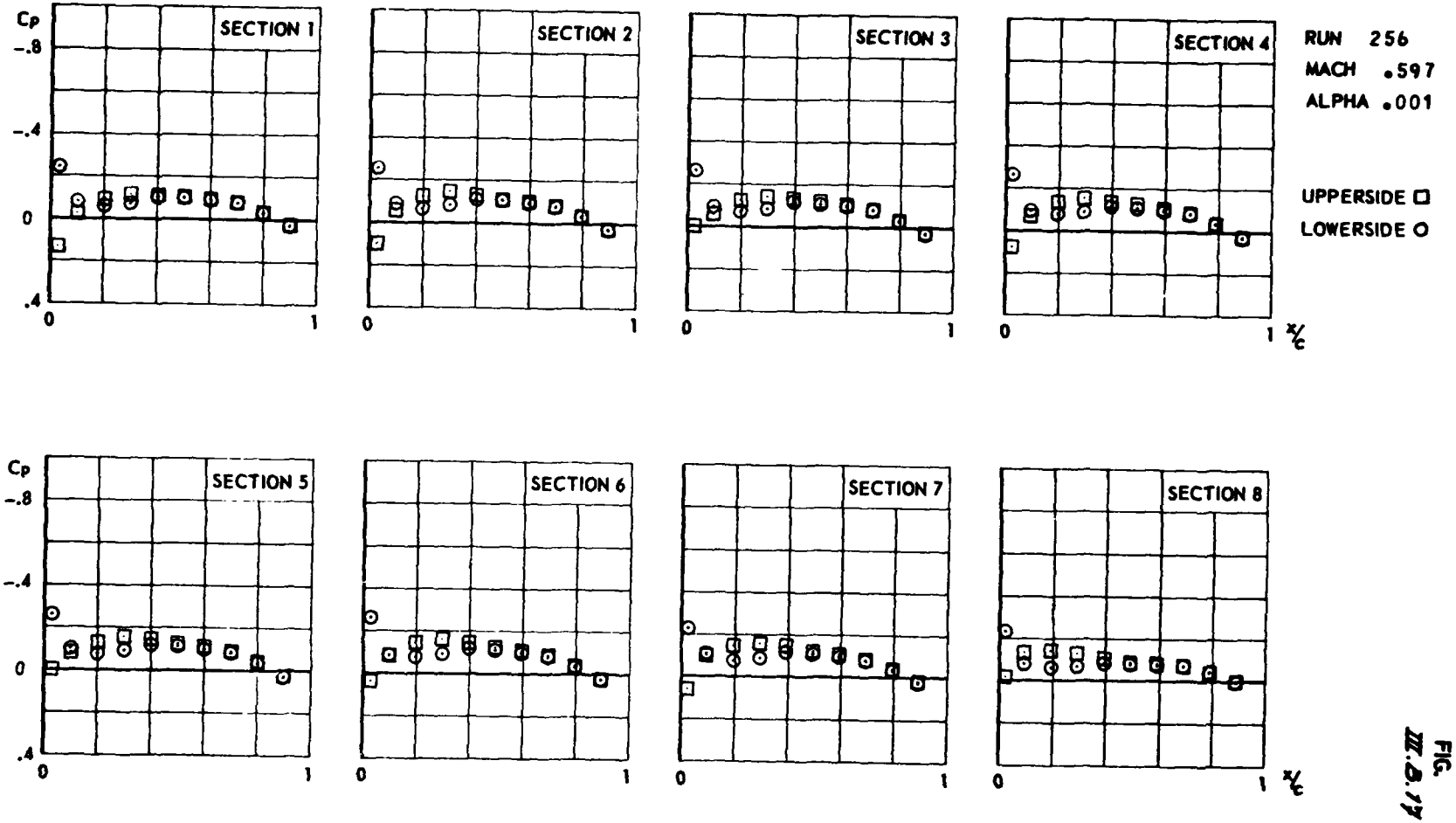

CONF.2 (WING + TIPLAUNCHER + MISSILEBODY)

FIG. III.B.17

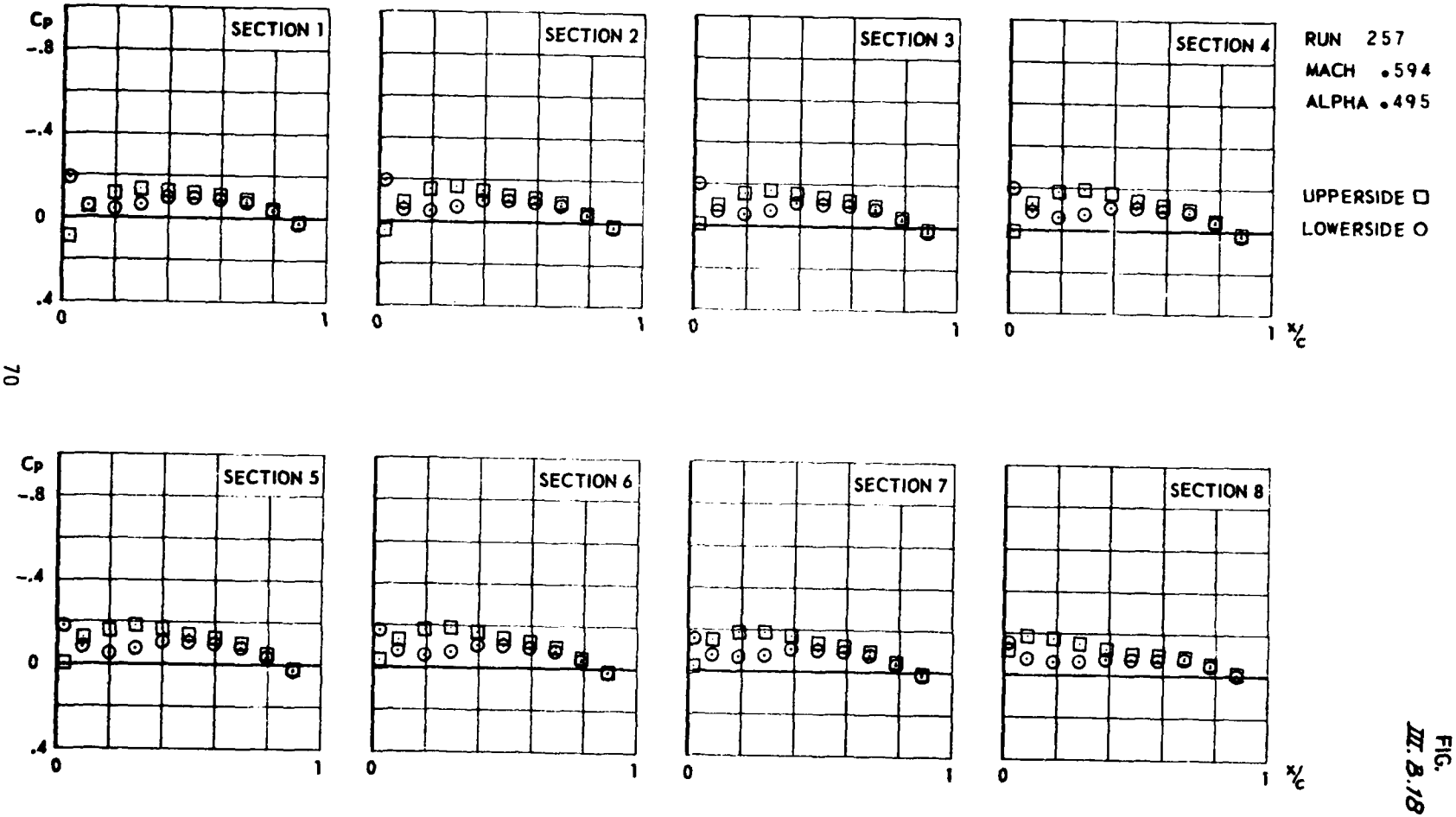

CONF.2 (WING + TIPLAUNCHER + MISSILEBODY)

FIG. III.B.18

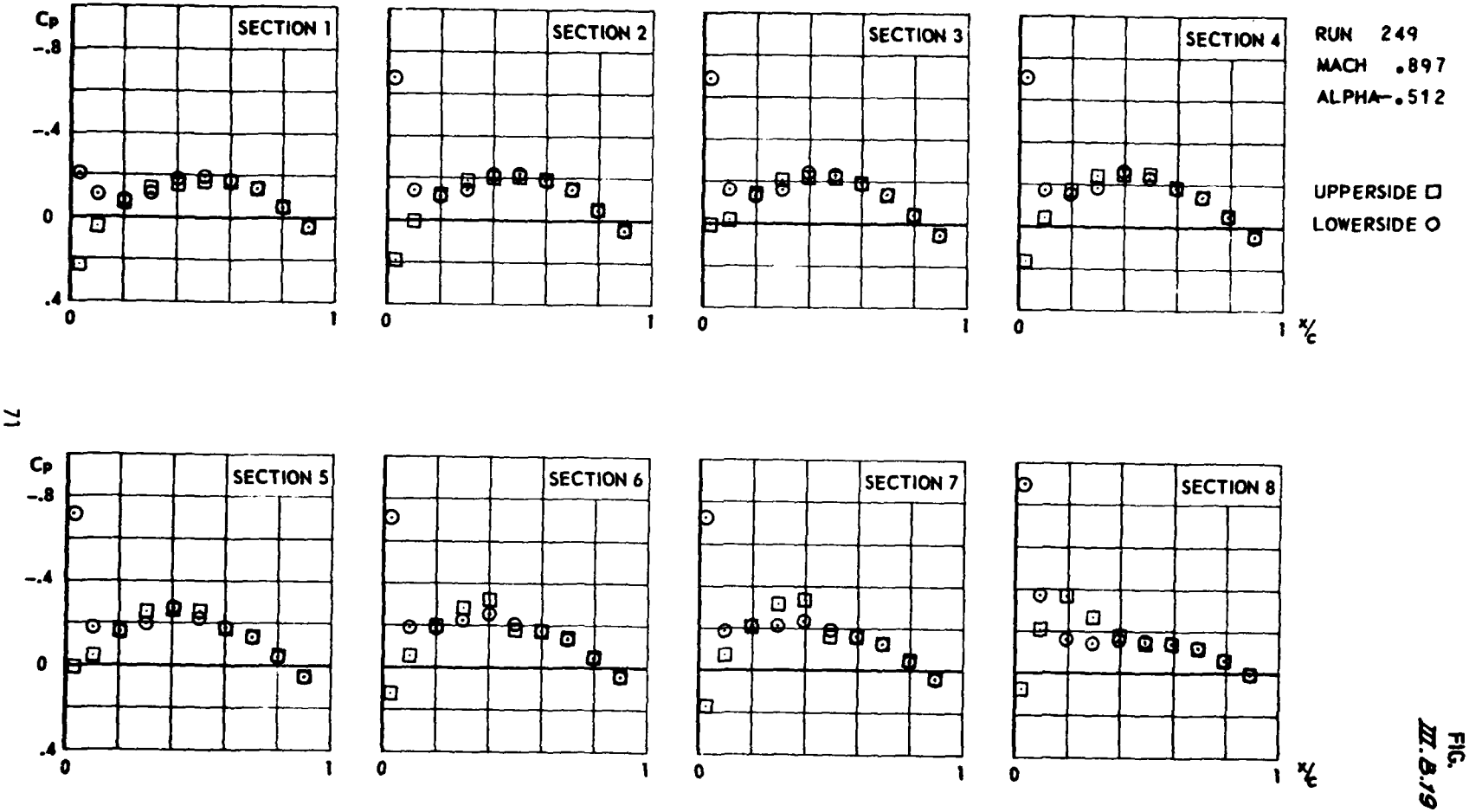

CONF.2 (WING + TIPLAUNCHER + MISSILEBODY)

FIG. III.B.19

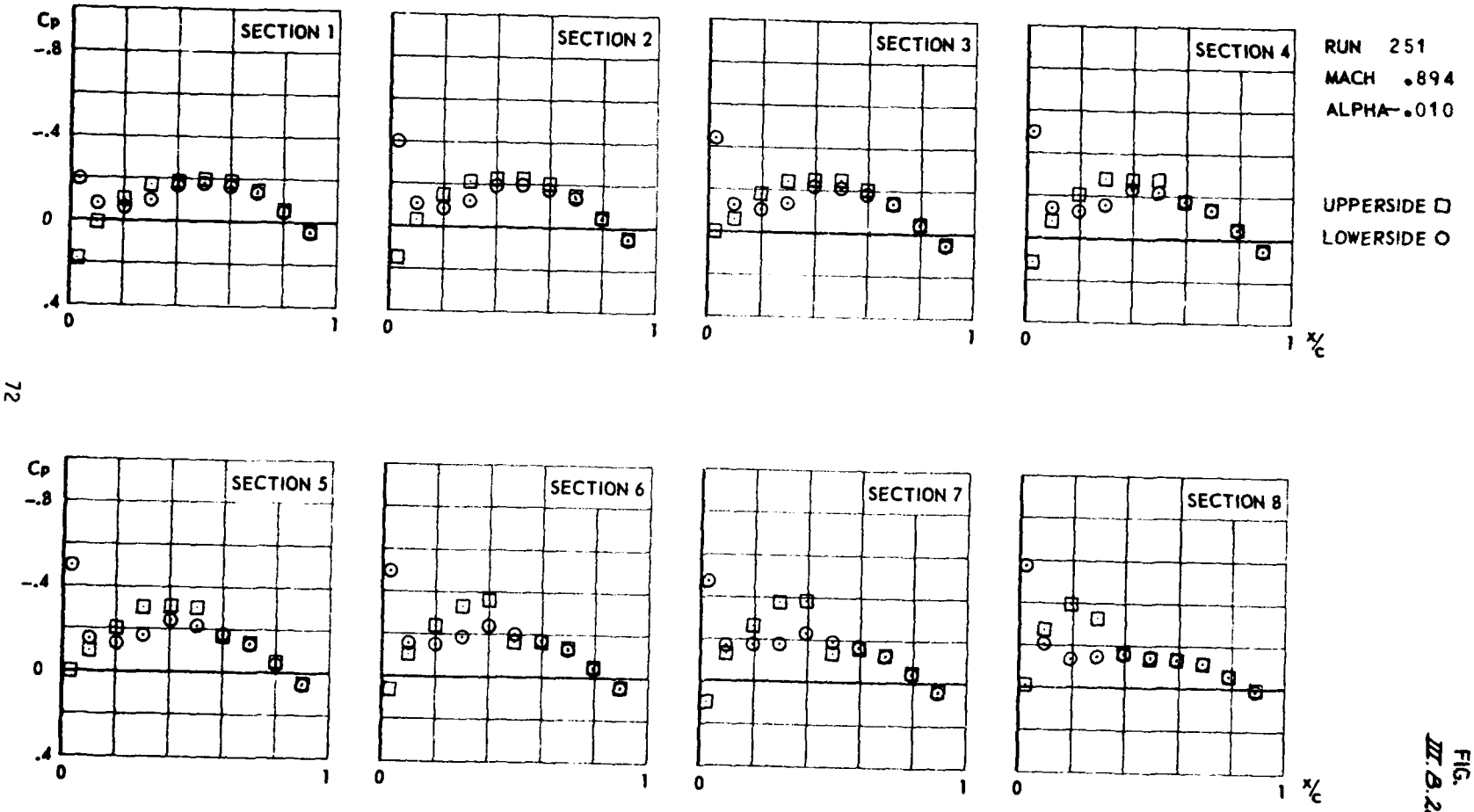

CONF.2 (WING + TIPLAUNCHER + MISSILEBODY)

FIG. III.B.20

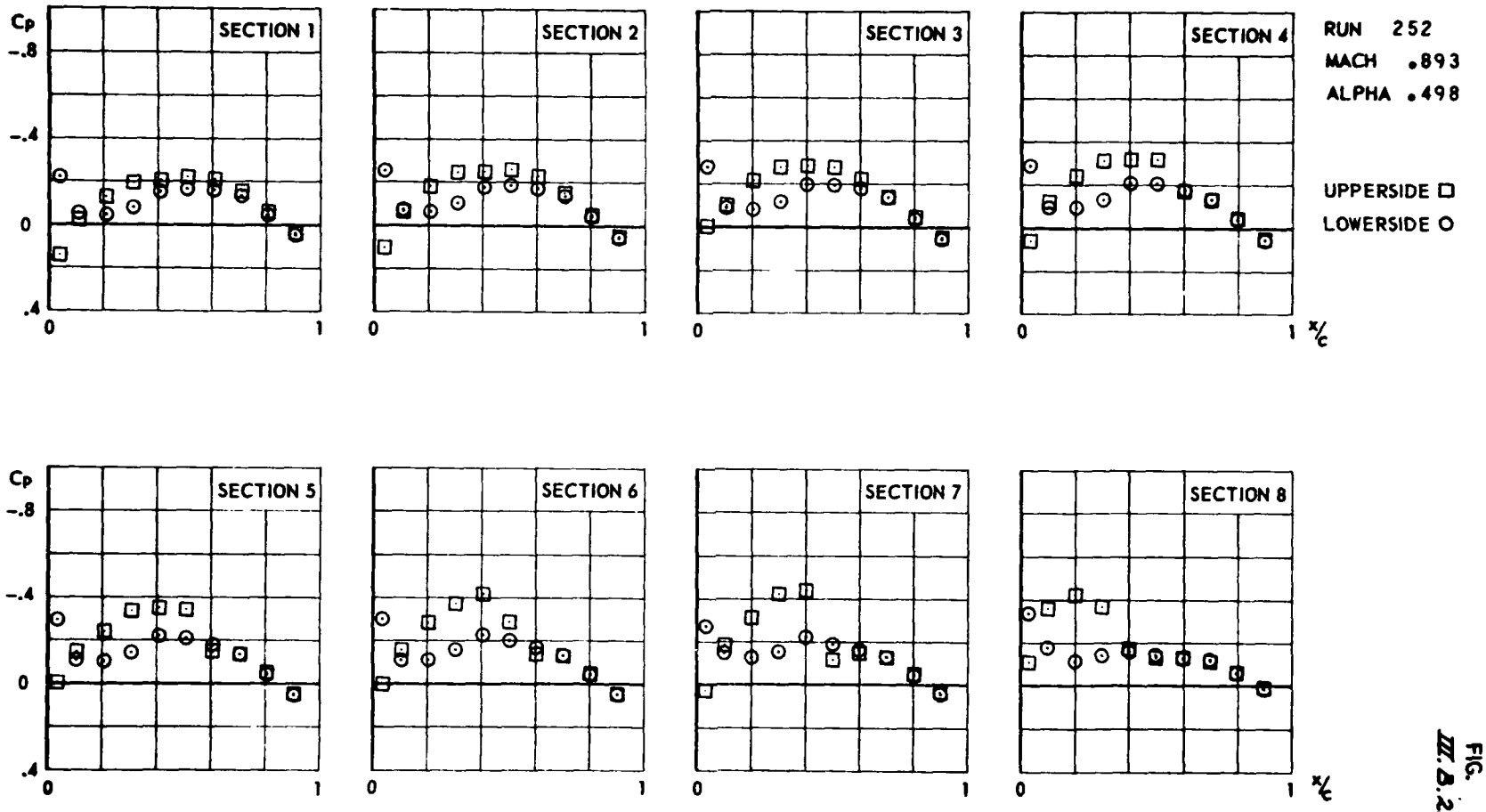

CONF.2 (WING + TIPLAUNCHER + MISSILEBODY)

FIG. III.B.27

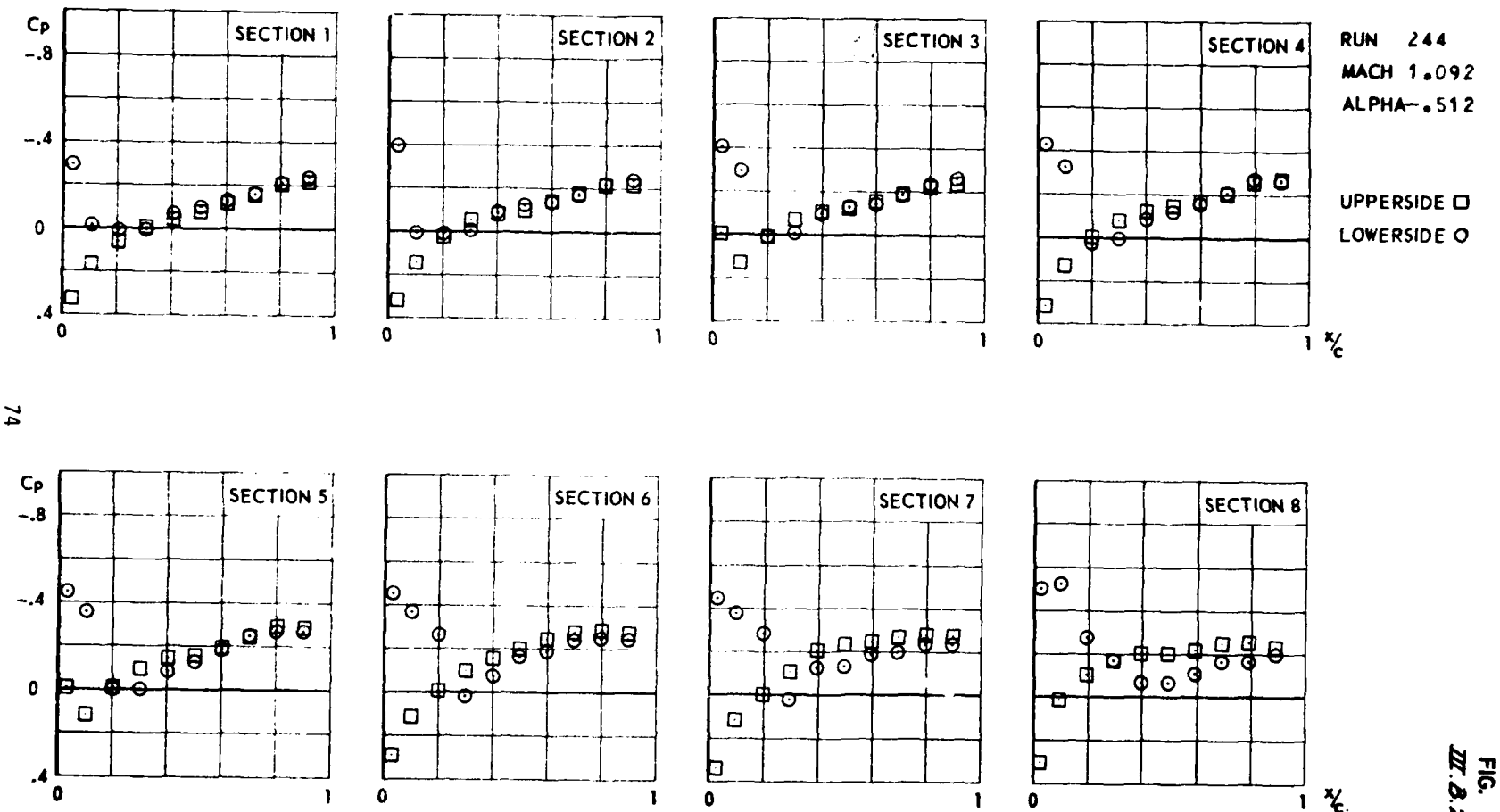

CONF.2 (WING + TIPLAUNCHER + MISSILEBODY)

FIG. III.B.22

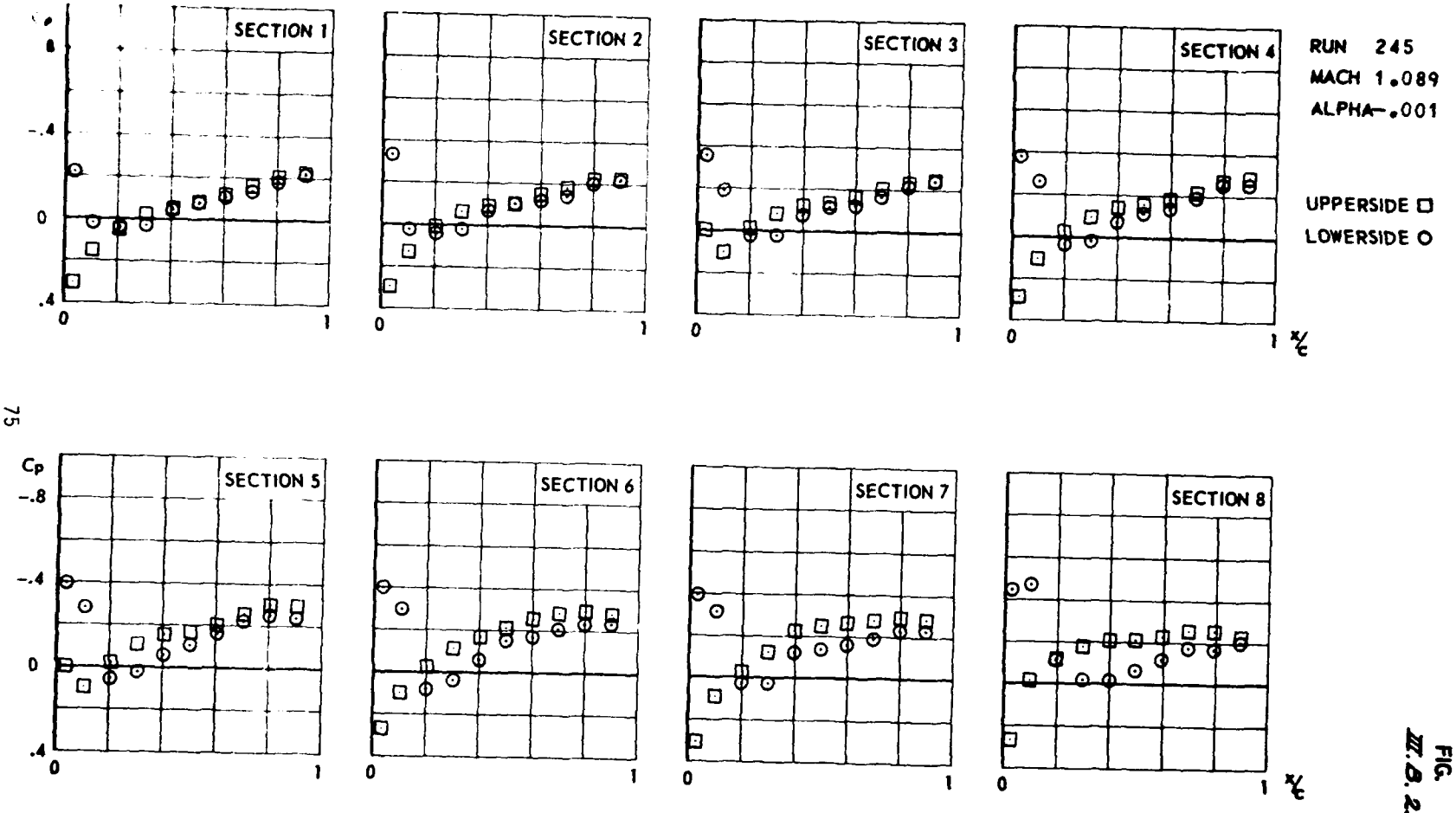

CONF.2 (WING + TIPLAUNCHER + MISSILEBODY)

FIG. III.B.23

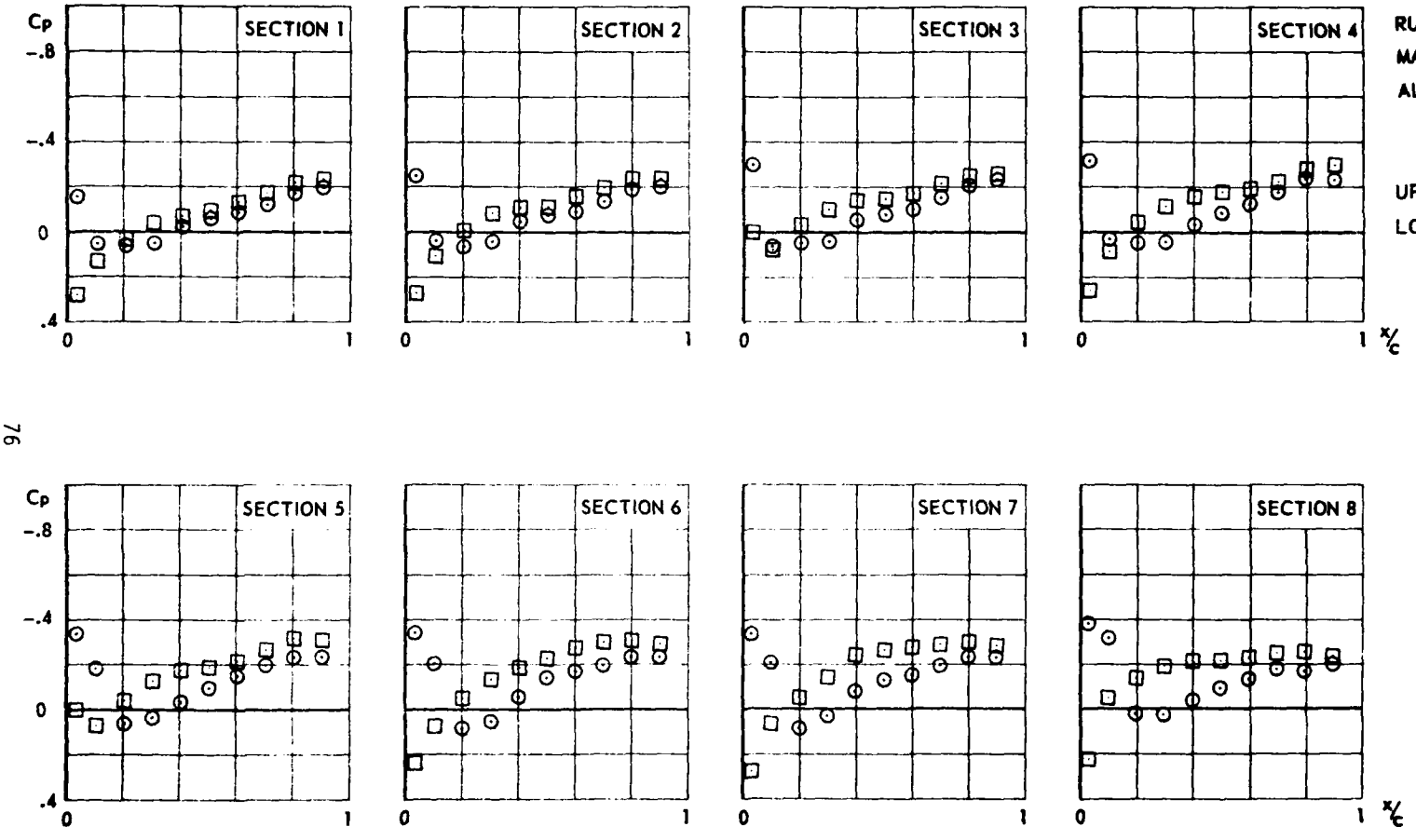

CONF.2 (WING + TIPLAUNCHER + MISSILEBODY)

FIG. III.B.24

FIG.
III.B.25

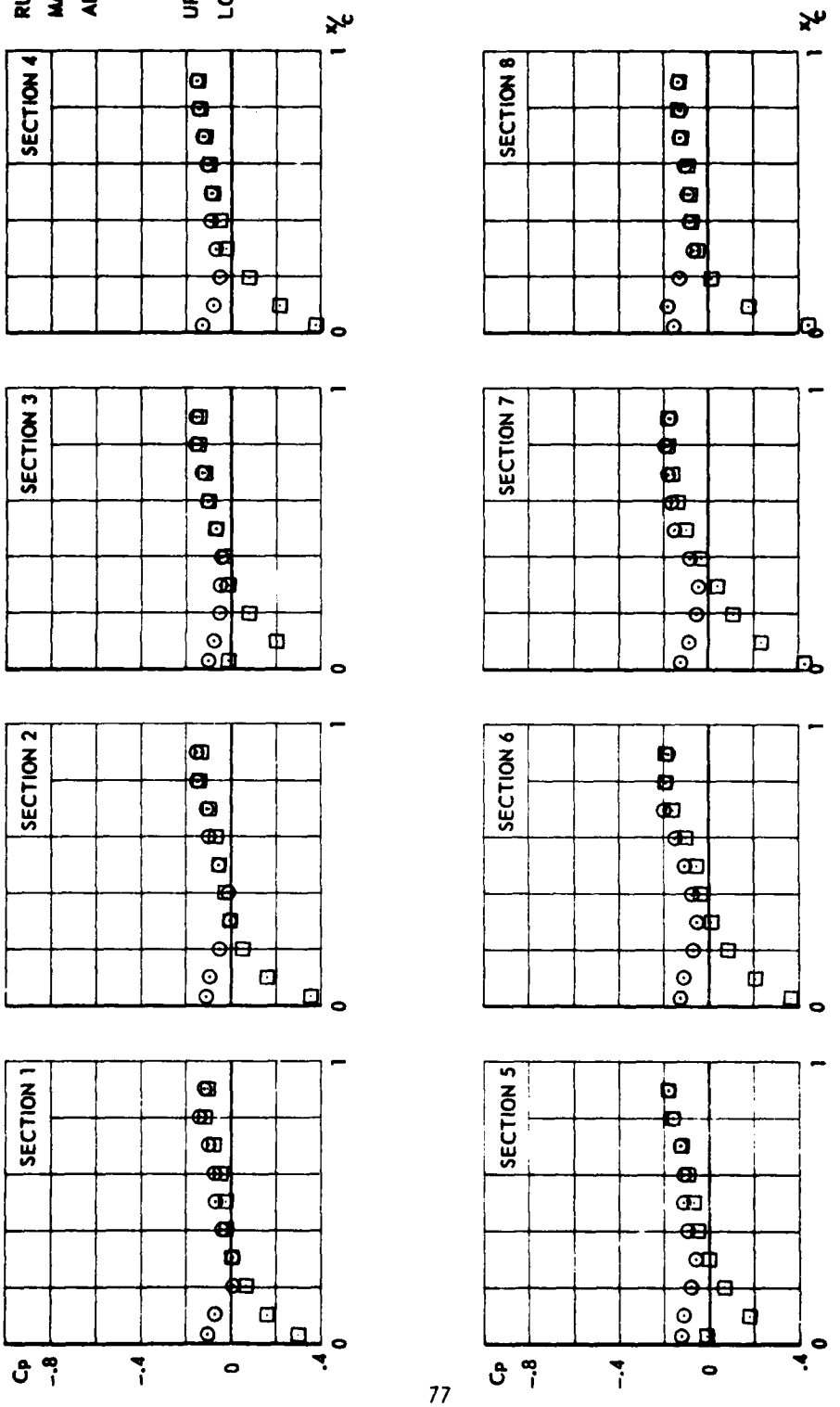

CONF.2 (WING + TIPLAUNCHER + MISSILEBODY)

FIG.
III. B. 26

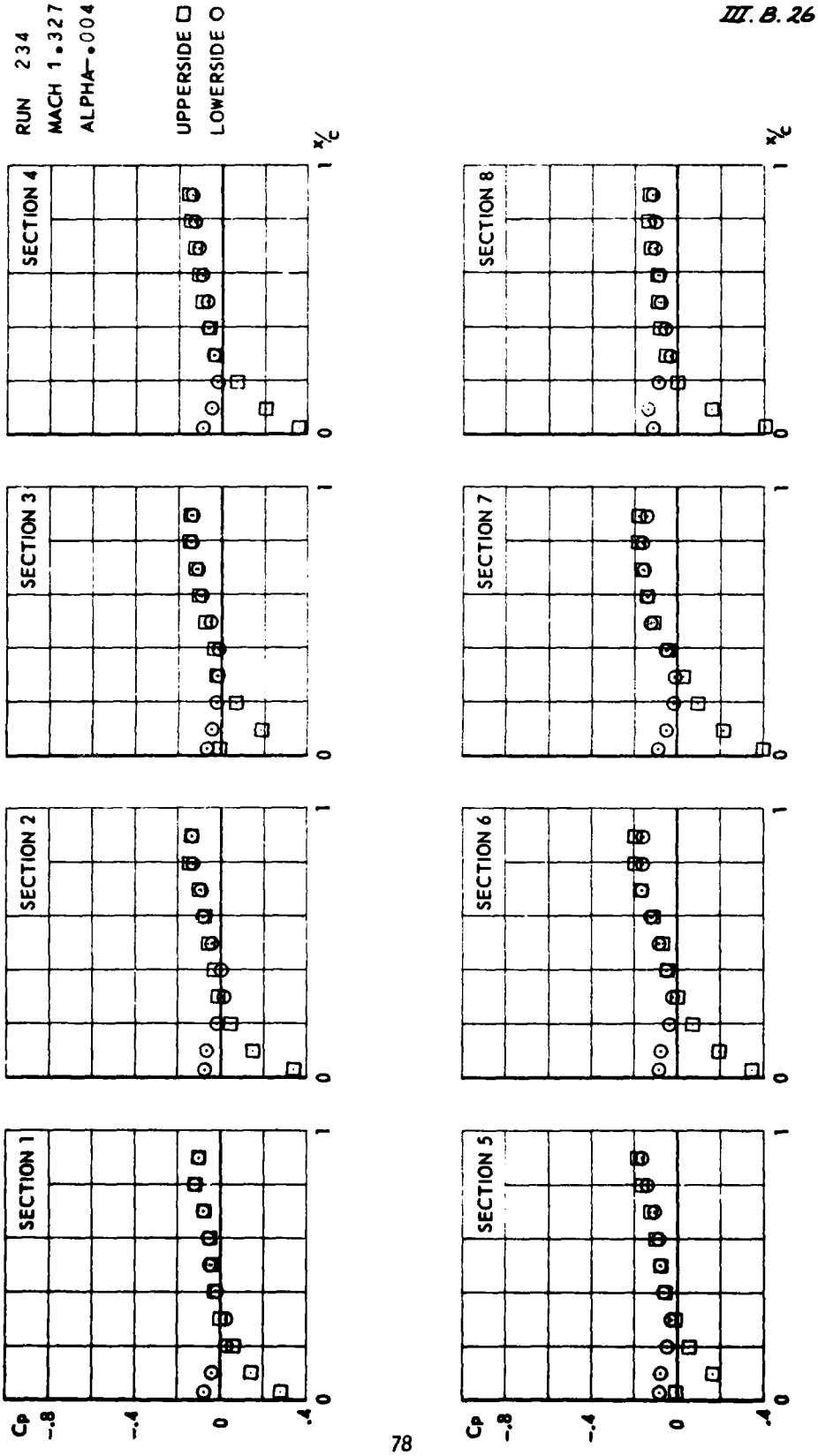

CONF.2 (WING + TIPLAUNCHER + MISSILEBODY)

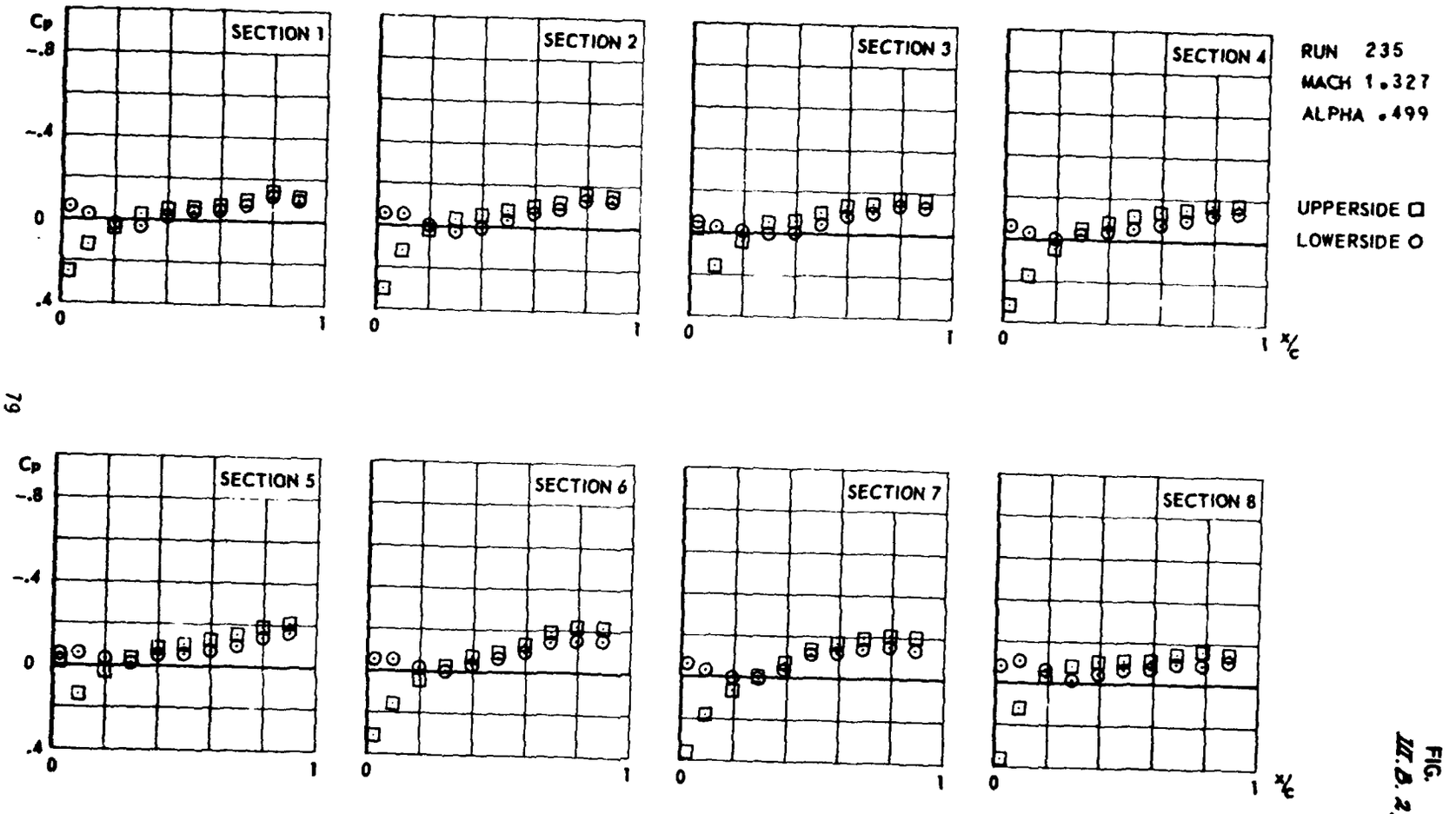

CONF.2 (WING + TIPLAUNCHER + MISSILEBODY)

FIG. III.B.27

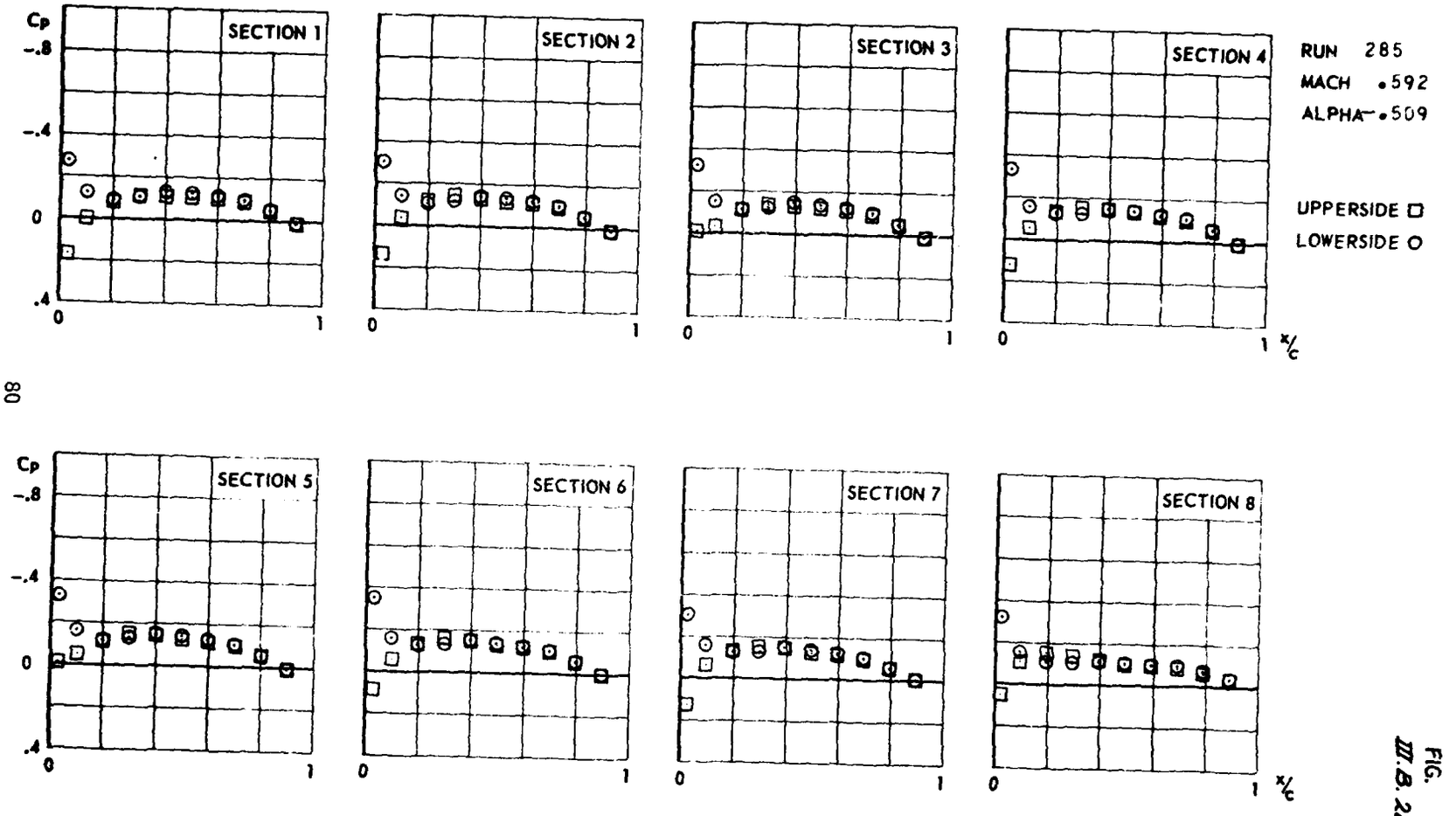

CONF.3 (WING + TIPLAUNCHER + MISSILEBODY WITH AFT WINGS)

FIG. III.B.28

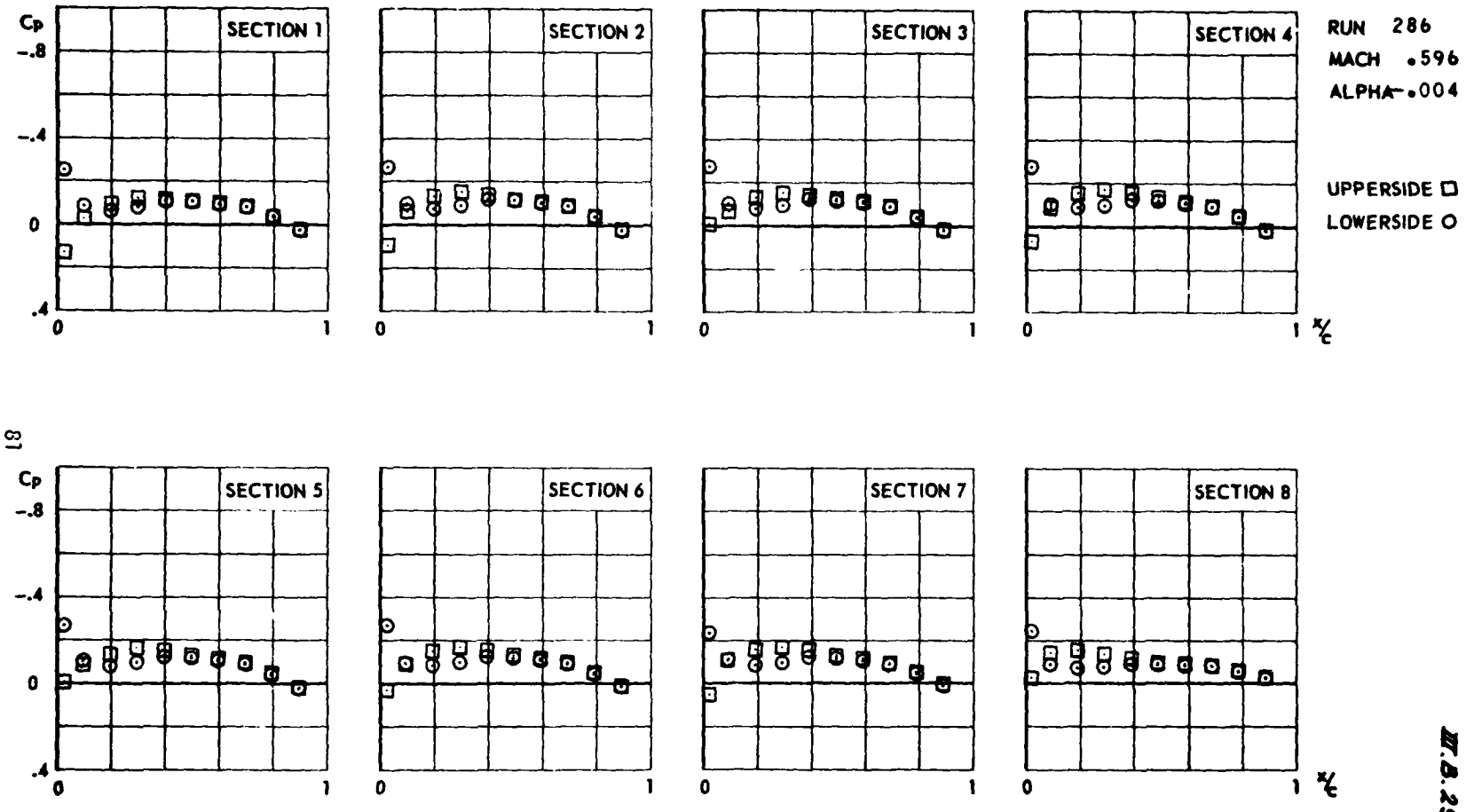

CONF.3 (WING + TIPLAUNCHER + MISSILEBODY WITH AFT WINGS)

FIG. III.B.29

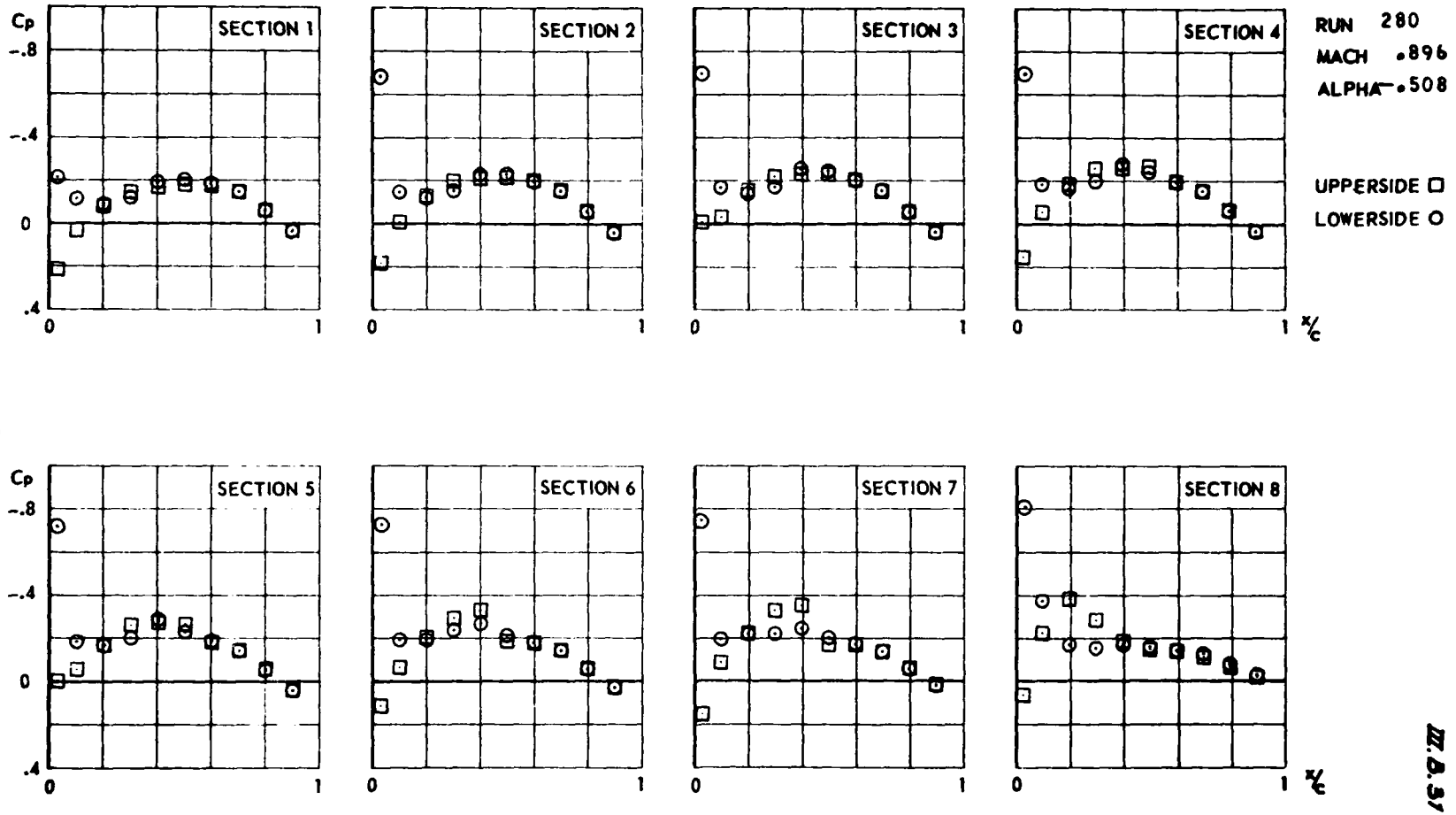

CONF.3 (WING + TIPLAUNCHER + MISSILEBODY WITH AFT WINGS)

FIG. III.B.5.f

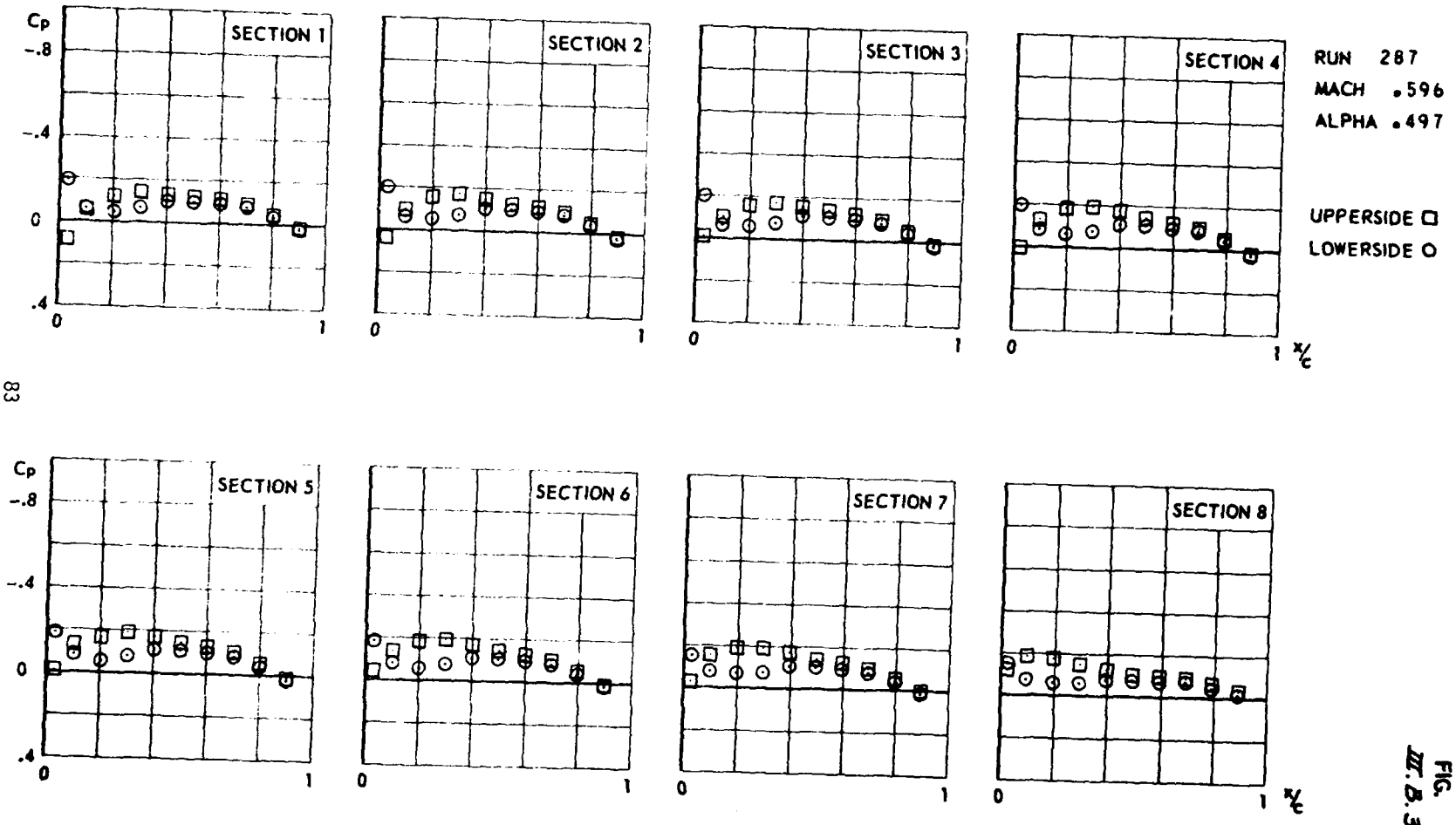

CONF.3 (WING + TIPLAUNCHER + MISSILEBODY WITH AFT WINGS)

FIG. III.B.30

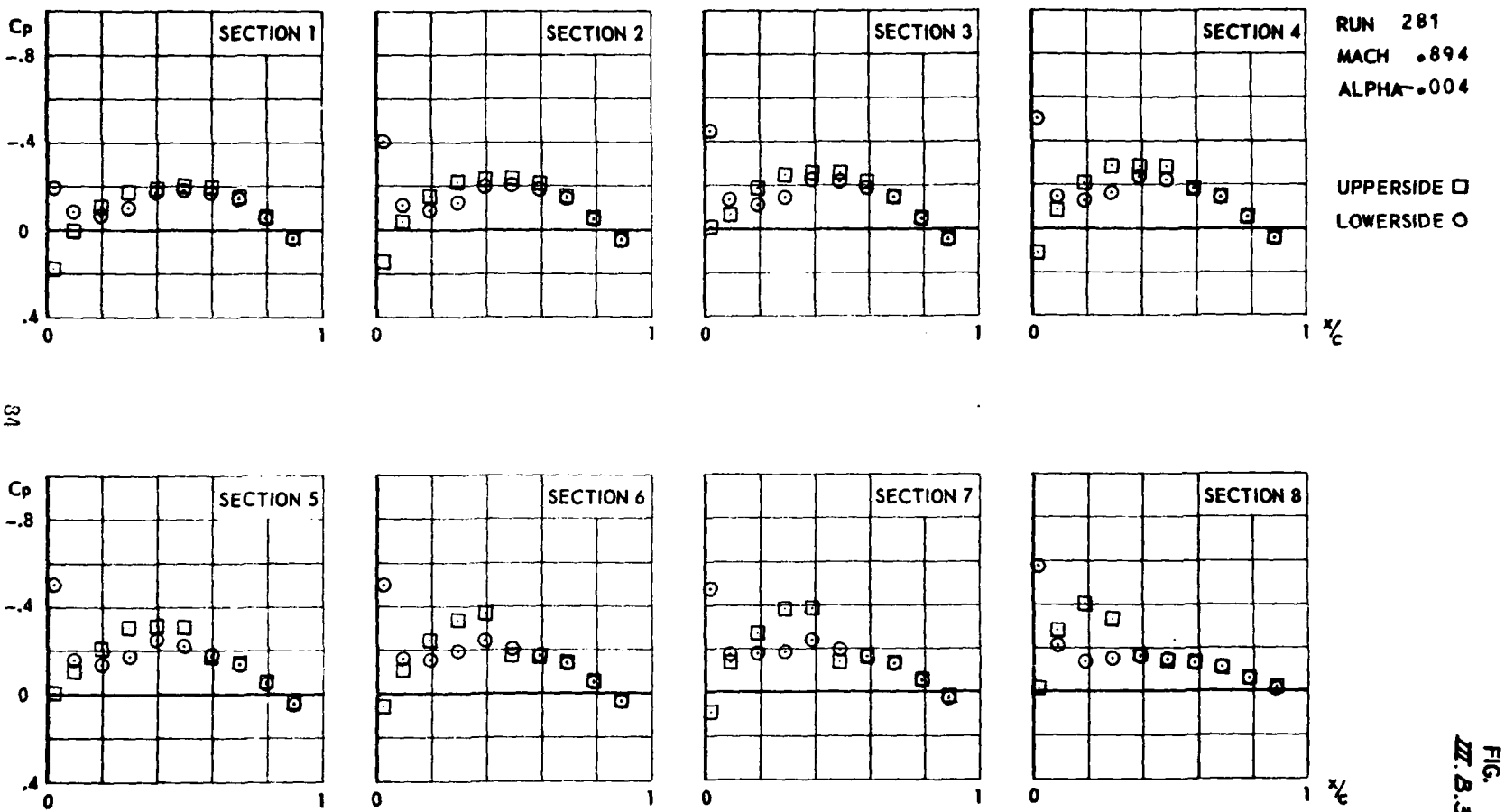

FIG. III.B.32

CONF.3 (WING + TIPLAUNCHER + MISSILEBODY WITH AFT WINGS)

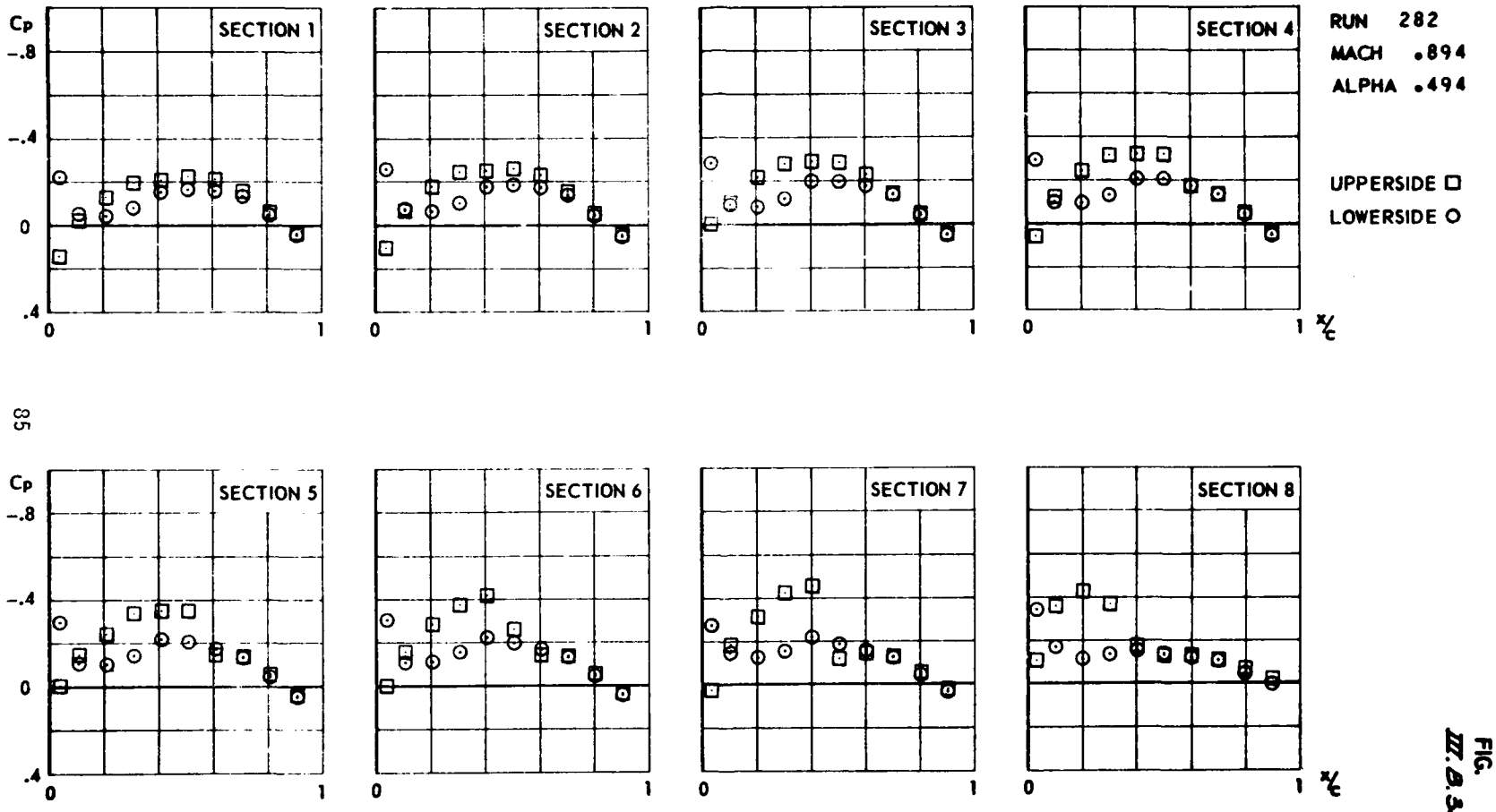

FIG. III.B.33

CONF.3 (WING + TIPLAUNCHER + MISSILEBODY WITH AFT WINGS)

FIG.
III.B.34

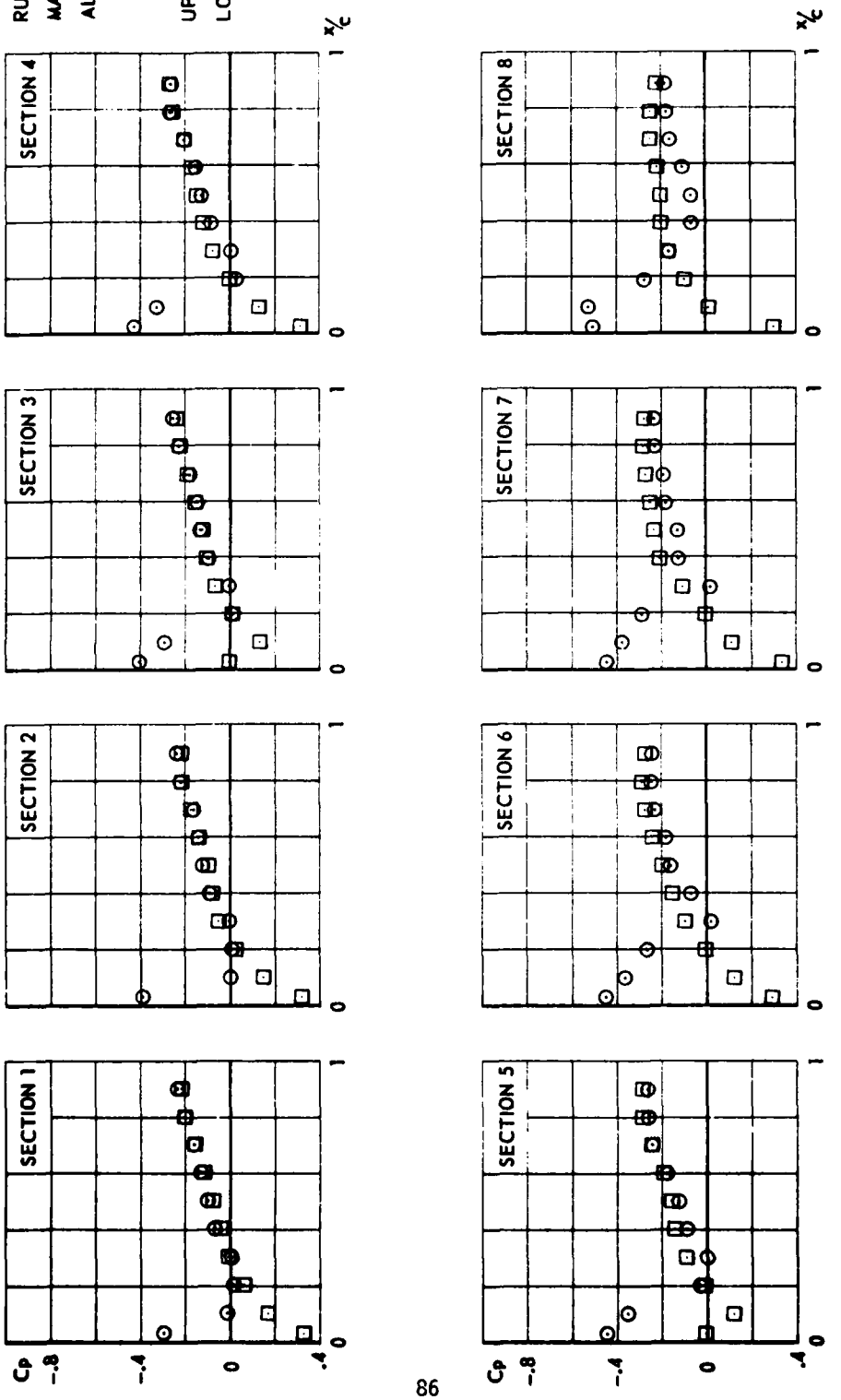

CONF.3 (WING + TIPLAUNCHER + MISSILEBODY WITH AFT WINGS)

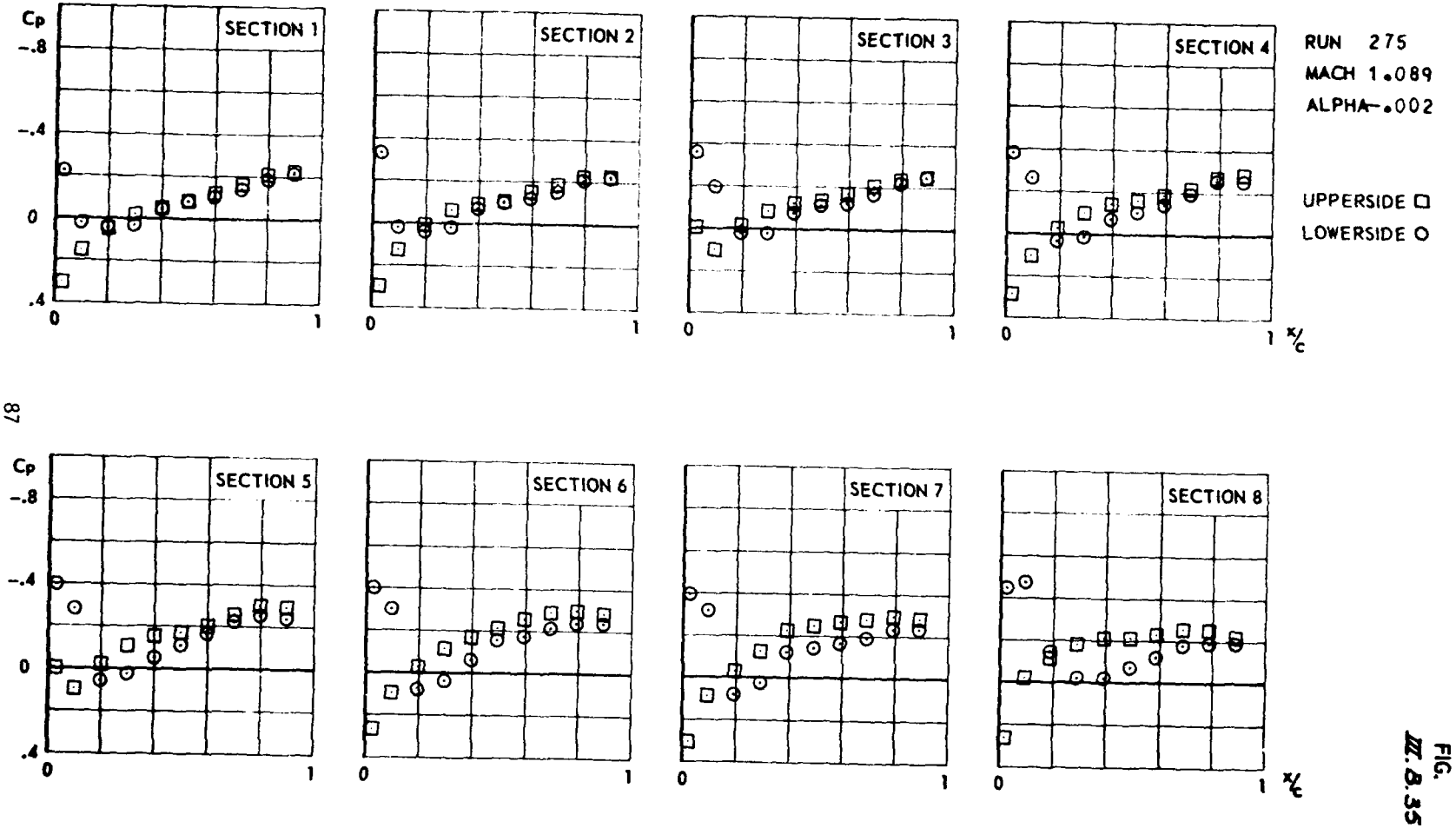

FIG. III.B.35

CONF.3 (WING + TIPLAUNCHER + MISSILEBODY WITH AFT WINGS)

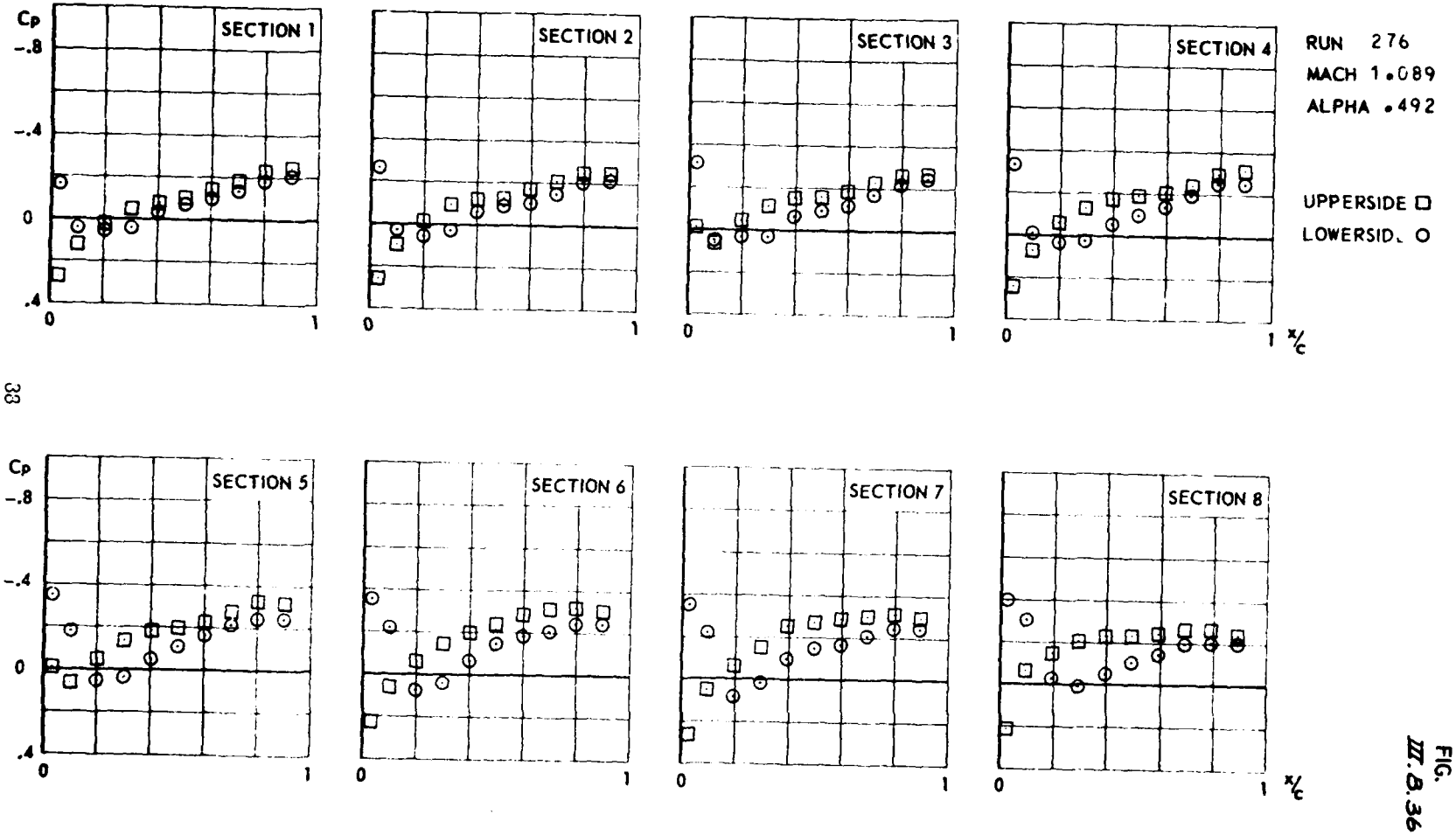

CONF.3 (WING + TIPLAUNCHER + MISSILEBODY WITH AFT WINGS)

FIG. III.B.36

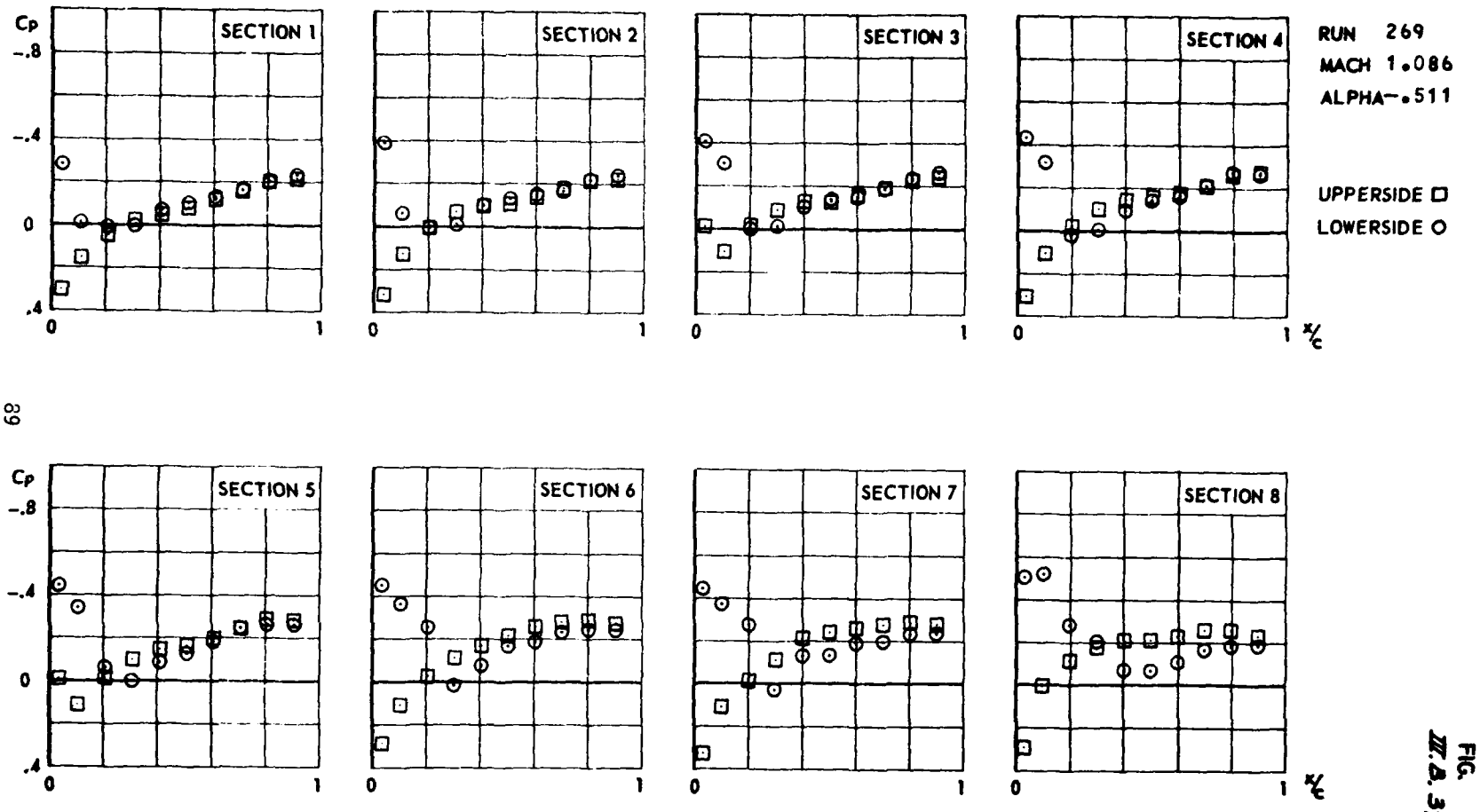

FIG. III.B.37

CONF.3 (WING + TIPLAUNCHER + MISSILEBODY WITH AFT WINGS)

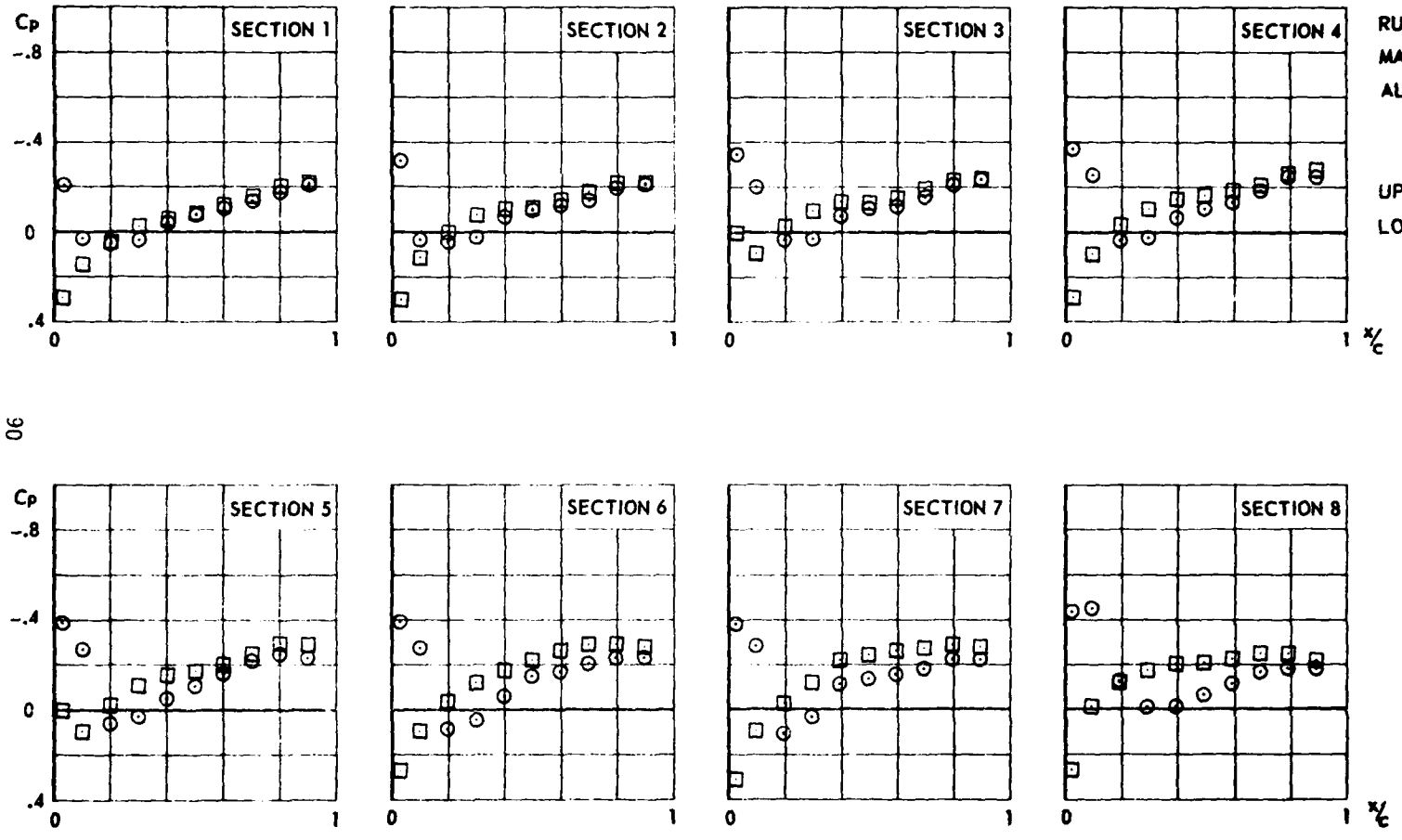

FIG. III.B.38

CONF.3 (WING + TIPLAUNCHER + MISSILEBODY WITH AFT WINGS)

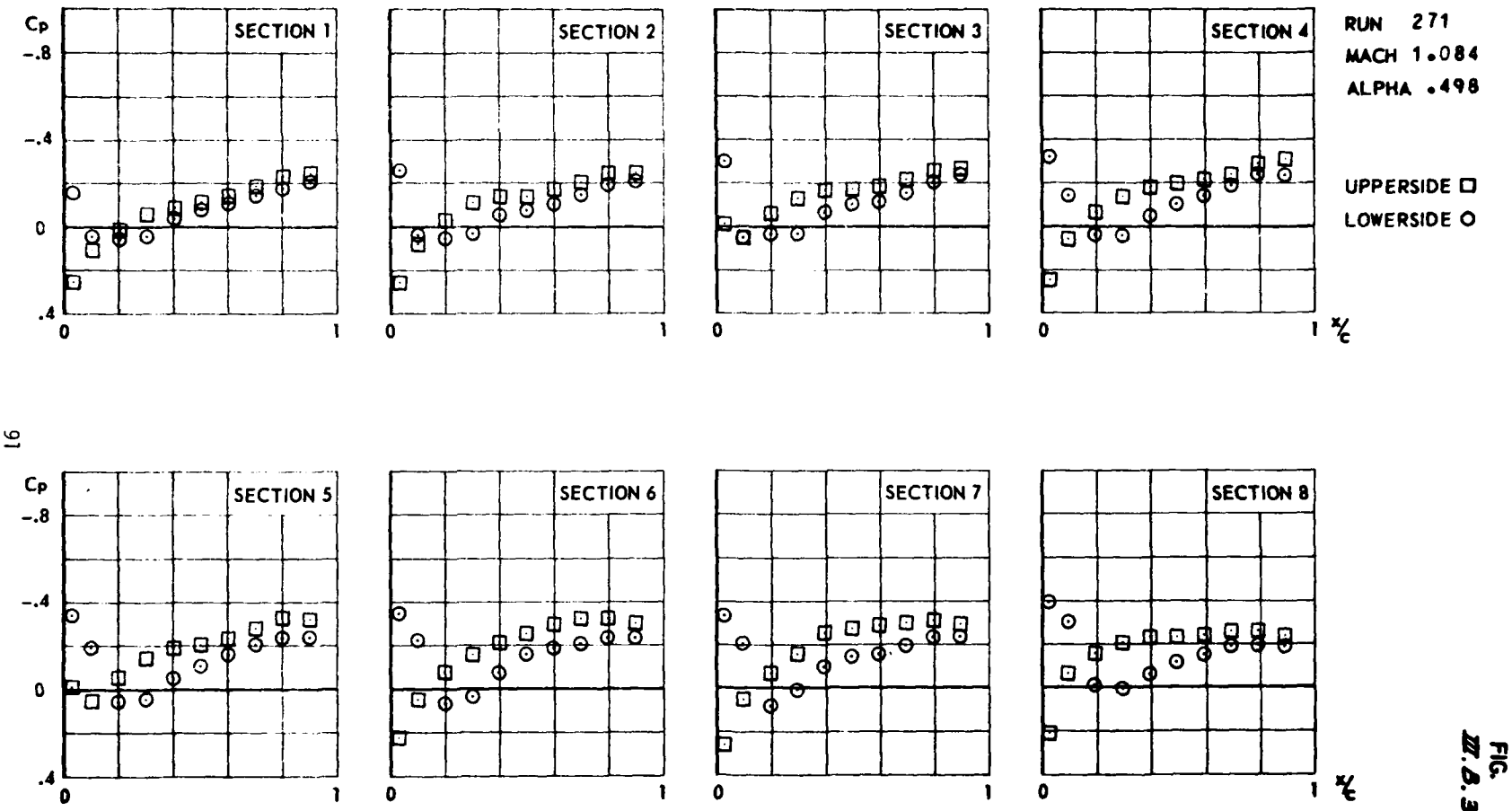

CONF.3 (WING + TIPLAUNCHER + MISSILEBODY WITH AFT WINGS)

FIG. III.B.39

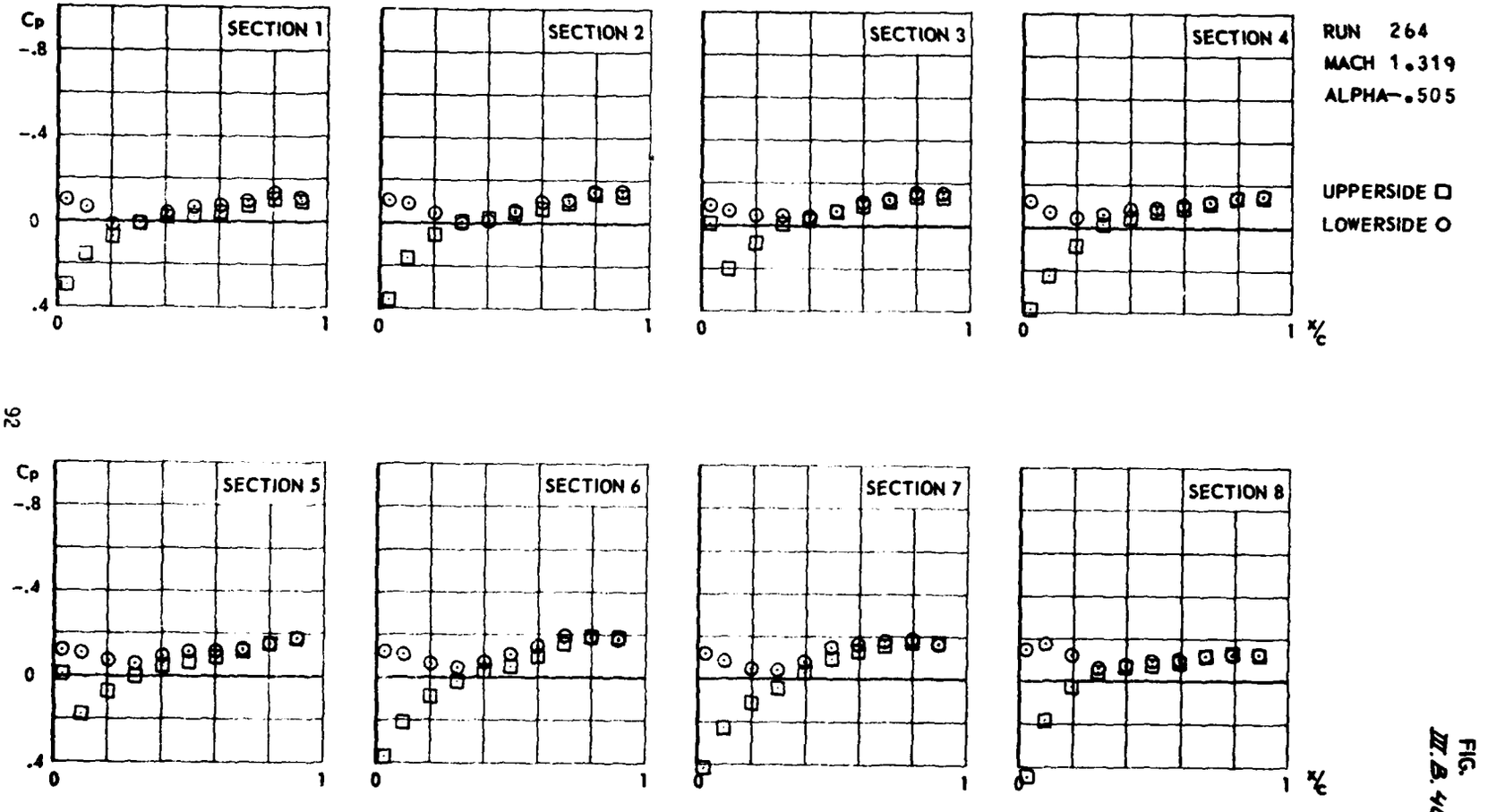

CONF.3 (WING + TIPLAUNCHER + MISSILEBODY WITH AFT WINGS)

FIG. III.B.40

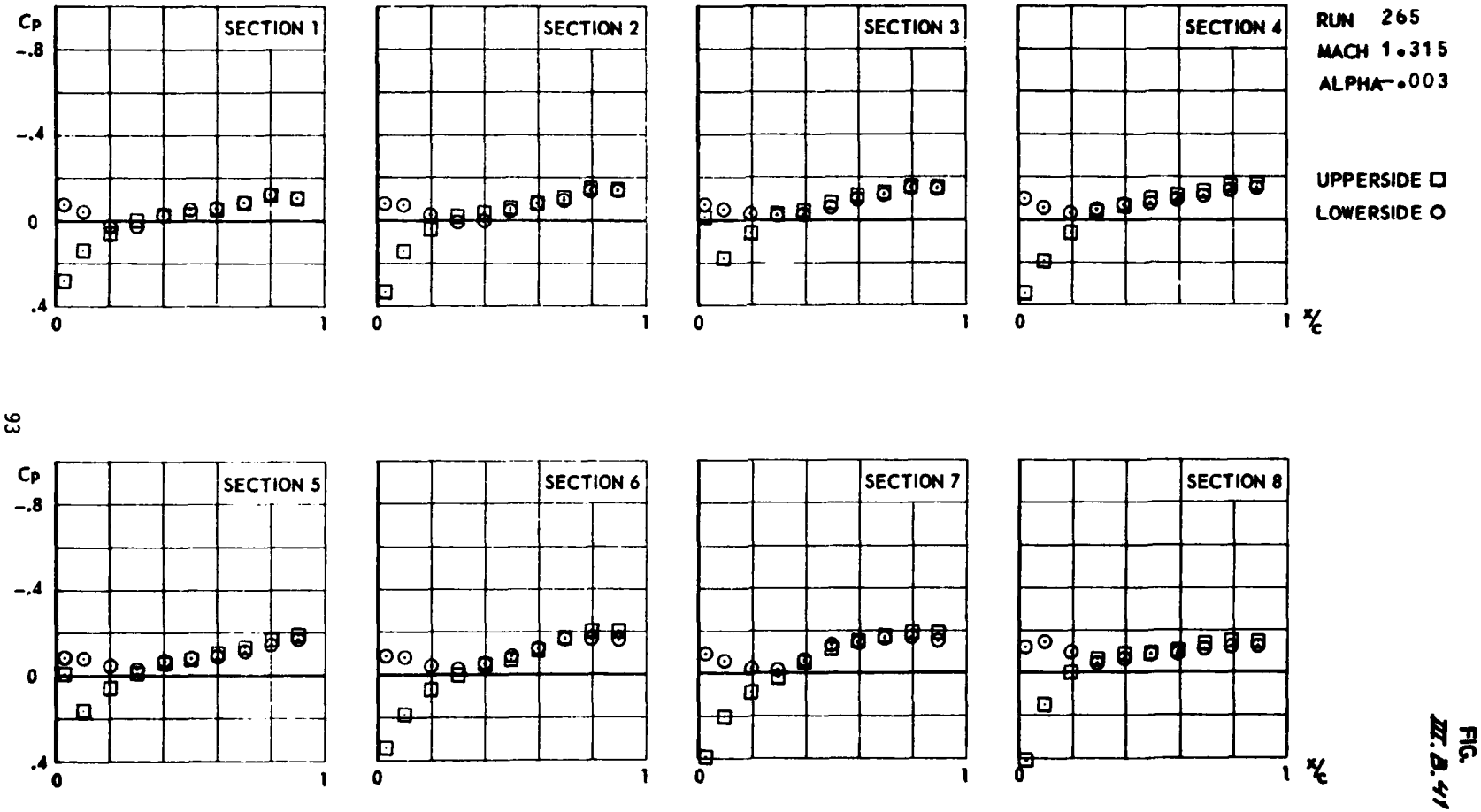

FIG. III.B.41

CONF.3 (WING + TIPLAUNCHER + MISSILEBODY WITH AFT WINGS)

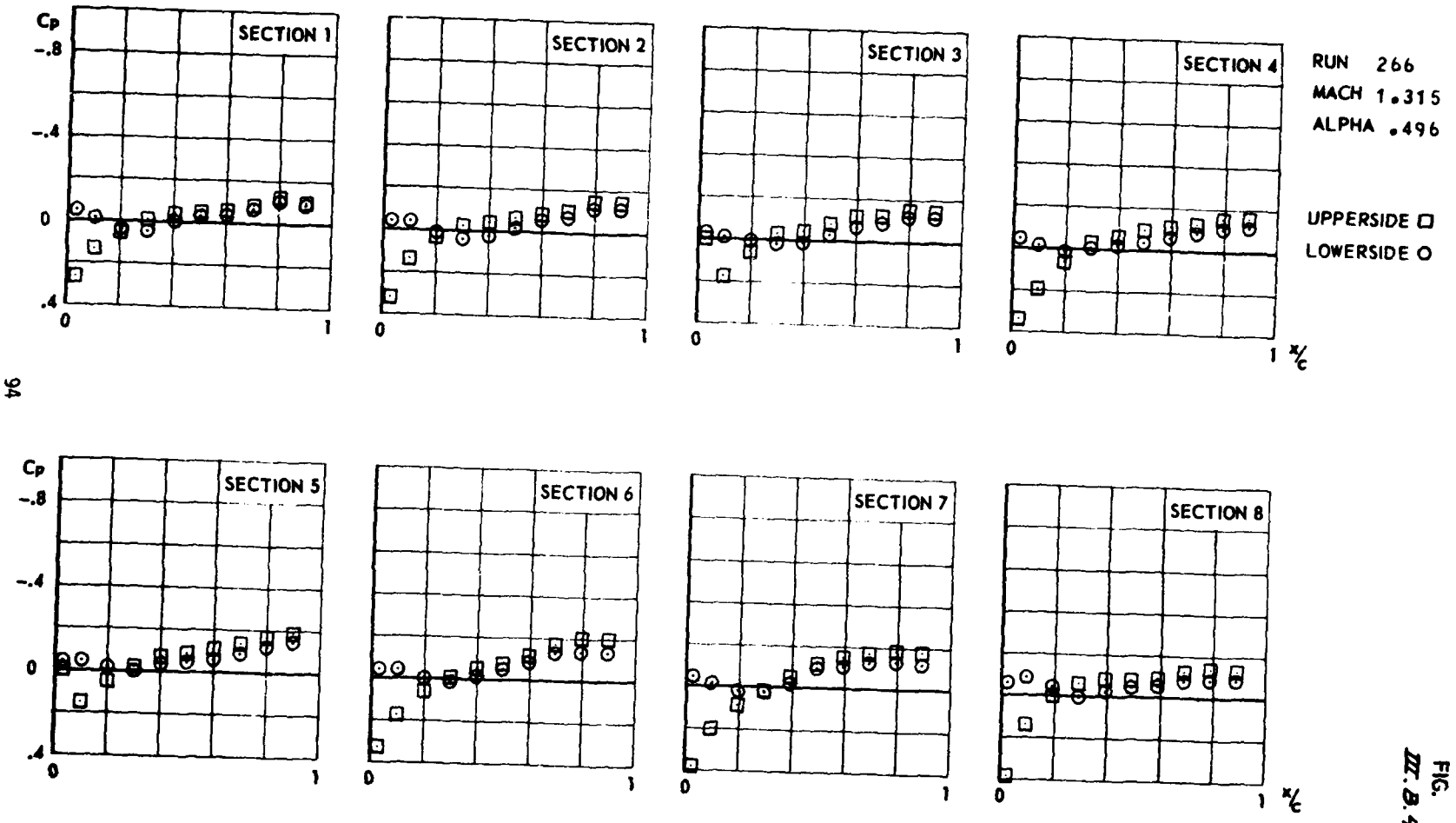

CONF.3 (WING + TIPLAUNCHER + MISSILEBODY WITH AFT WINGS)

FIG. III.B.42

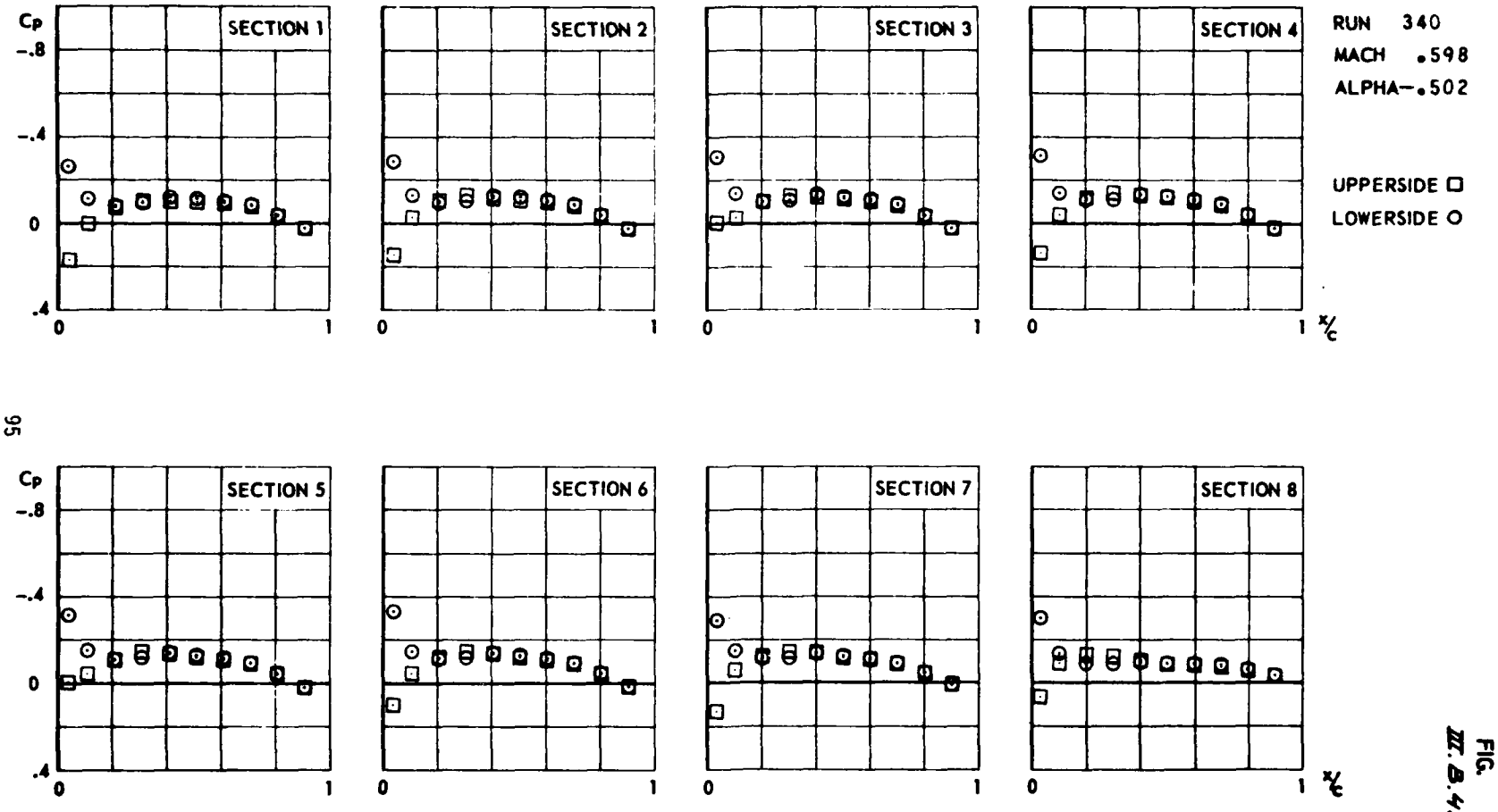

CONF.4 (WING + TIPLAUNCHER + COMPLETE MISSILE)

FIG. III.B.43

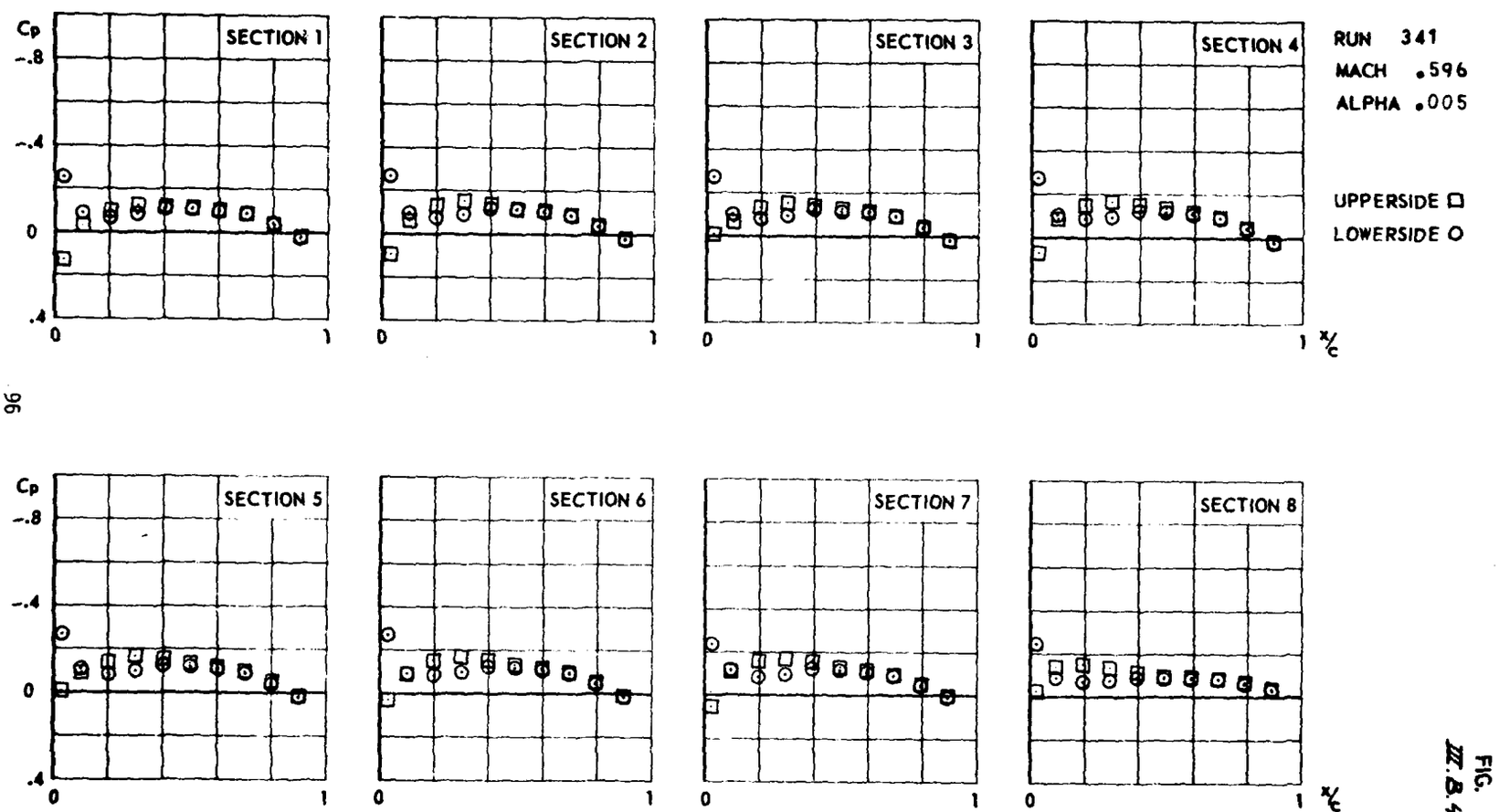

CONF.4 (WING + TIPLAUNCHER + COMPLETE MISSILE)

FIG. III.B.44

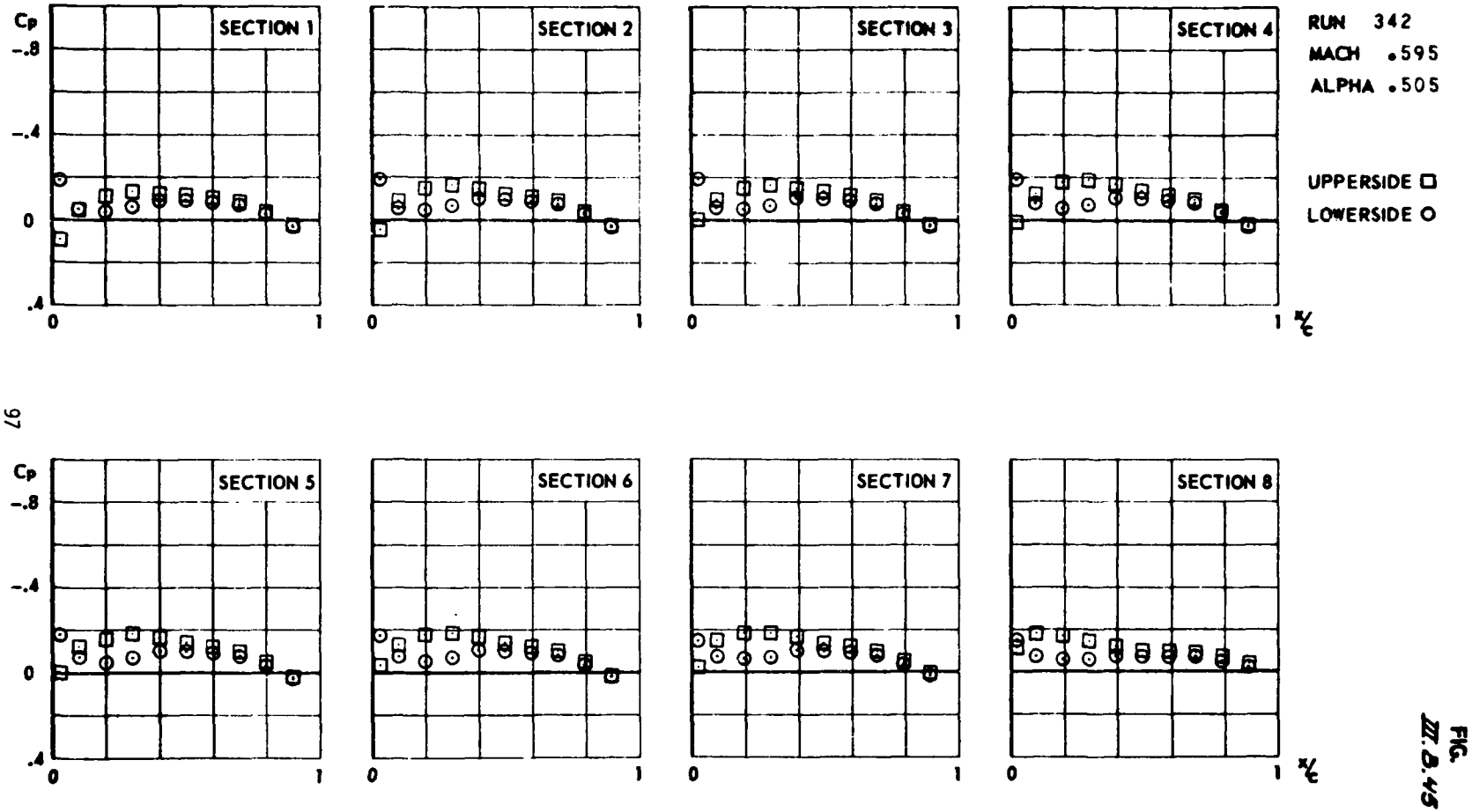

CONF.4 (WING + TIPLAUNCHER + COMPLETE MISSILE)

FIG. III.B.49

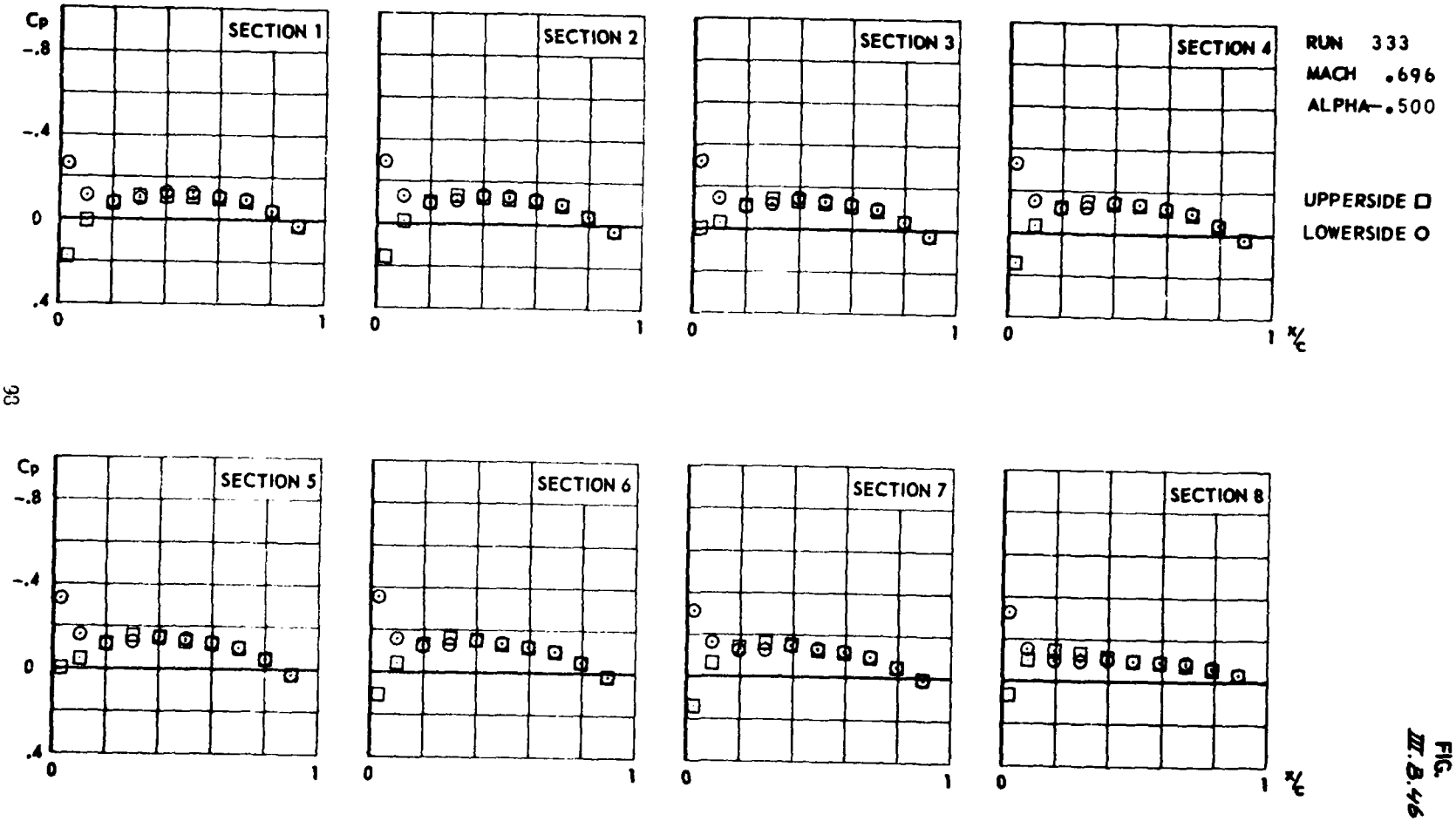

CONF.4 (WING + TIPLAUNCHER + COMPLETE MISSILE)

FIG. III.B.46

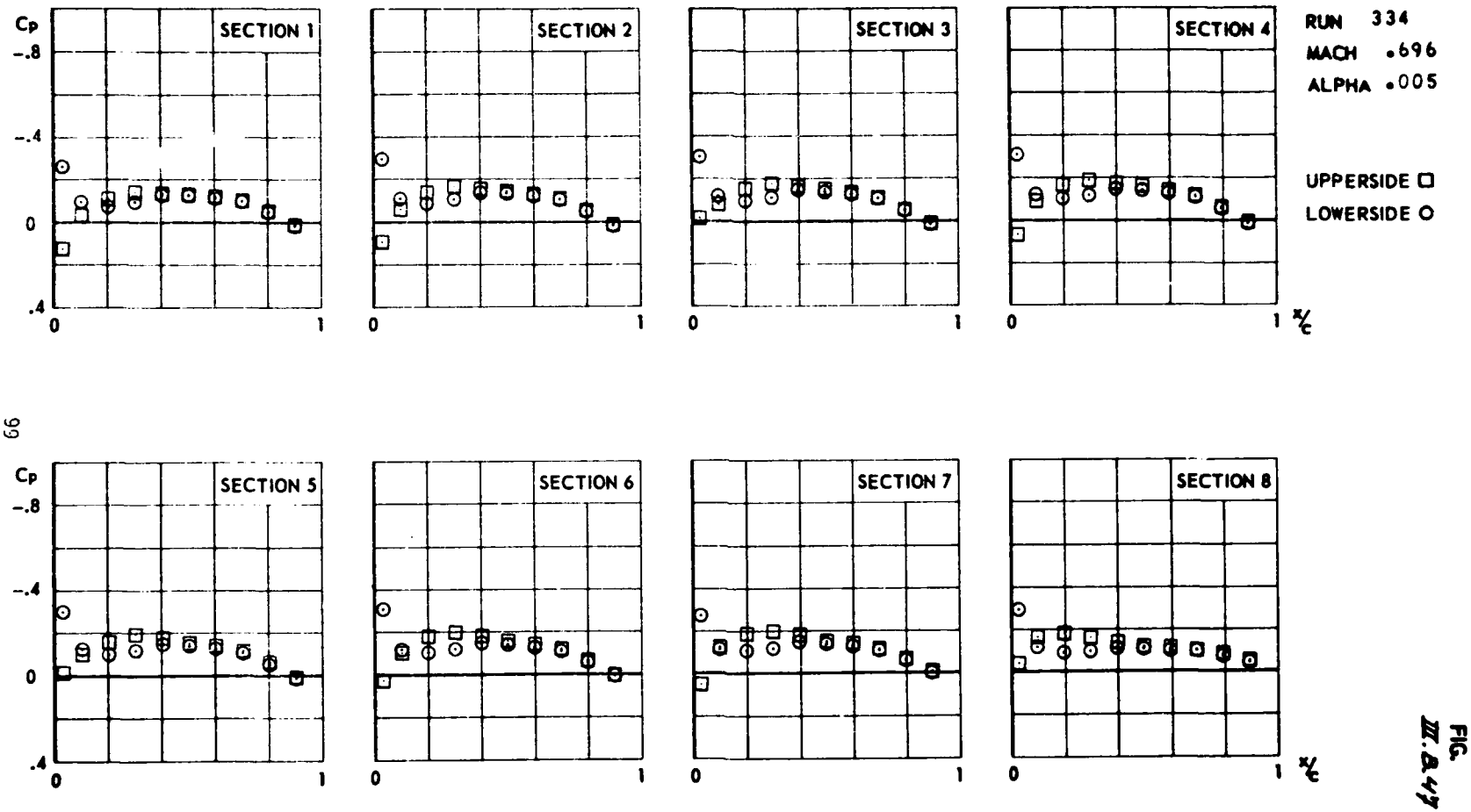

CONF.4 (WING + TIPLAUNCHER + COMPLETE MISSILE)

FIG. III.A.47

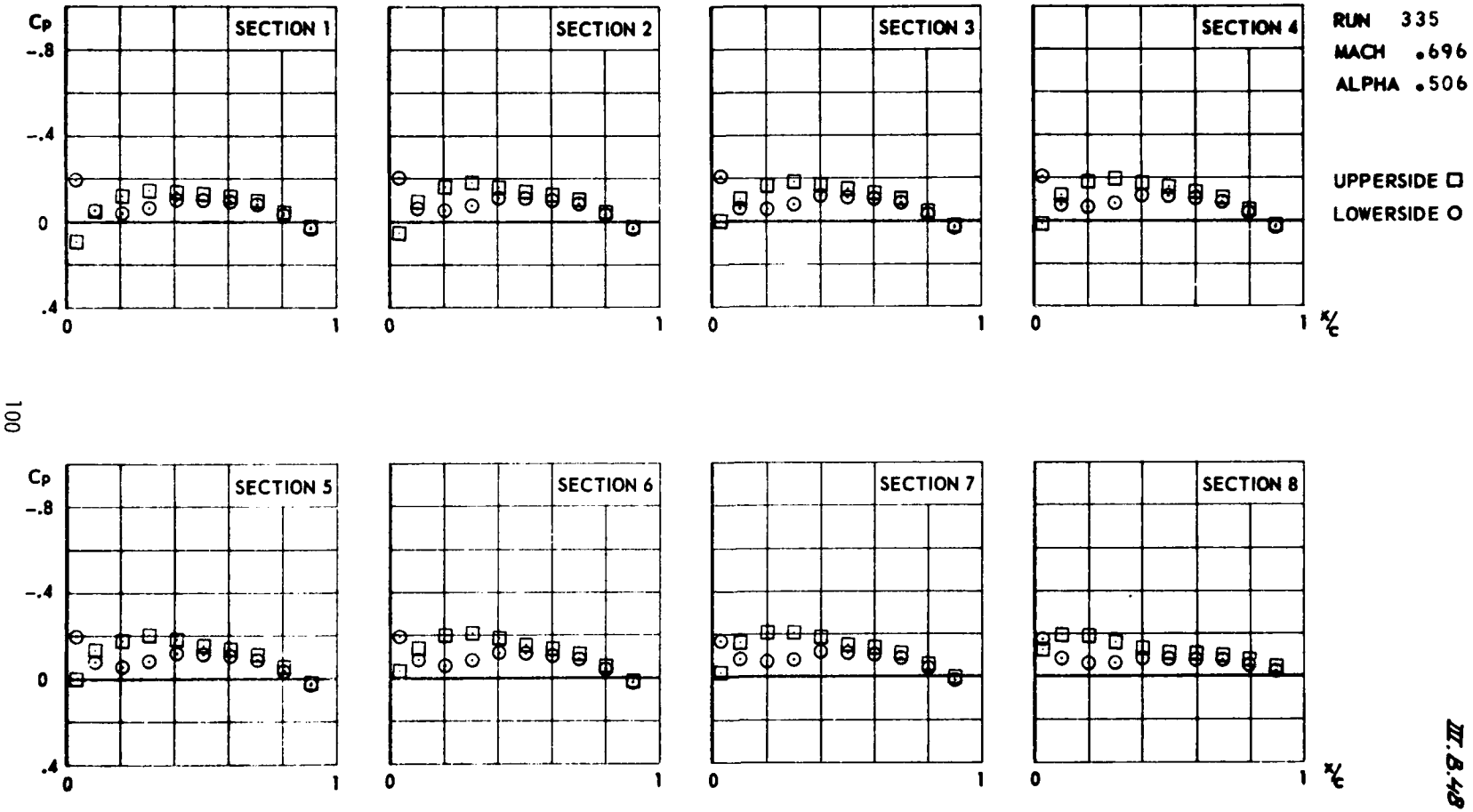

CONF.4 (WING + TIPLAUNCHER + COMPLETE MISSILE)

FIG. III.B.48

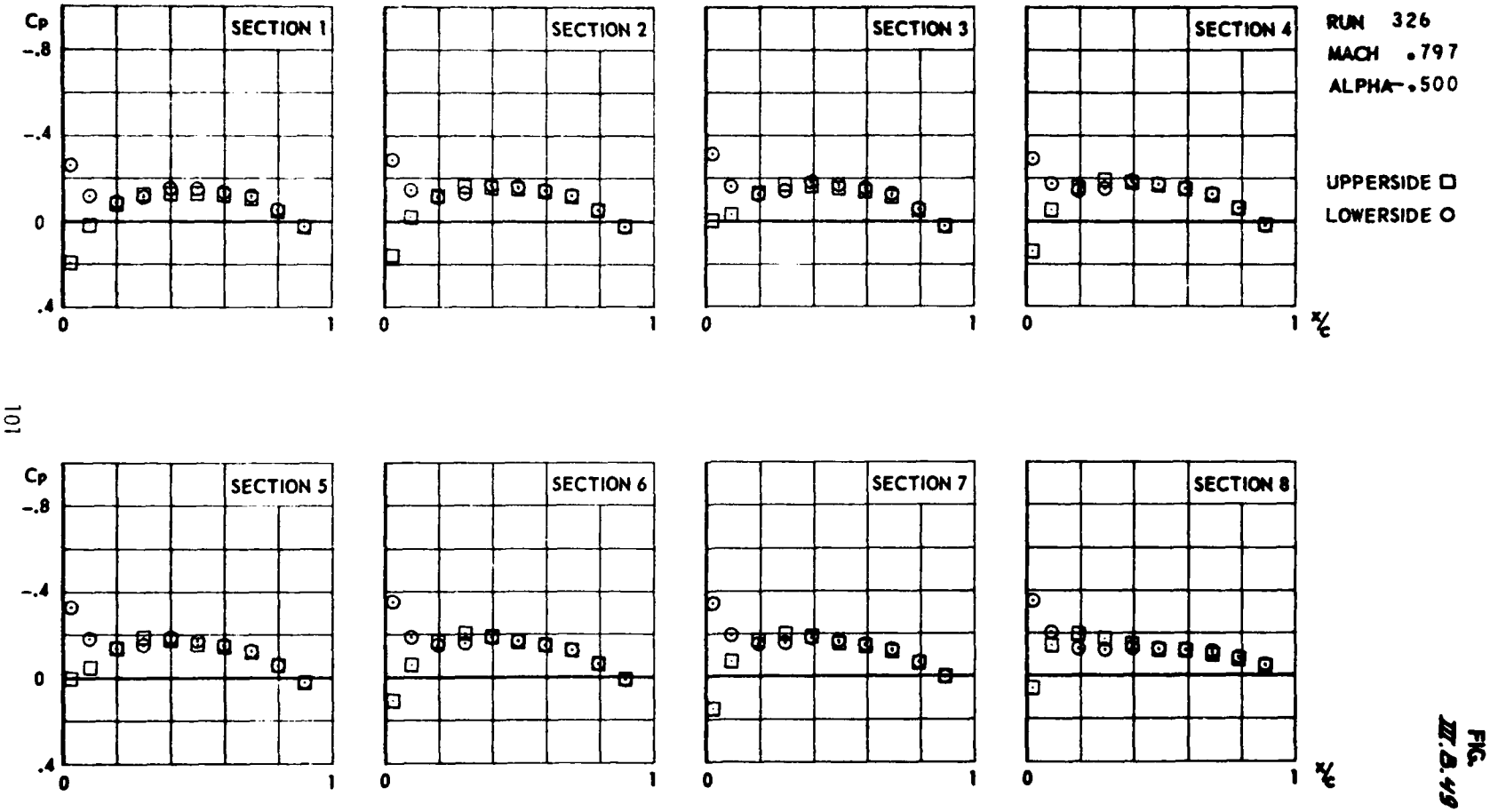

CONF.4 (WING + TIPLAUNCHER + COMPLETE MISSILE)

FIG. III.B.49

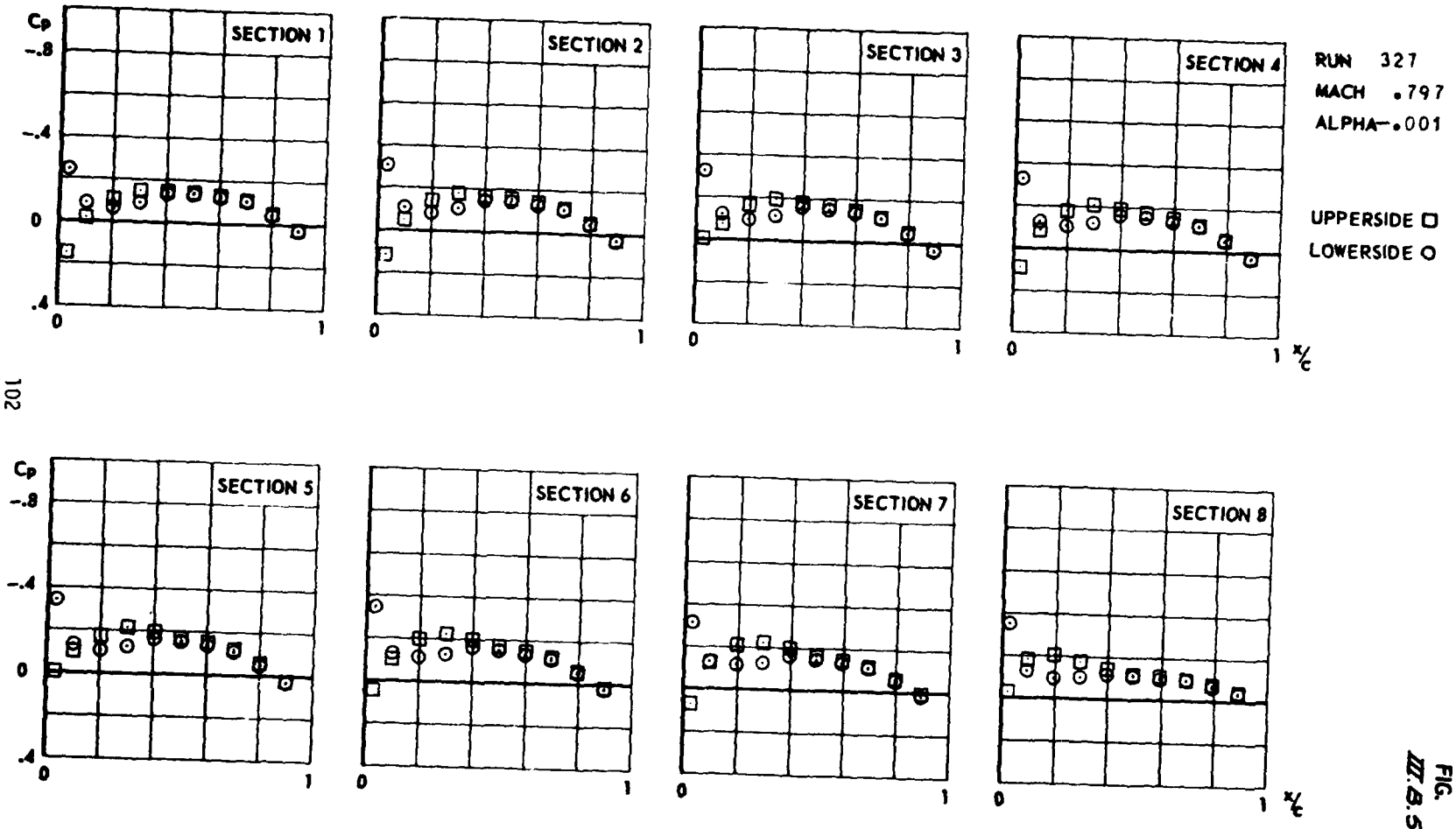

CONF.4 (WING + TIPLAUNCHER + COMPLETE MISSILE)

FIG. III.B.50

FIG.
III.B.51

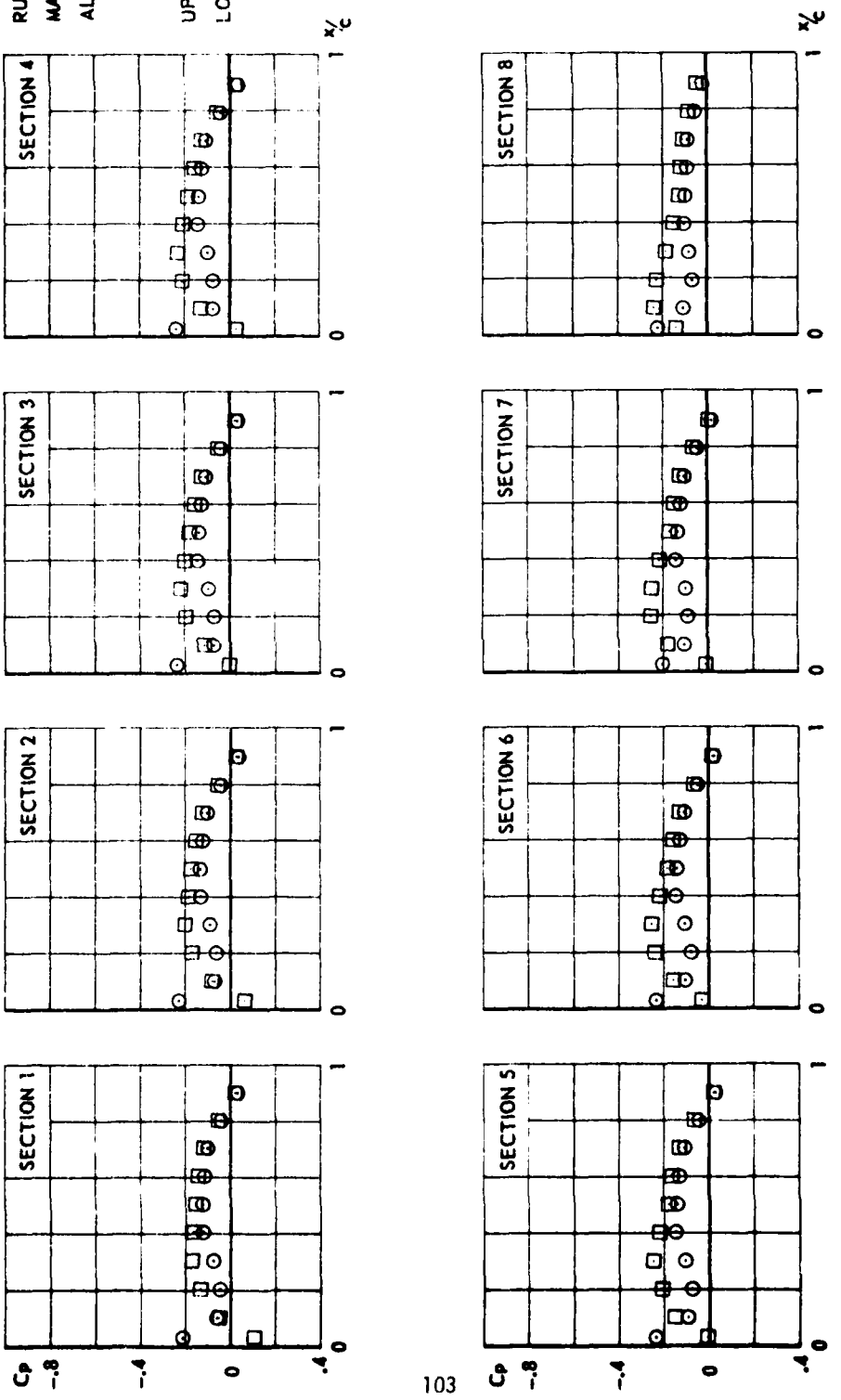

CONF.4 (WING + TIPLAUNCHER + COMPLETE MISSILE)

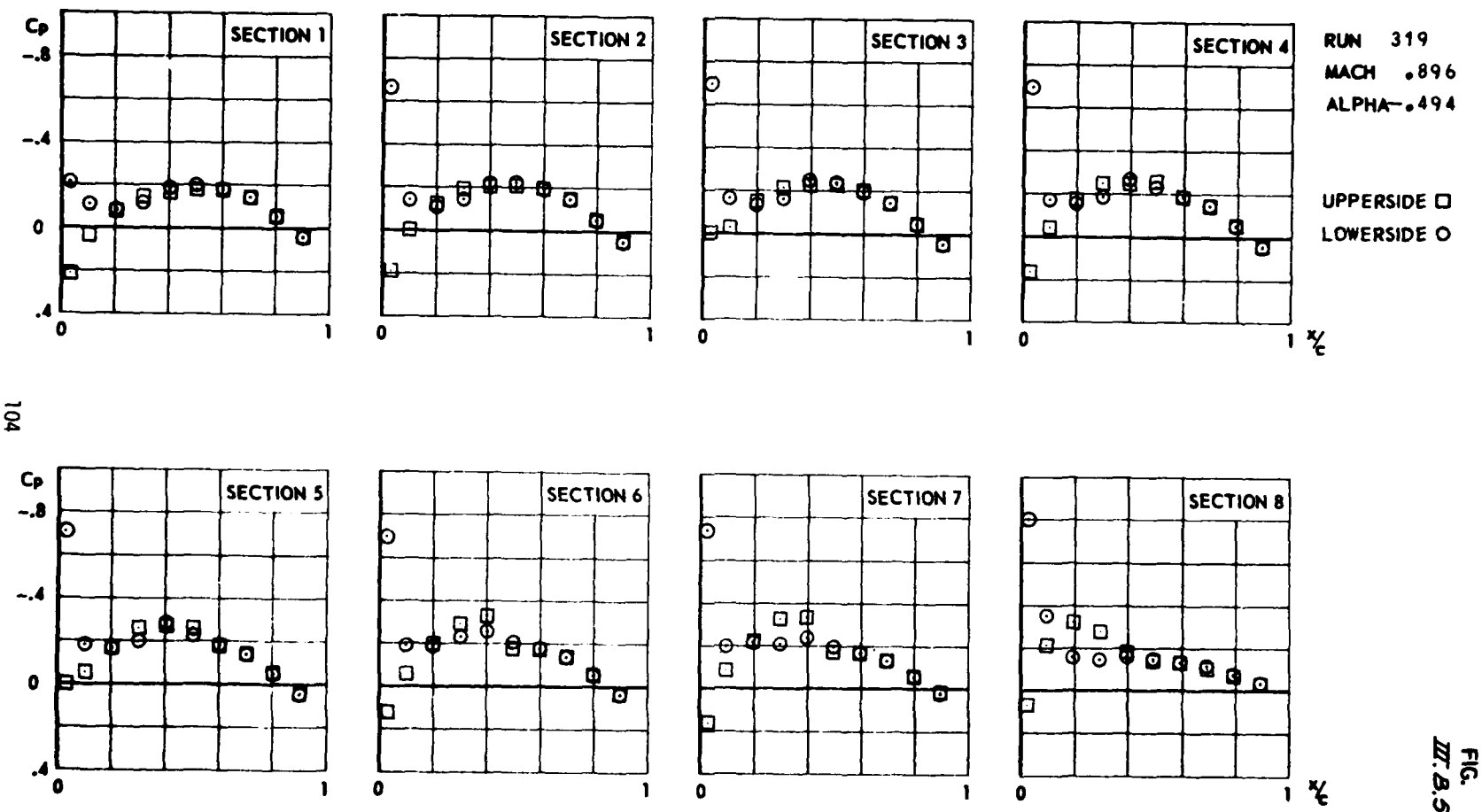

CONF.4 (WING + TIPLAUNCHER + COMPLETE MISSILE)

FIG. III.B.52

FIG.
III.B.53

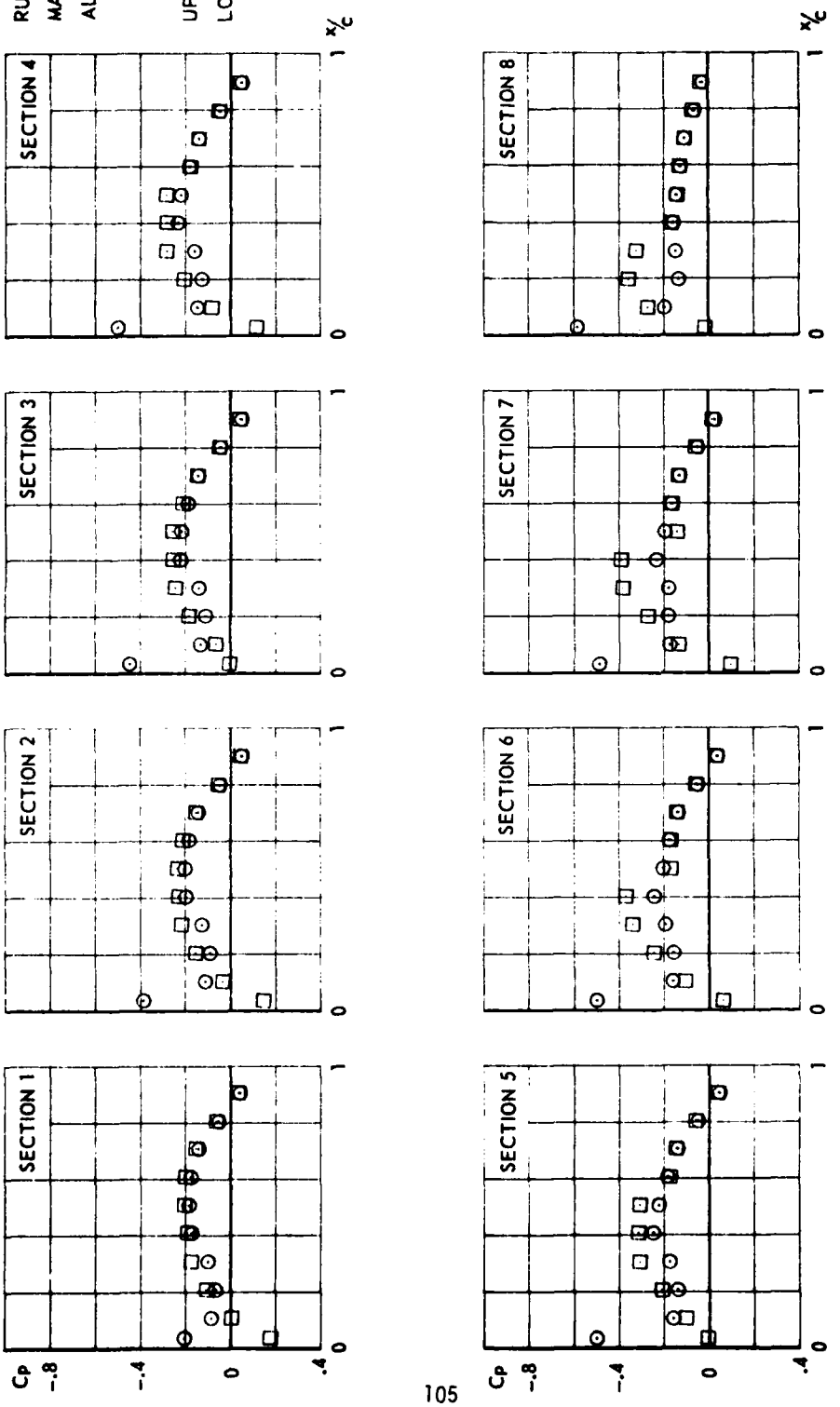

CONF.4 (W.G + TIPLAUNCHER + COMPLETE MISSILE)

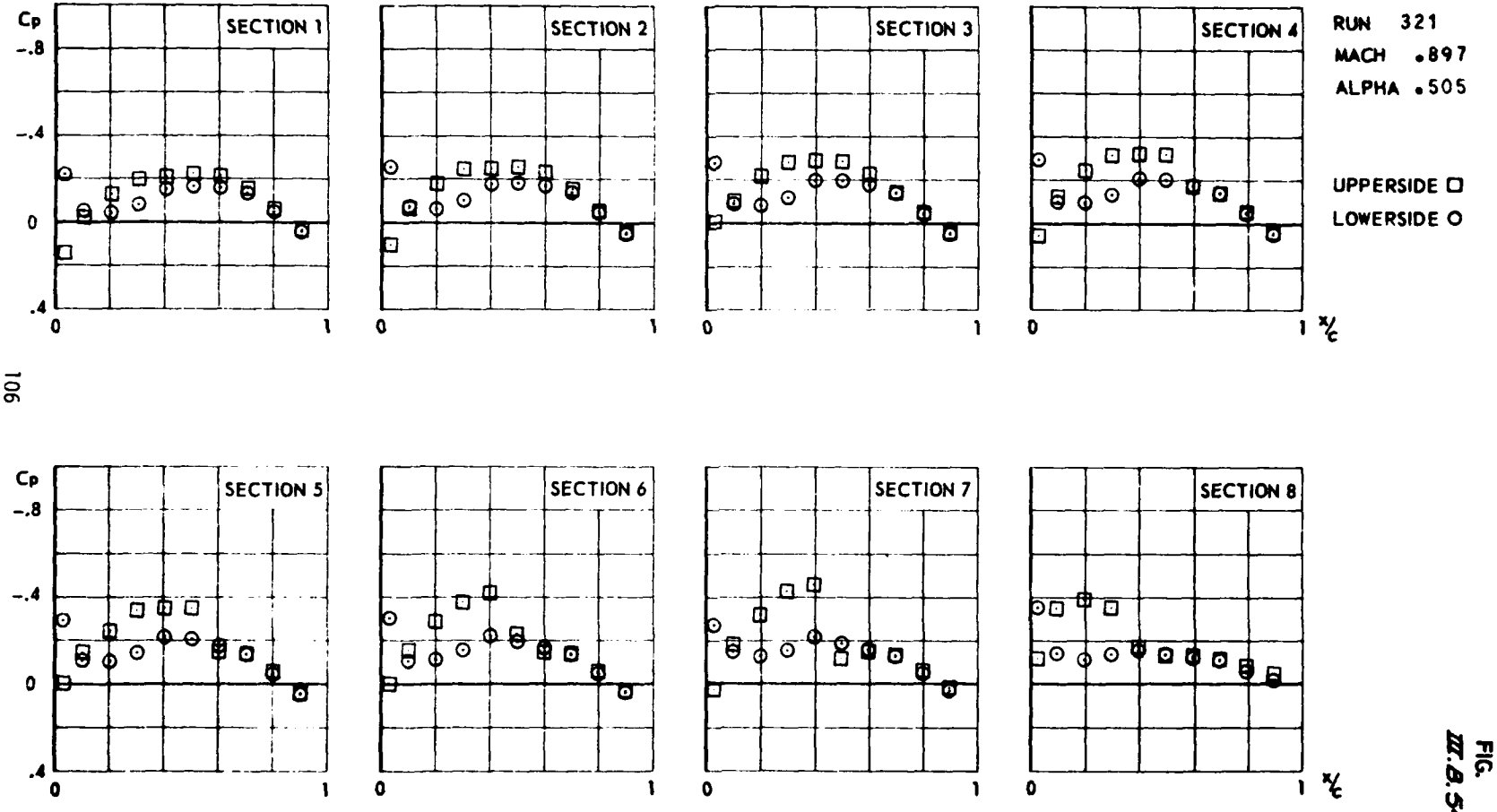

CONF.4 (WING + TIPLAUNCHER + COMPLETE MISSILE)

FIG. III.B.54

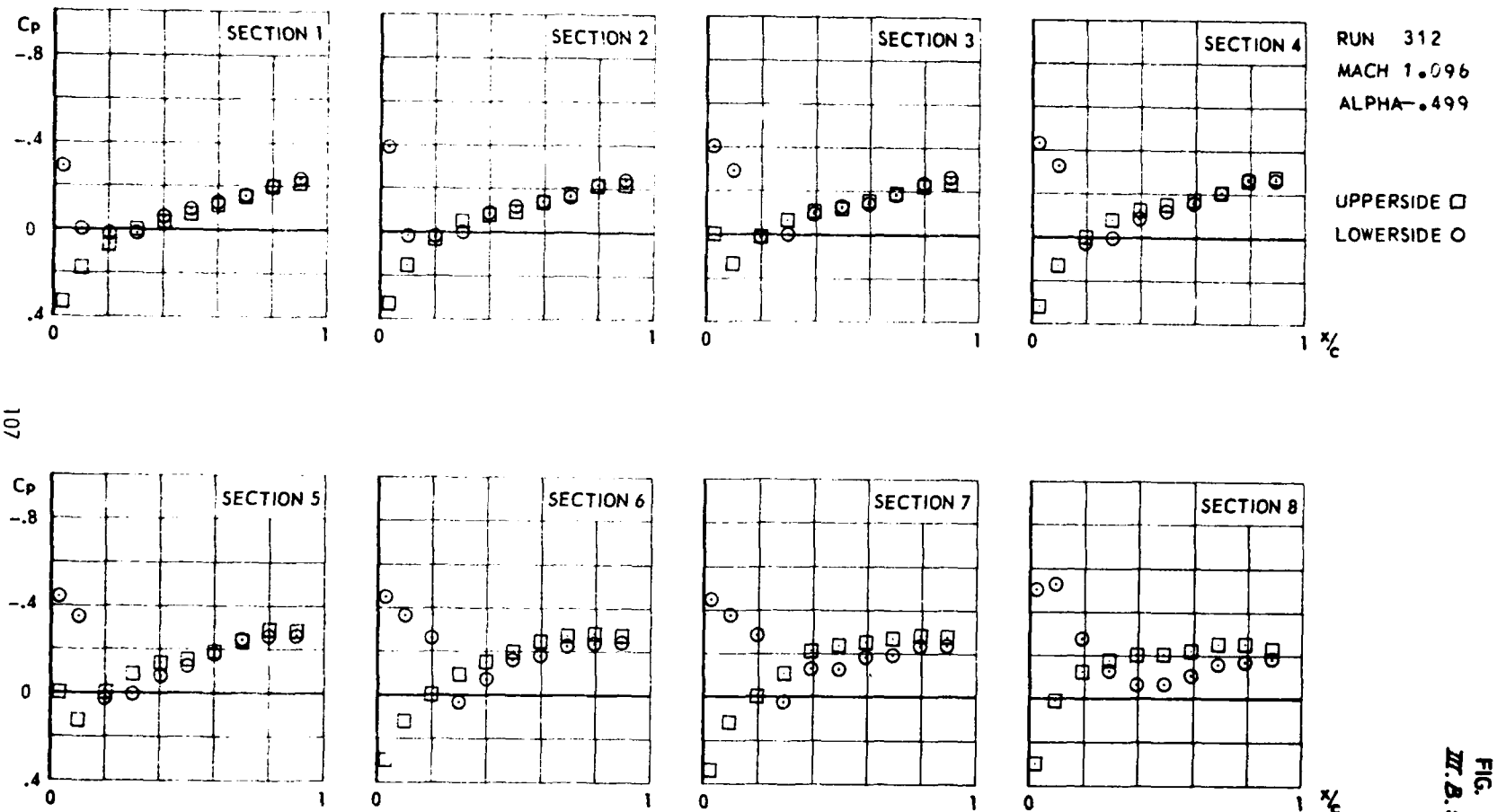

CONF.4 (WING + TIPLAUNCHER + COMPLETE MISSILE)

FIG. III.B.55

FIG.
III.B.56

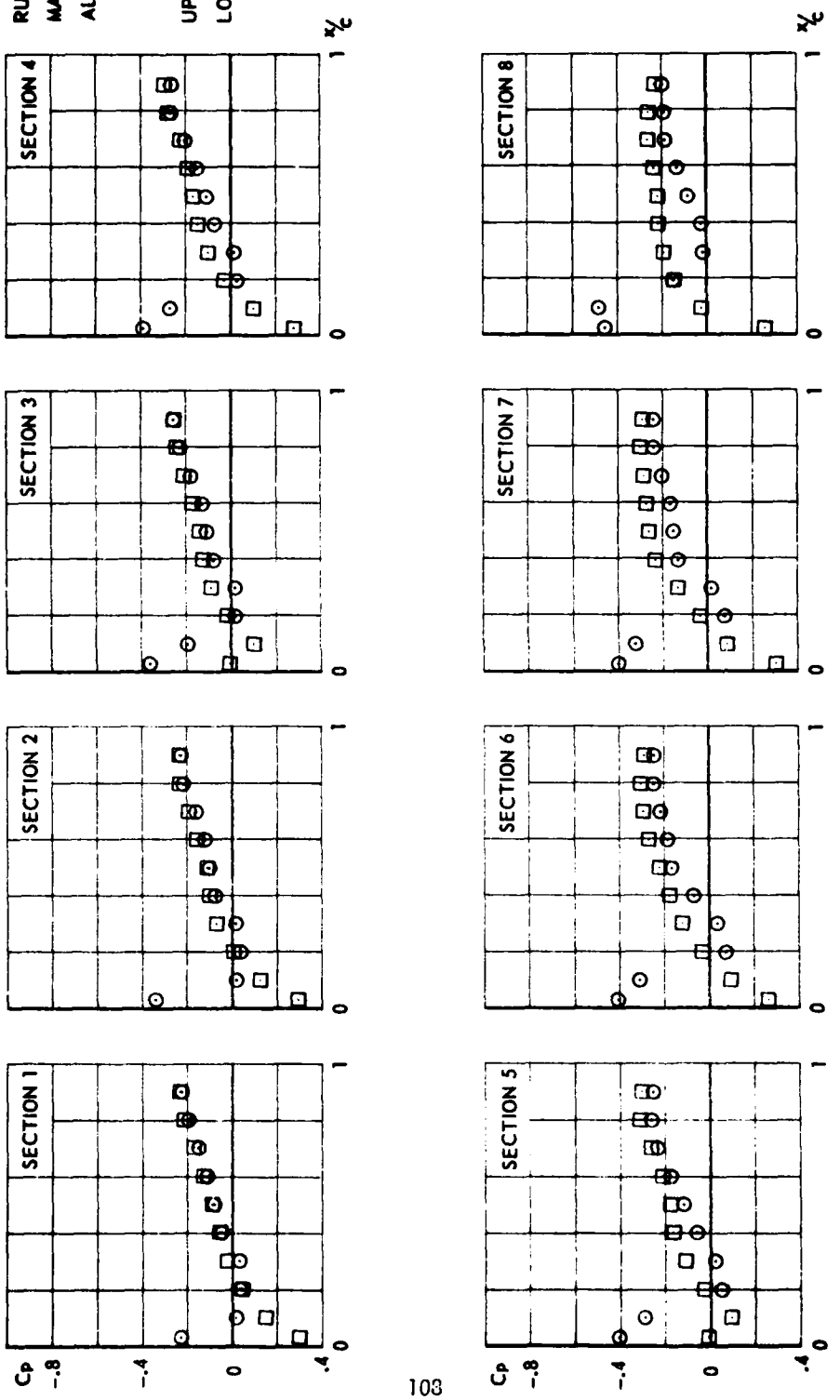

CONF.4 (WING + TIPLAUNCHER + COMPLETE MISSILE)

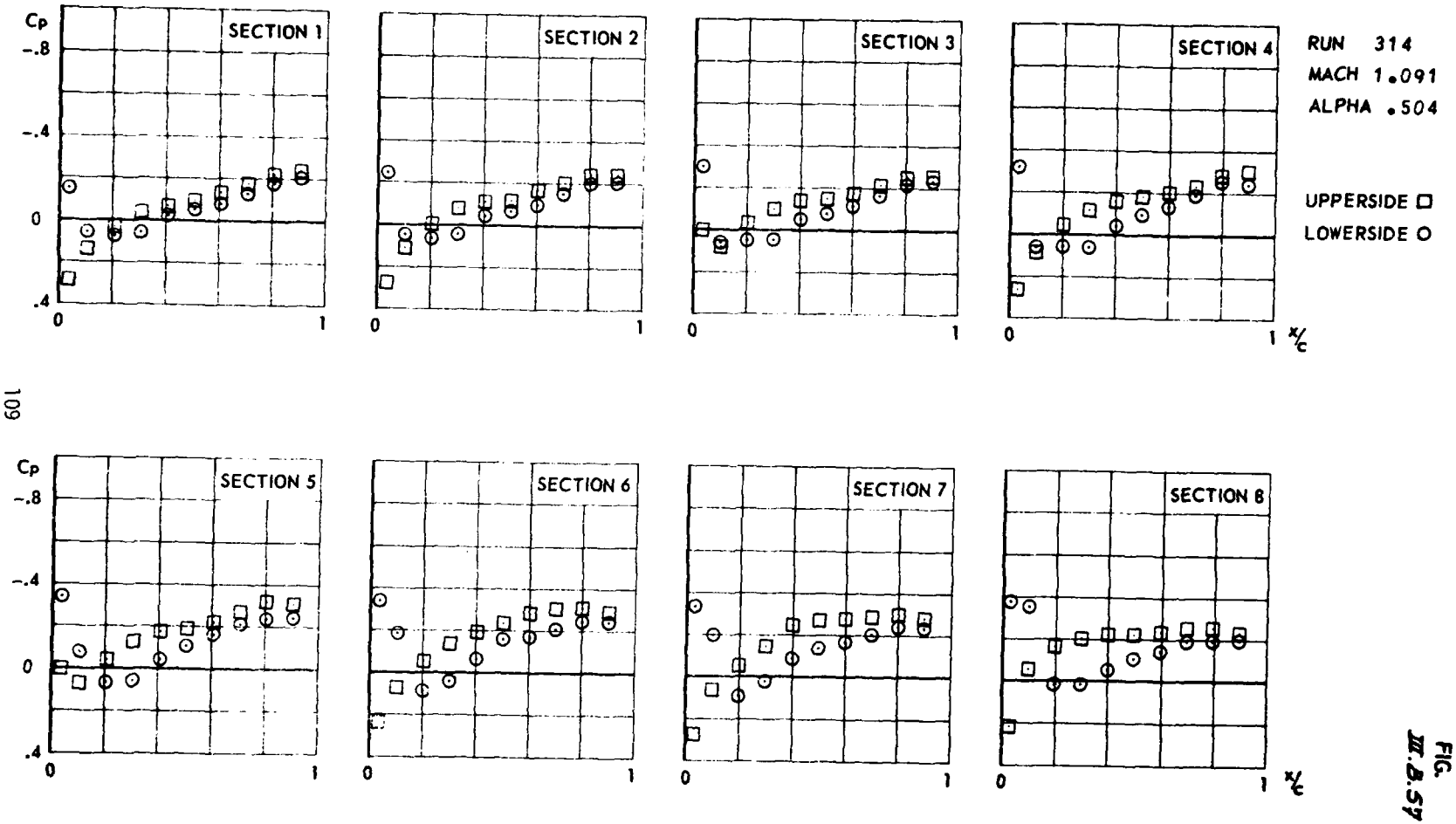

CONF.4 (WING + TIPLAUNCHER + COMPLETE MISSILE)

FIG. III.B.57

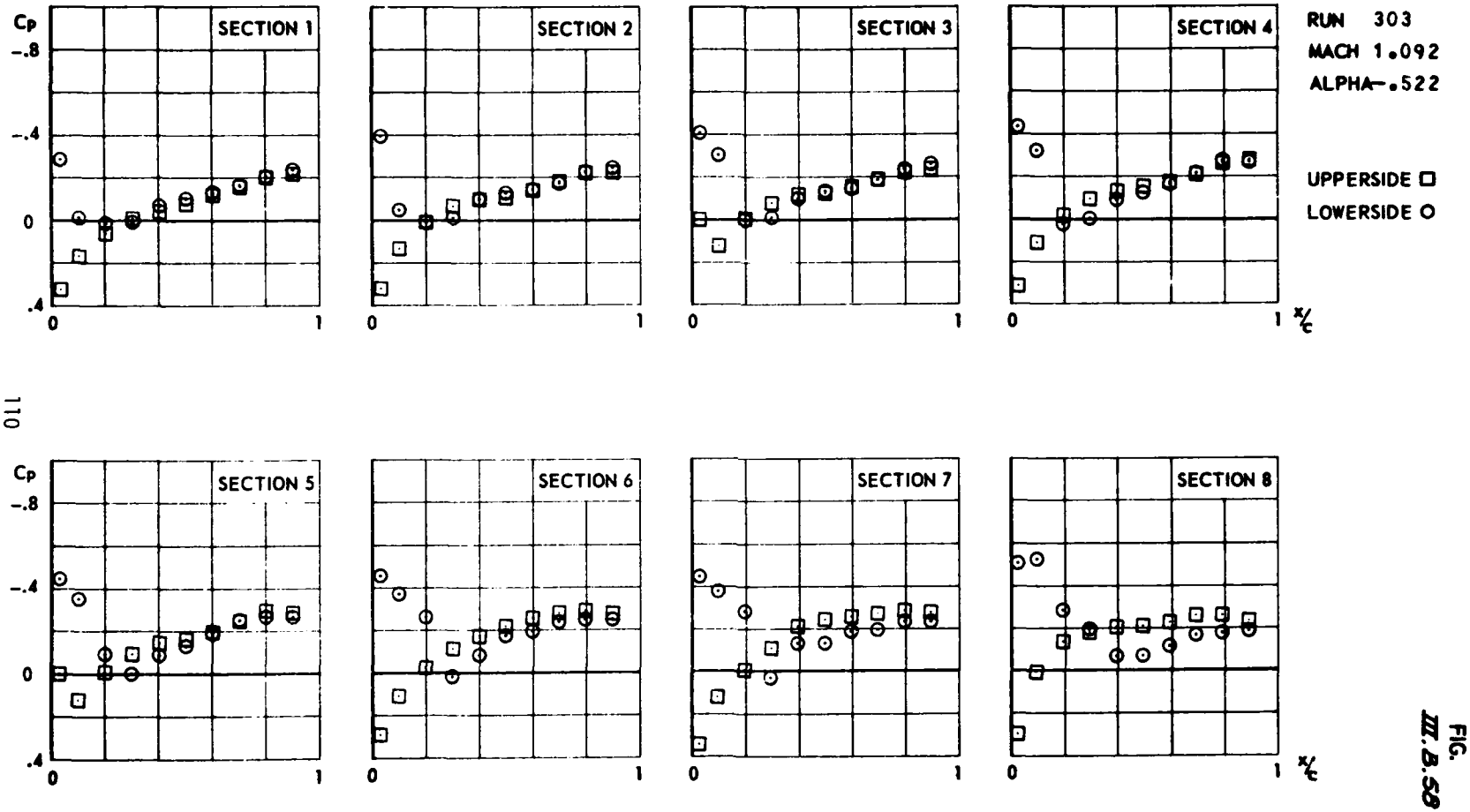

CONF.4 (WING + TIPLAUNCHER + COMPLETE MISSILE)

FIG. III.B.58

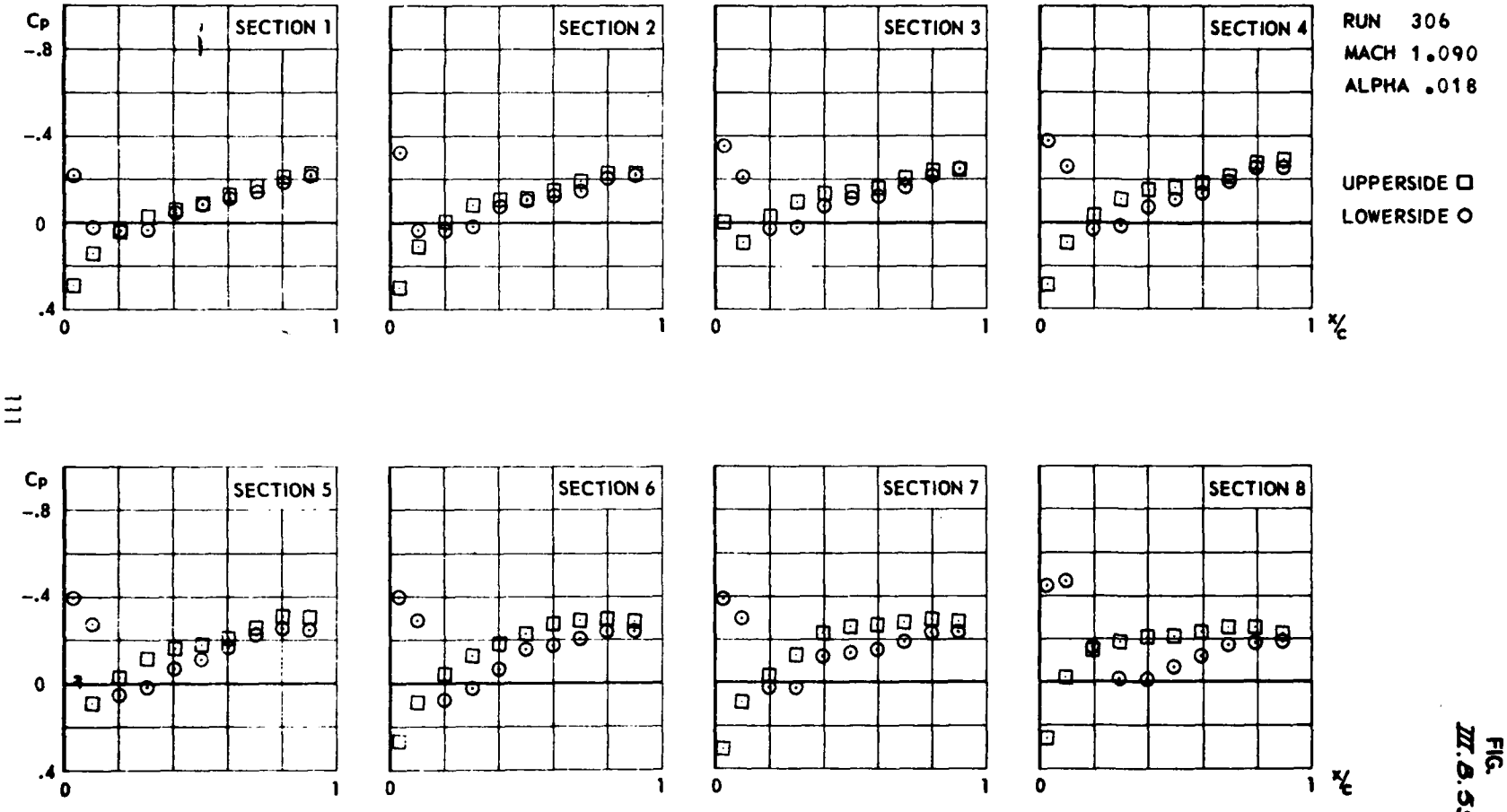

CONF.4 (WING + TIPLAUNCHER + COMPLETE MISSILE)

FIG. III.B.59

FIG.
III.B.60

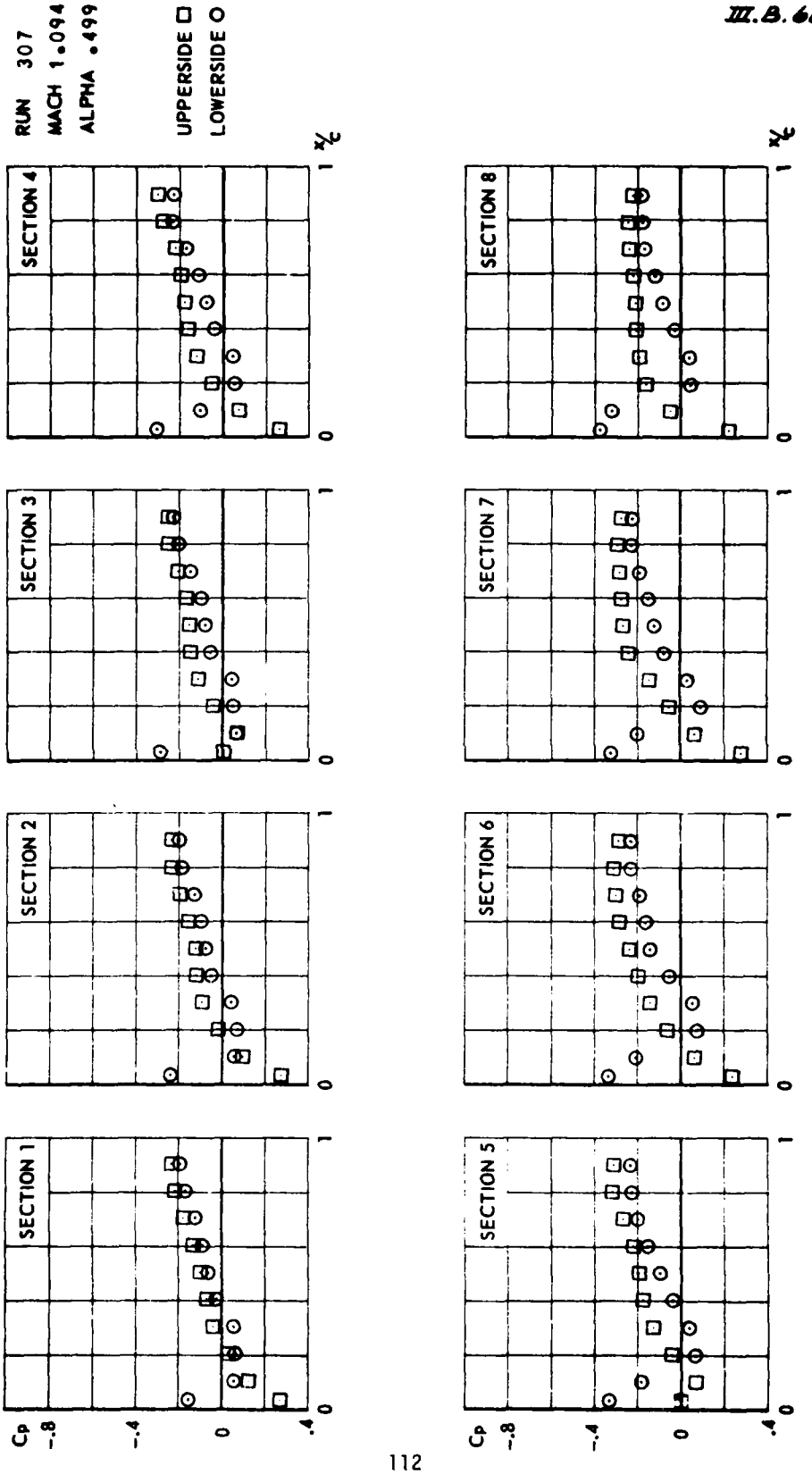

CONF.4 (WING + TIPLAUNCHER + COMPLETE MISSILE)

FIG.
III.B.61

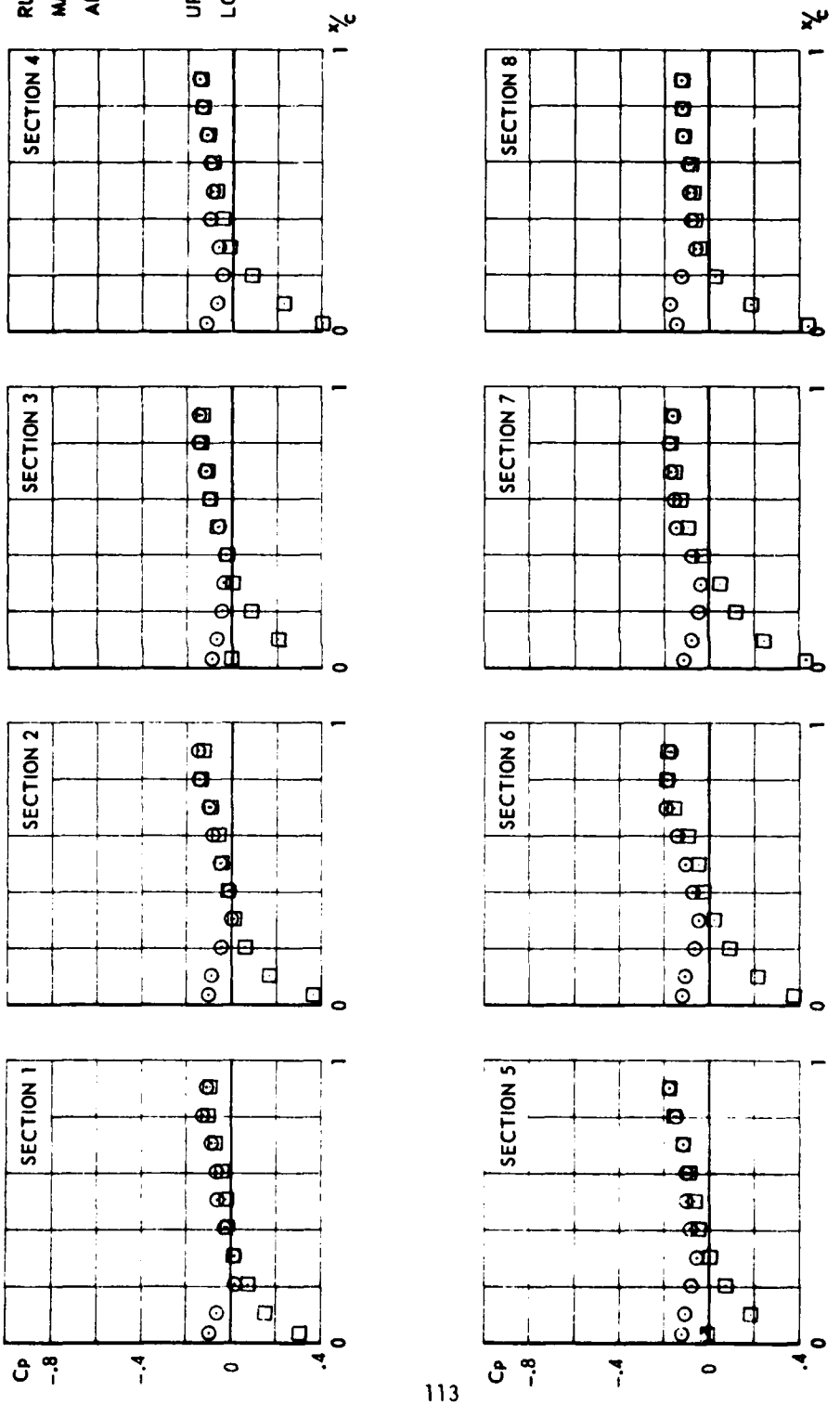

CONF.4 (WING + TIPLAUNCHER + COMPLETE MISSILE)

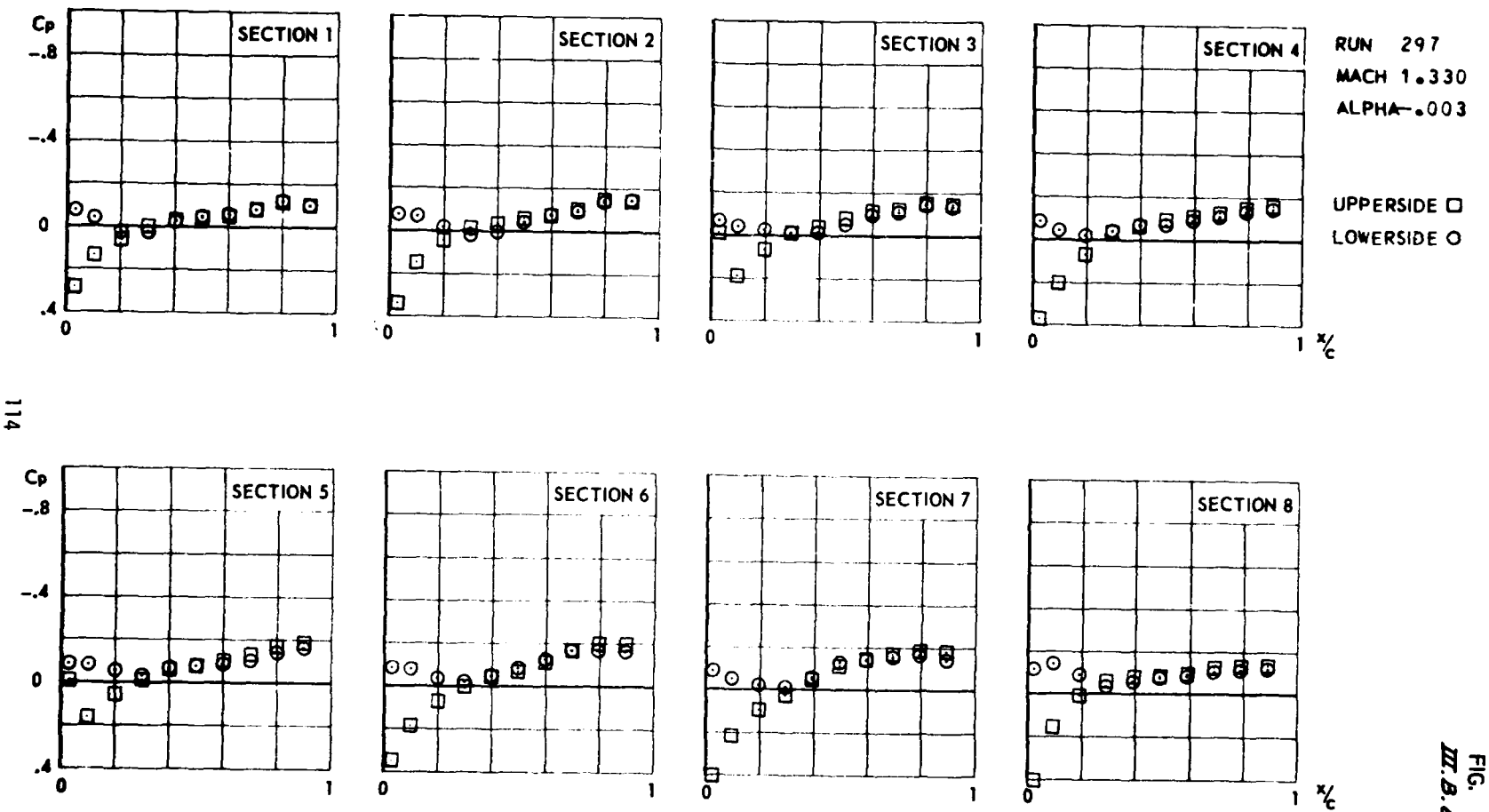

CONF.4 (WING + TIPLAUNCHER + COMPLETE MISSILE)

FIG. III.B.62

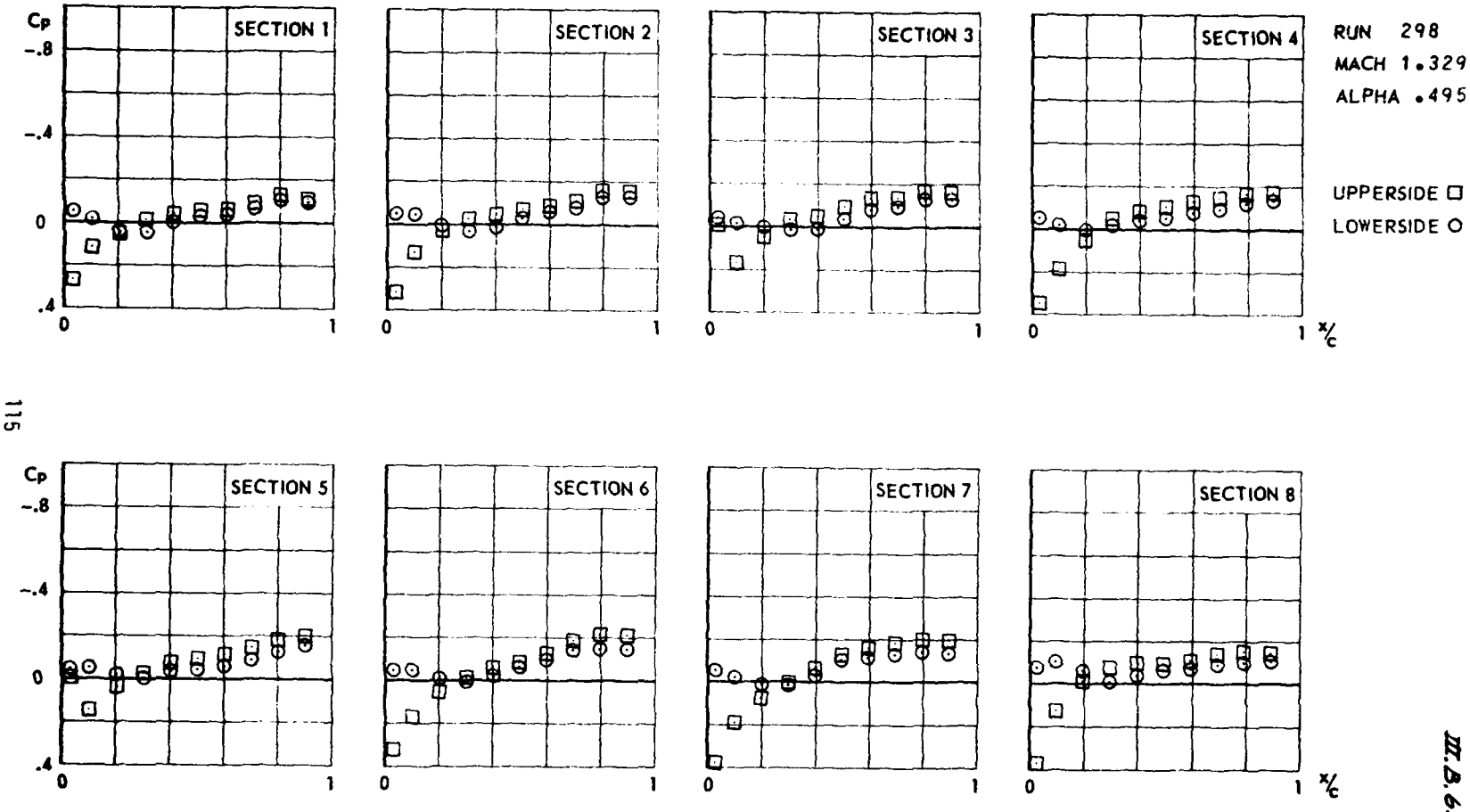

CONF.4 (WING + TIPLAUNCHER + COMPLETE MISSILE)

FIG. III.B.63

APPENDIX III.C

Unsteady Pressure Distributions*)

Wing + Tiplauncher (Conf. 1)

Run No.	Nominal Ma	Nominal $P_o \times 10^{-5}$ (Pa)	F (Hz)	K	Oscillation amplitude (degrees)	Fig. No.
202	0.6	1.0	20	0.202	0.11	III.C. 1
204			40	0.402	0.11	2
210	0.9		20	0.138	0.53	III.C. 3
211			40	0.276	0.22	4
215	1.10		20	0.116	0.53	III.C. 5
216		1.0	40	0.232	0.23	6
226	1.10	0.7	20	0.117	0.53	III.C. 7
227			40	0.234	0.12	8
221	1.35		20	0.100	0.53	III.C. 9
222		0.7	40	0.200	0.11	10

*)Note that in sections 3 and 5 the first point on the upperside, showing a zero value, is wrong. It should not be used in any evaluation. Further the values for the upperside are plotted with a reversed sign.

Wing + Tiplauncher + Missile Body (Conf. 2)

Run No.	Nominal Ma	Nominal $P_o \times 10^{-5}$ (Pa)	F (Hz)	K	Oscillation amplitude (degrees)	Fig. No.
258	0.6	1.0	20	0.201	0.52	III.C.11
259			40	0.402	0.22	12
253	0.9		20	0.138	0.53	III.C.13
254			40	0.276	0.22	14
247	1.10		20	0.116	0.53	III.C.15
248		1.0	40	0.232	0.23	16
242	1.10	0.7	20	0.116	0.52	III.C.17
243			40	0.232	0.22	18
236	1.35		20	0.100	0.53	III.C.19
237		0.7	40	0.199	0.11	20

Wing + Tiplauncher + Missile Body + Aft Wings (Conf. 3)

Run No.	Nominal Ma	Nominal $P_o \times 10^{-5}$ (Pa)	F (Hz)	K	Oscillation amplitude (degrees)	Fig. No.
288	0.6	1.0	20	0.201	0.52	III.C.21
289			40	0.402	0.22	22
283	0.9		20	0.139	0.53	III.C.23
284			40	0.279	0.22	24
277	1.10		20	0.116	0.52	III.C.25
278		1.0	40	0.232	0.23	26
272	1.10	0.7	20	0.117	0.52	III.C.27
273			40	0.234	0.11	28
267	1.35		20	0.100	0.53	III.C.29
268		0.7	40	0.200	0.22	30

Wing + Tiplauncher + Complete Missile (Conf. 4)

Run No.	Nominal Ma	Nominal $P_o \times 10^{-5}$ (Pa)	F (Hz)	K	Oscillation amplitude (degrees)	Fig. No.
351	0.6	1.0	10	0.100	0.11	III.C.31
350			20	0.200	0.11	32
344			20	0.200	0.53	33
349			30	0.300	0.11	34
348			40	0.401	0.11	35
336	0.7		10	0.086	0.53	III.C.36
337			20	0.173	0.53	37
338			30	0.260	0.37	38
339			40	0.346	0.22	39
357	0.8		10	0.076	0.11	III.C.40
358			20	0.153		41
359			30	0.229		42
360			40	0.305		43
352	0.9		10	0.069		III.C.44
353			20	0.138		45
354			30	0.207		46
355			40	0.275	0.11	47
315	1.10		10	0.058	0.55	III.C.48
316			20	0.116	0.53	49
317			30	0.174	0.38	50
318		1.0	40	0.231	0.23	51
308	1.10	0.7	10	0.058	0.54	III.C.52
309			20	0.117	0.52	53
310			30	0.175	0.37	54
311			40	0.234	0.22	55
299	1.35		10	0.051	0.53	III.C.56
300			20	0.101	0.53	57
301			30	0.149	0.37	58
302		0.7	40	0.199	0.22	59

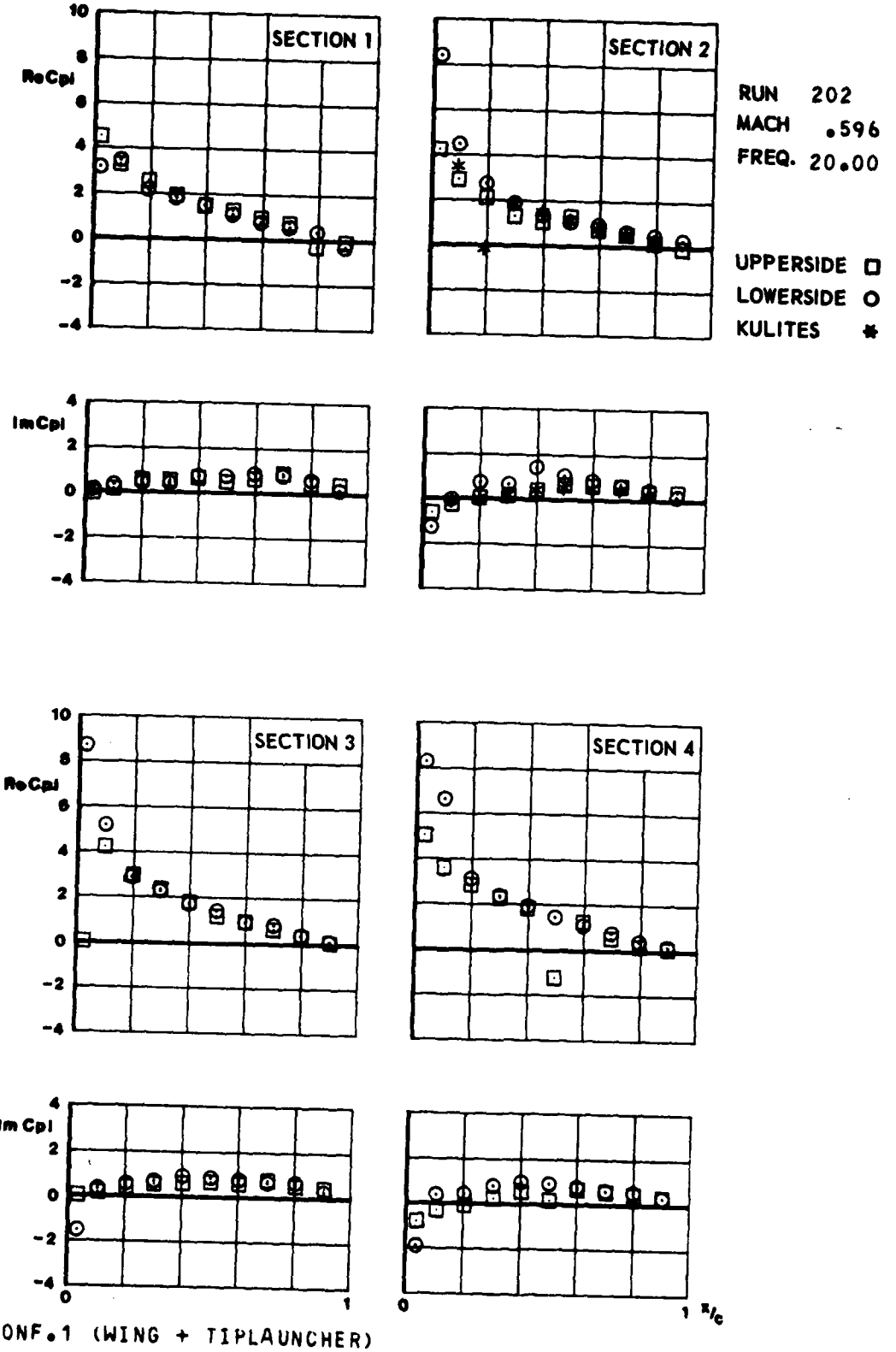

CONF.1 (WING + TIPLAUNCHER)

FIG.
III.C.1.b

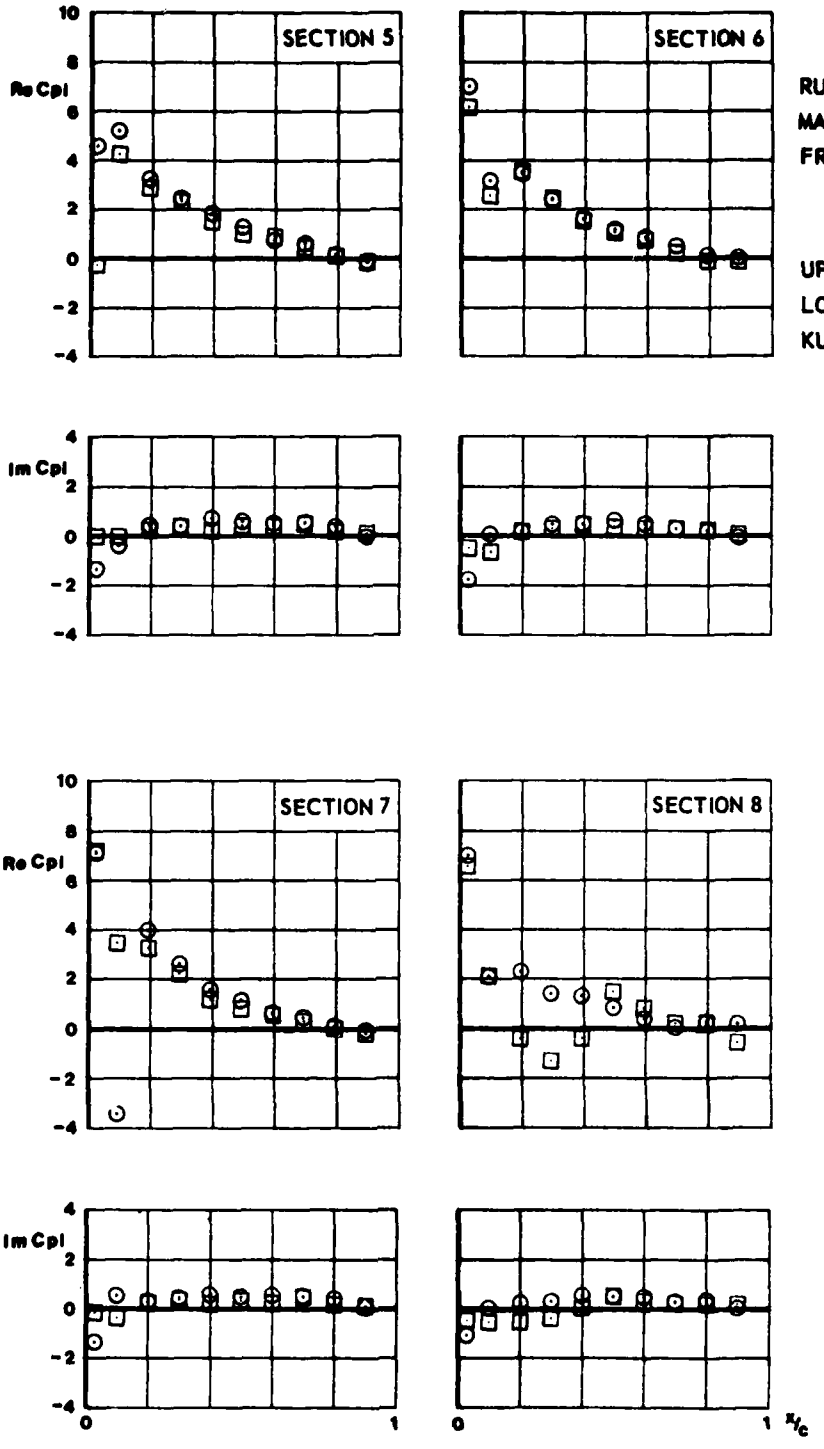

CONF. 1 (WING + TIPLAUNCHER)

FIG.
III.C.2.a

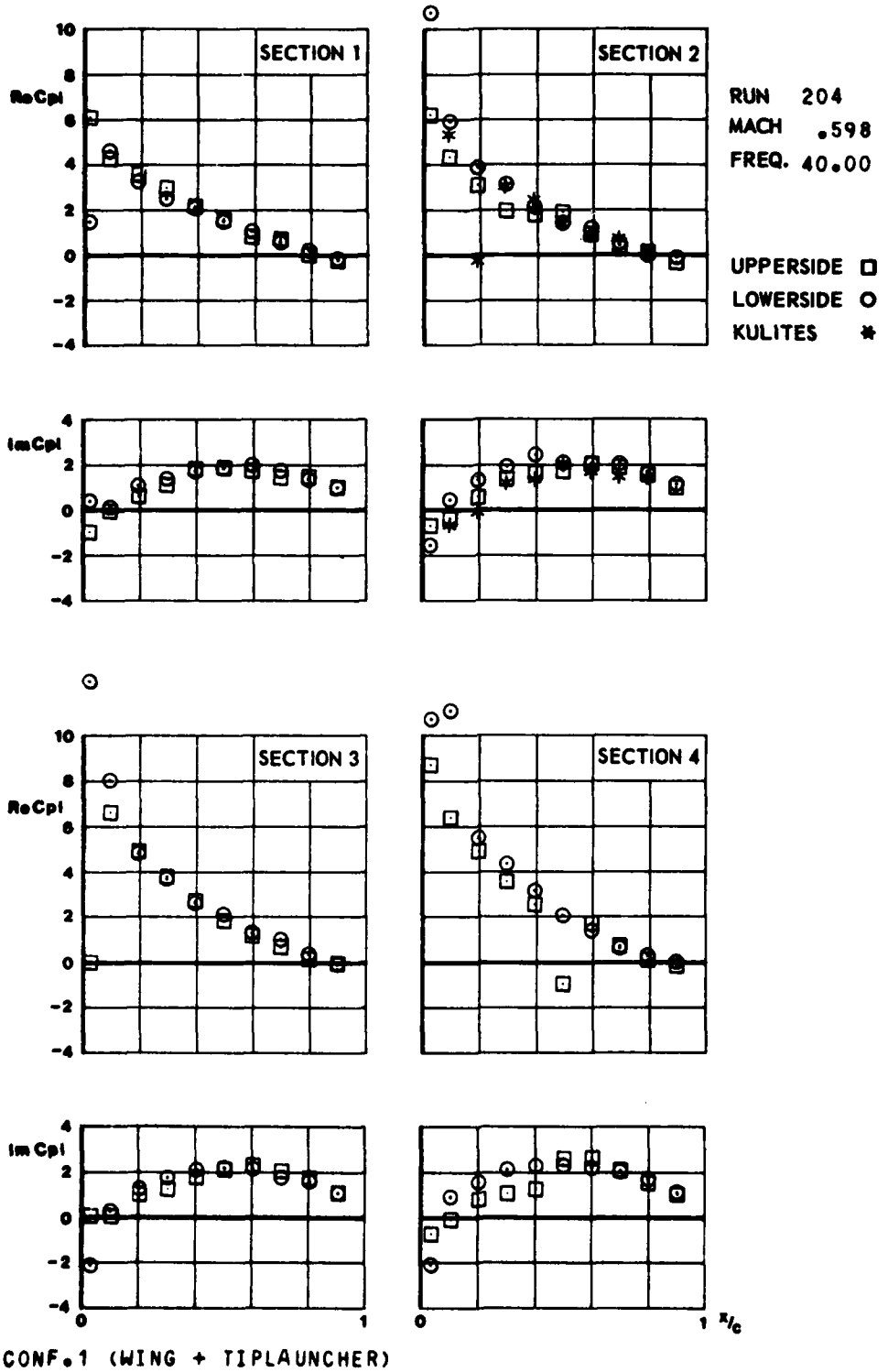

CONF.1 (WING + TIPLAUNCHER)

FIG.
III.C.2.6

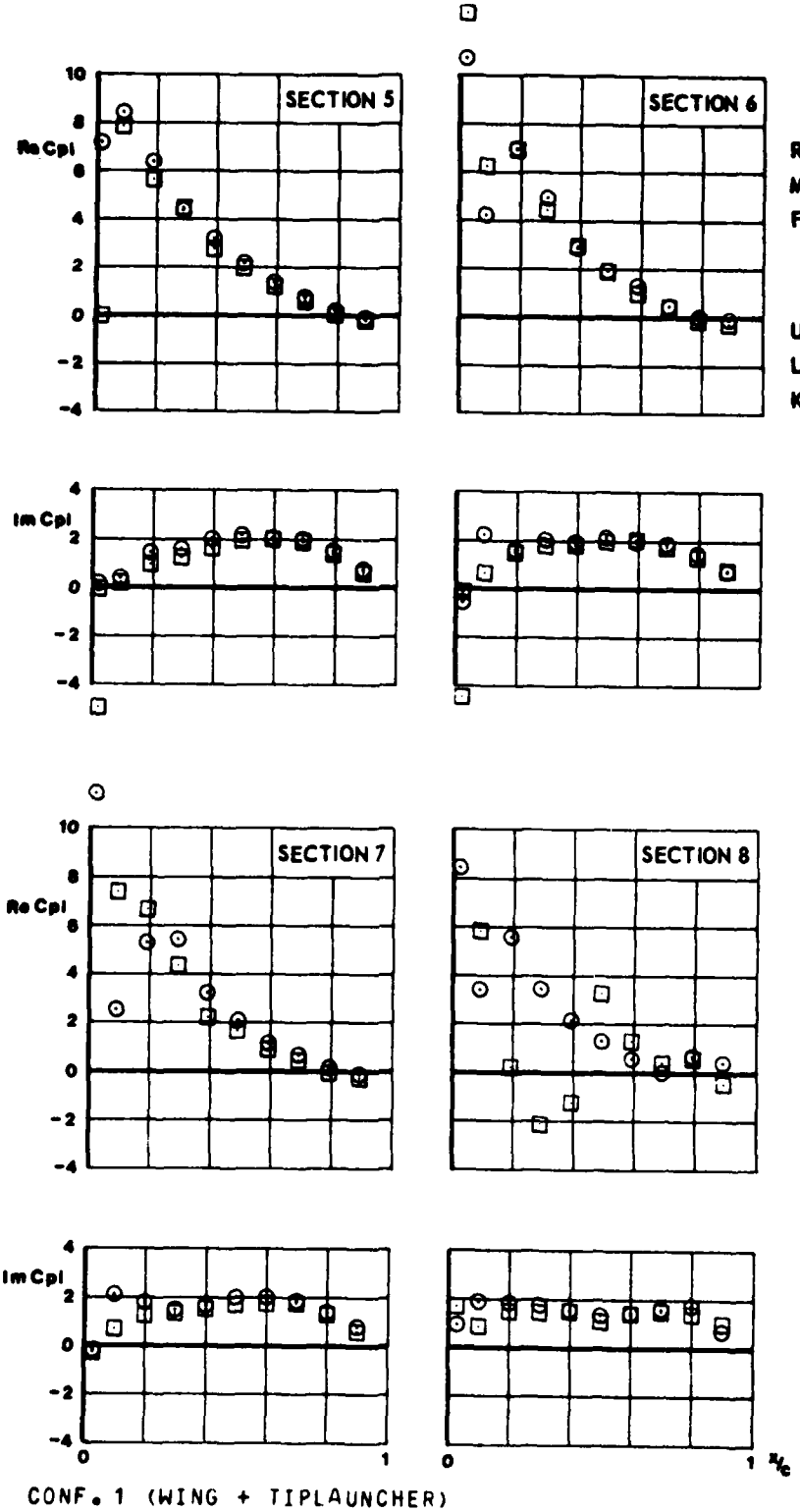

CONF. 1 (WING + TIPLAUNCHER)

FIG.
III.C.3.a

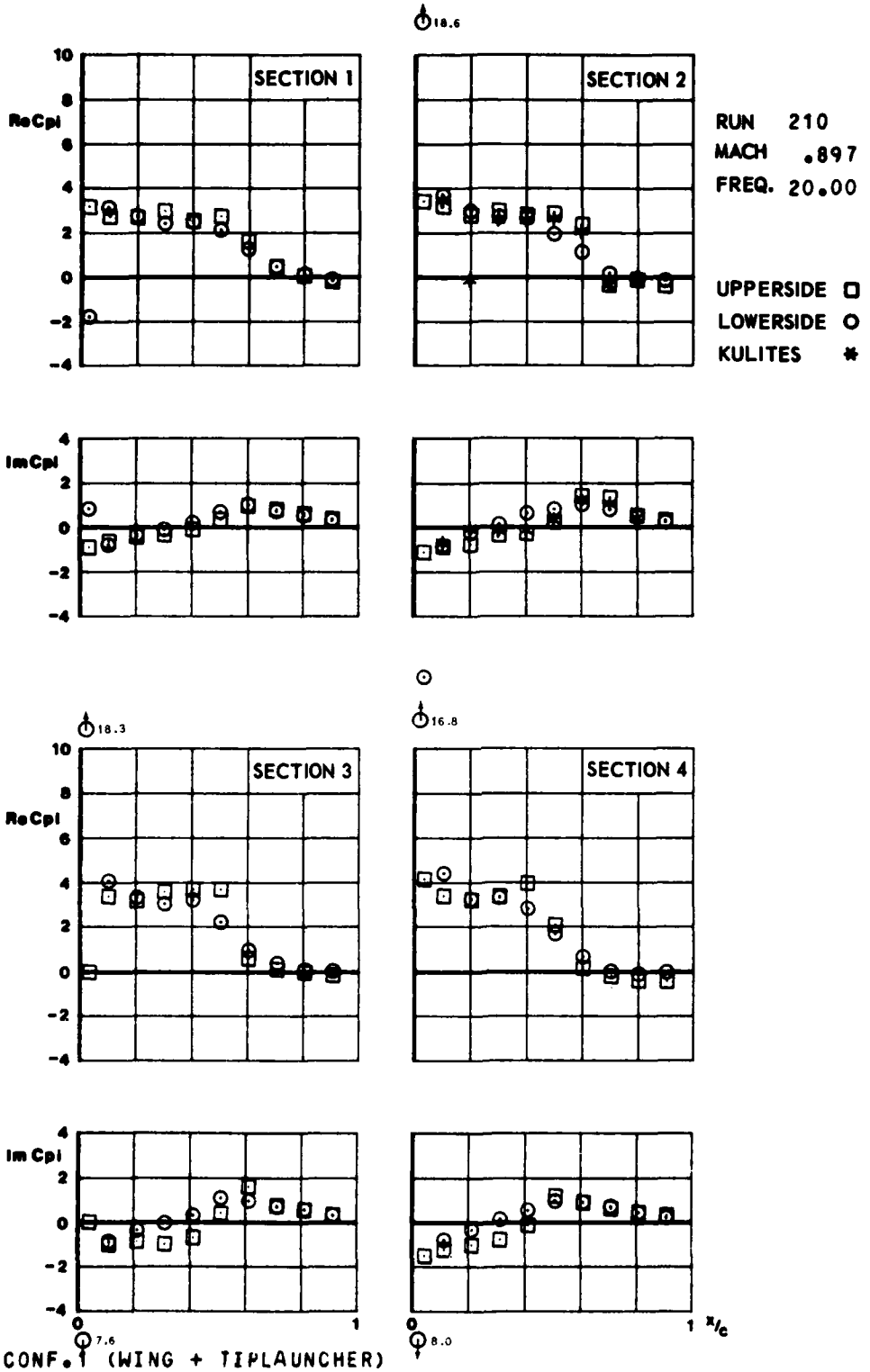
18.6
SECTION 1
SECTION 2
ReCpl
ImCpl
RUN 210
MACH .897
FREQ. 20.00
UPPERSIDE
LOWERSIDE
KULITES
18.3
16.8
SECTION 3
SECTION 4
ReCpl
Im Cpl
7.6
8.0
x/c
CONF. 1 (WING + TIPLAUNCHER)

FIG.
III.C.3.b

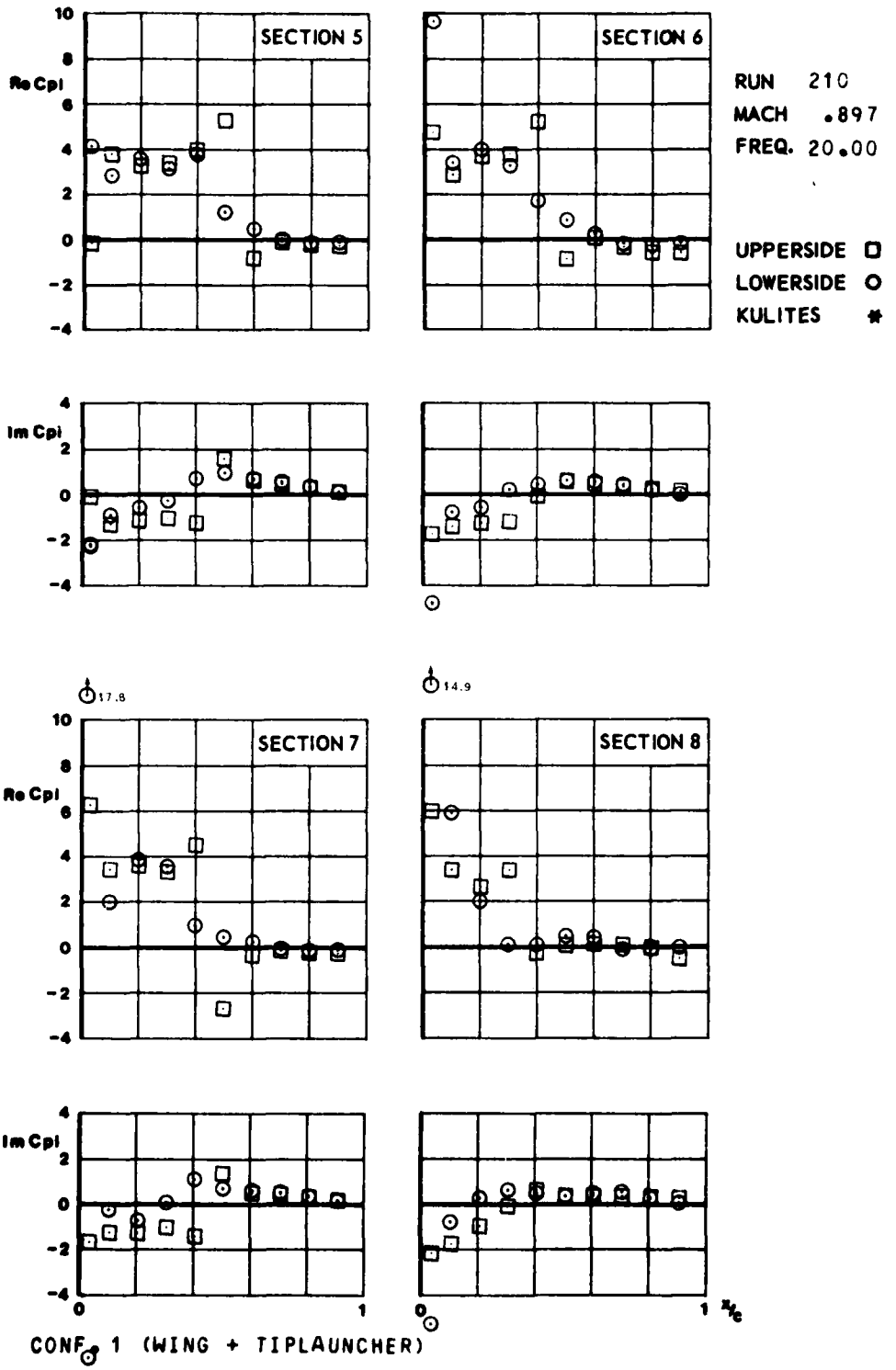

CONF 1 (WING + TIPLAUNCHER)

FIG.
III.C.4.a

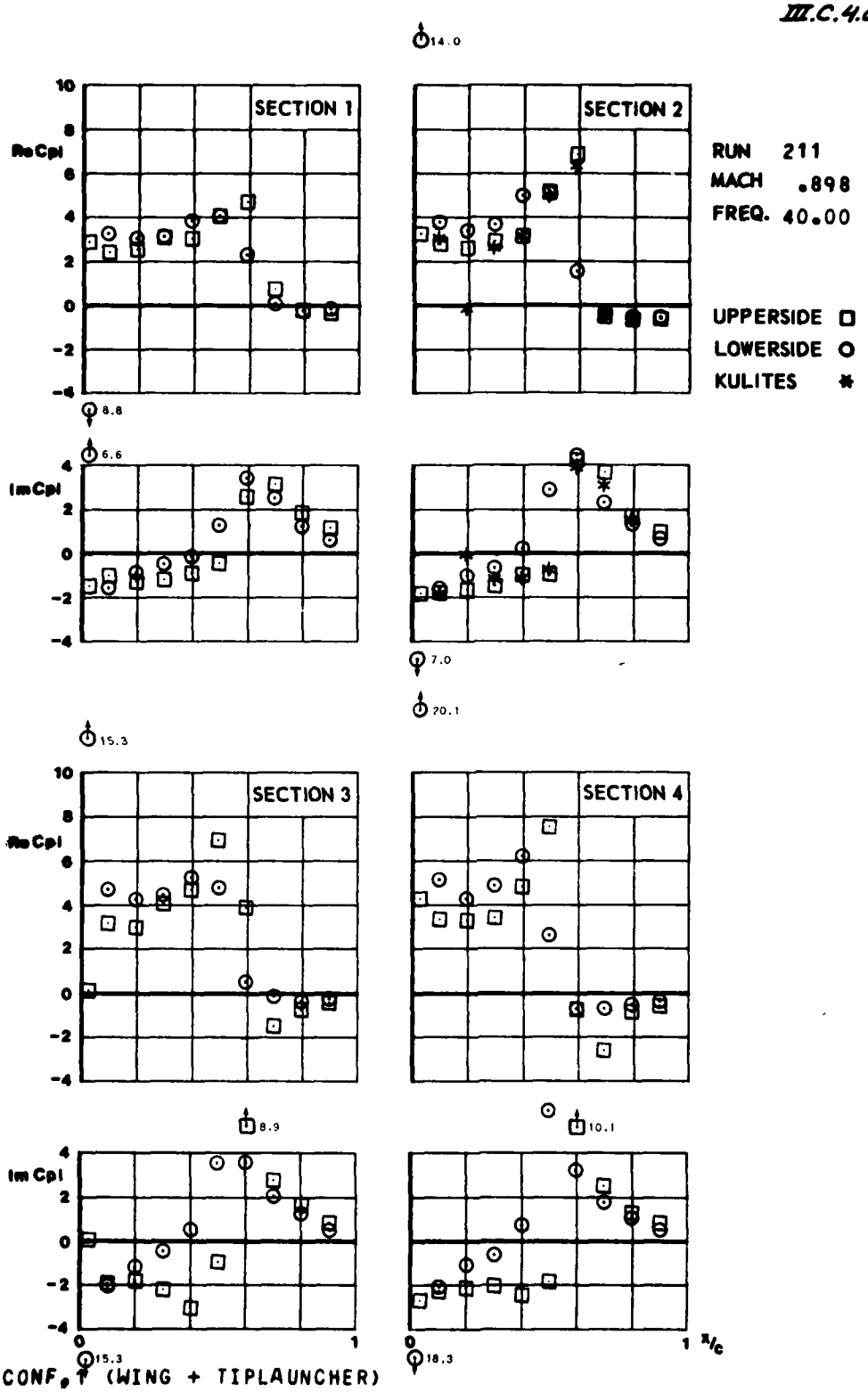

CONF. 1 (WING + TIPLAUNCHER)

FIG.
III.C.4.b

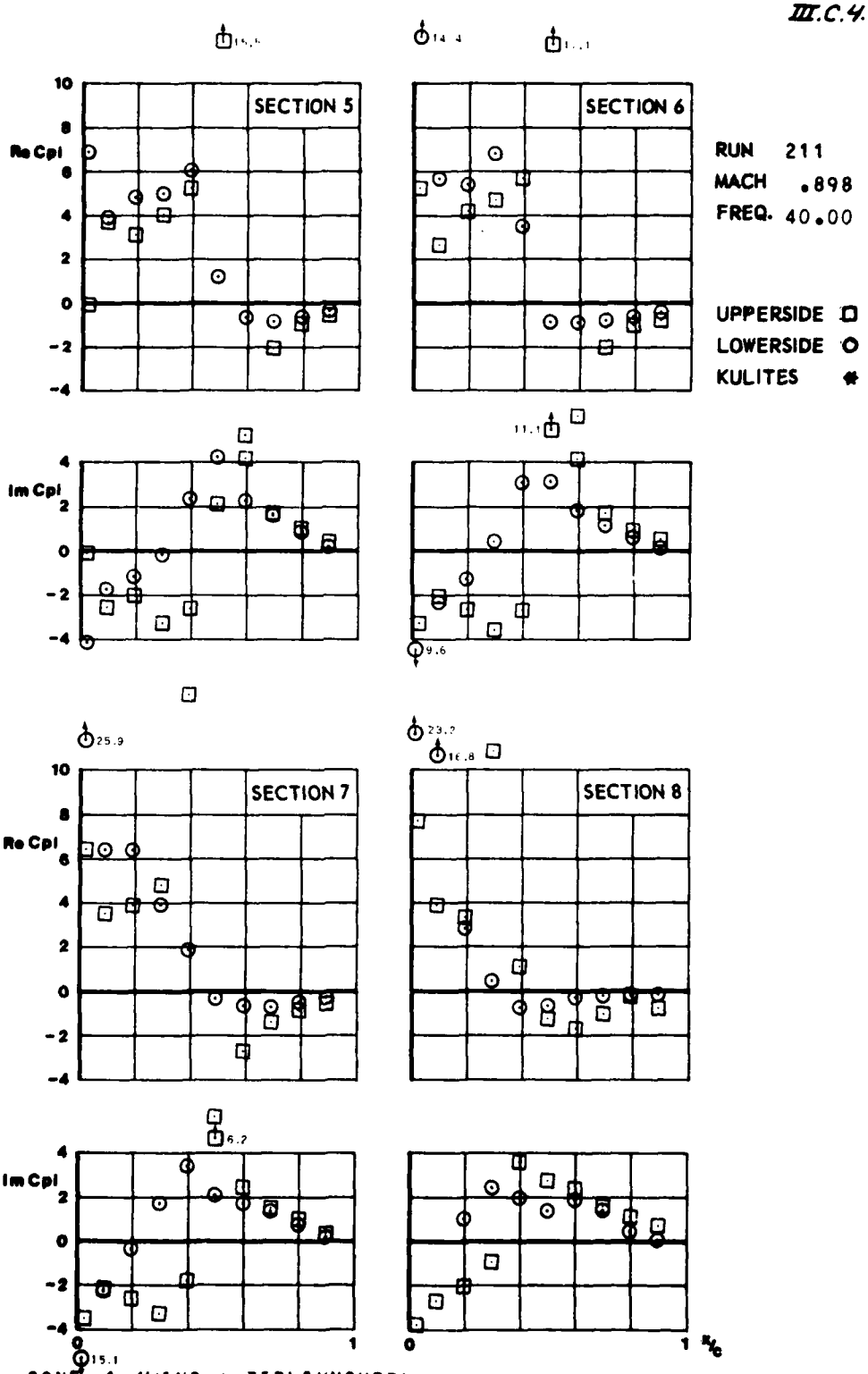

CONF. 1 (WING + TIPLAUNCHER)

FIG.
III.C.5.a

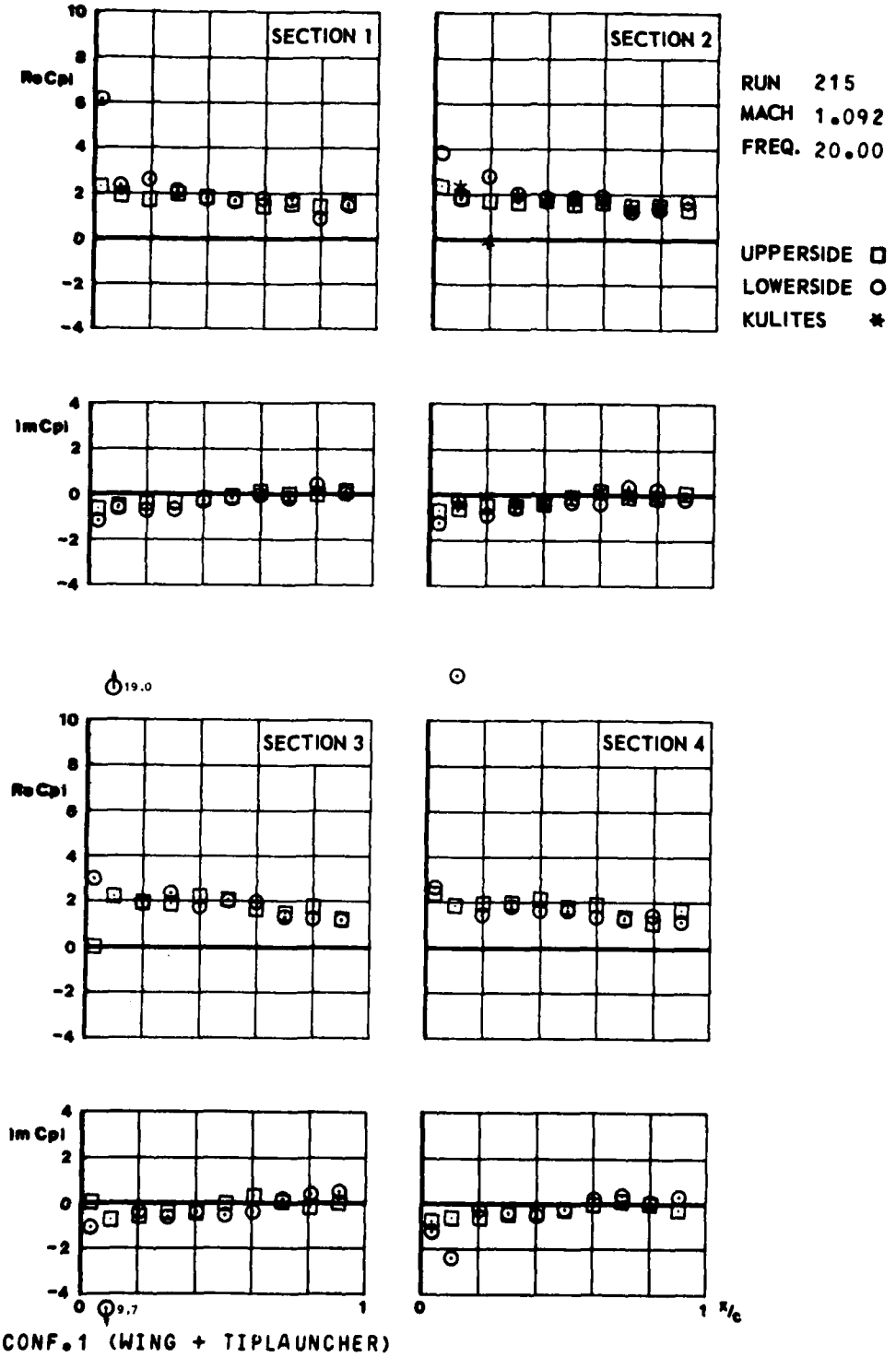

CONF.1 (WING + TIPLAUNCHER)

FIG.
III.C.5.b

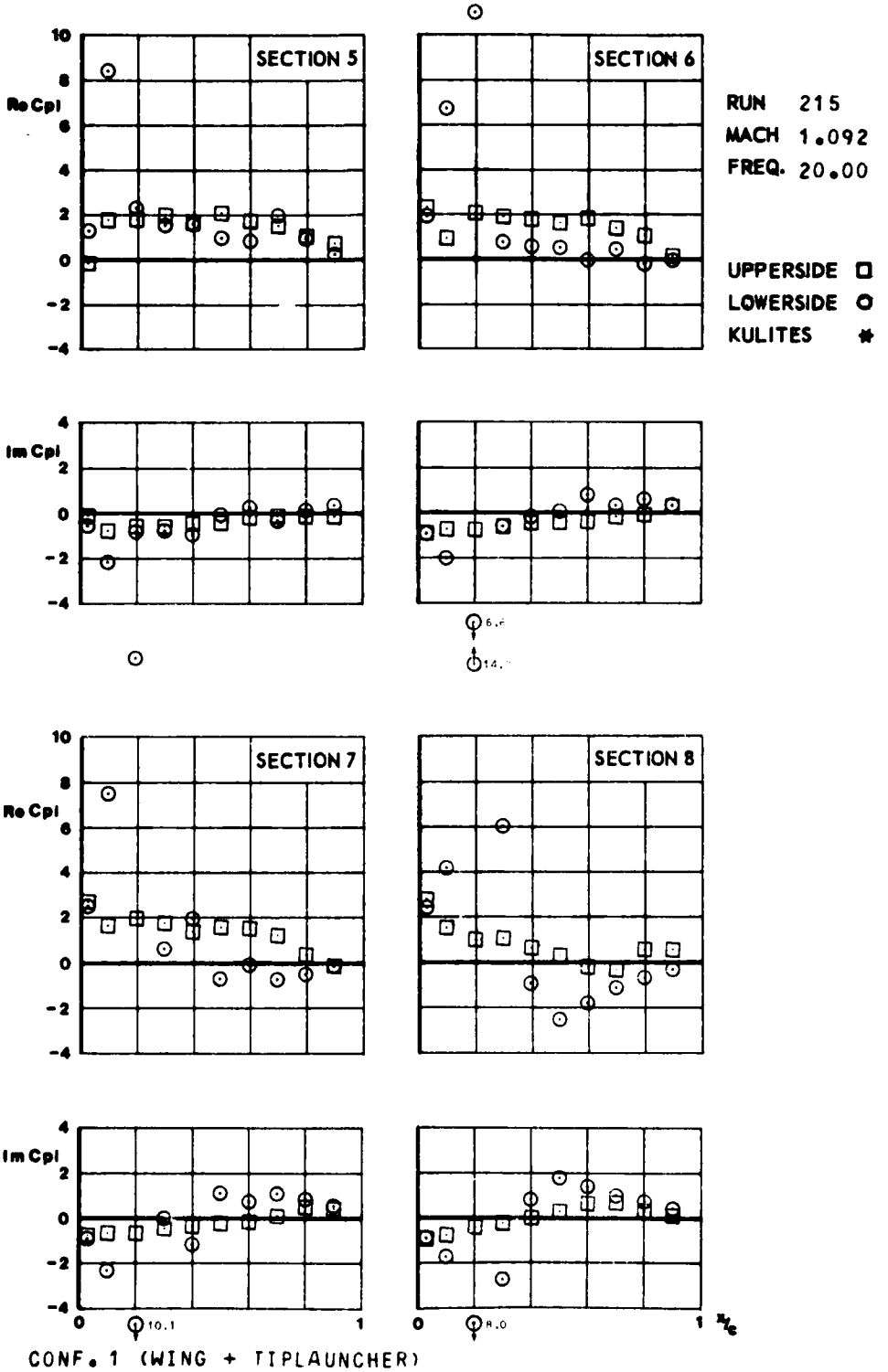

CONF. 1 (WING + TIPLAUNCHER)

FIG.
III.C.6.a

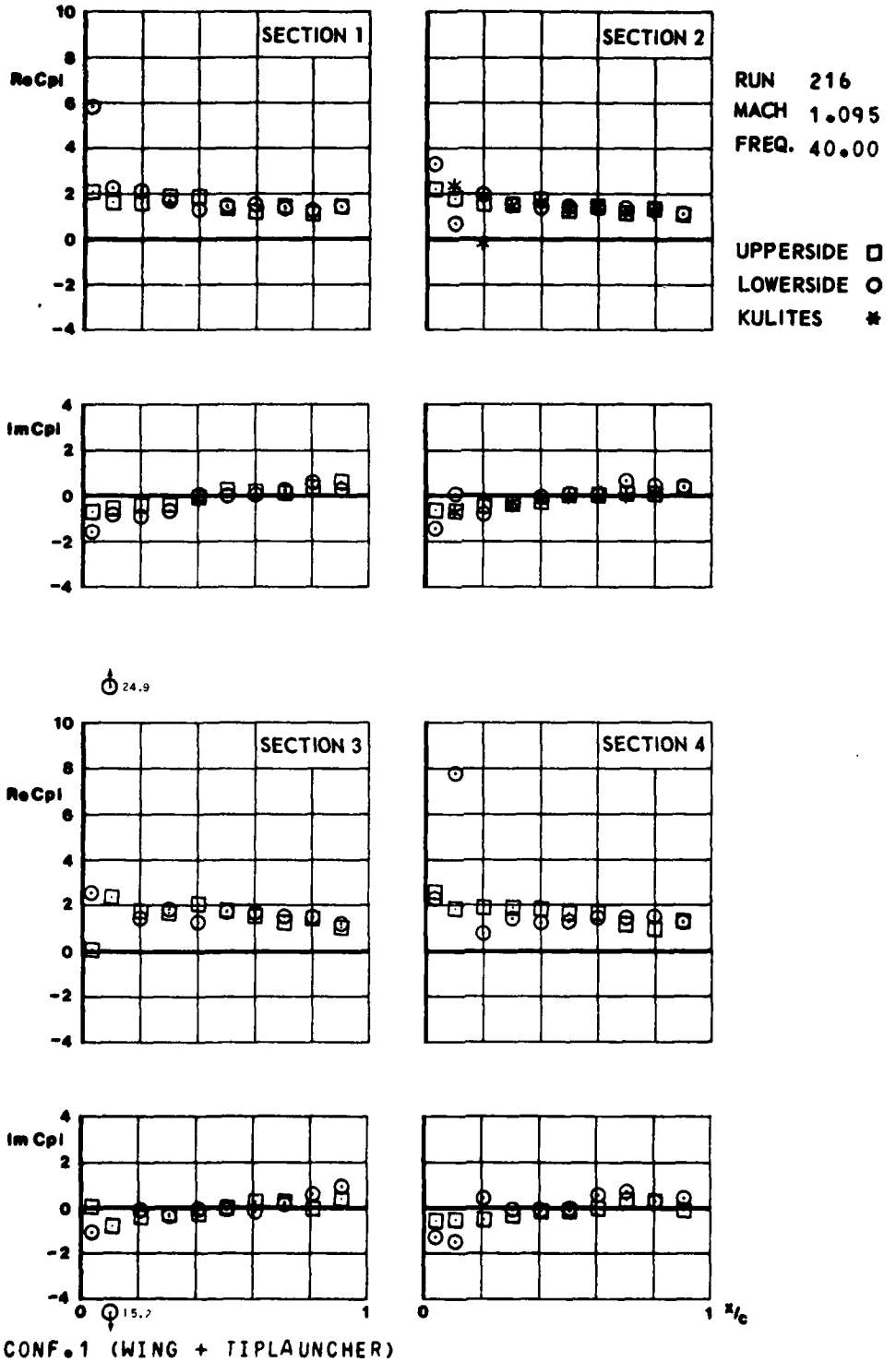

CONF.1 (WING + TIPLAUNCHER)

FIG.
III.C.6.b

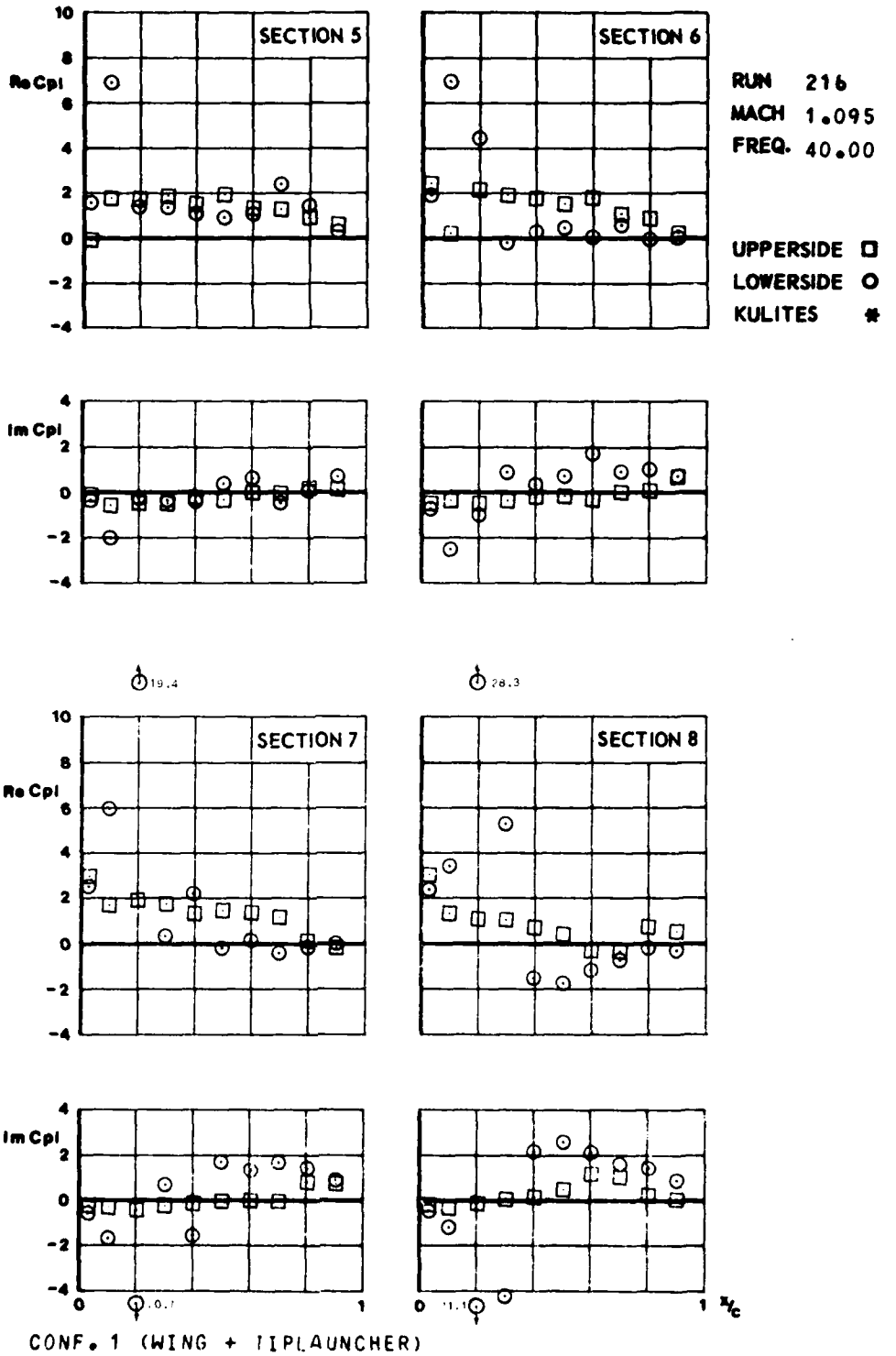

CONF. 1 (WING + TIPLAUNCHER)

FIG.
III.C.7.a

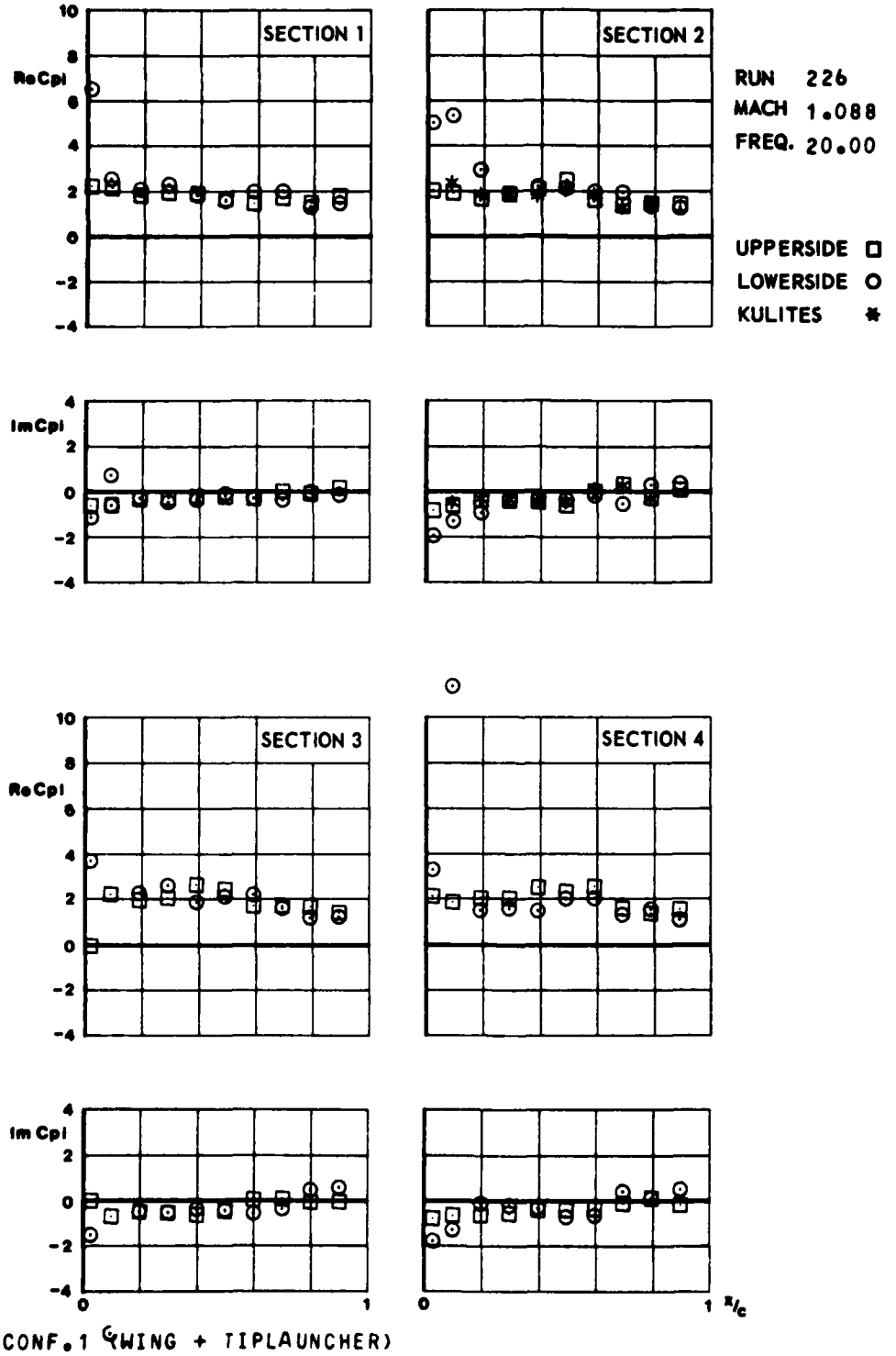

CONF.1 (WING + TIPLAUNCHER)

FIG.
III.C.7.b

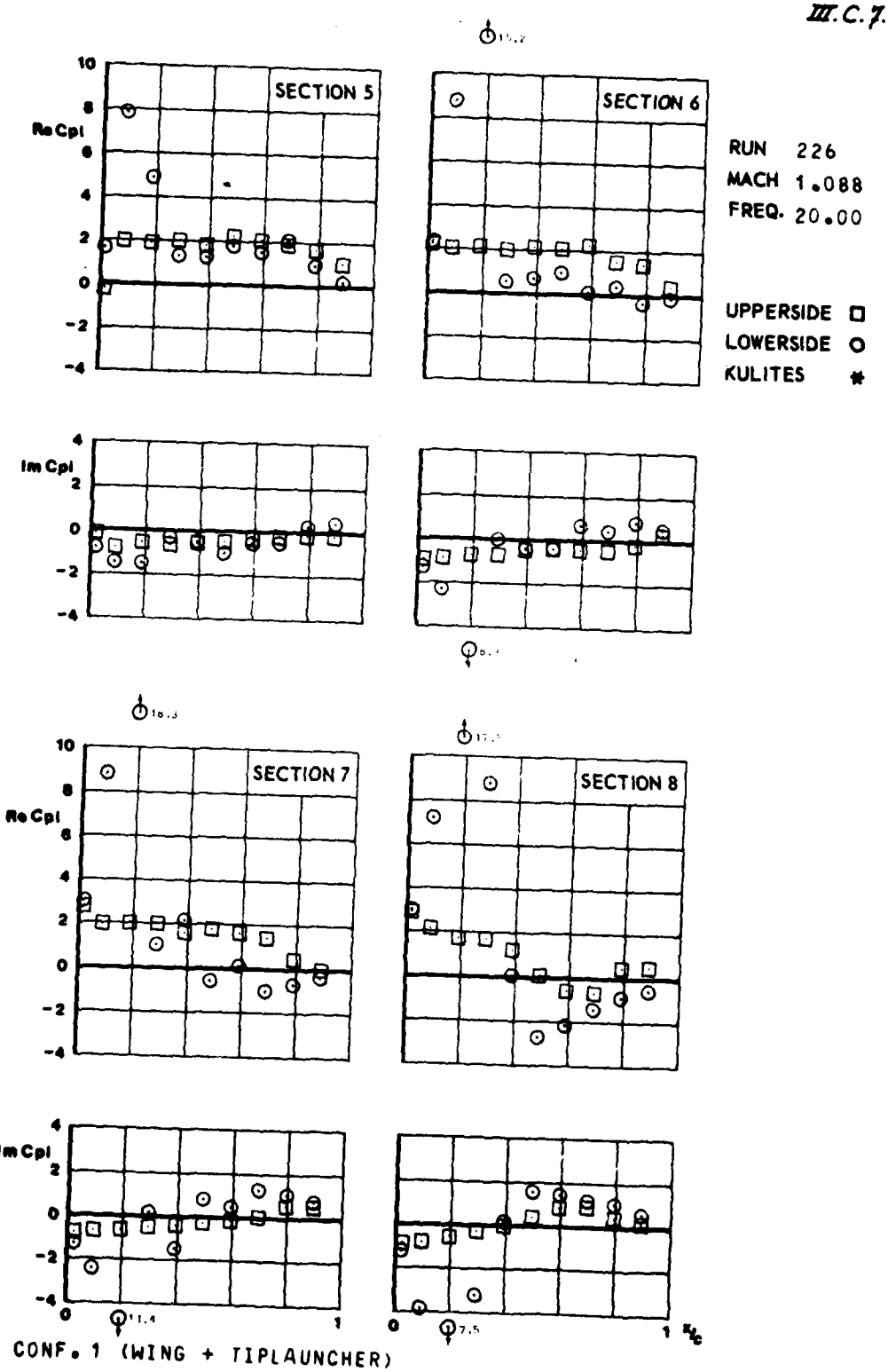

CONF. 1 (WING + TIPLAUNCHER)

FIG.
III.C.8.a

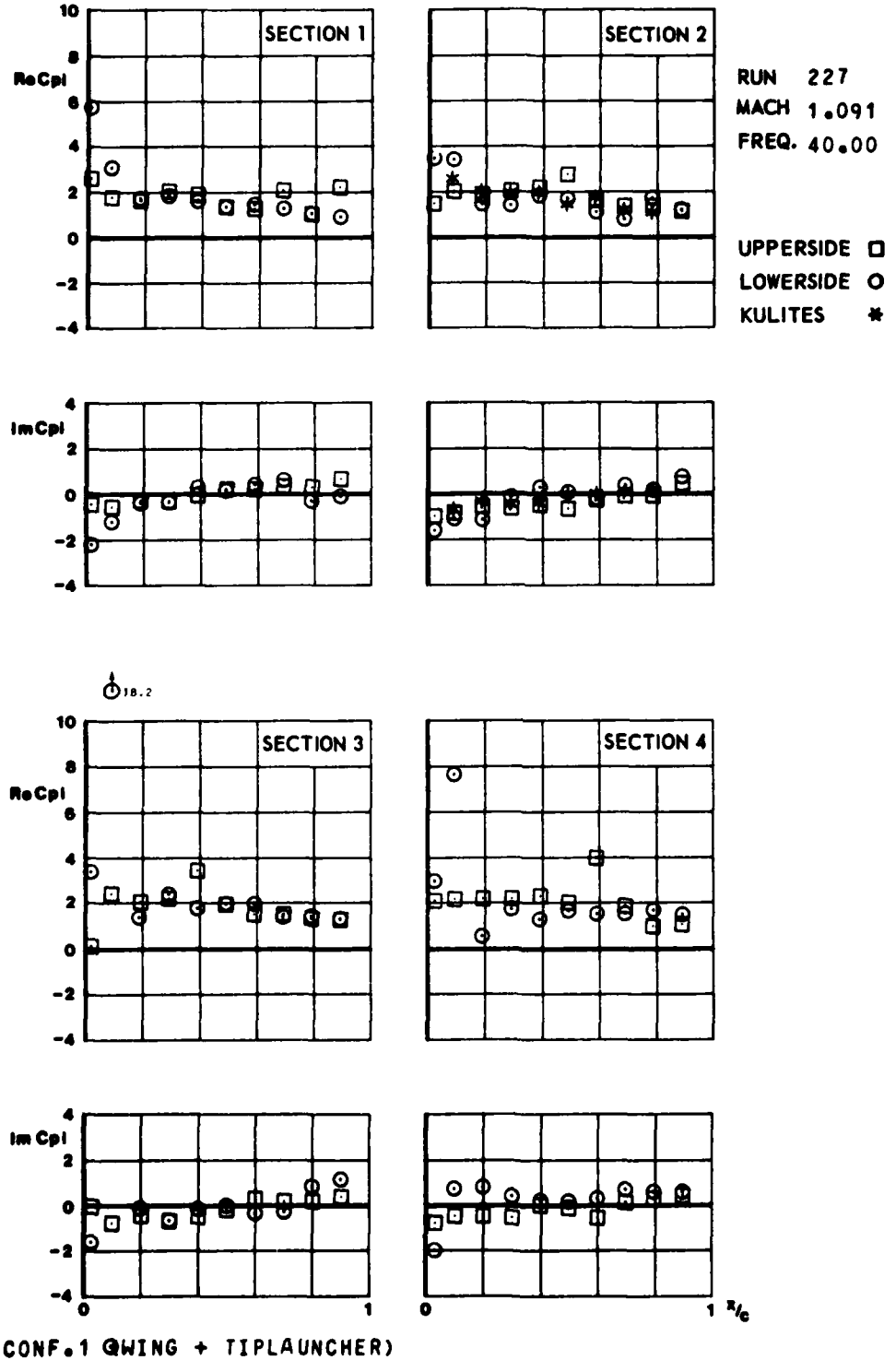

CONF.1 (WING + TIPLAUNCHER)

FIG.
III.C.8.b

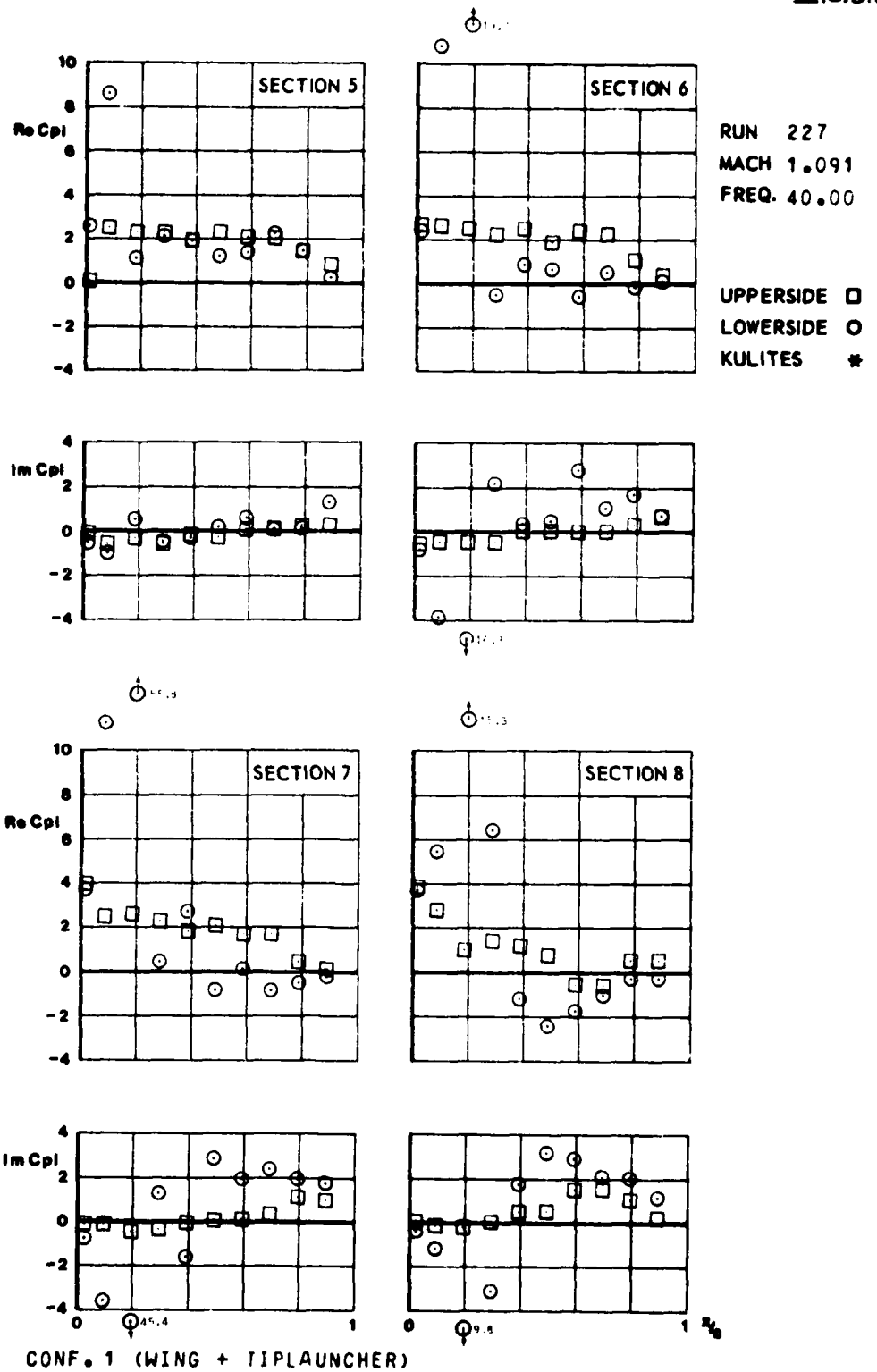

CONF. 1 (WING + TIPLAUNCHER)

FIG.
III.C.9.a

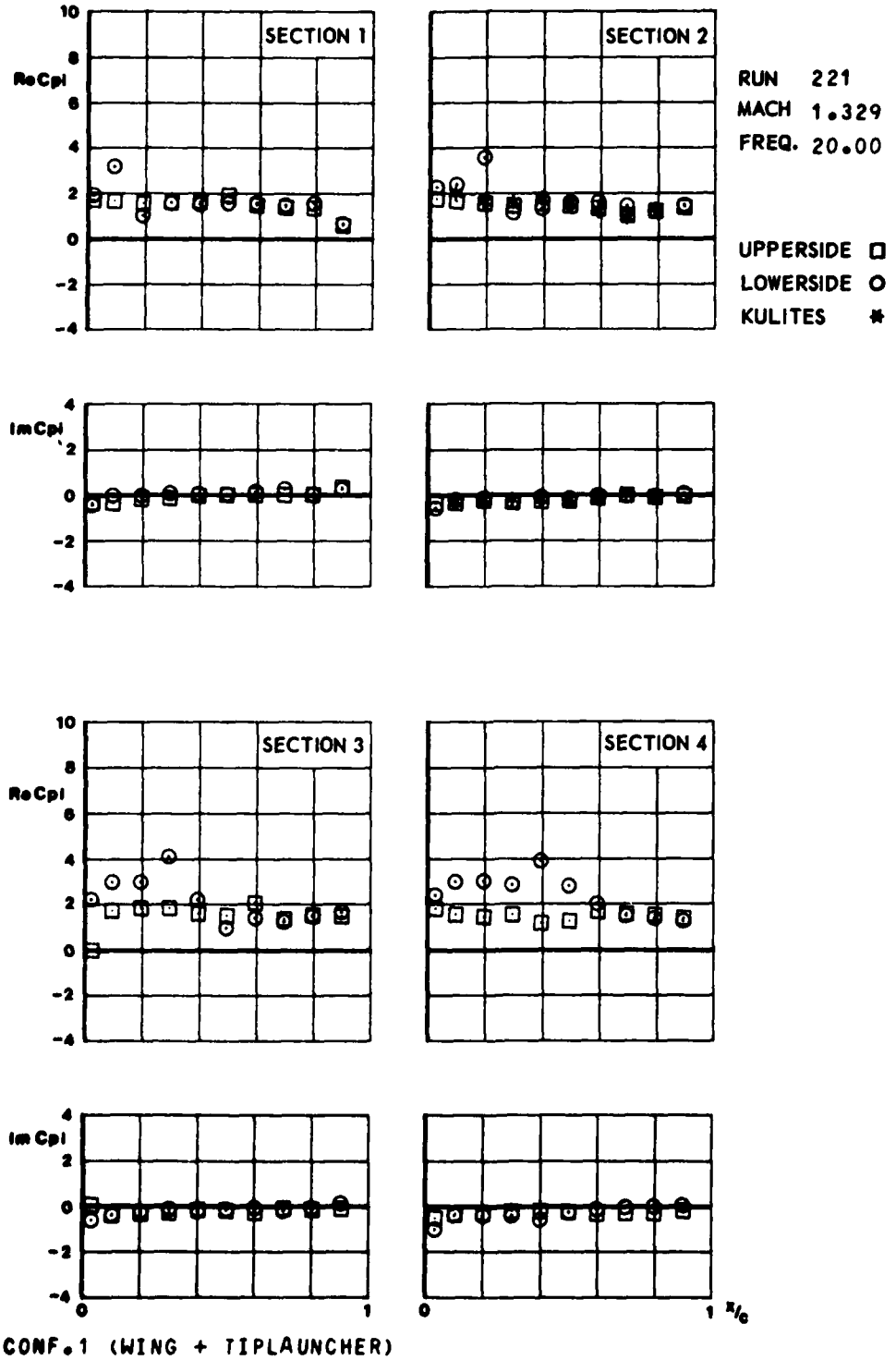

CONF.1 (WING + TIPLAUNCHER)

FIG.
III.C.9.b

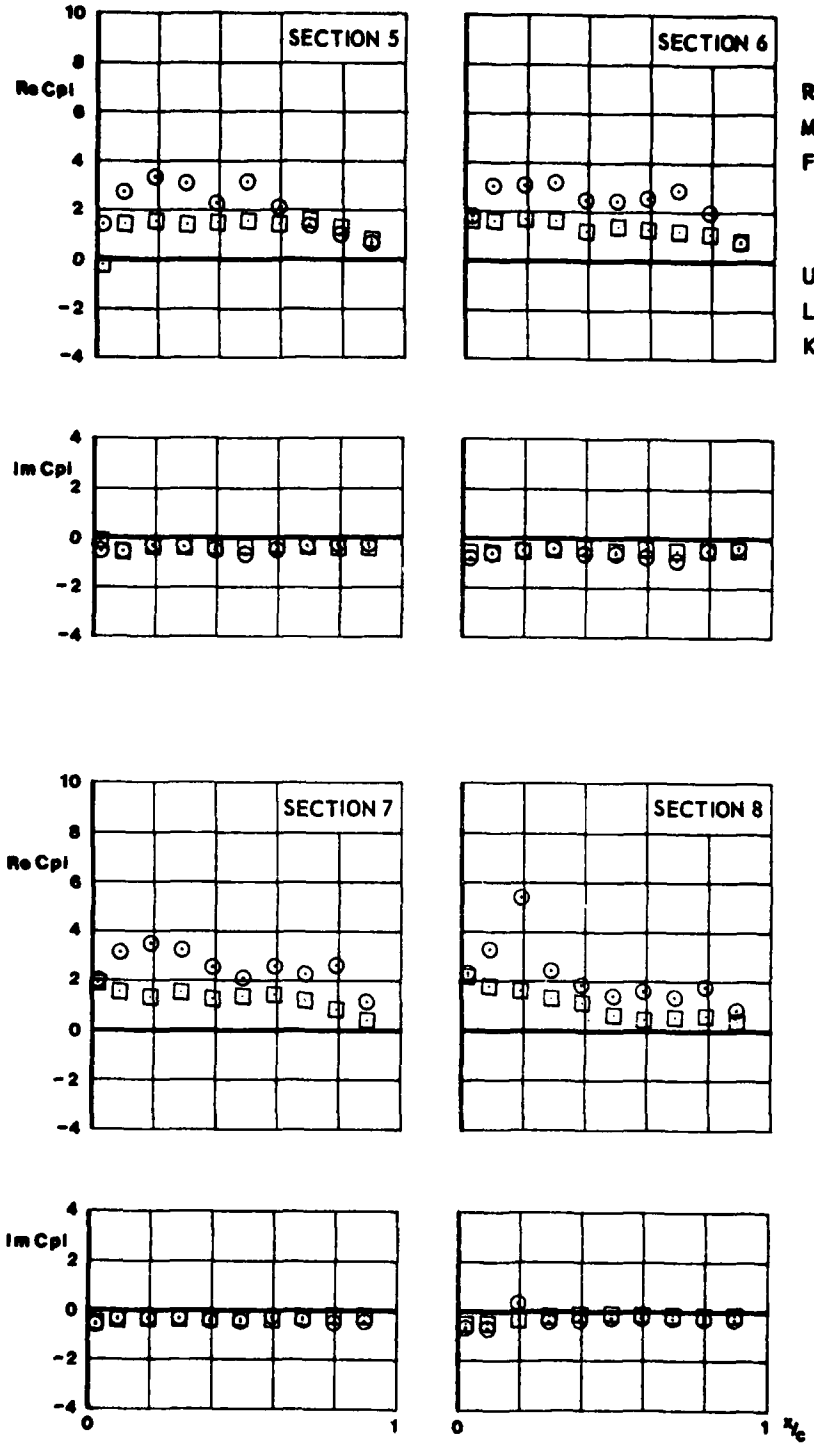

CONF. 1 (WING + TIPLAUNCHER)

FIG.
III.C.10.a

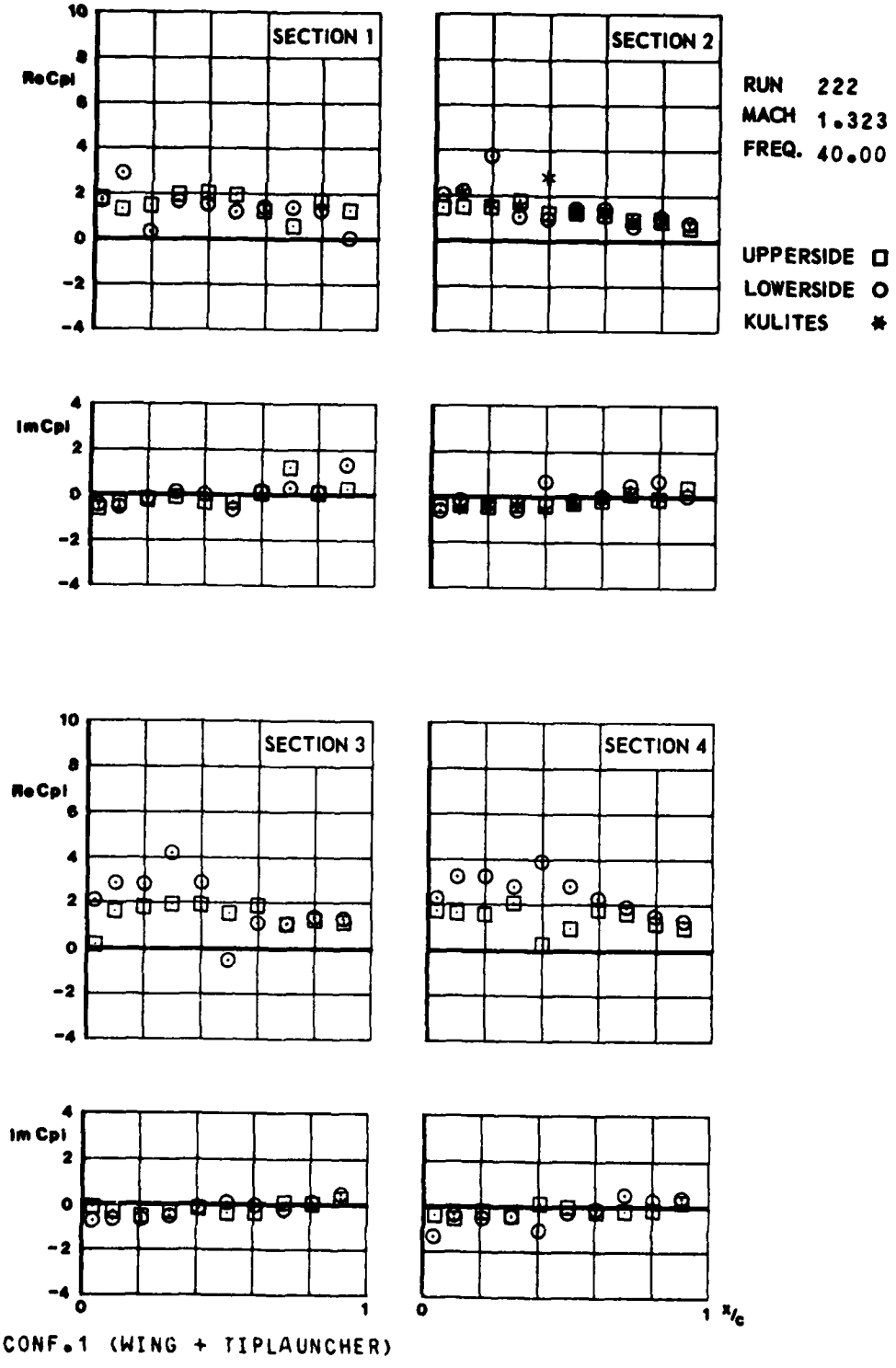

CONF.1 (WING + TIPLAUNCHER)

FIG.
III.C.10.b

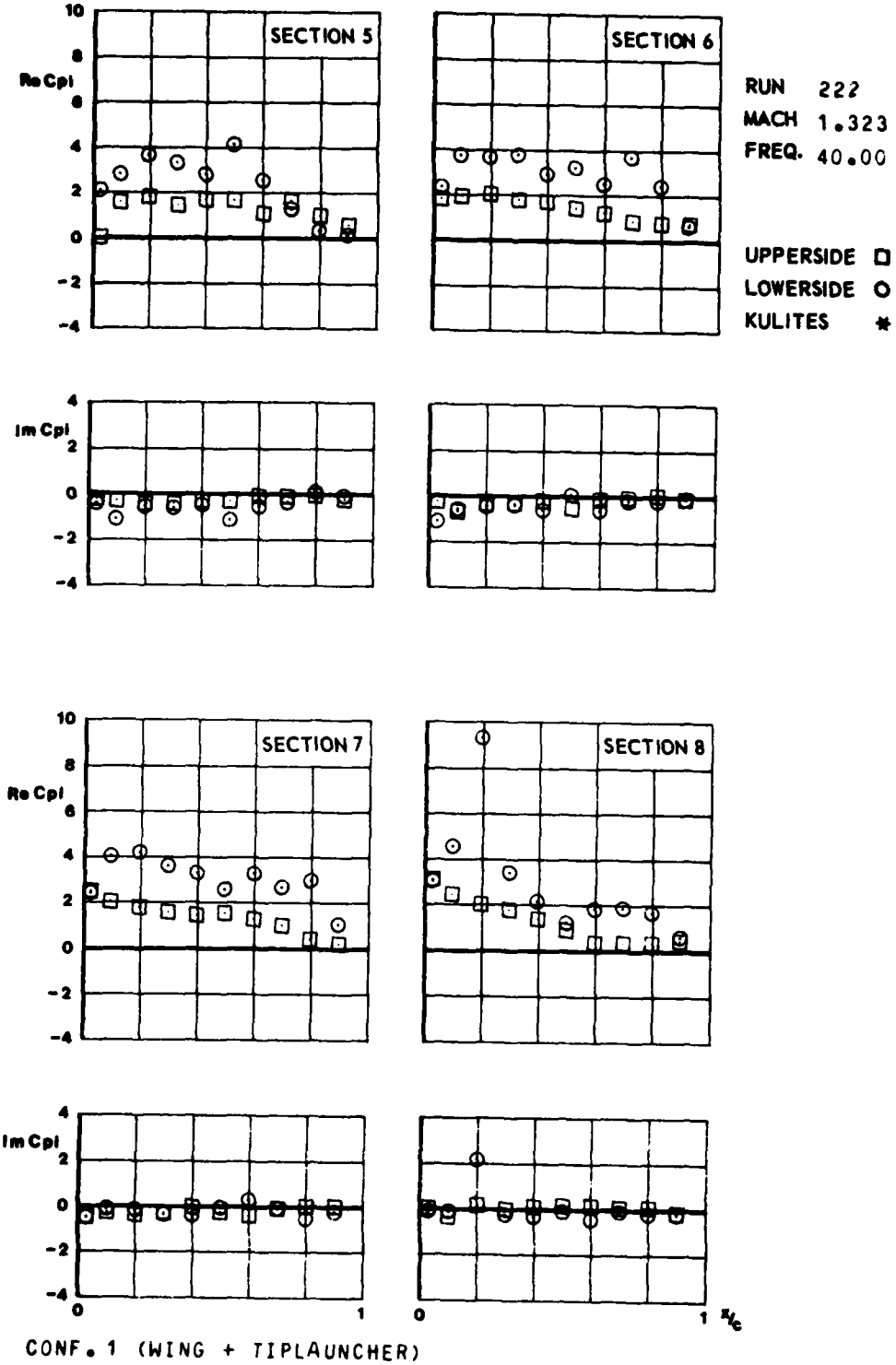

CONF. 1 (WING + TIPLAUNCHER)

FIG.
III.C.11.a

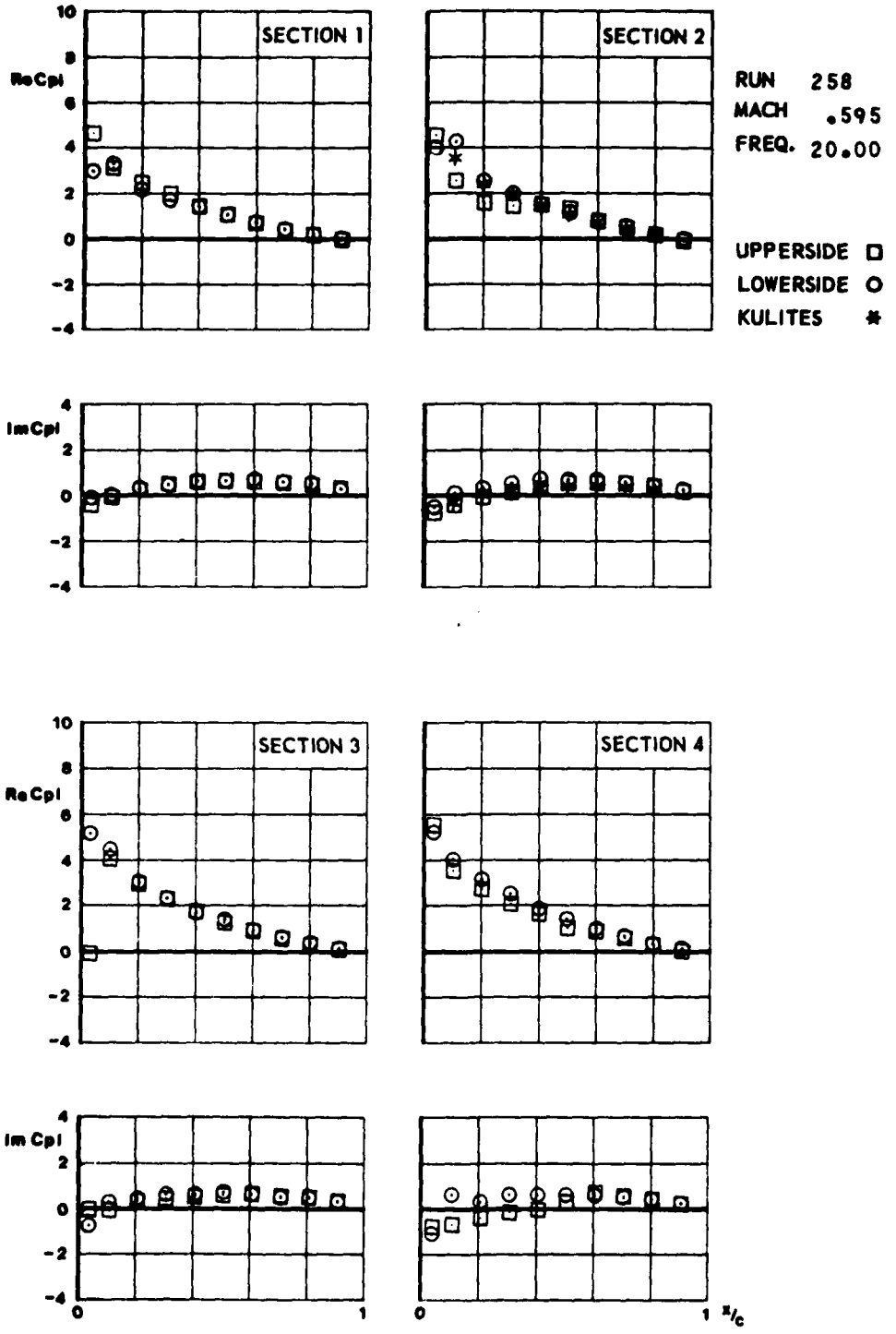

CONF.2 (WING + TIPLAUNCHER + MISSILEBODY)

FIG.
III.C.11.6

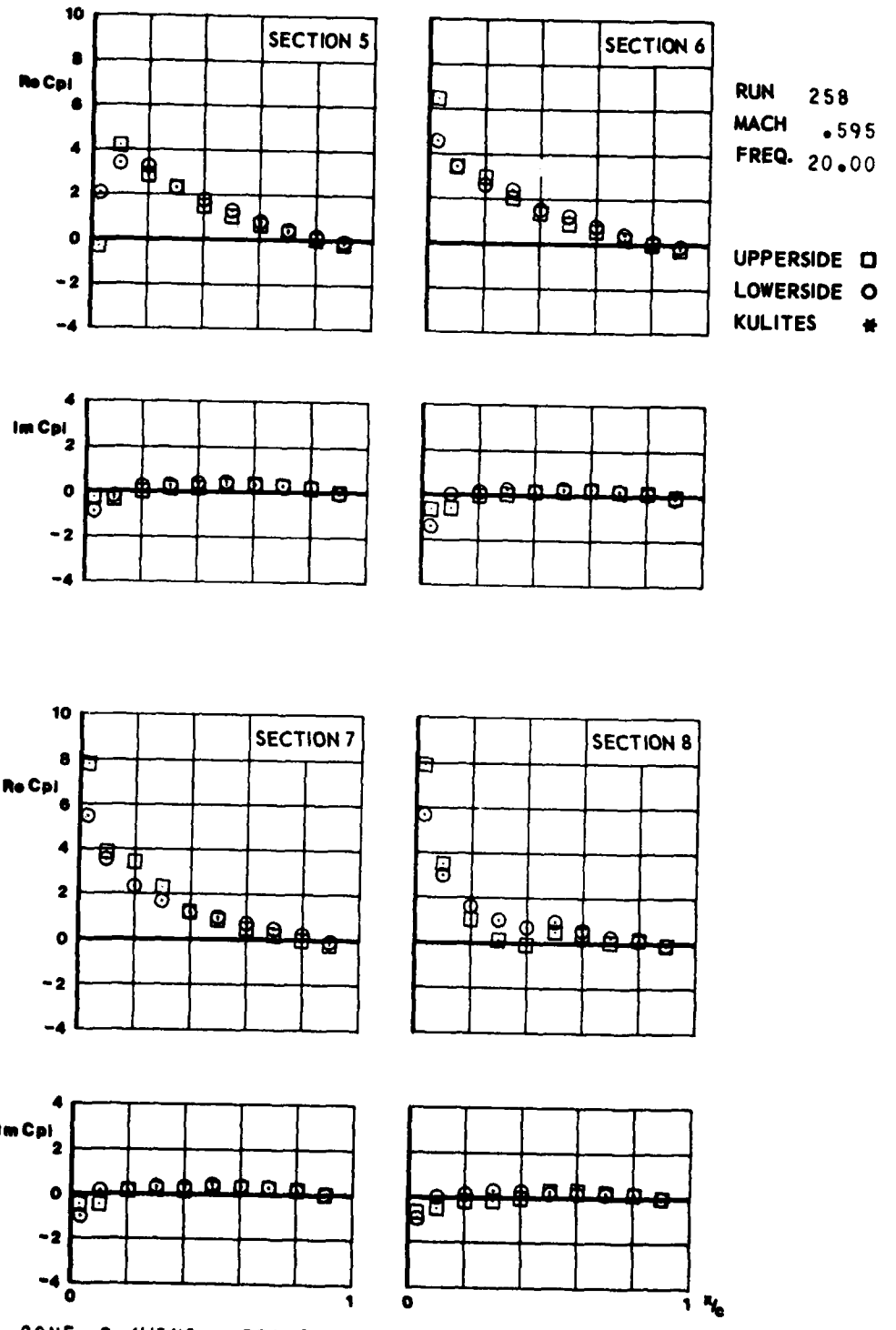

CONF. 2 (WING + TIPLAUNCHER + MISSILEBODY)

FIG.
III.C.12.a

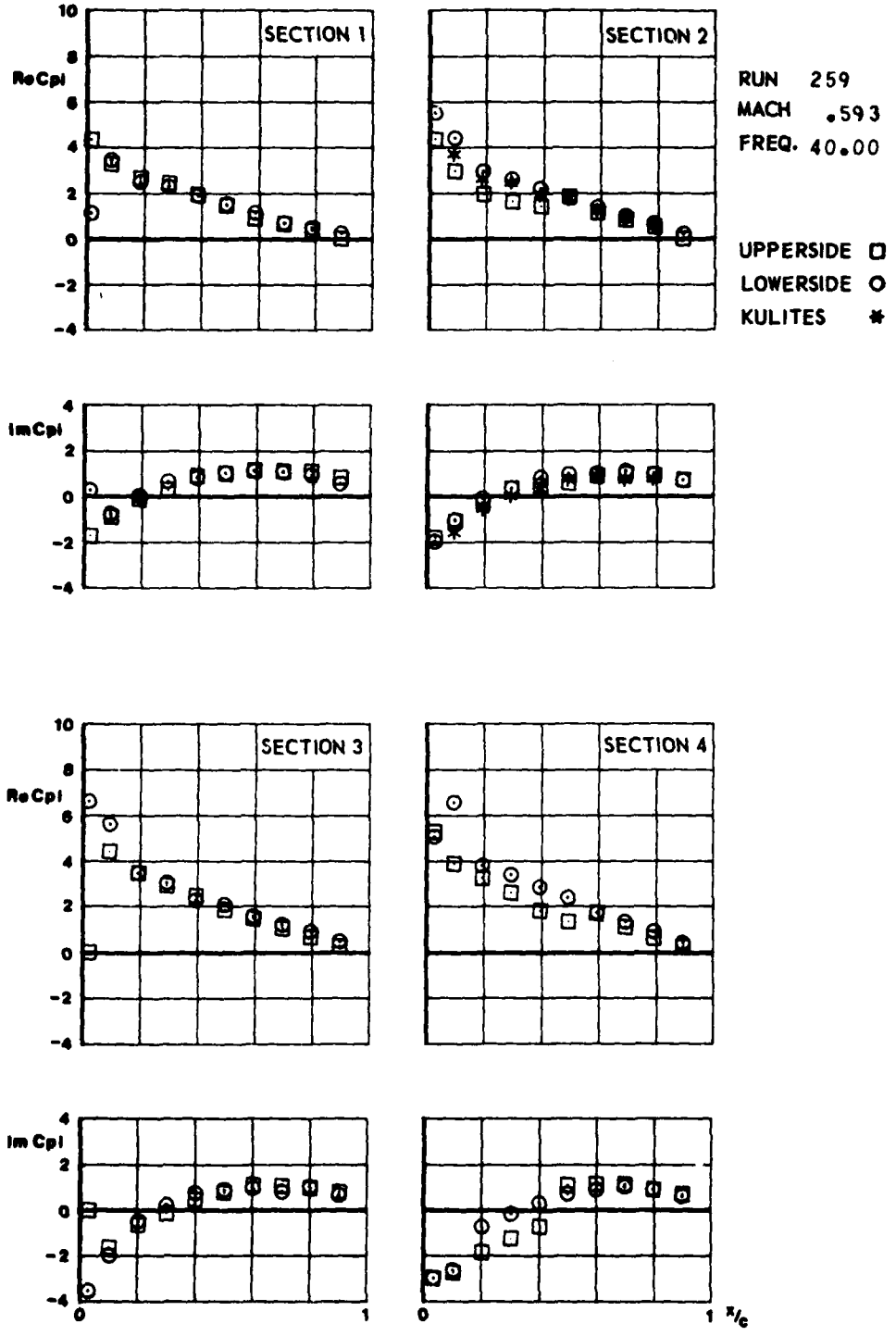

CONF.2 (WING + TIPLAUNCHER + MISSILEBODY)

FIG.
III.C.12.b

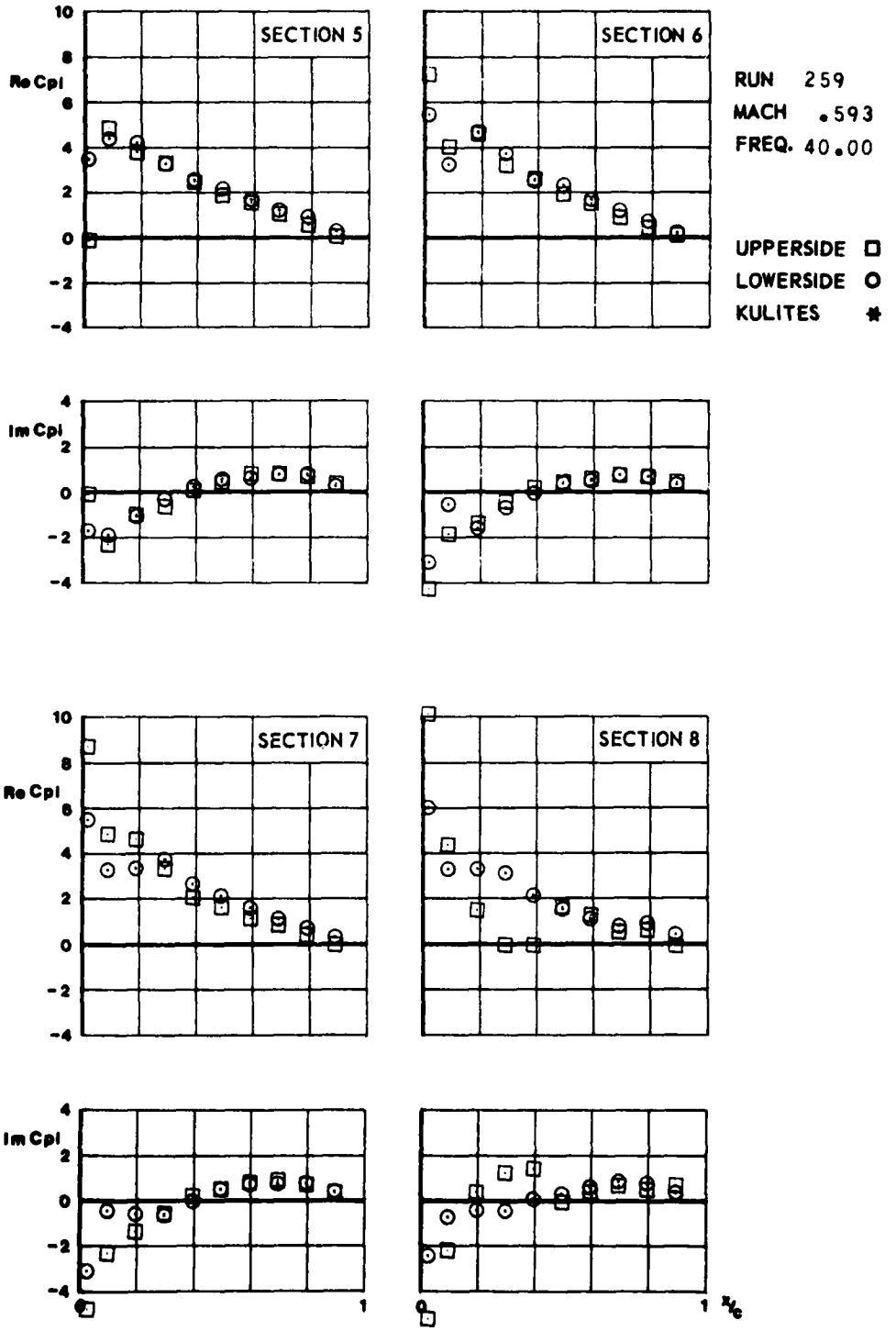

CONF. 2 (WING + TIPLAUNCHER + MISSILEBODY)

FIG.
III.C.13.a

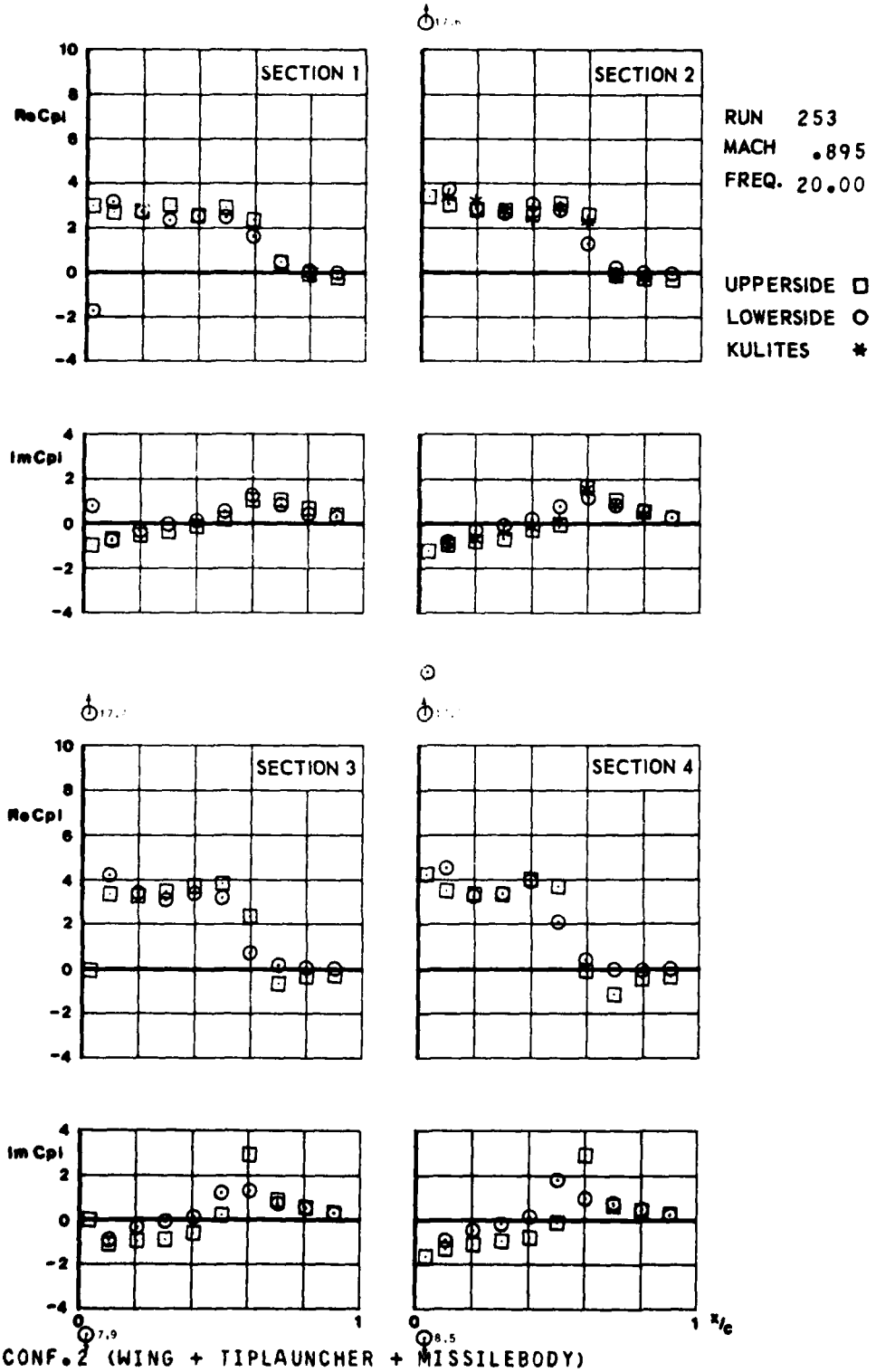

CONF. 2 (WING + TIPLAUNCHER + MISSILEBODY)

FIG.
III.C.13.8

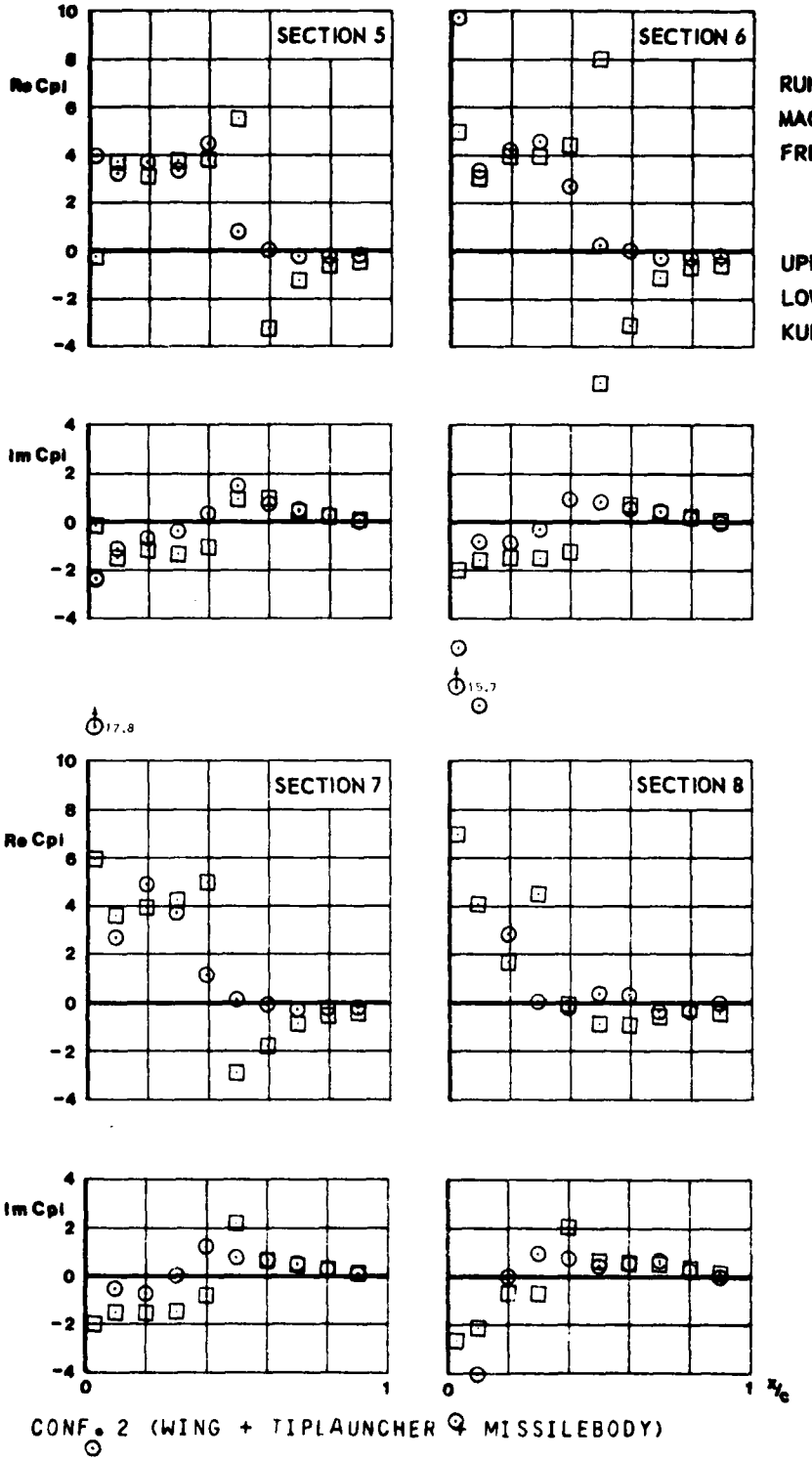

CONF. 2 (WING + TIPLAUNCHER + MISSILEBODY)

FIG.
III.C.14.a

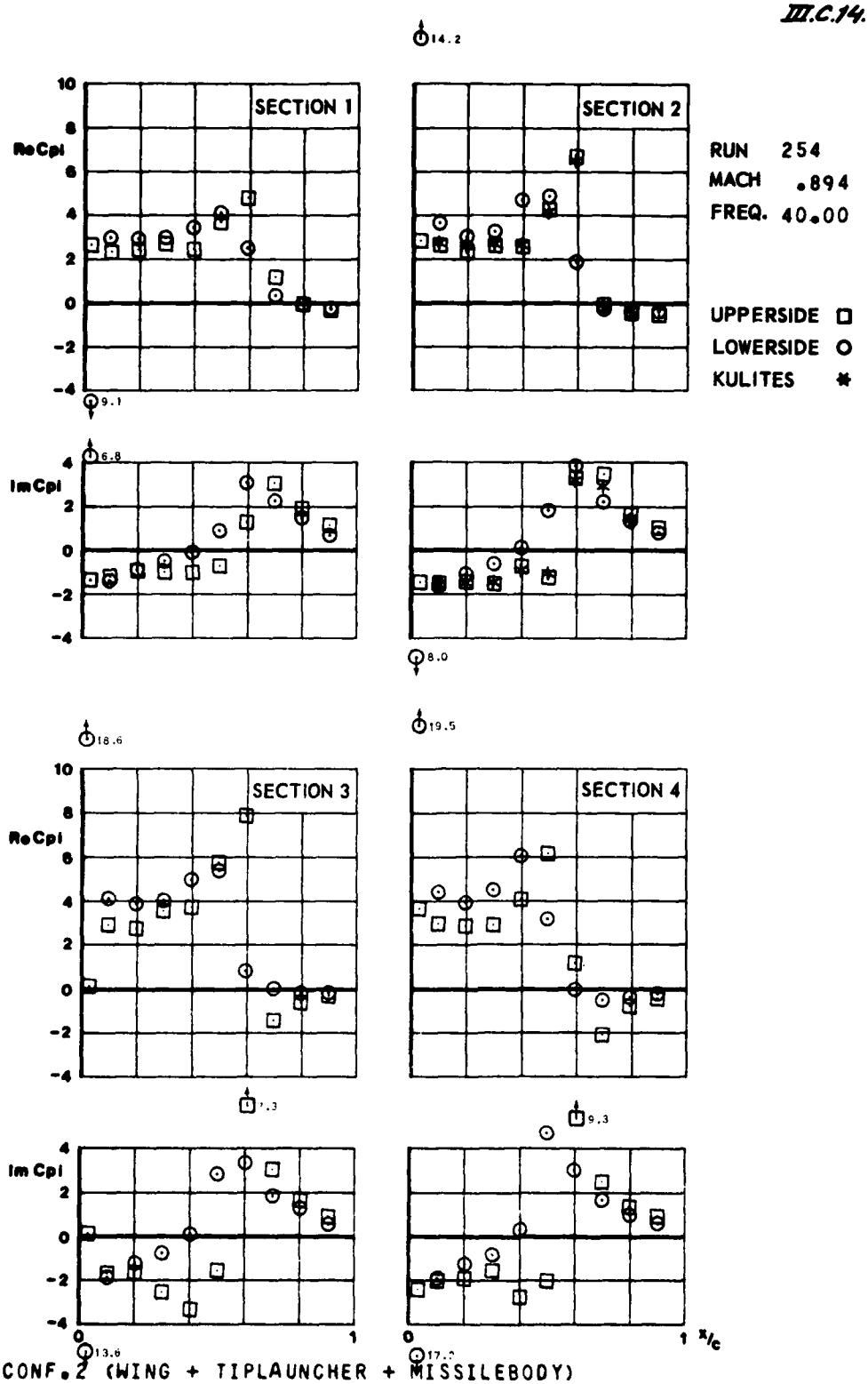

CONF.2 (WING + TIPLAUNCHER + MISSILEBODY)

FIG.
III.C.14.b

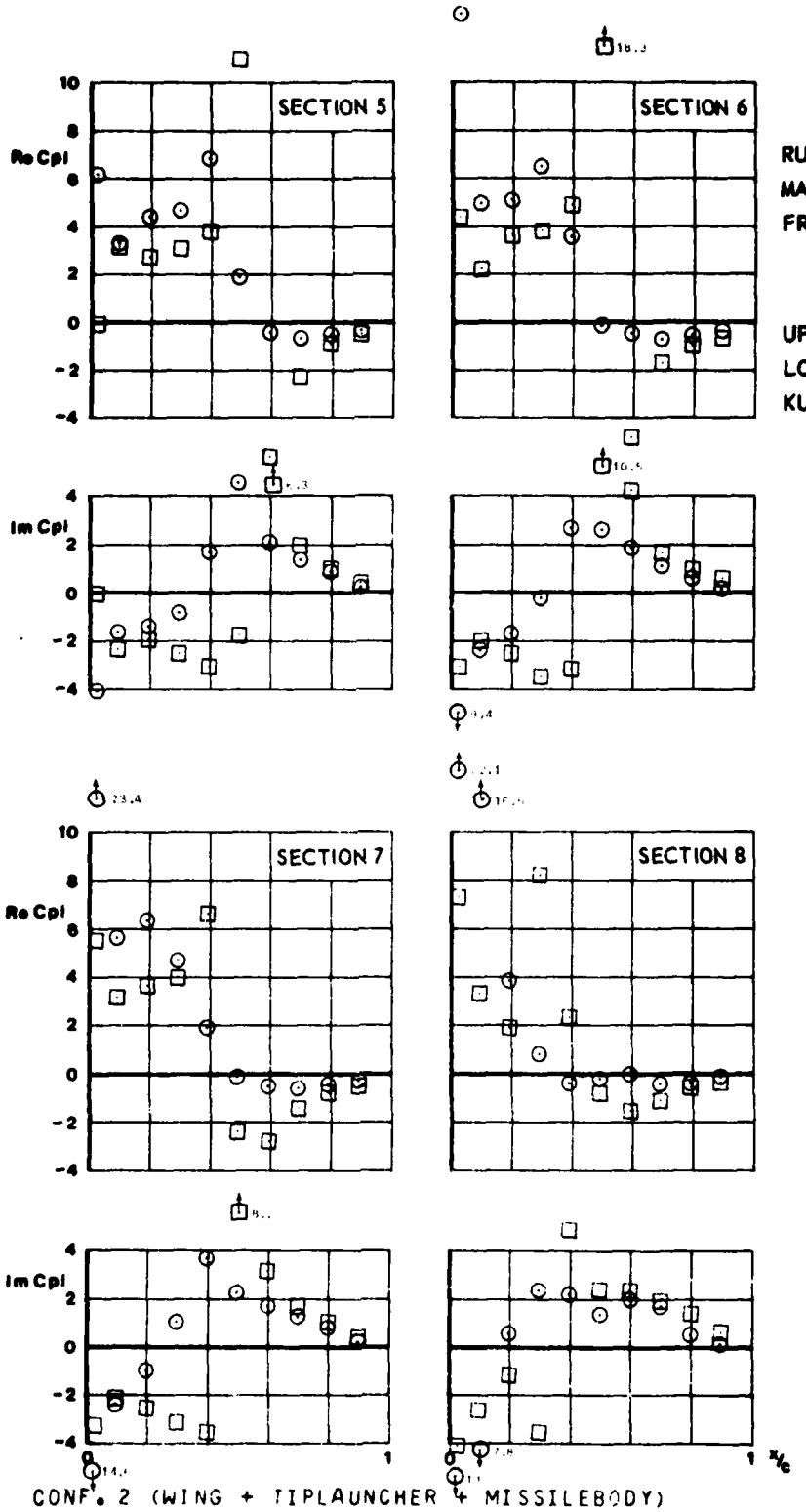

CONF. 2 (WING + TIPLAUNCHER + MISSILEBODY)

FIG.
III.C.15.a

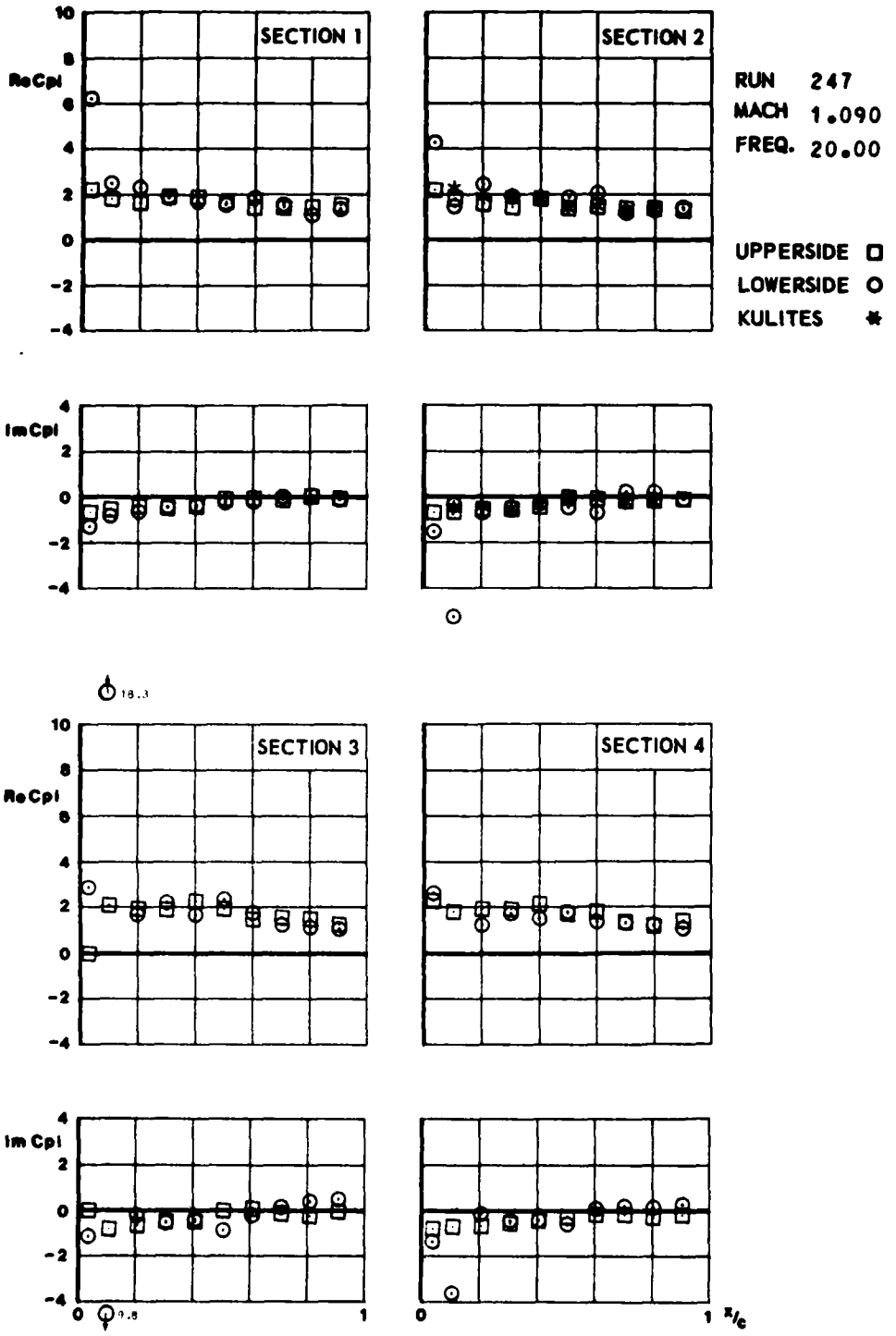

CONF.2 (WING + TIPLAUNCHER + MISSILEBODY)

FIG.
III.C.15.b

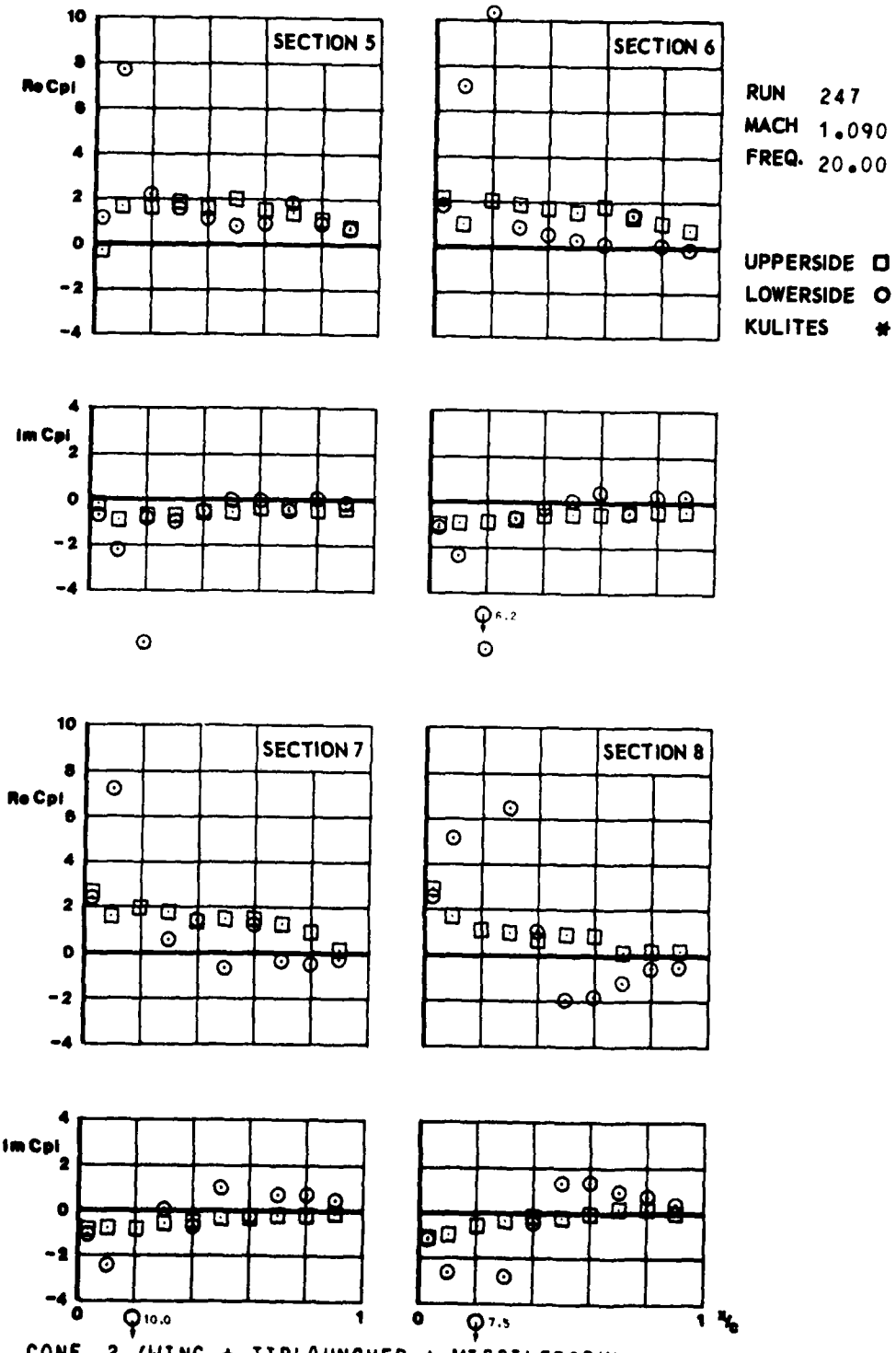

CONF. 2 (WING + TIPLAUNCHER + MISSILEBODY)

FIG.
III.C.16.a

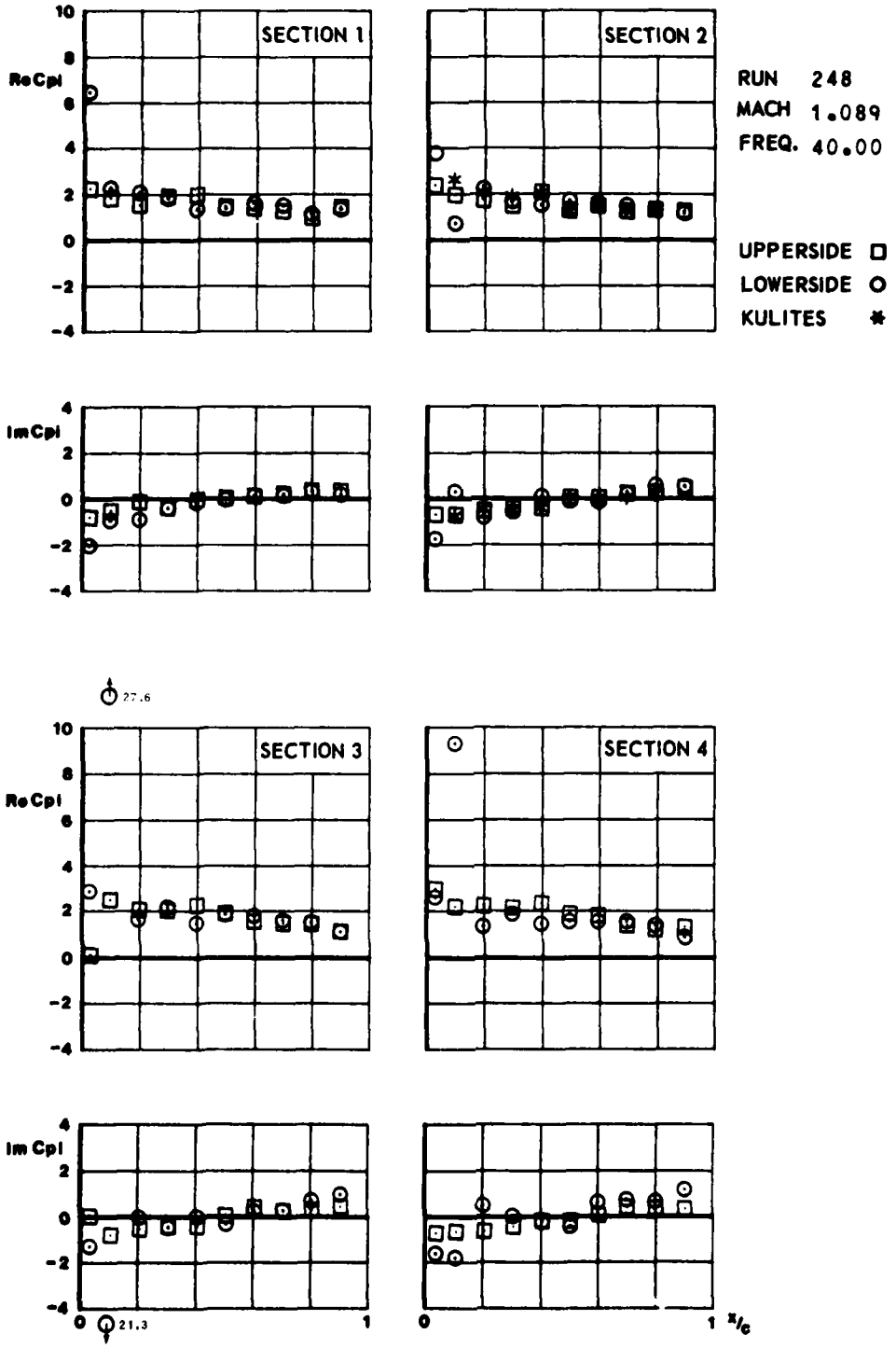

CONF. 2 (WING + TIPLAUNCHER + MISSILEBODY)

FIG.
III.C.16.b

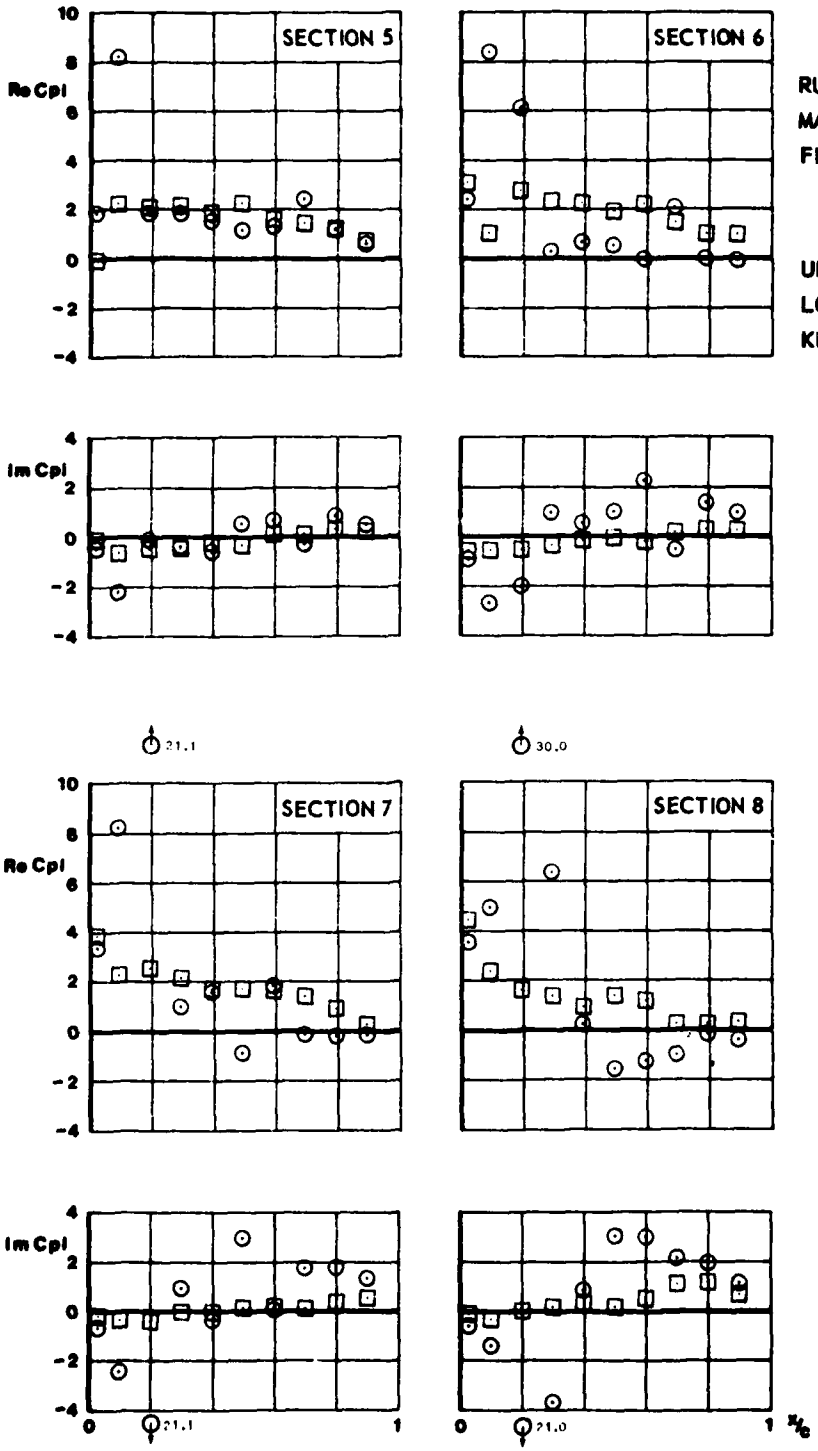

CONF. 2 (WING + TIPLAUNCHER + MISSILEBODY)

FIG.
III.C.17.a

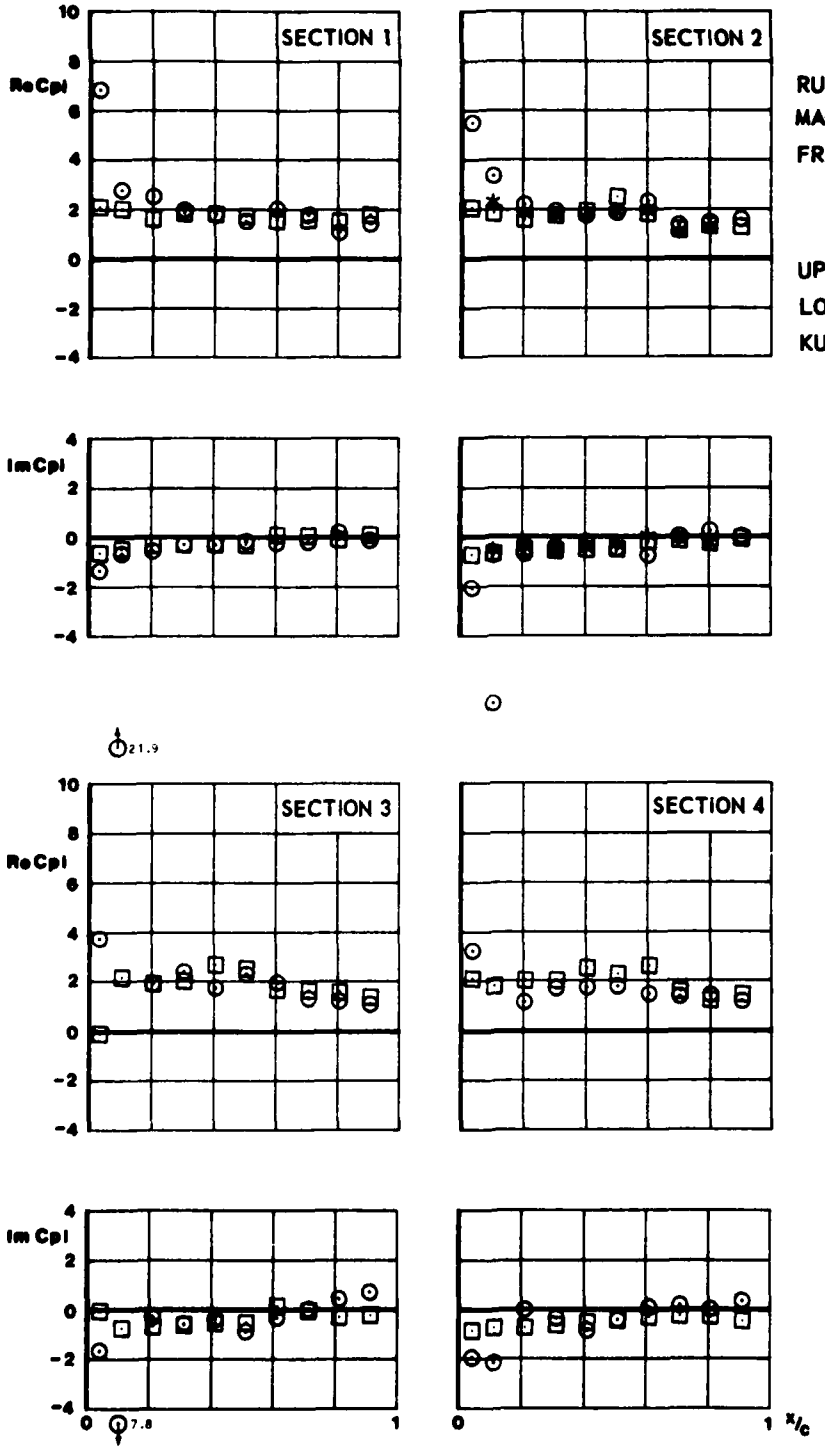

CONF.2 (WING + TIPLAUNCHER + MISSILEBODY)

FIG.
III.C.17.b

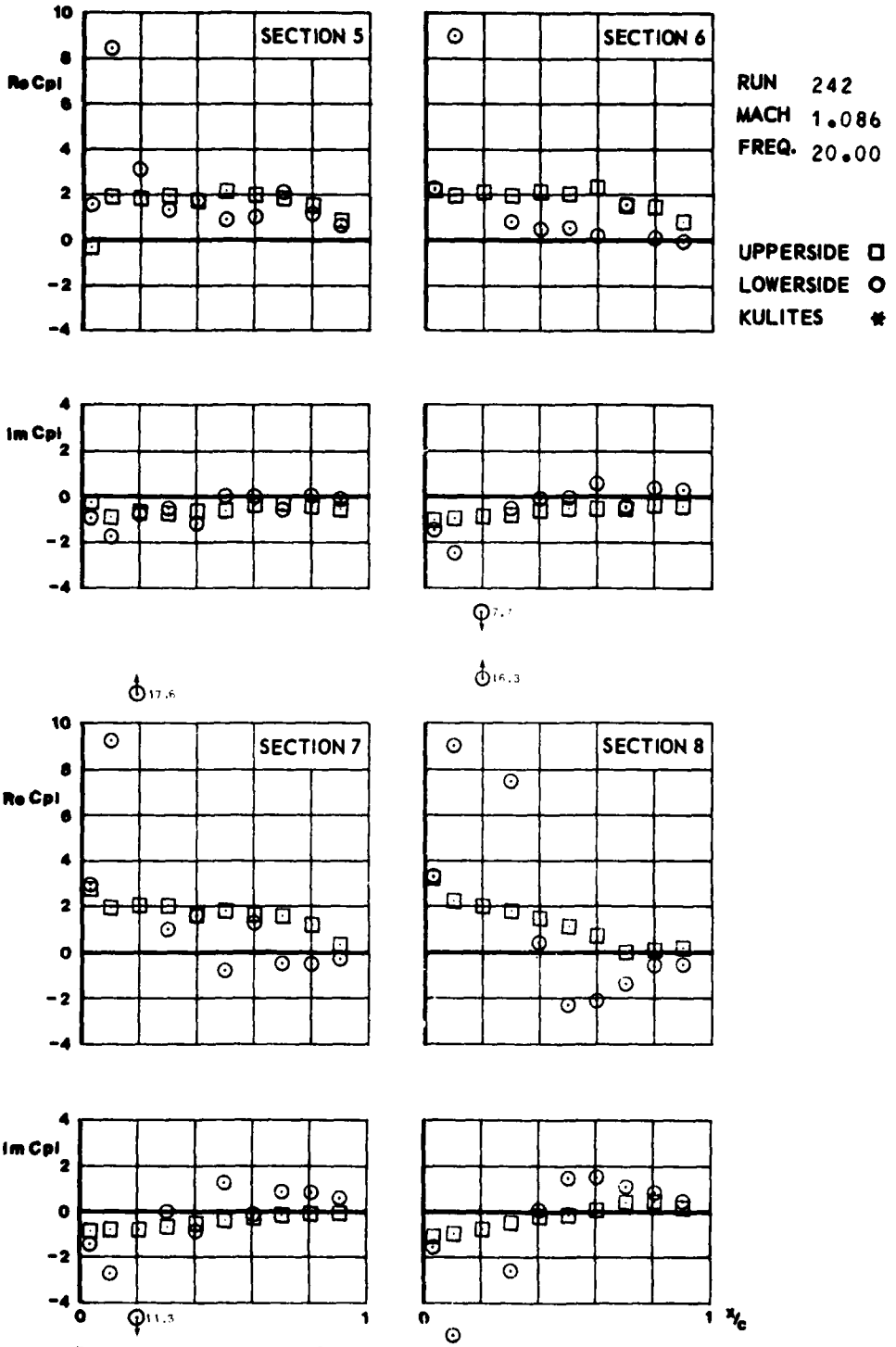

CONF. 2 (WING + TIPLAUNCHER + MISSILEBODY)

FIG.
III.C.18.a

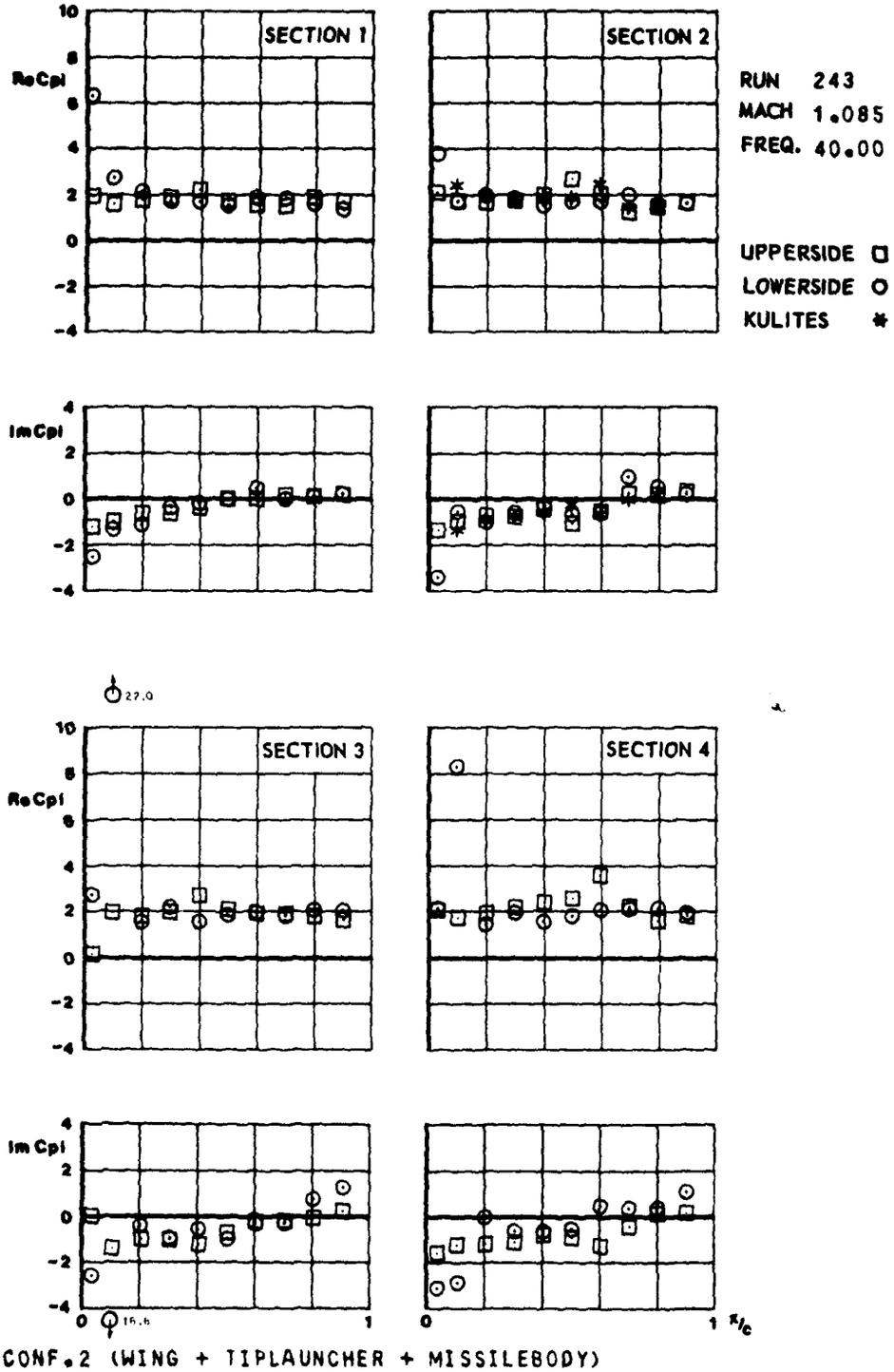

CONF.2 (WING + TIPLAUNCHER + MISSILEBODY)

FIG.
III.C.18.6

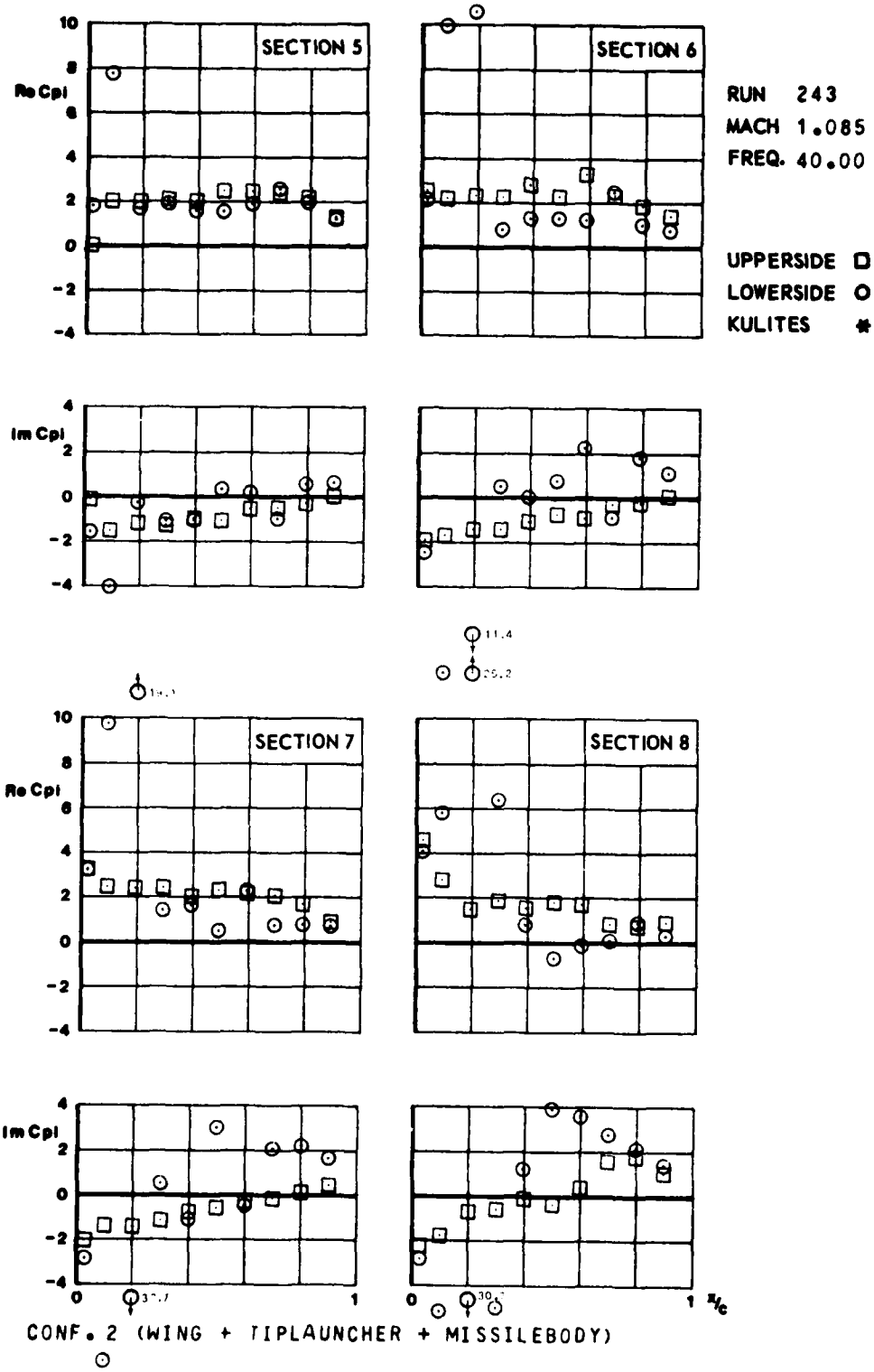

CONF. 2 (WING + TIPLAUNCHER + MISSILEBODY)

FIG.
III.C.19a

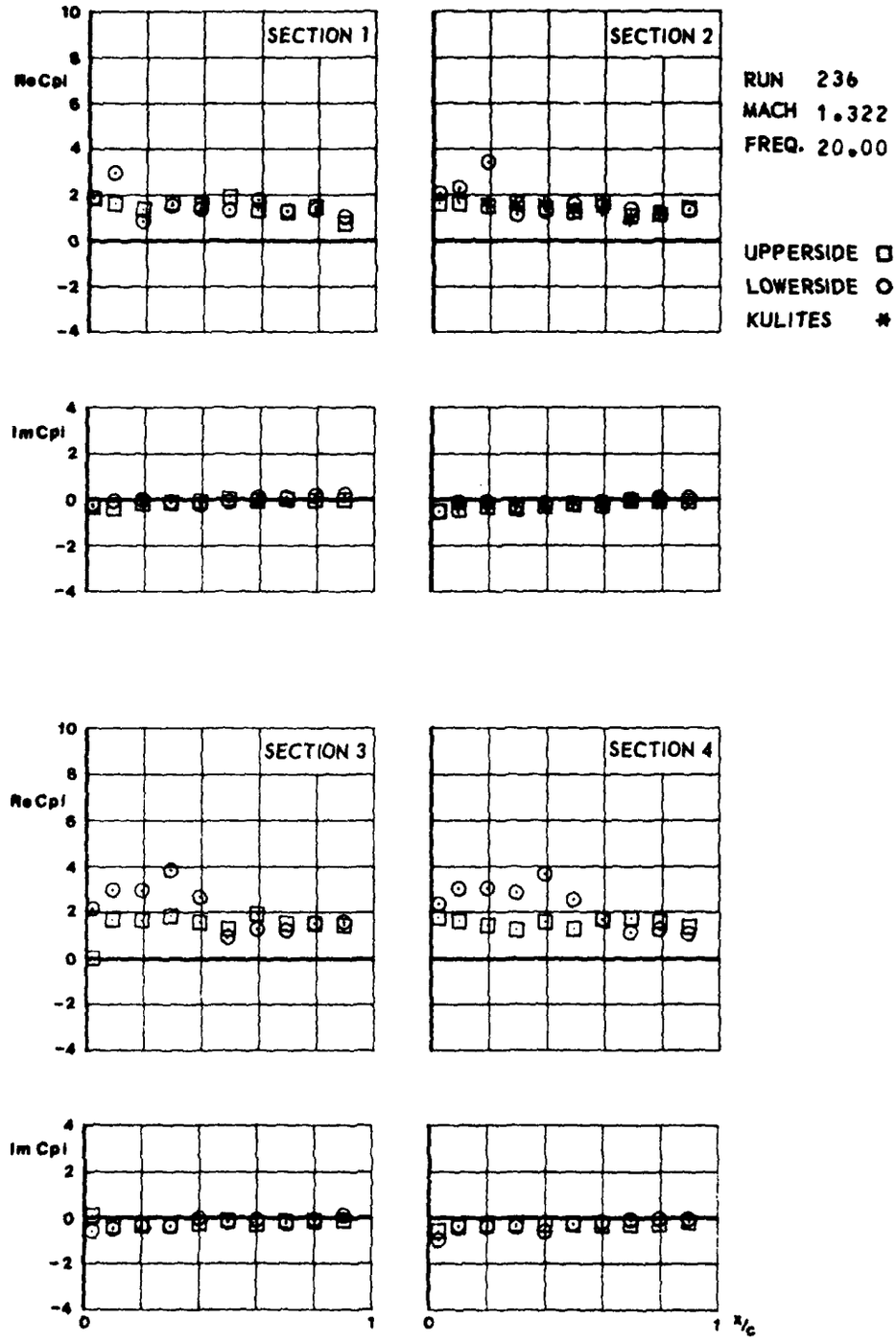

CONF.2 (WING + TIPLAUNCHER + MISSILEBODY)

FIG.
III.C.19.b

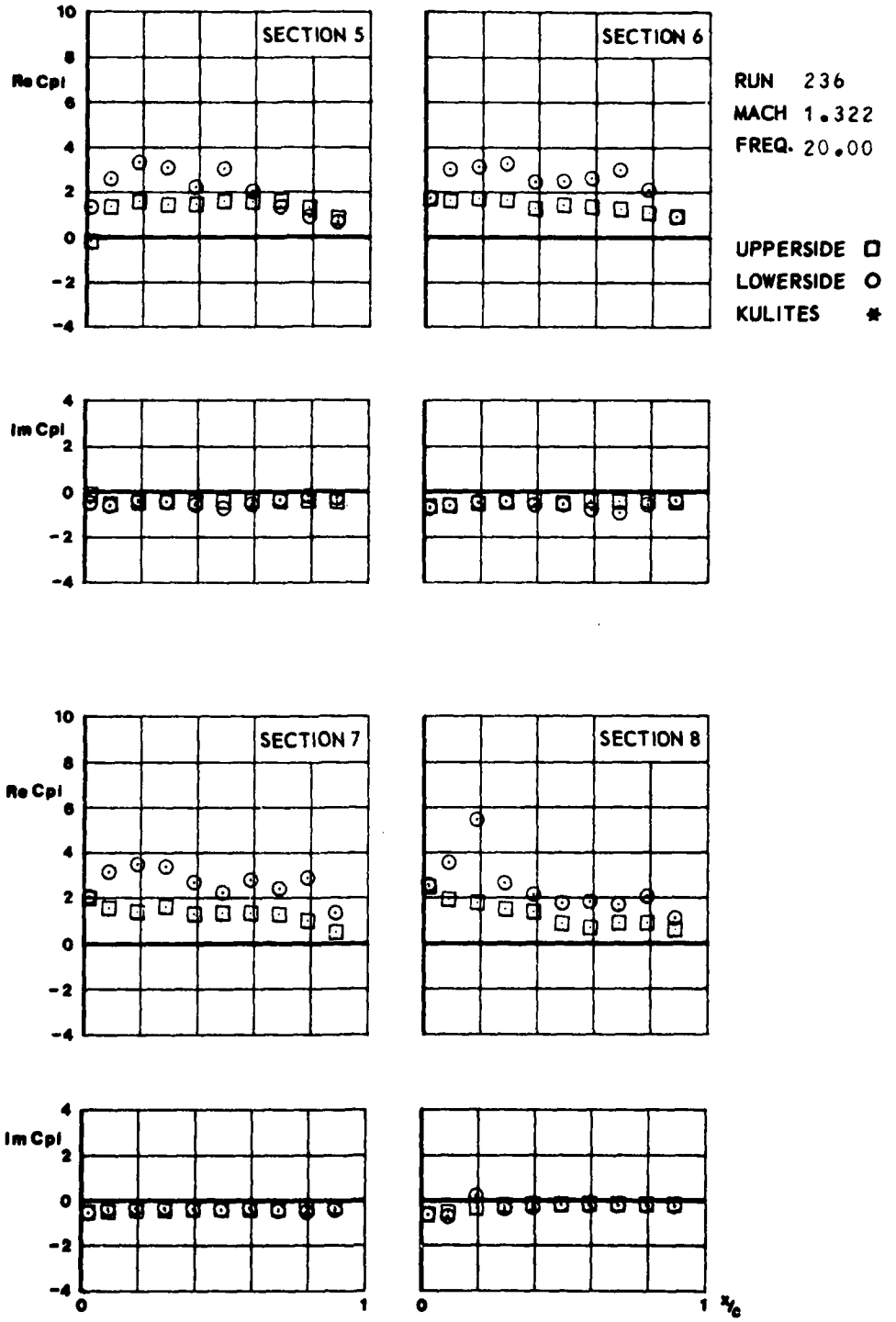

CONF. 2 (WING + TIPLAUNCHER + MISSILEBODY)

FIG.
III.C.20a

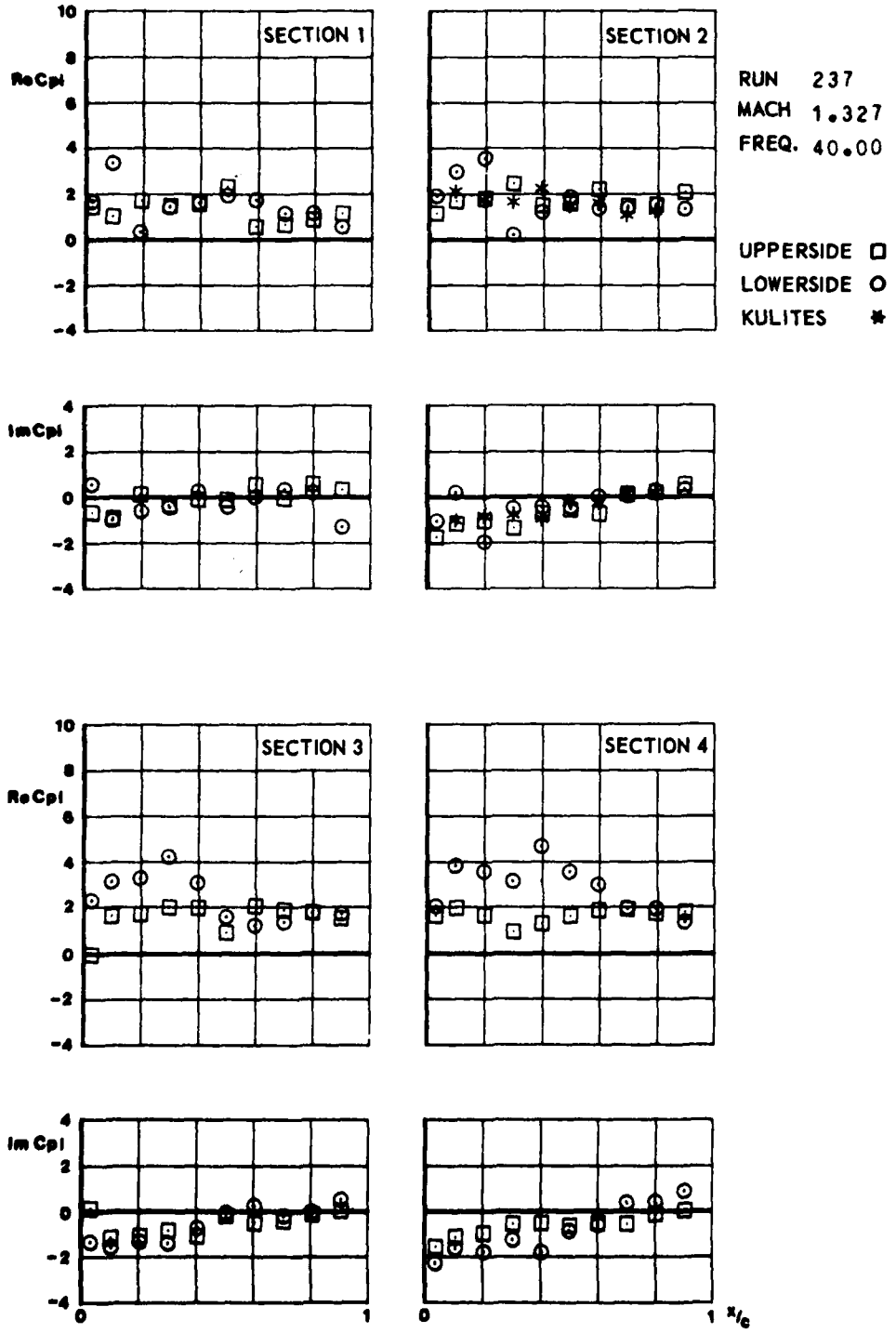

CONF.2 (WING + TIPLAUNCHER + MISSILEBODY)

FIG.
III.C.20b

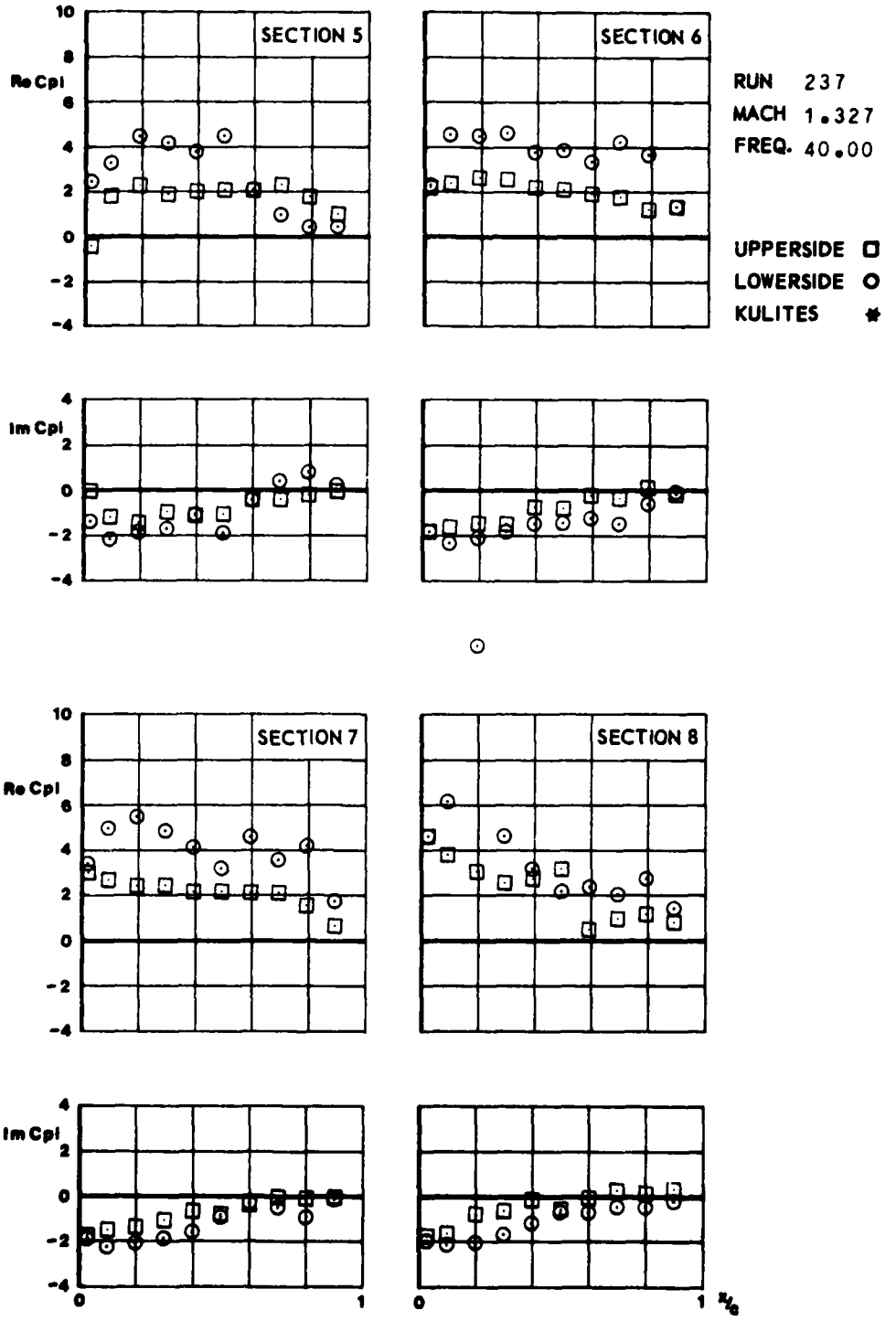

CONF. 2 (WING + TIPLAUNCHER + MISSILEBODY)

FIG.
III.C.21.a

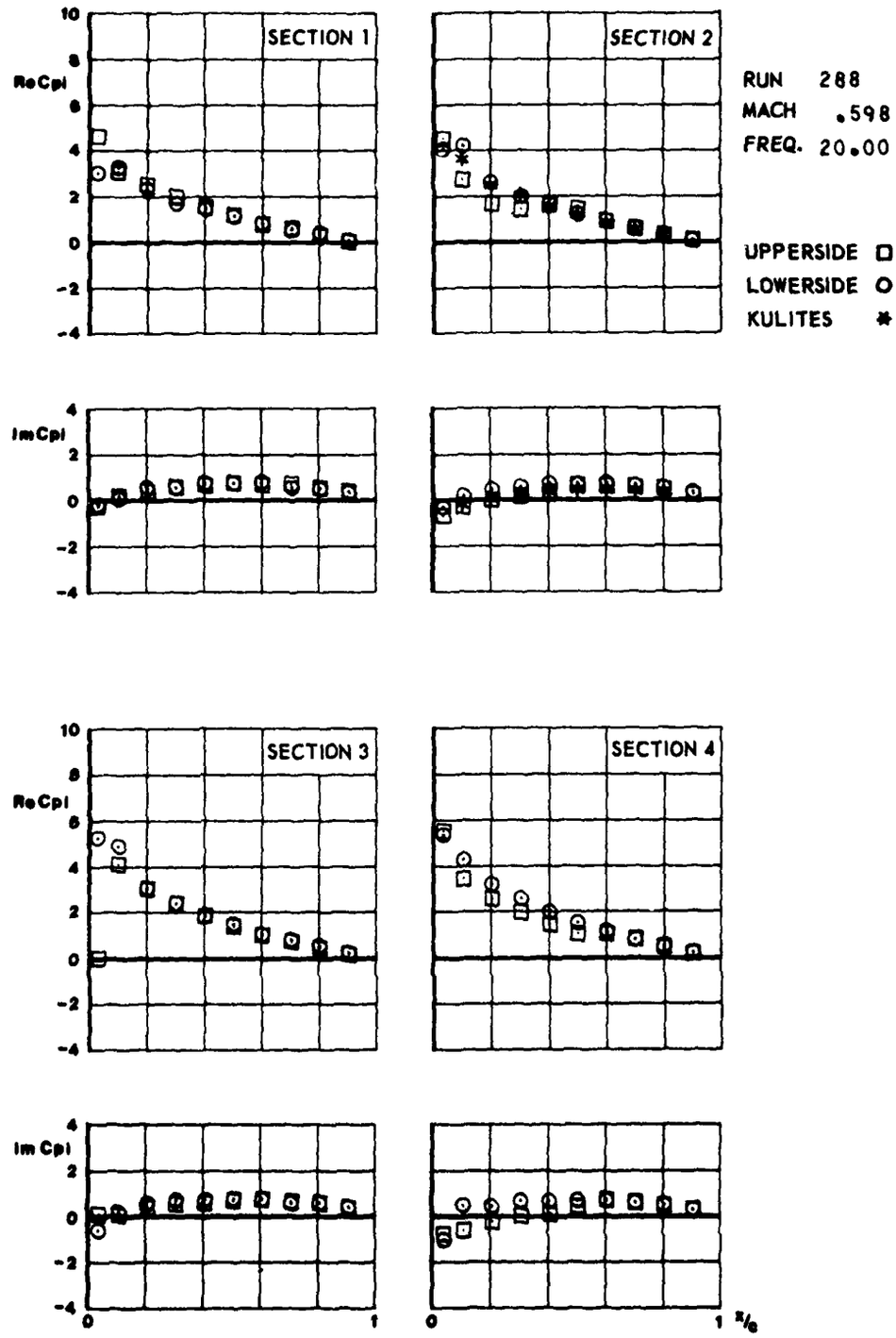

CONF. 3 (WING + TIPLAUNCHER + MISSILEBODY WITh AFT WINGS)

FIG.
III.C.21.b

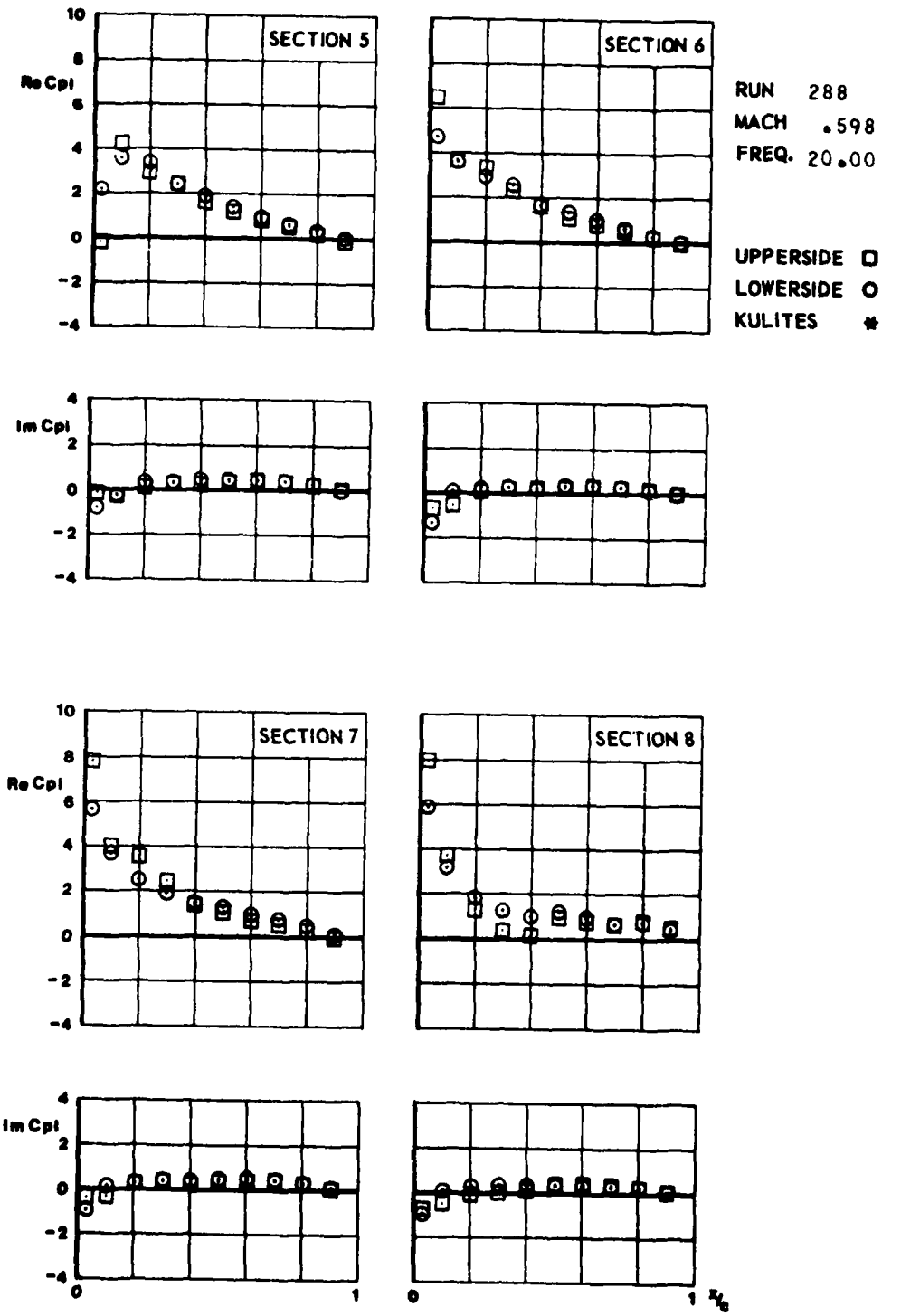

CONF. 3 (WING + TIPLAUNCHER + MISSILEBODY WITH AFT WINGS)

FIG.
III.C.22.a

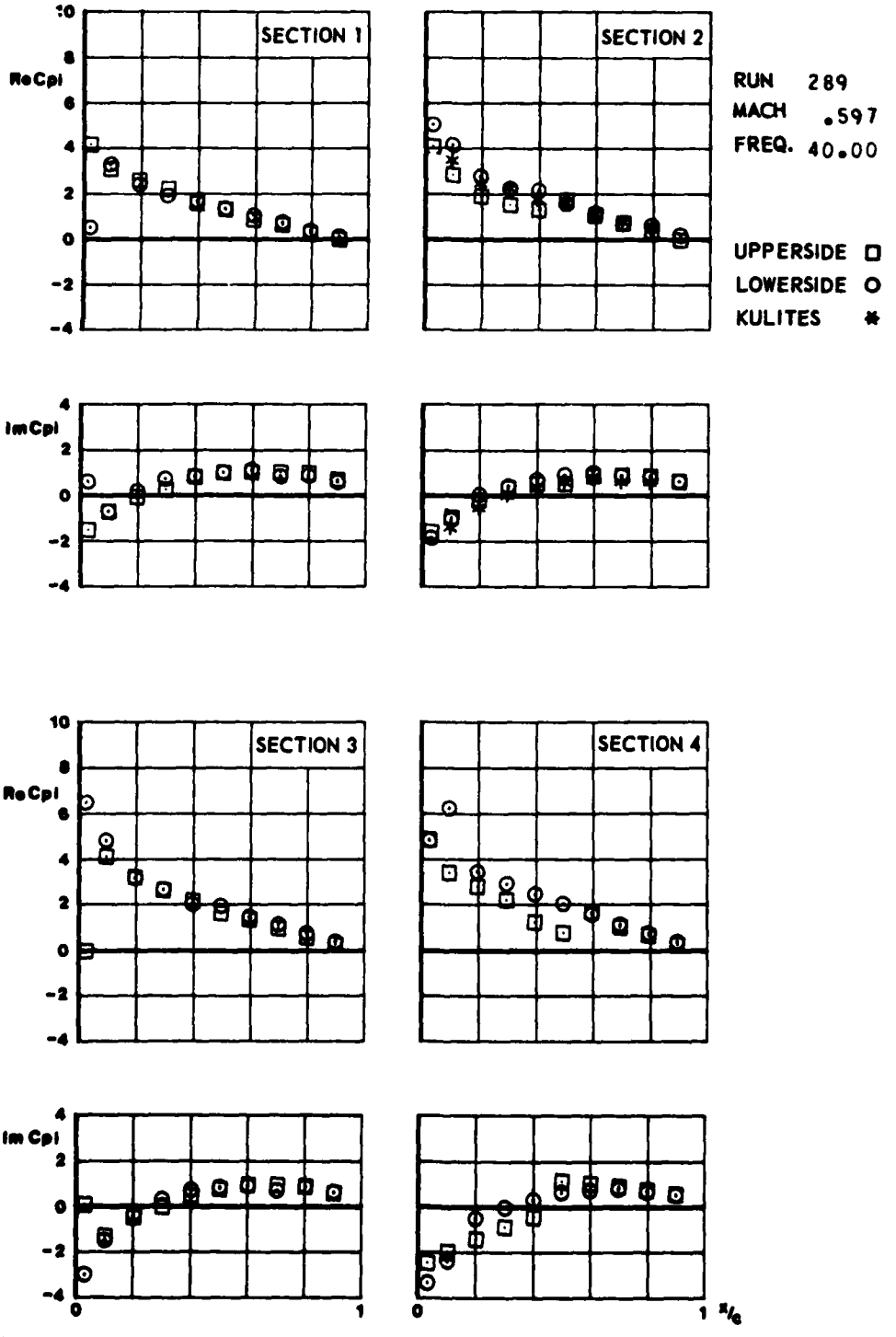

CONF. 3 (WING + TIPLAUNCHER + MISSILEBODY WITH AFT WINGS)

FIG.
III.C.22.b

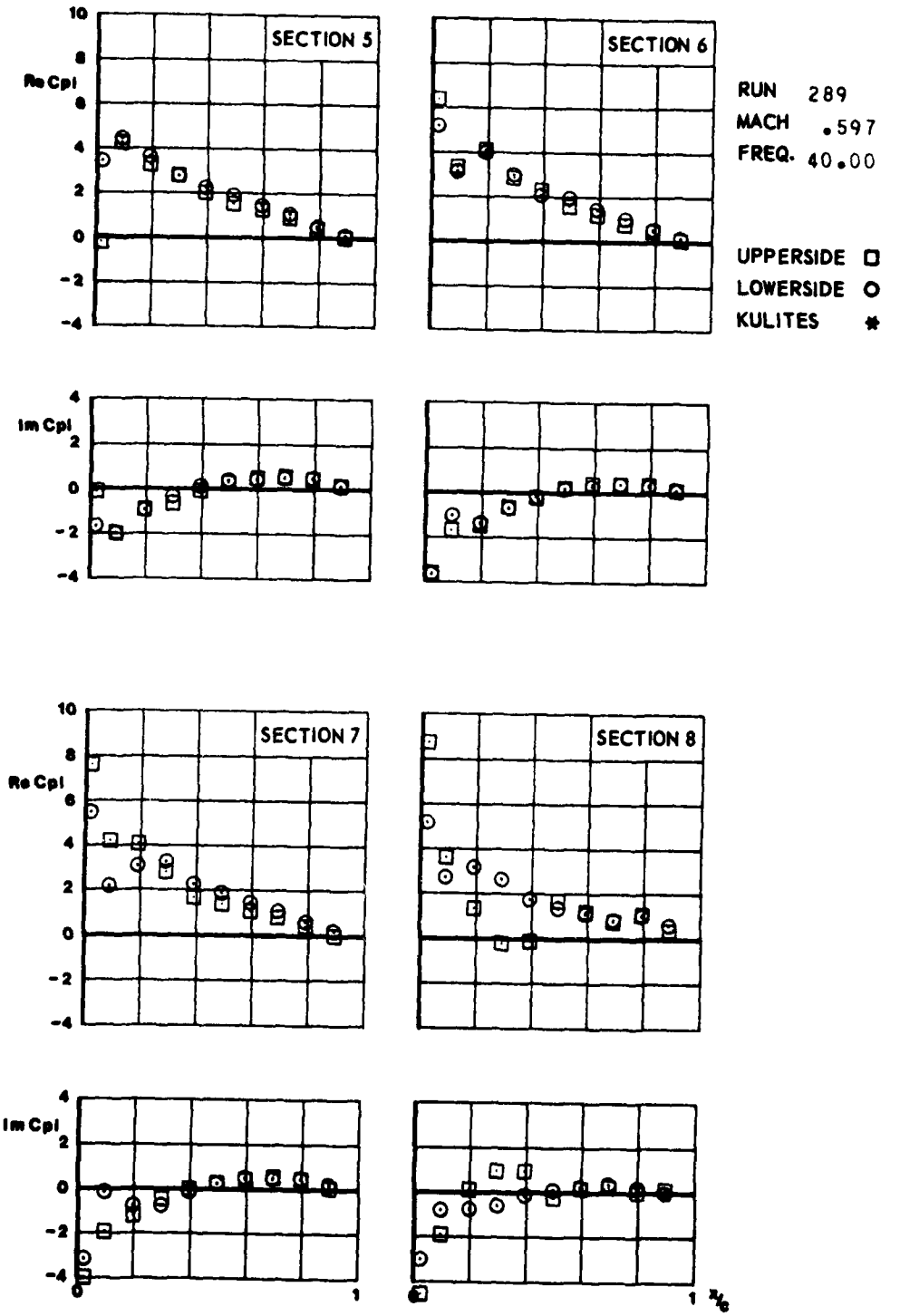

CONF. 3 (WING + TIPLAUNCHER + MISSILEBODY WITH AFT WINGS)

FIG.
III.C.23.a

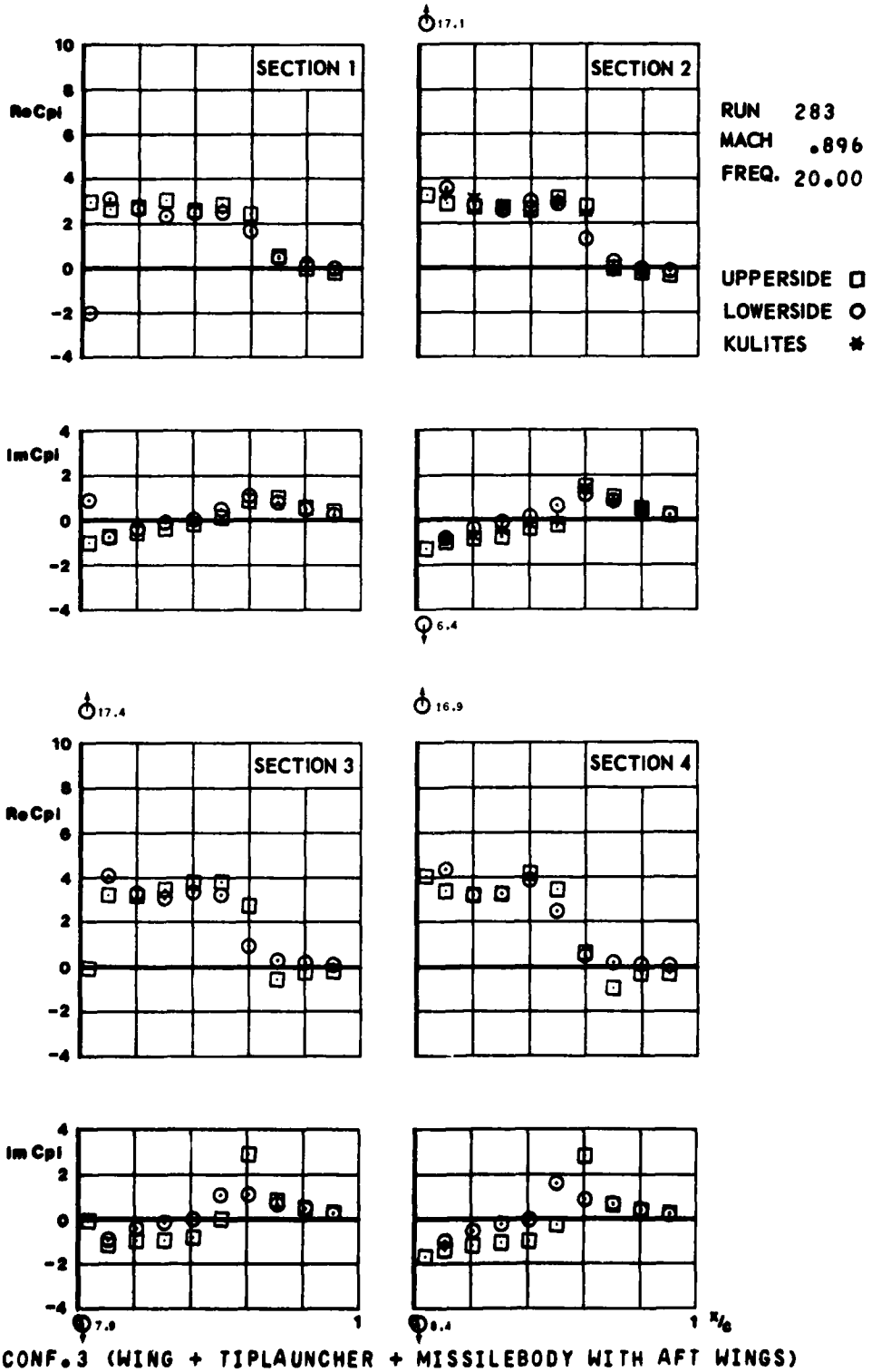

CONF. 3 (WING + TIPLAUNCHER + MISSILEBODY WITH AFT WINGS)

FIG.
III.C.23.b

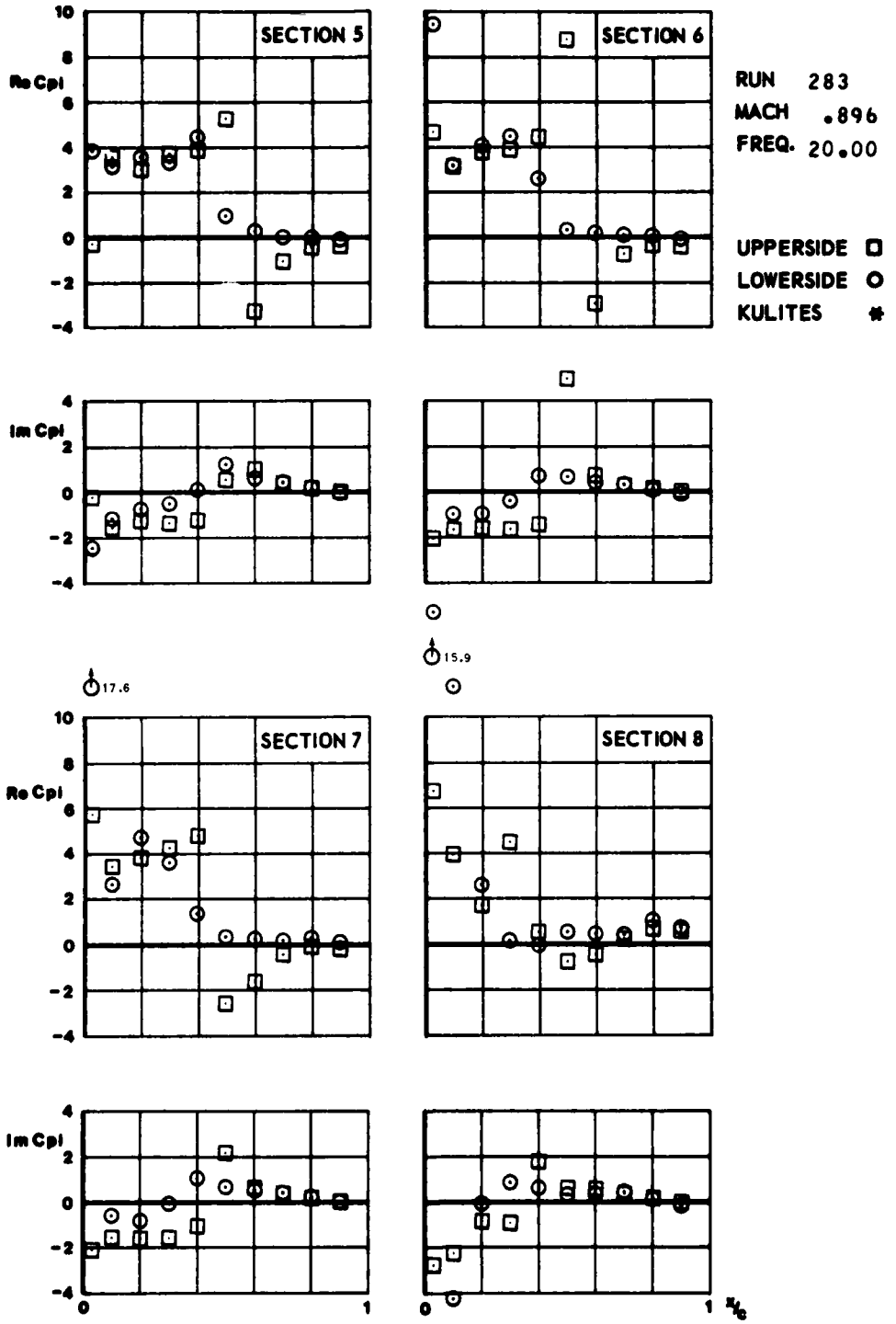

CONF. 3 (WING + TIPLAUNCHER ⊙ MISSILEBODY WITH AFT WINGS)

FIG.
III.C.24.a

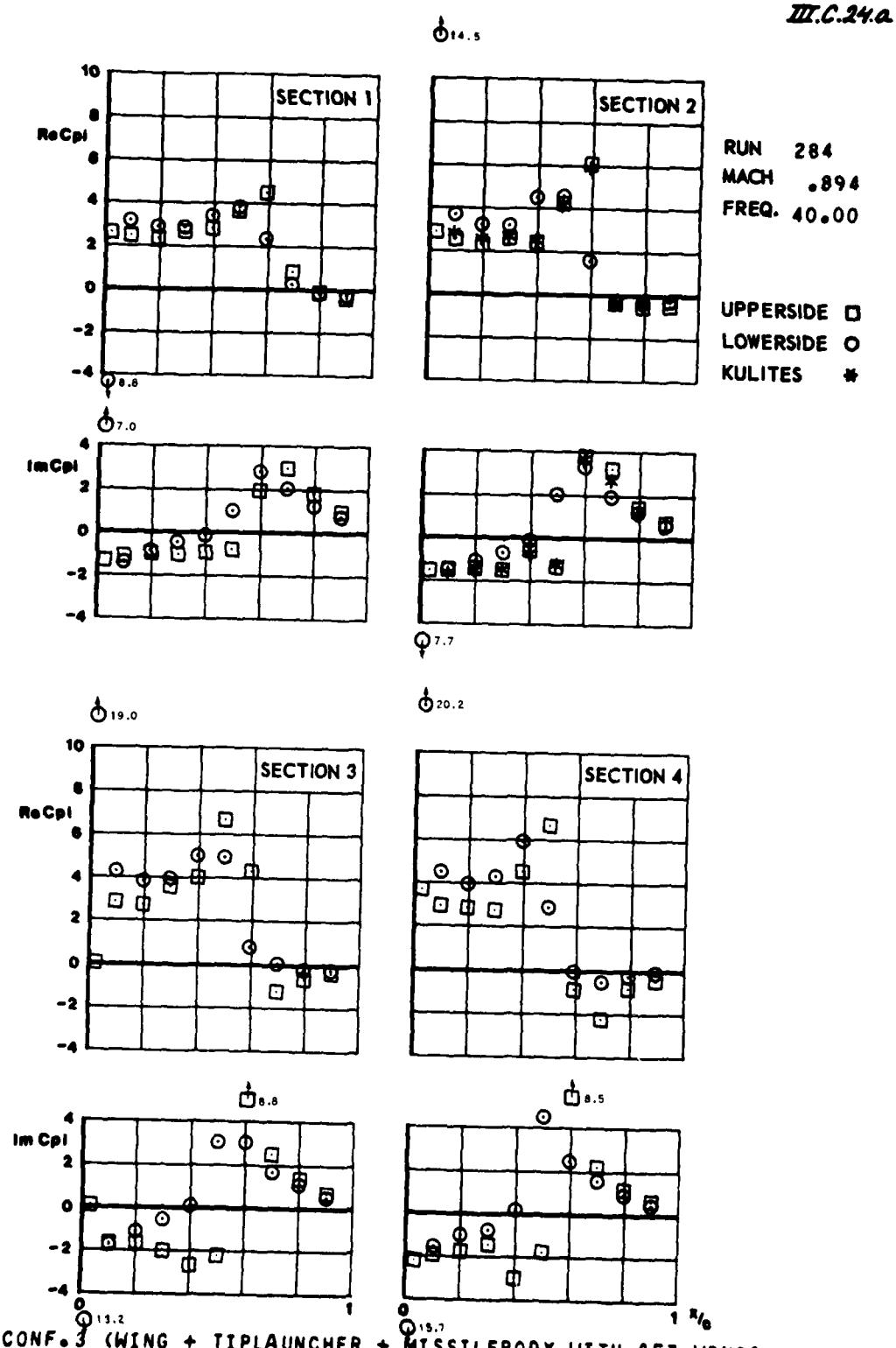

CONF. 3 (WING + TIPLAUNCHER + MISSILEBODY WITH AFT WINGS)

FIG.
III.C.24.b

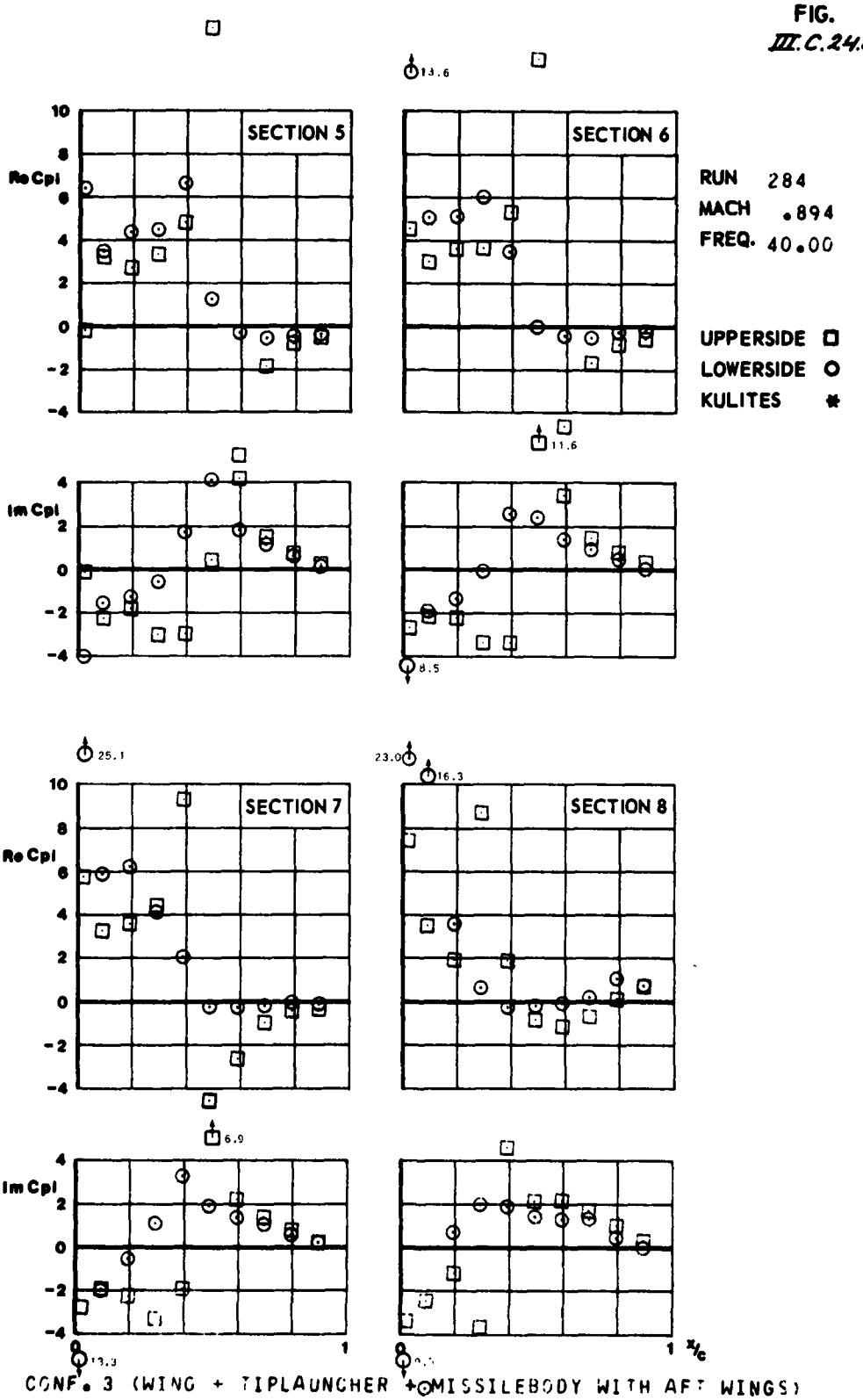

CONF. 3 (WING + TIPLAUNCHER + MISSILEBODY WITH AFT WINGS)

FIG.
III.C.25.a

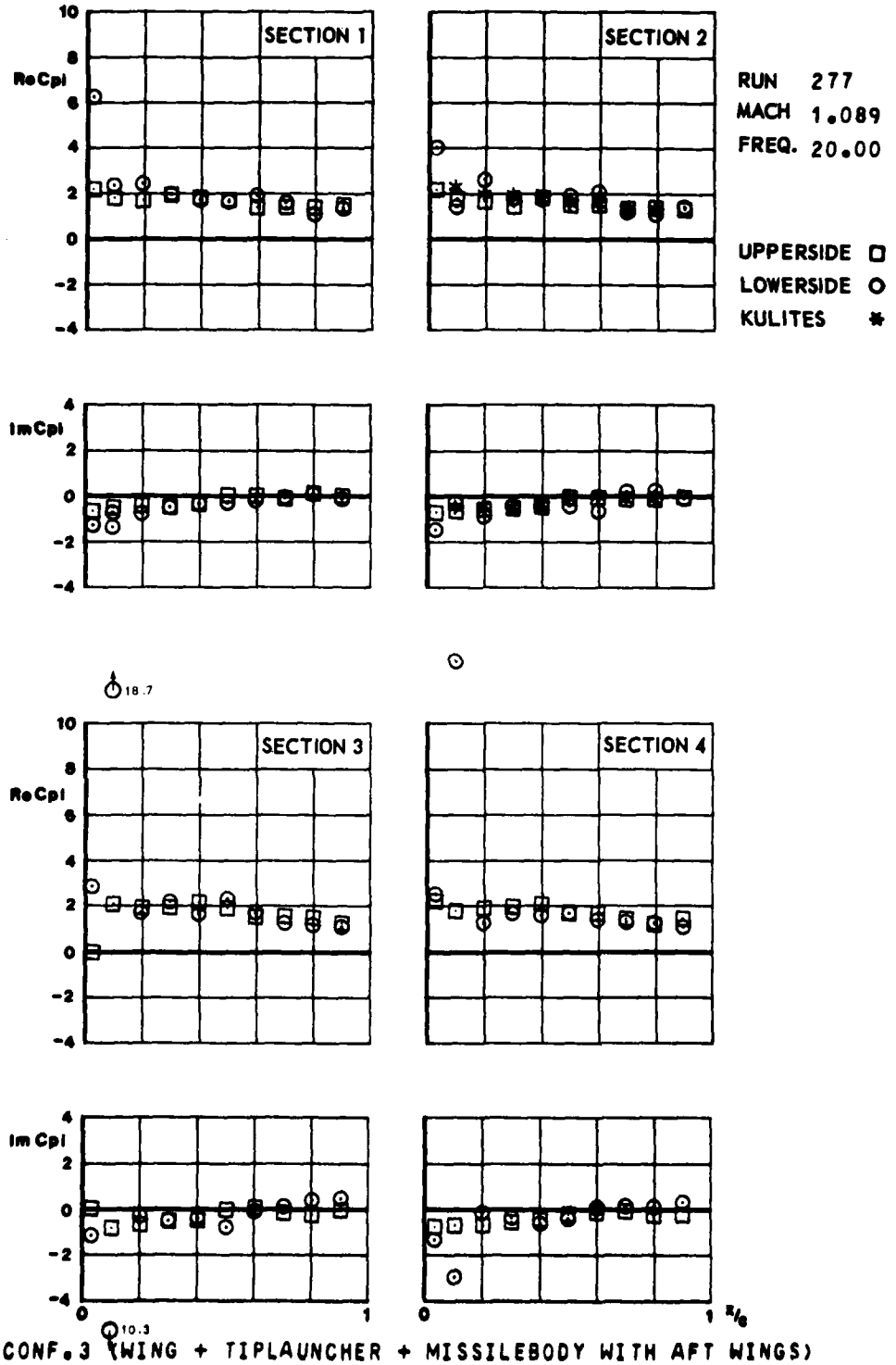

CONF. 3 (WING + TIPLAUNCHER + MISSILEBODY WITH AFT WINGS)

FIG.
III.C.25.b

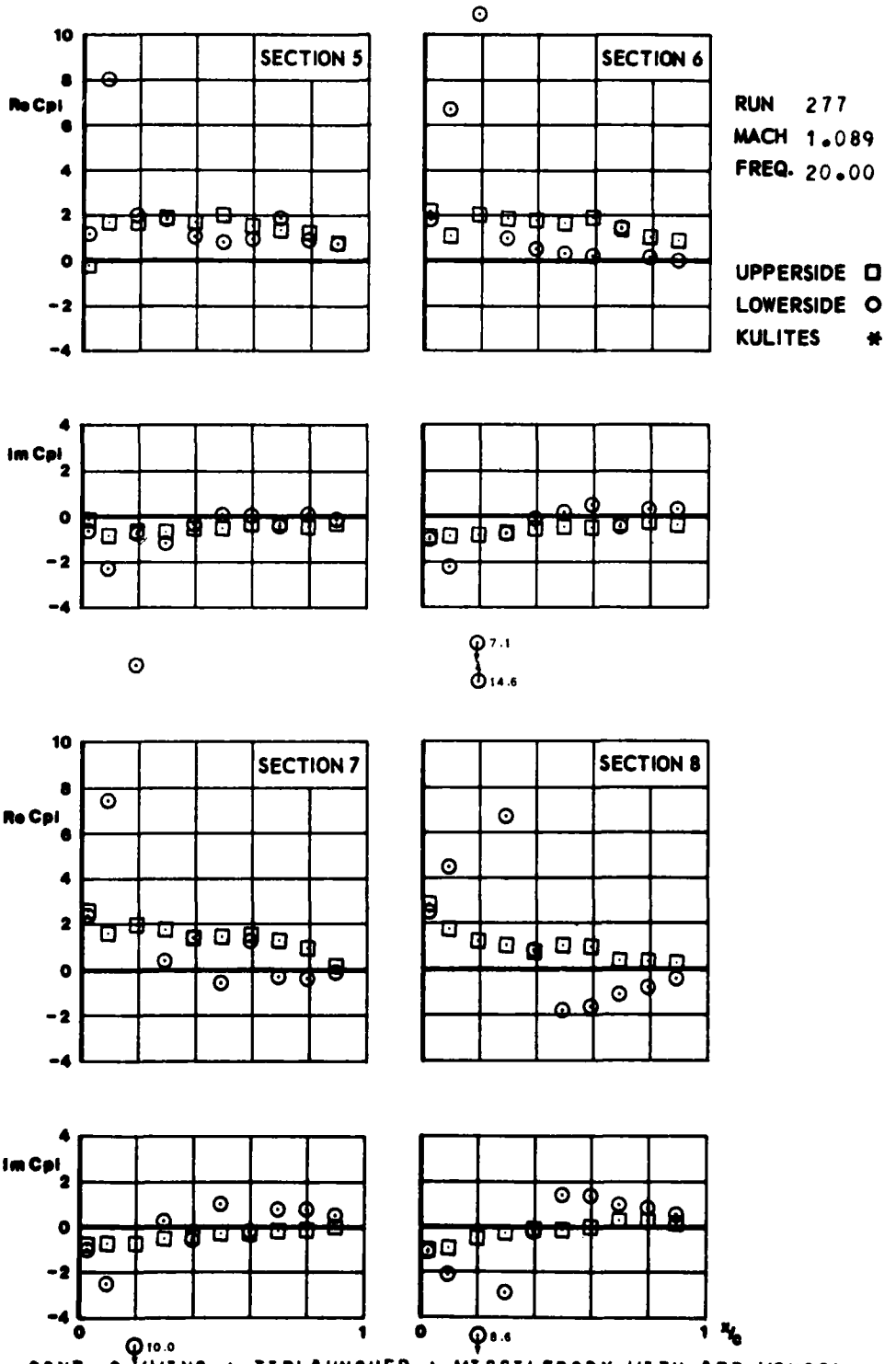

CONF. 3 (WING + TIPLAUNCHER + MISSILEBODY WITH AFT WINGS)

FIG.
III.C.26.a

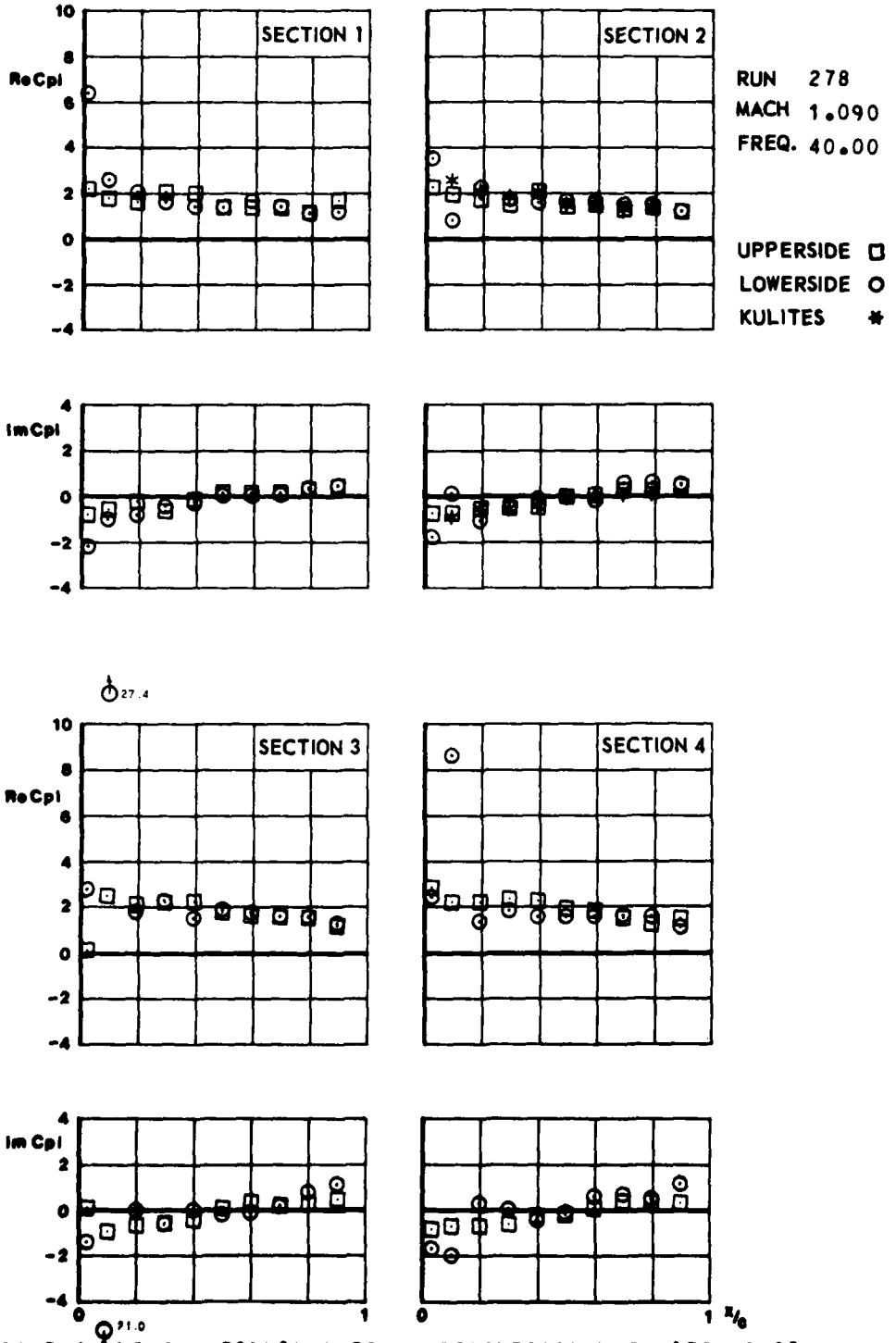

CONF.3 (WING + TIPLAUNCHER + MISSILEBODY WITH AFT WINGS)

FIG.
III.C.26.b

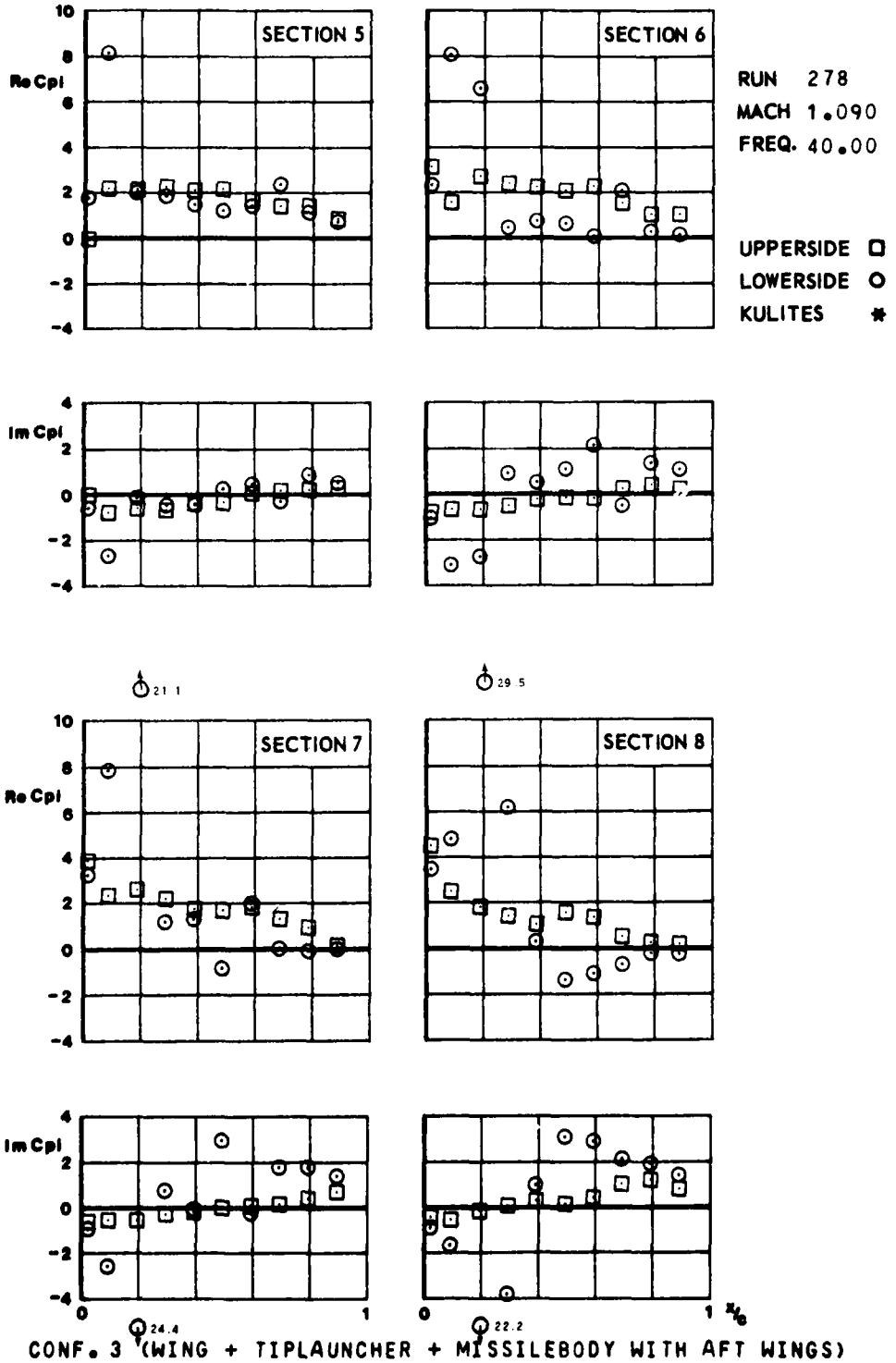

CONF. 3 (WING + TIPLAUNCHER + MISSILEBODY WITH AFT WINGS)

FIG.
III.C.27.a

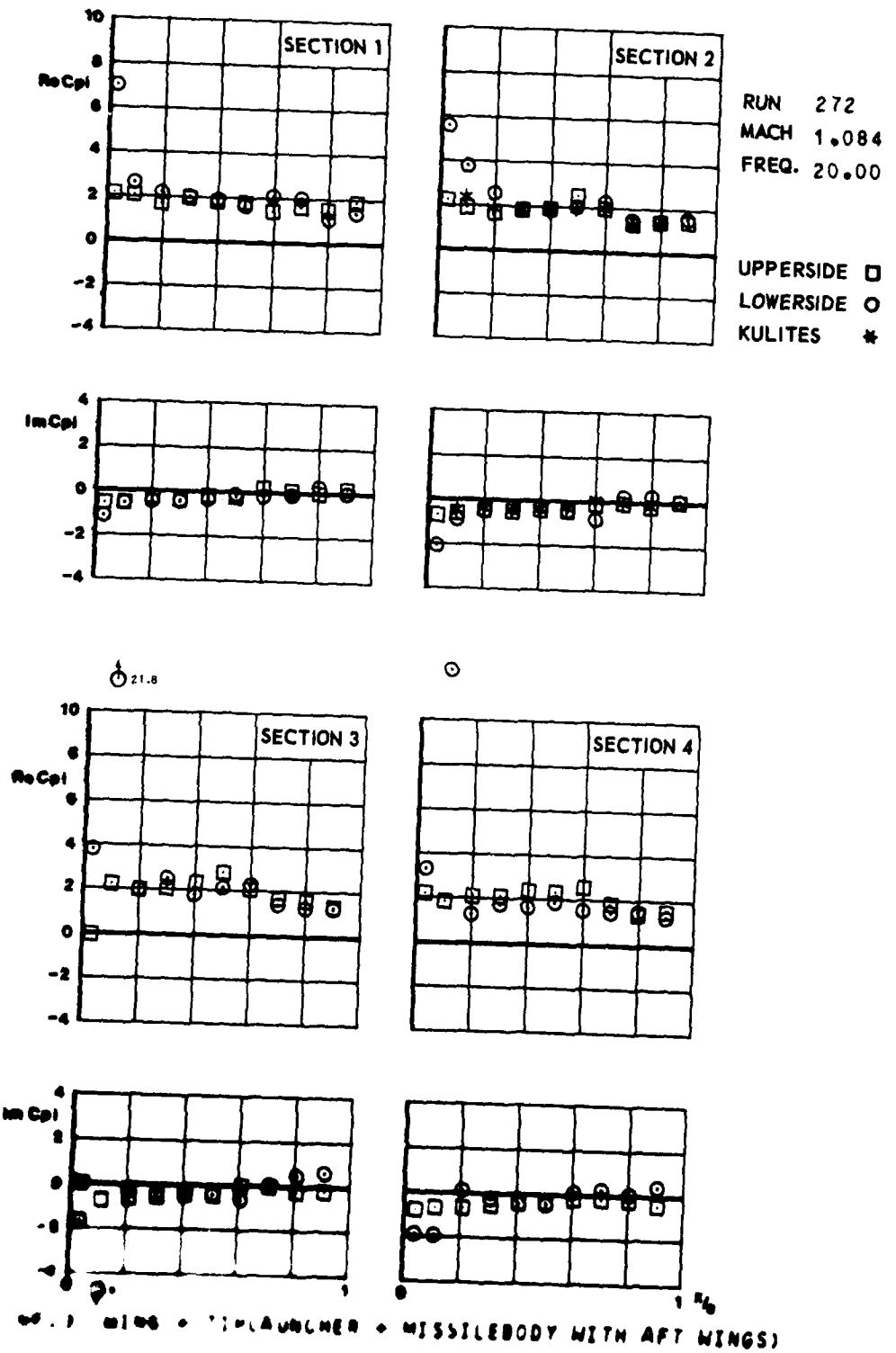
SECTION 1
SECTION 2
SECTION 3
SECTION 4
Re Cpl
Im Cpl
RUN 272
MACH 1.084
FREQ. 20.00
UPPERSIDE
LOWERSIDE
KULITES
21.8
MISSILEBODY WITH AFT WINGS)

FIG.
III.C.27.6

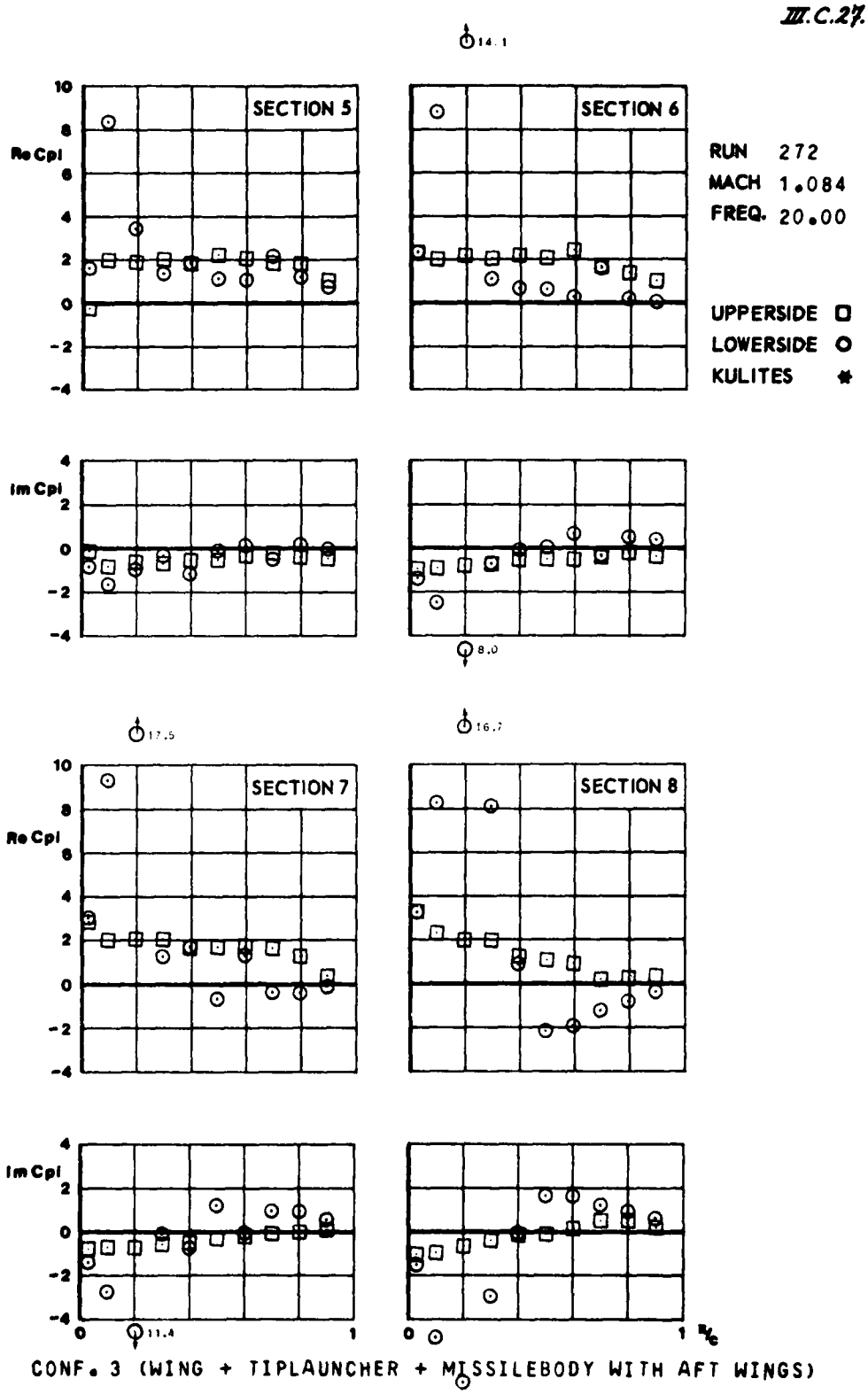

CONF. 3 (WING + TIPLAUNCHER + MISSILEBODY WITH AFT WINGS)

FIG.
III.C.28.a

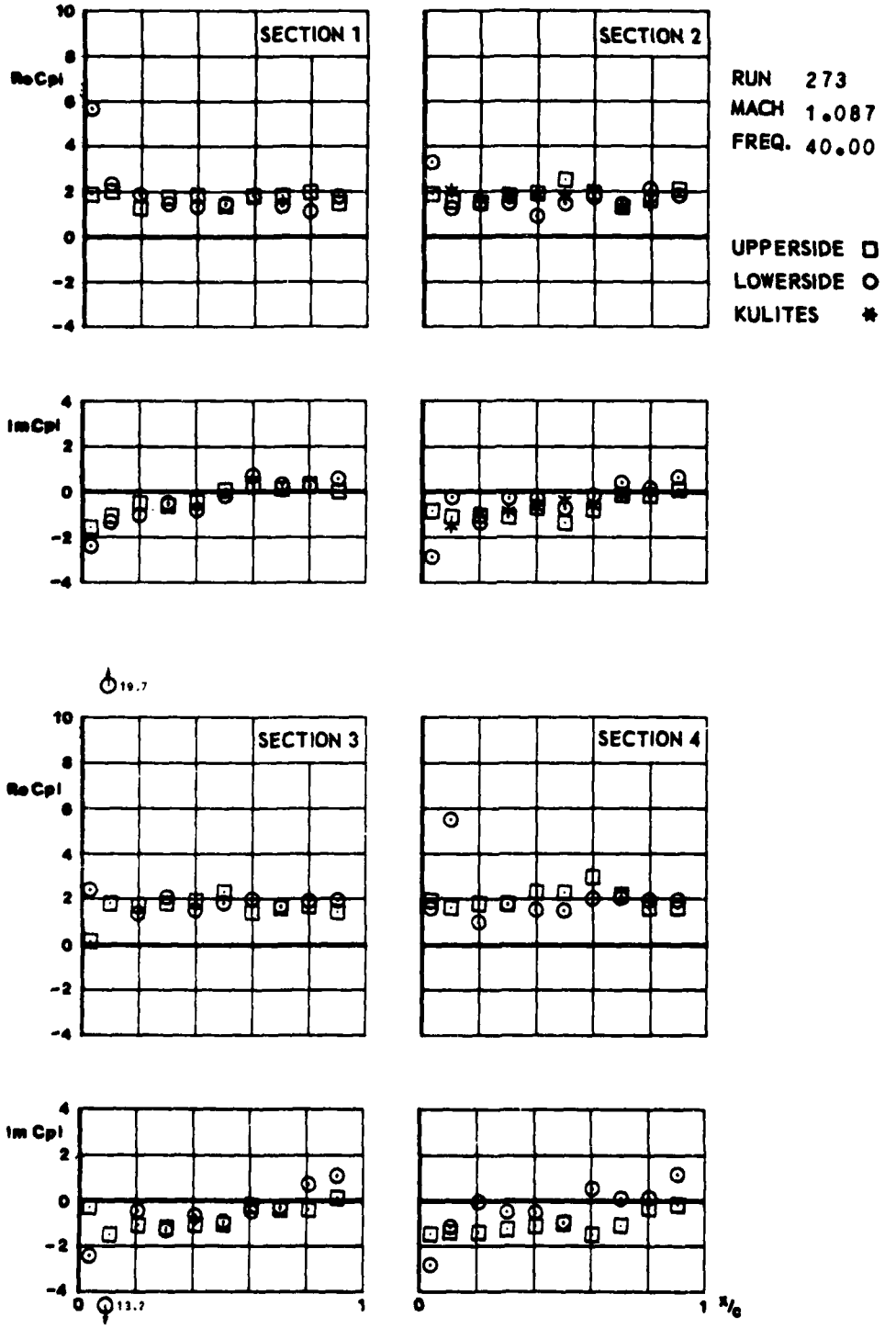

CONF.3 (WING + TIPLAUNCHER + MISSILEBODY WITH AFT WINGS)

FIG.
III.C.28.b

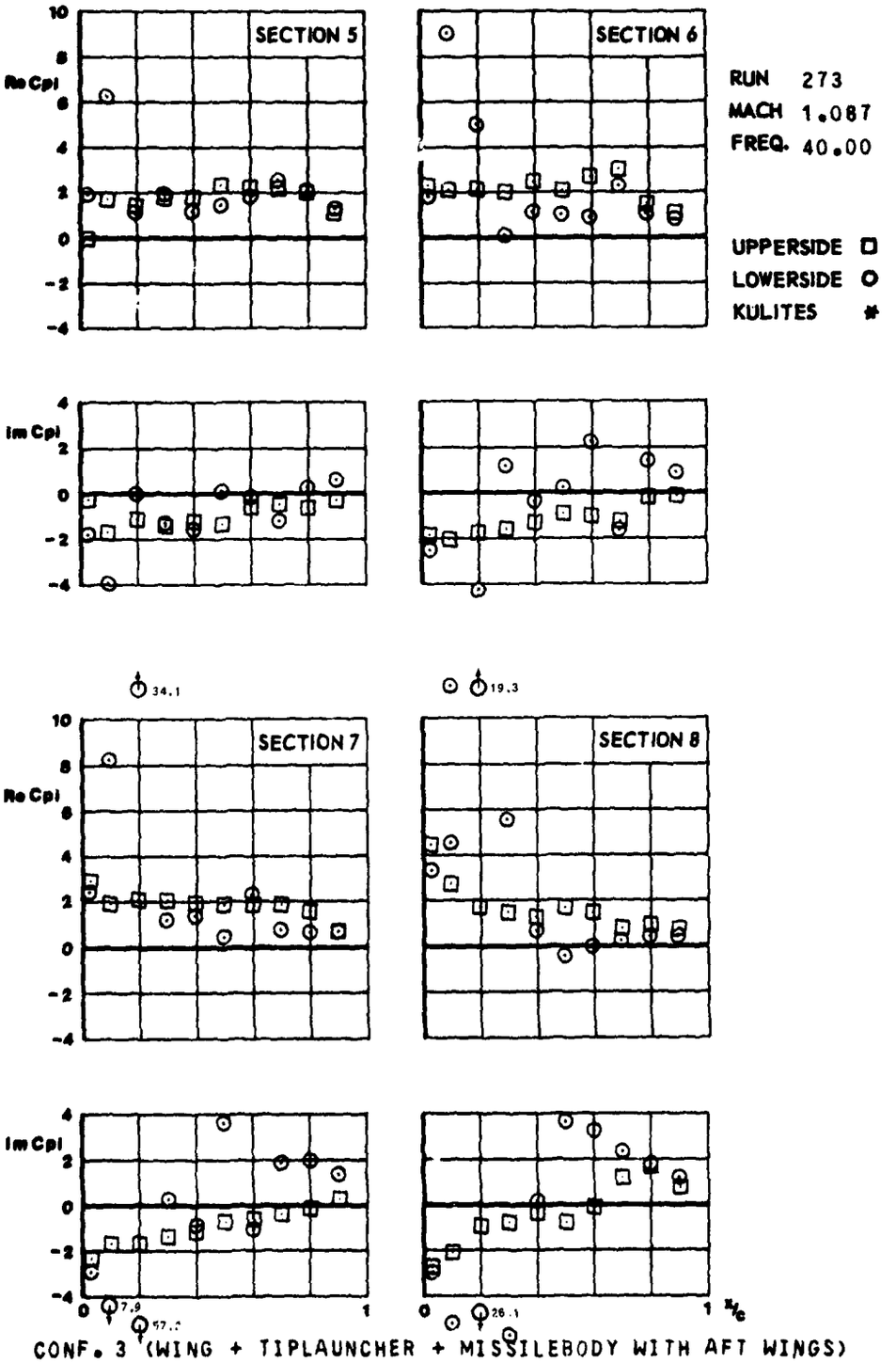

CONF. 3 (WING + TIPLAUNCHER + MISSILEBODY WITH AFT WINGS)

FIG.
III.C.29.a

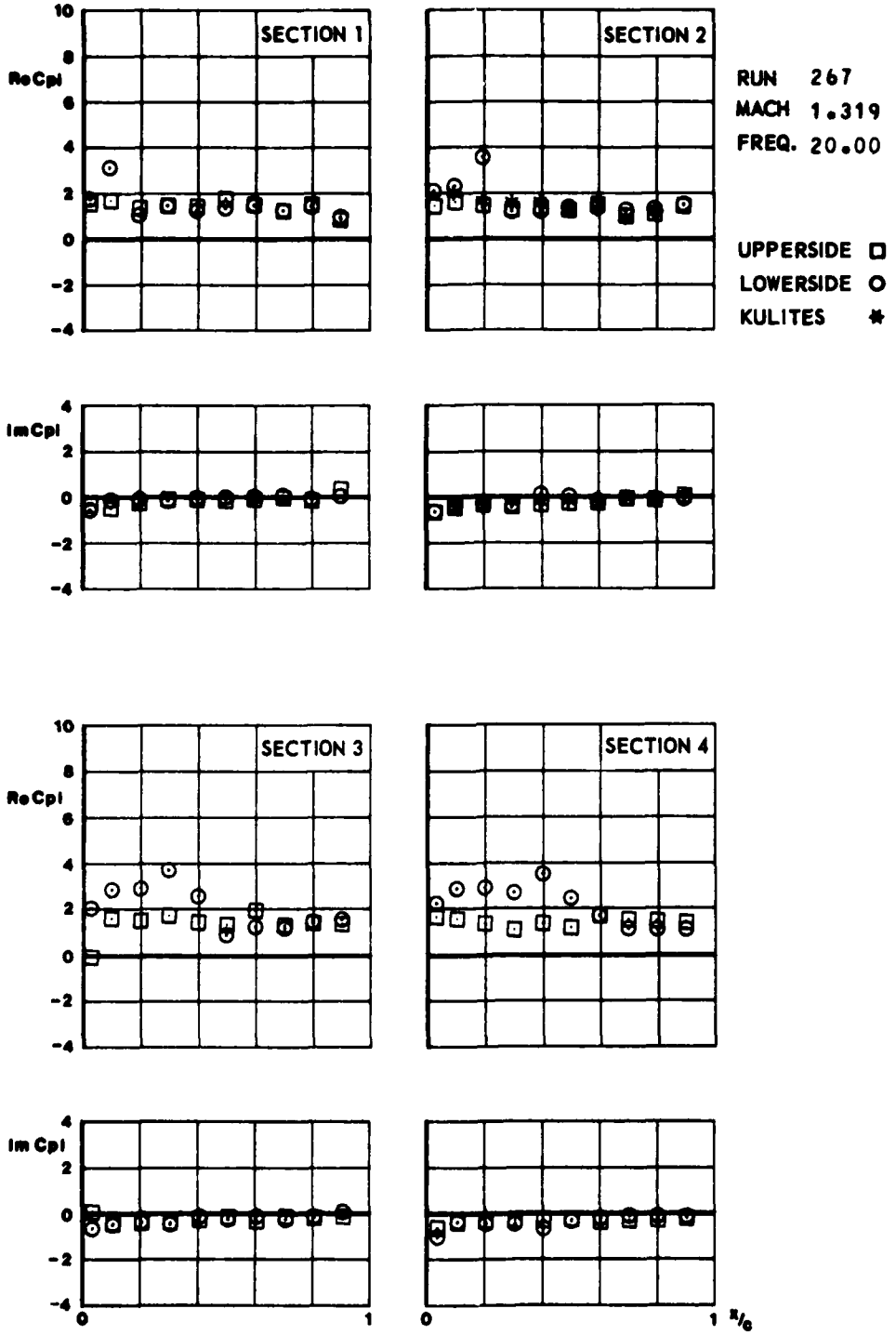

CONF.3 (WING + TIPLAUNCHER + MISSILEBODY WITH AFT WINGS)

FIG.
III.C.29.b

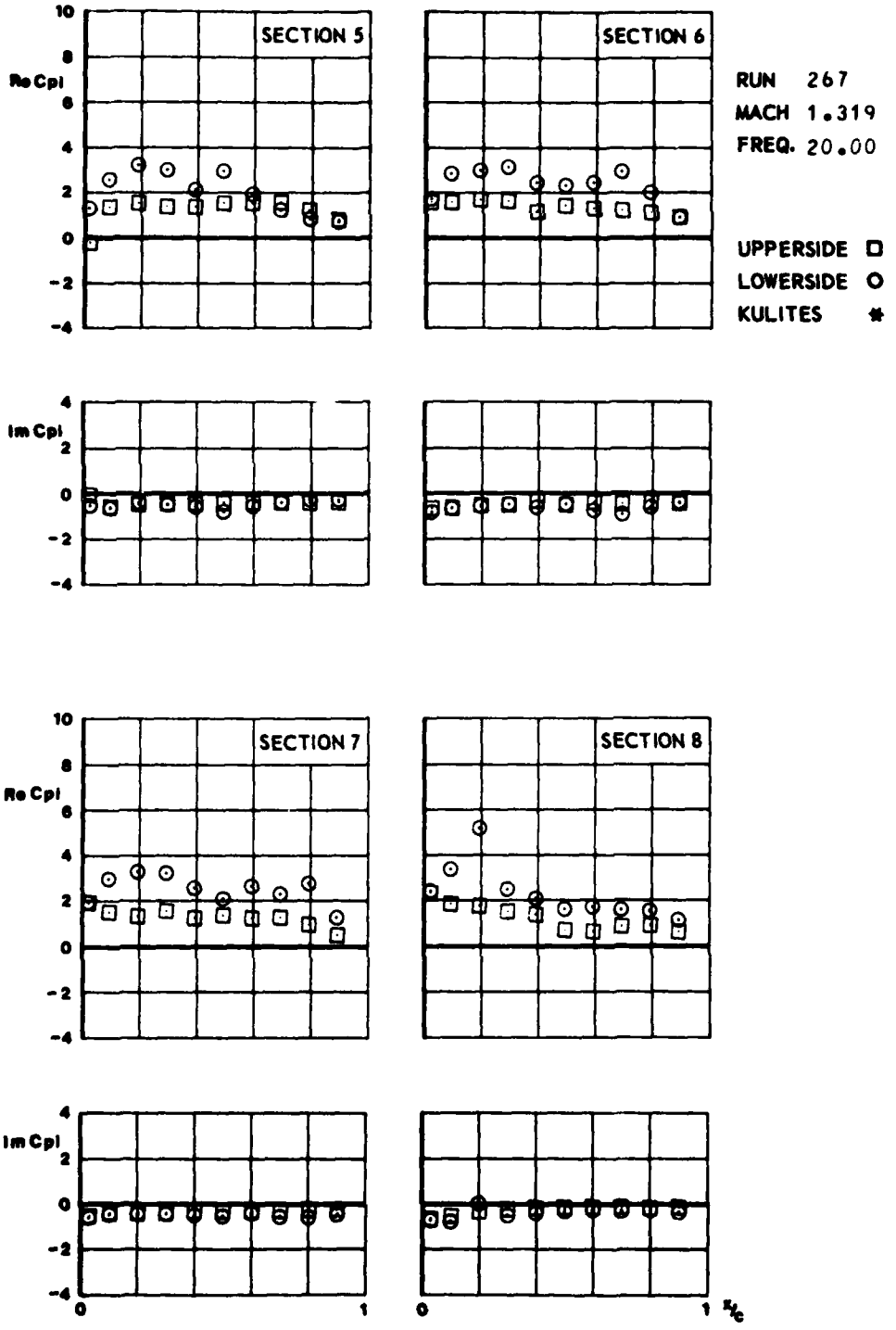

CONF. 3 (WING + TIPLAUNCHER + MISSILEBODY WITH AFT WINGS)

FIG.
III.C.30.a

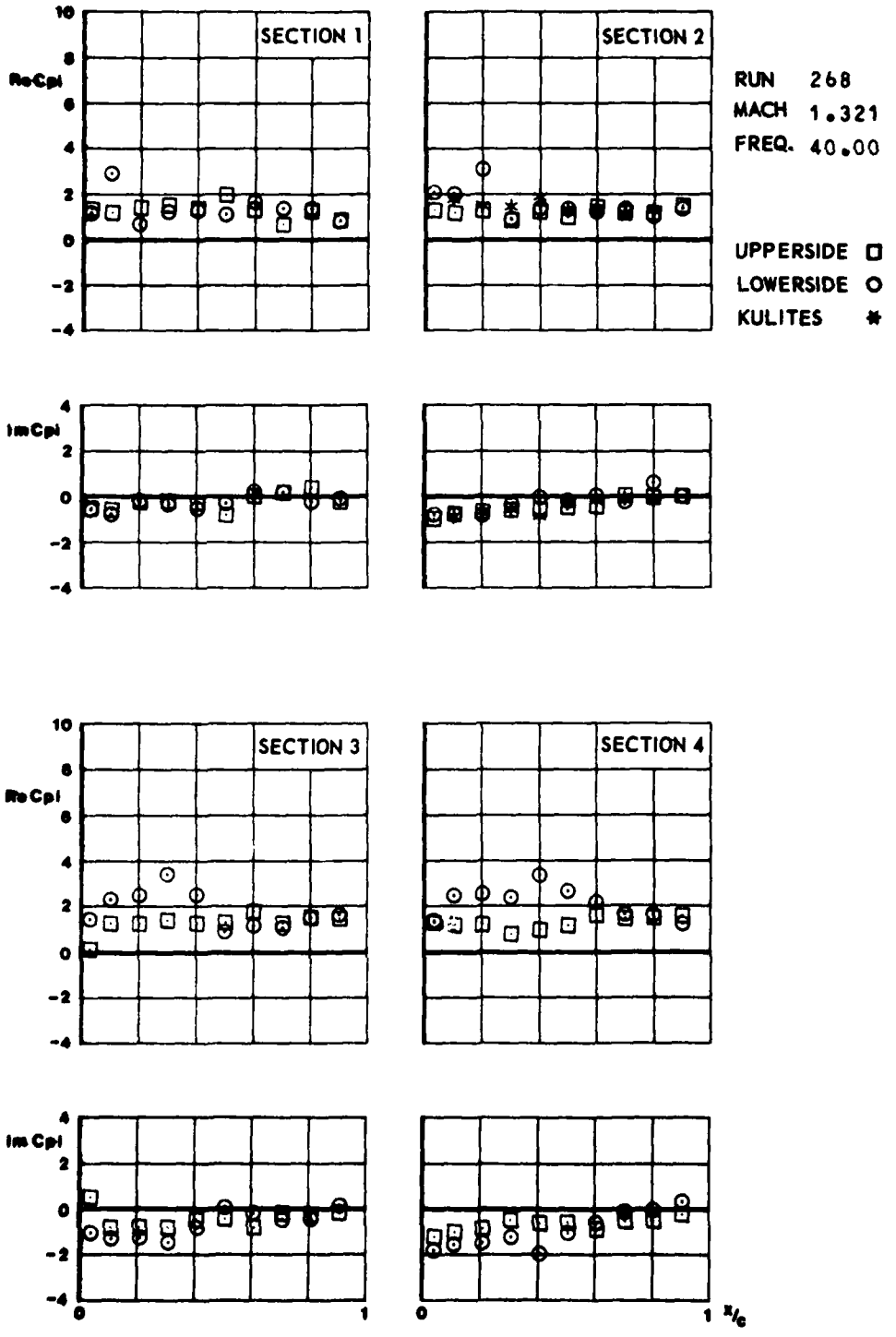

CONF.3 (WING + TIPLAUNCHER + MISSILEBODY WITH AFT WINGS)

FIG.
III.C.30.b

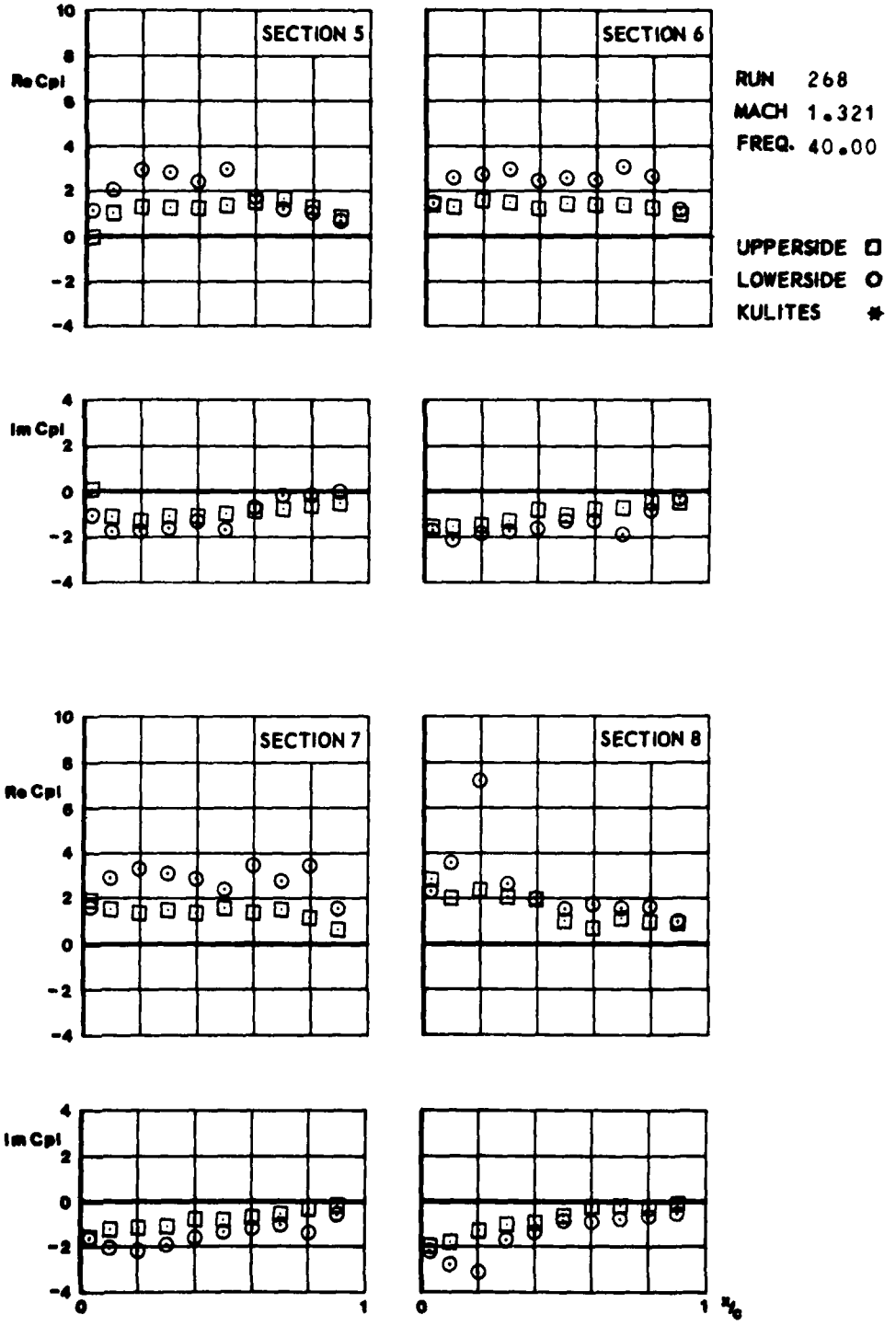

CONF. 3 (WING + TIPLAUNCHER + MISSILEBODY WITH AFT WINGS)

FIG.
III.C.31.a

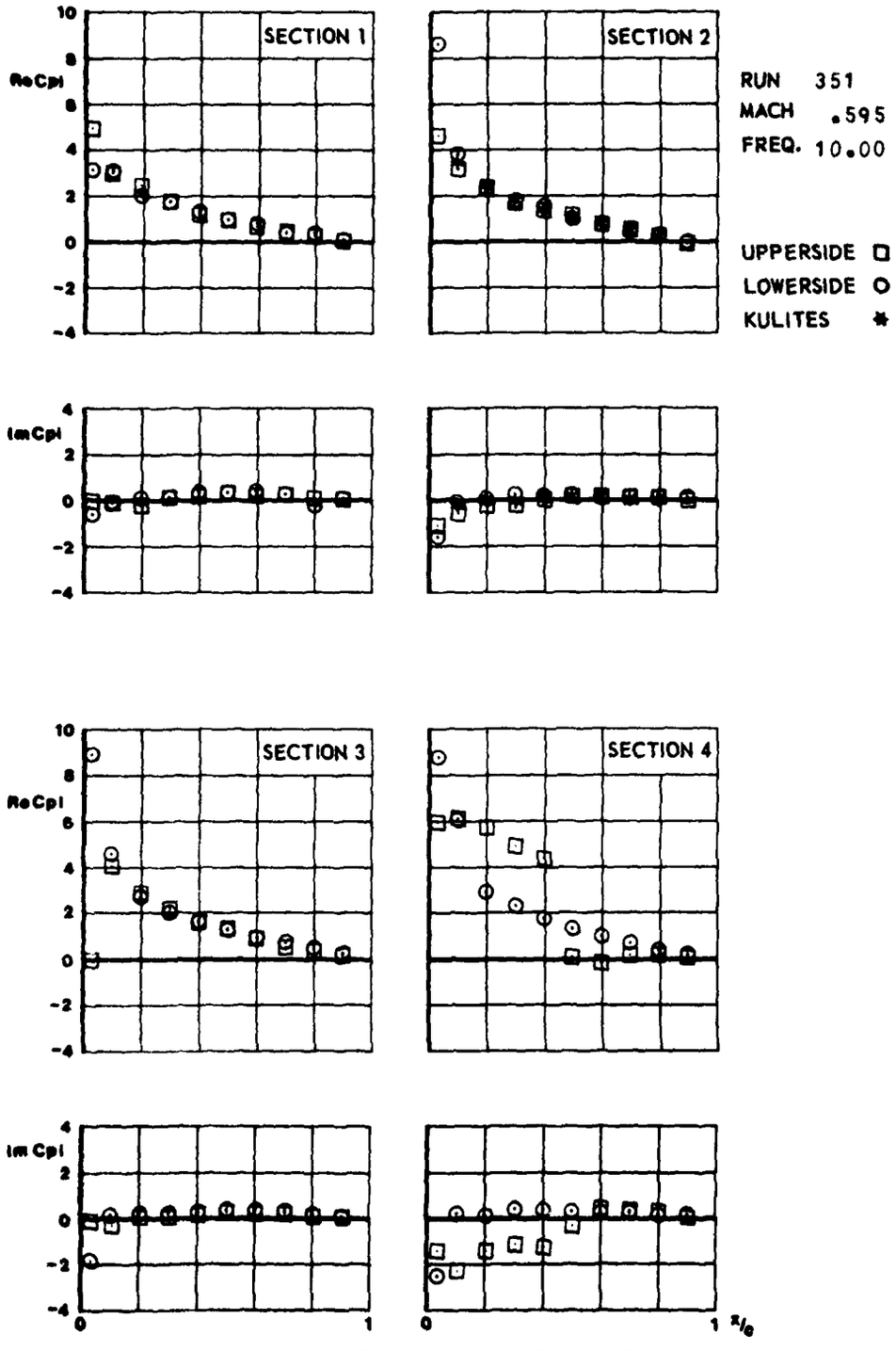

CONF.4 (WING + TIPLAUNCHER + COMPLETE MISSILE)

FIG.
III.C.31.6

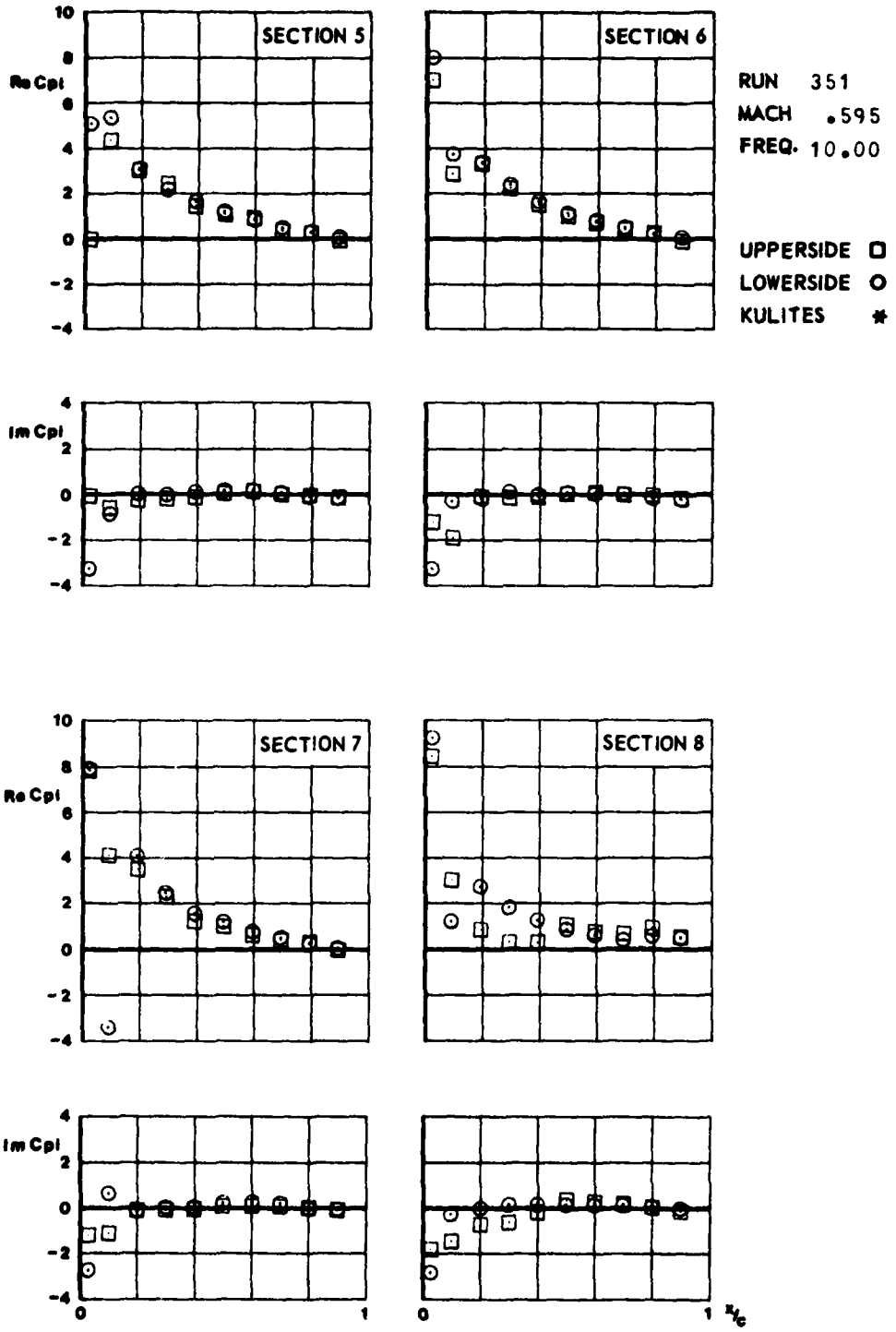

CONF. 4 (WING + TIPLAUNCHER + COMPLETE MISSILE)

FIG.
III.C.32.a

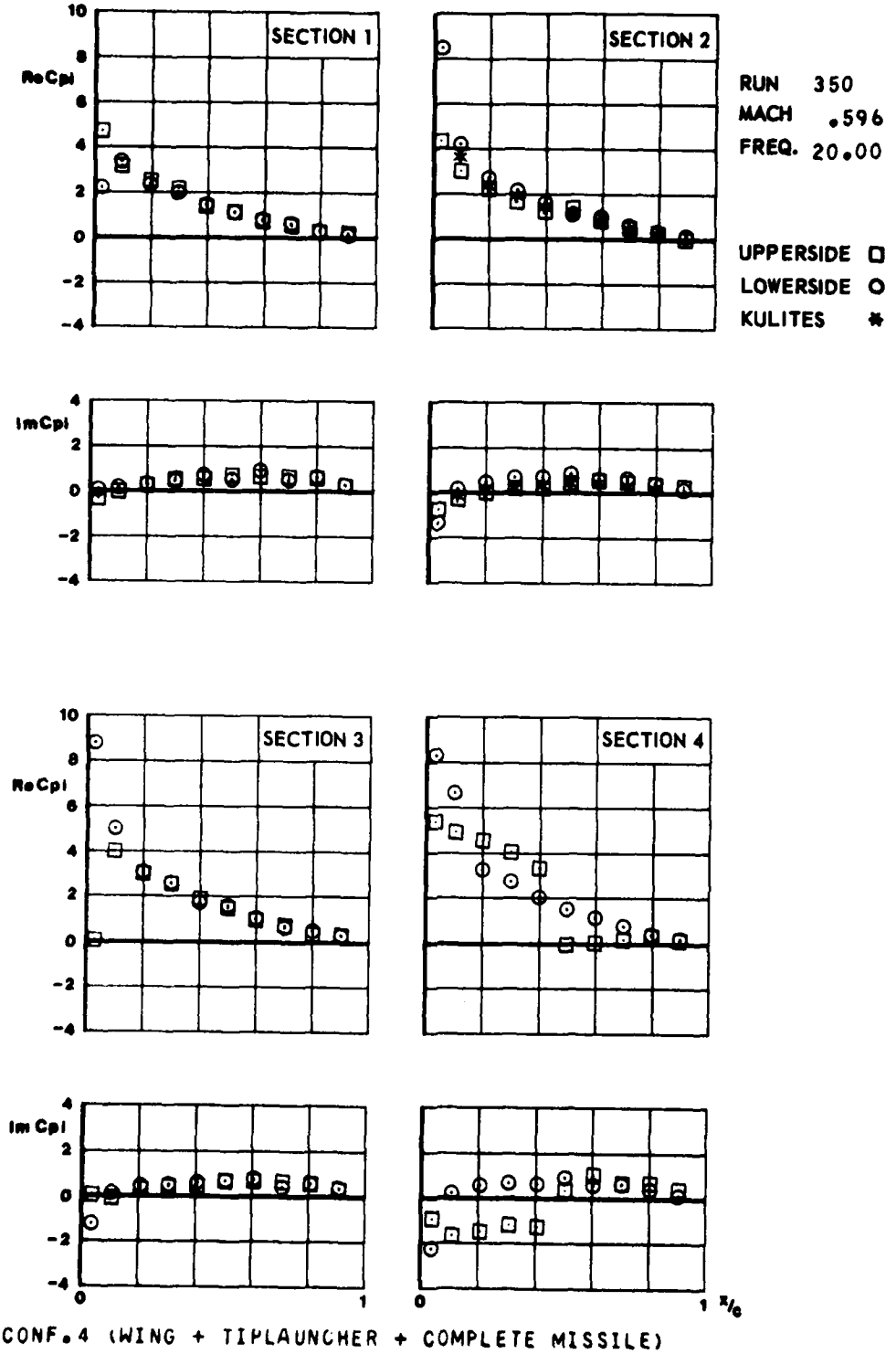

CONF. 4 (WING + TIPLAUNCHER + COMPLETE MISSILE)

FIG.
III.C.32.b

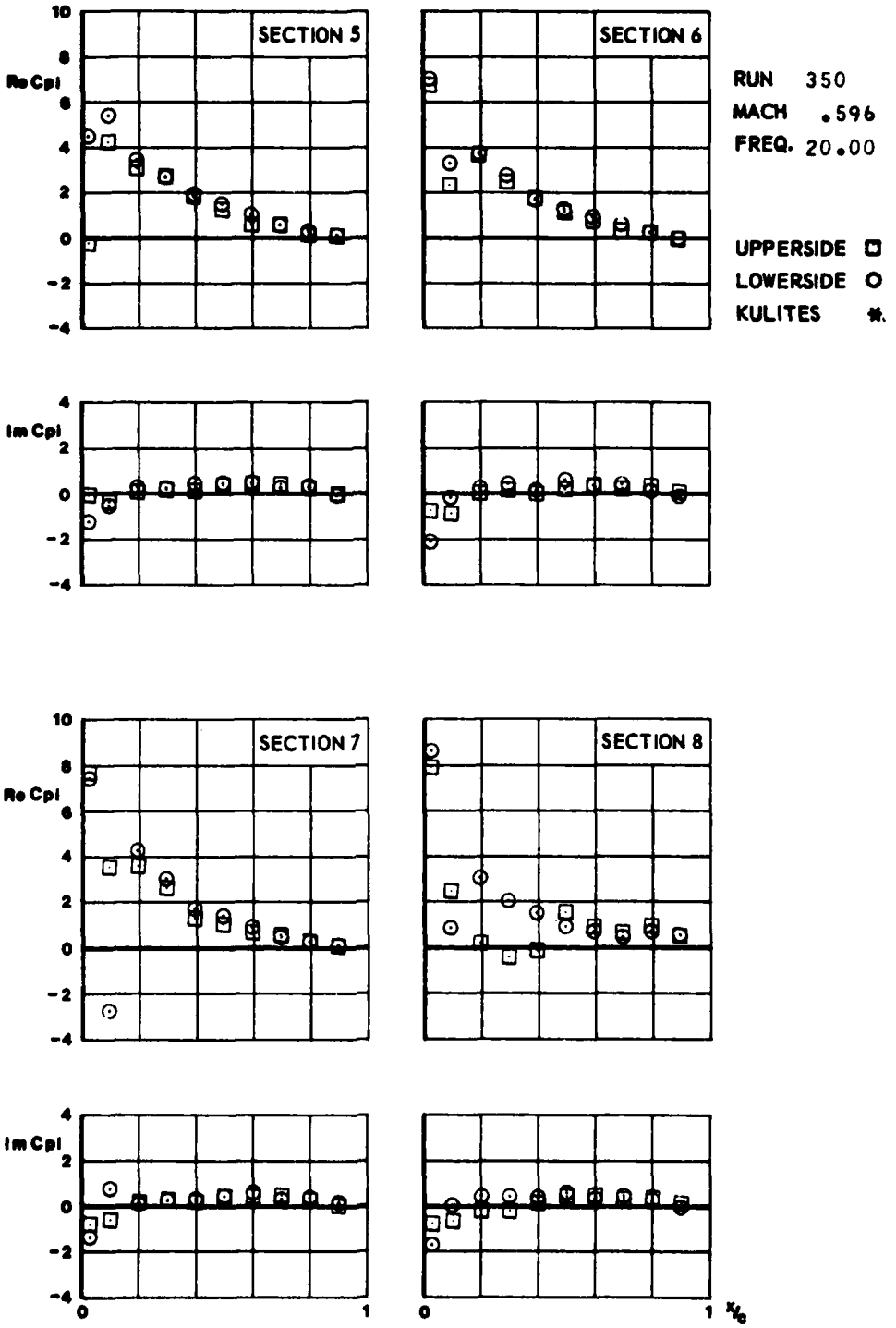

CONF. 4 (WING + TIPLAUNCHER + COMPLETE MISSILE)

FIG.
III.C.33a

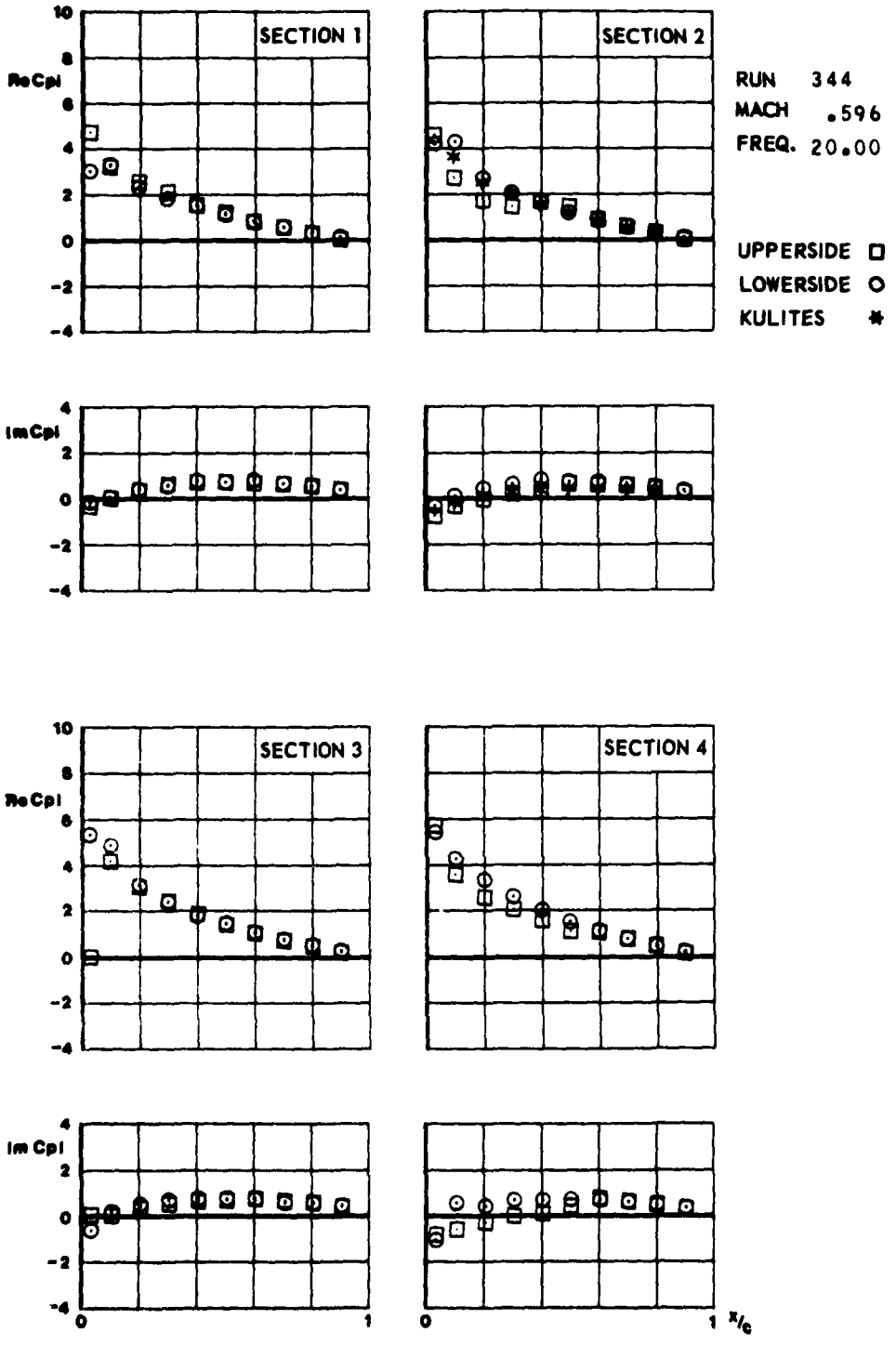

CONF.4 (WING + TIPLAUNCHER + COMPLETE MISSILE)

FIG.
III.C.33.6

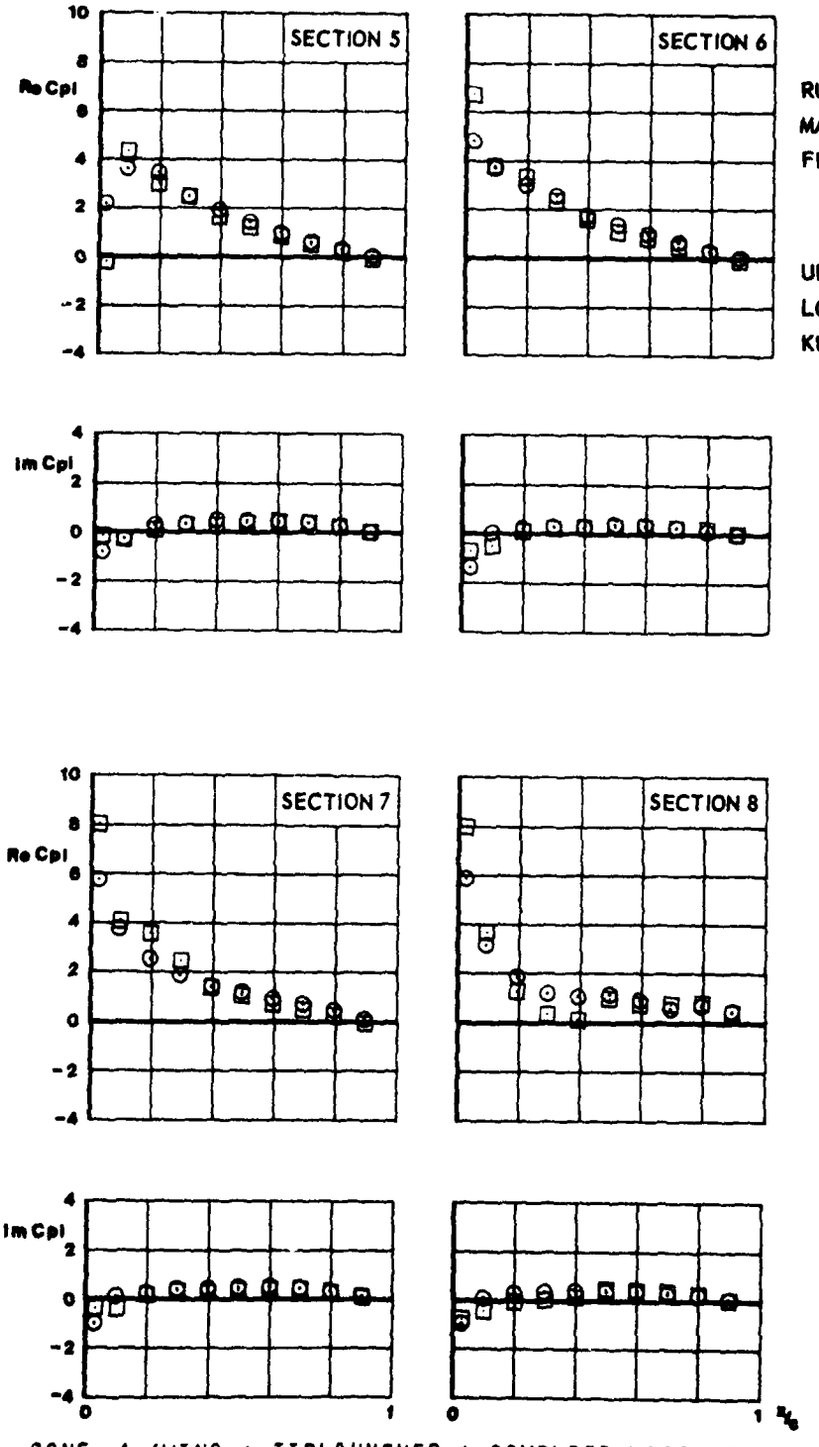

CONF. 4 (WING + TIPLAUNCHER + COMPLETE MISSILE)

FIG.
III.C.34a

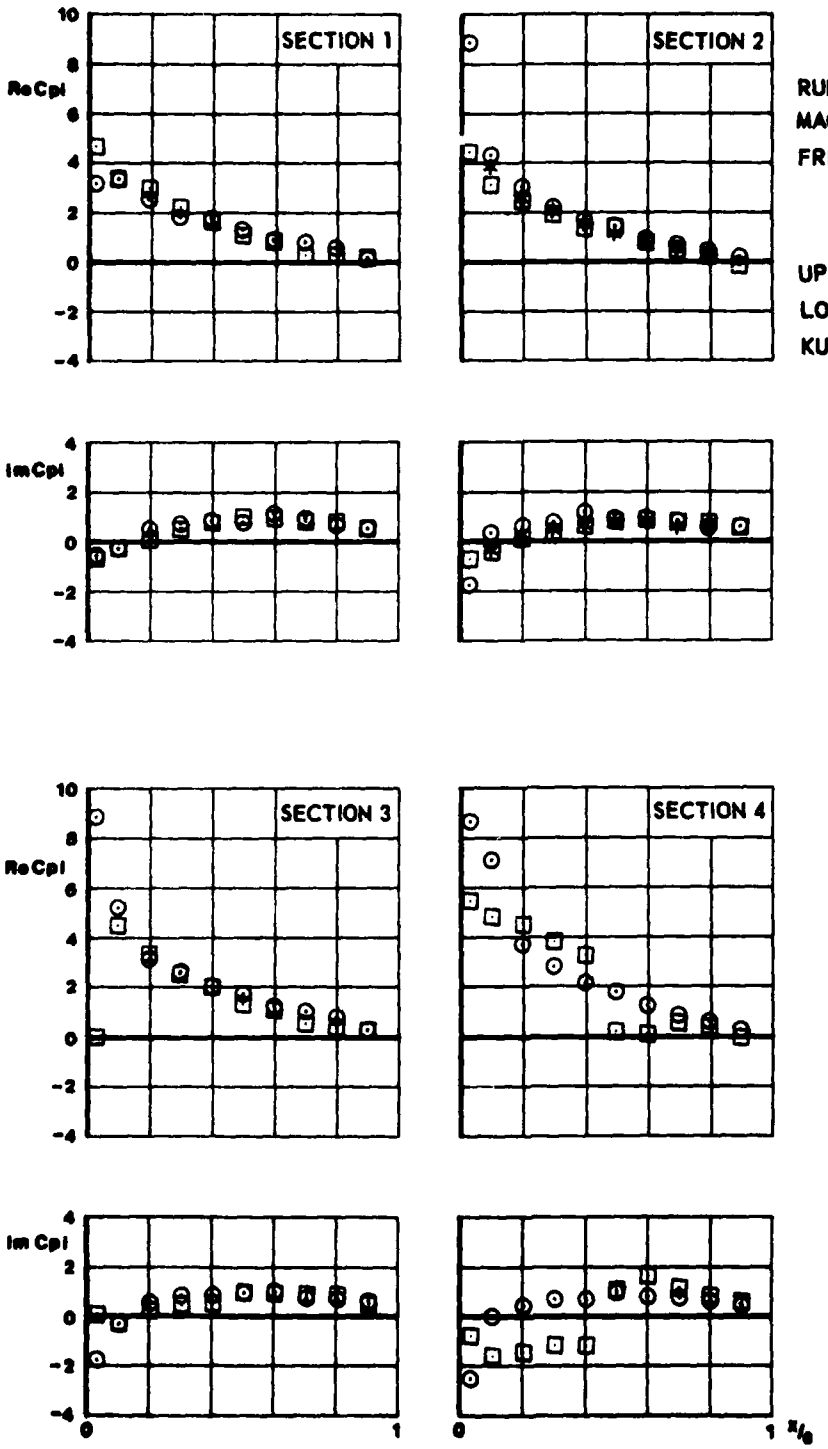

CONF.4 (WING + TIPLAUNCHER + COMPLETE MISSILE)

FIG.
III.C.34.b

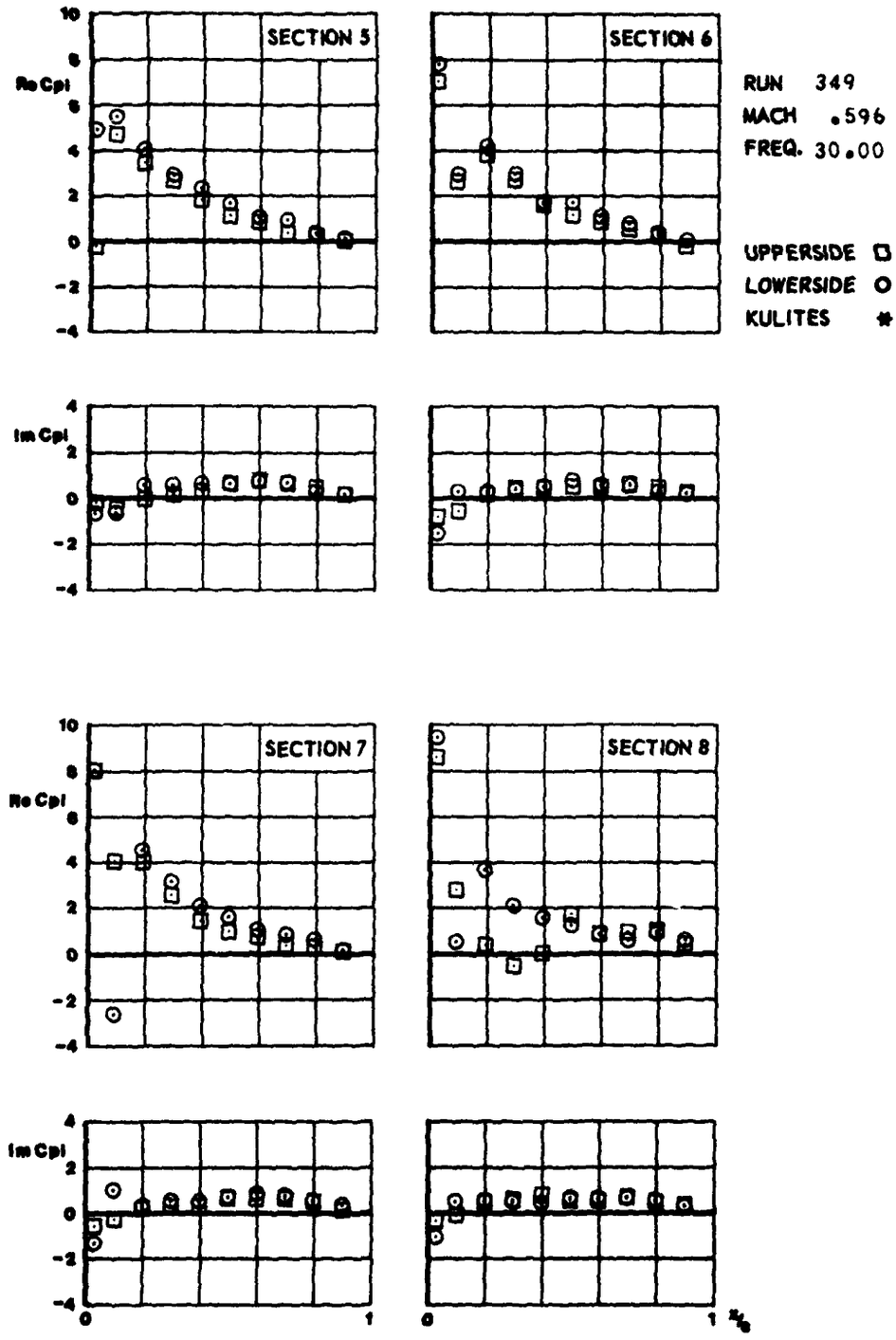

CONF. 4 (WING + TIPLAUNCHER + COMPLETE MISSILE)

FIG.
III.C.35.a

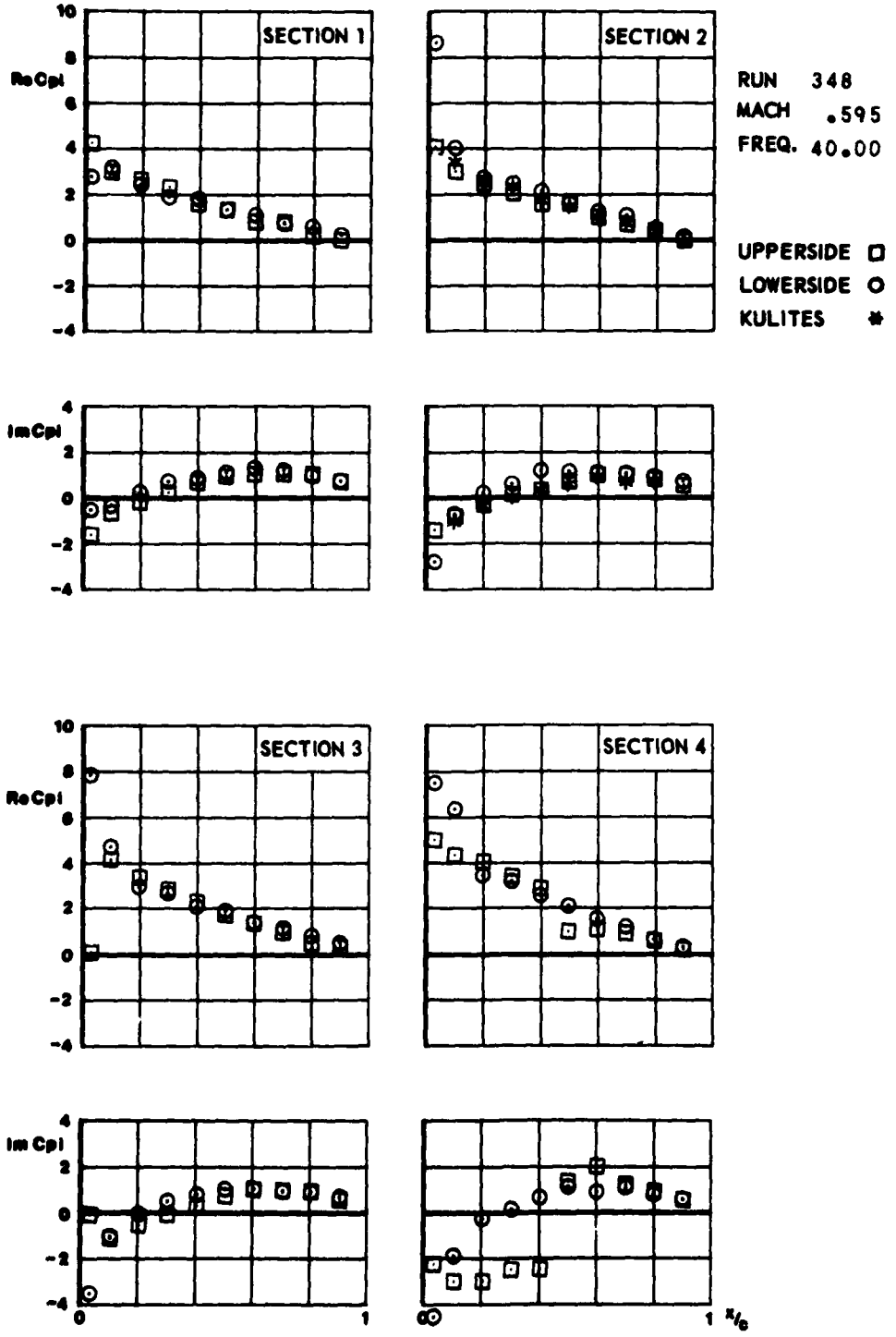

CONF.4 (WING + TIPLAUNCHER + COMPLETE MISSILE)

FIG.
III.C.35.b

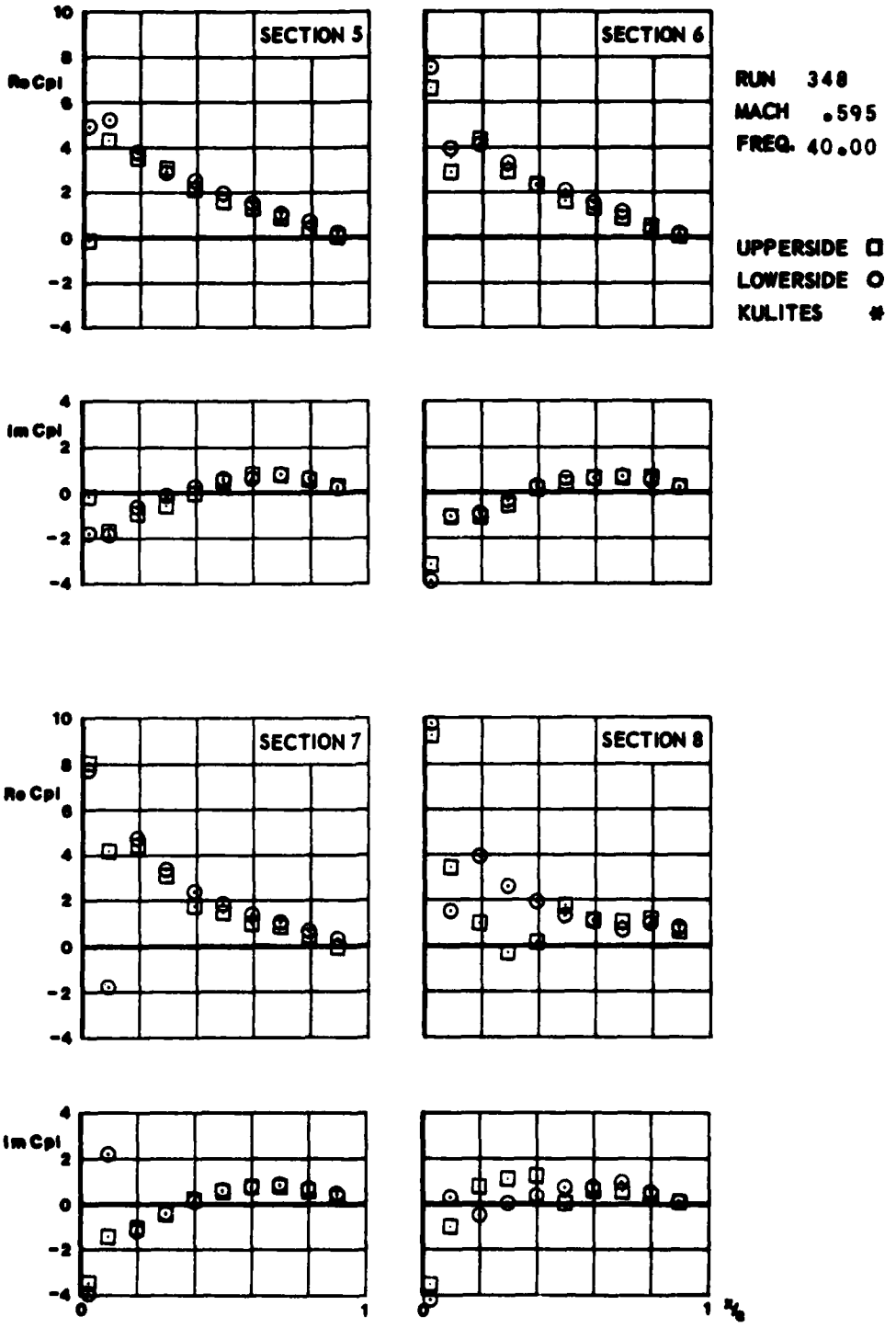

CONF. 4 (WING + TIPLAUNCHER + COMPLETE MISSILE)

FIG.
III.C.36.a

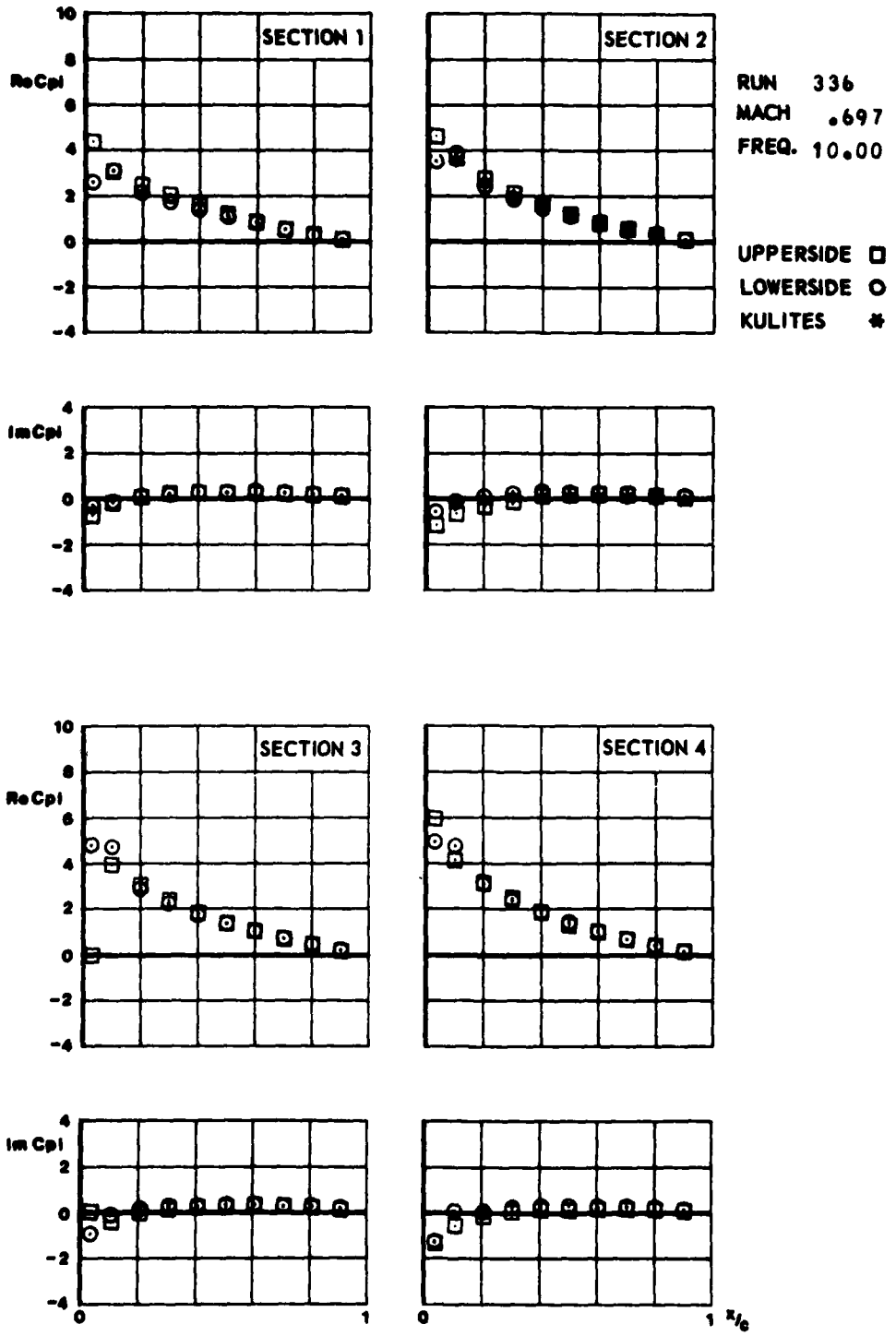

CONF.4 (WING + TIPLAUNCHER + COMPLETE MISSILE)

FIG.
III.C.36.b

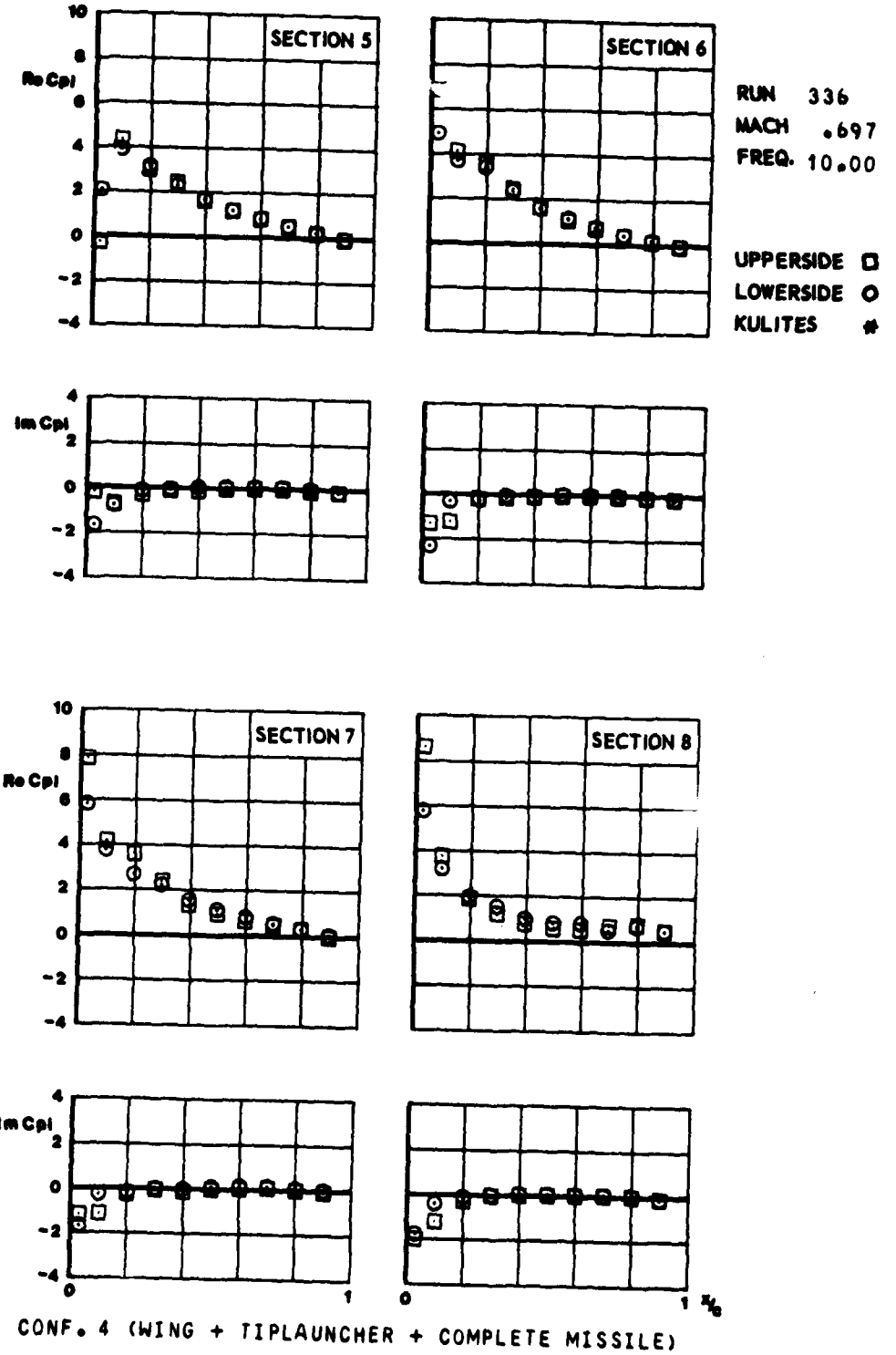

CONF. 4 (WING + TIPLAUNCHER + COMPLETE MISSILE)

FIG.
III.C.37.a

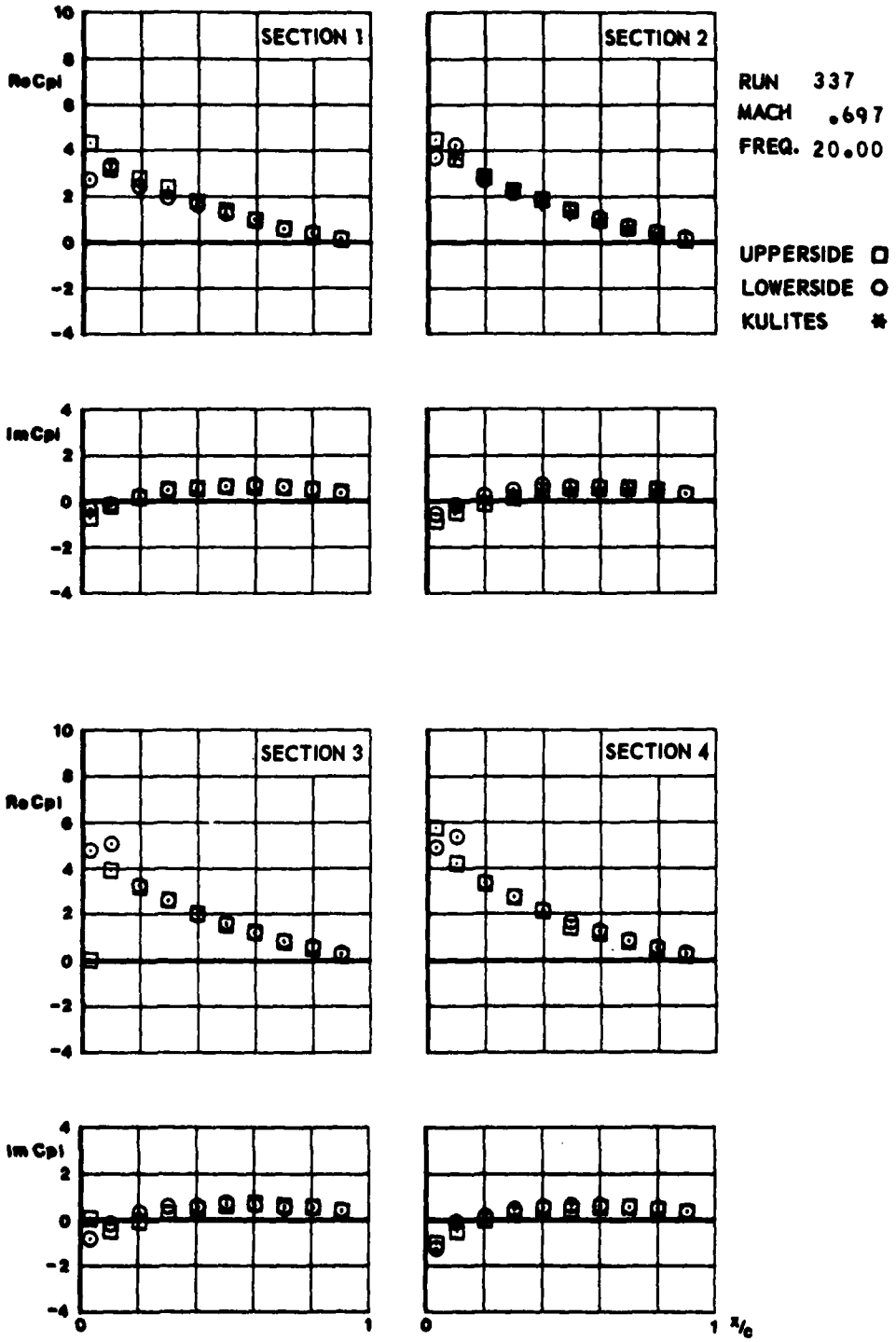

CONF.4 (WING + TIPLAUNCHER + COMPLETE MISSILE)

FIG.
III.C.37.6

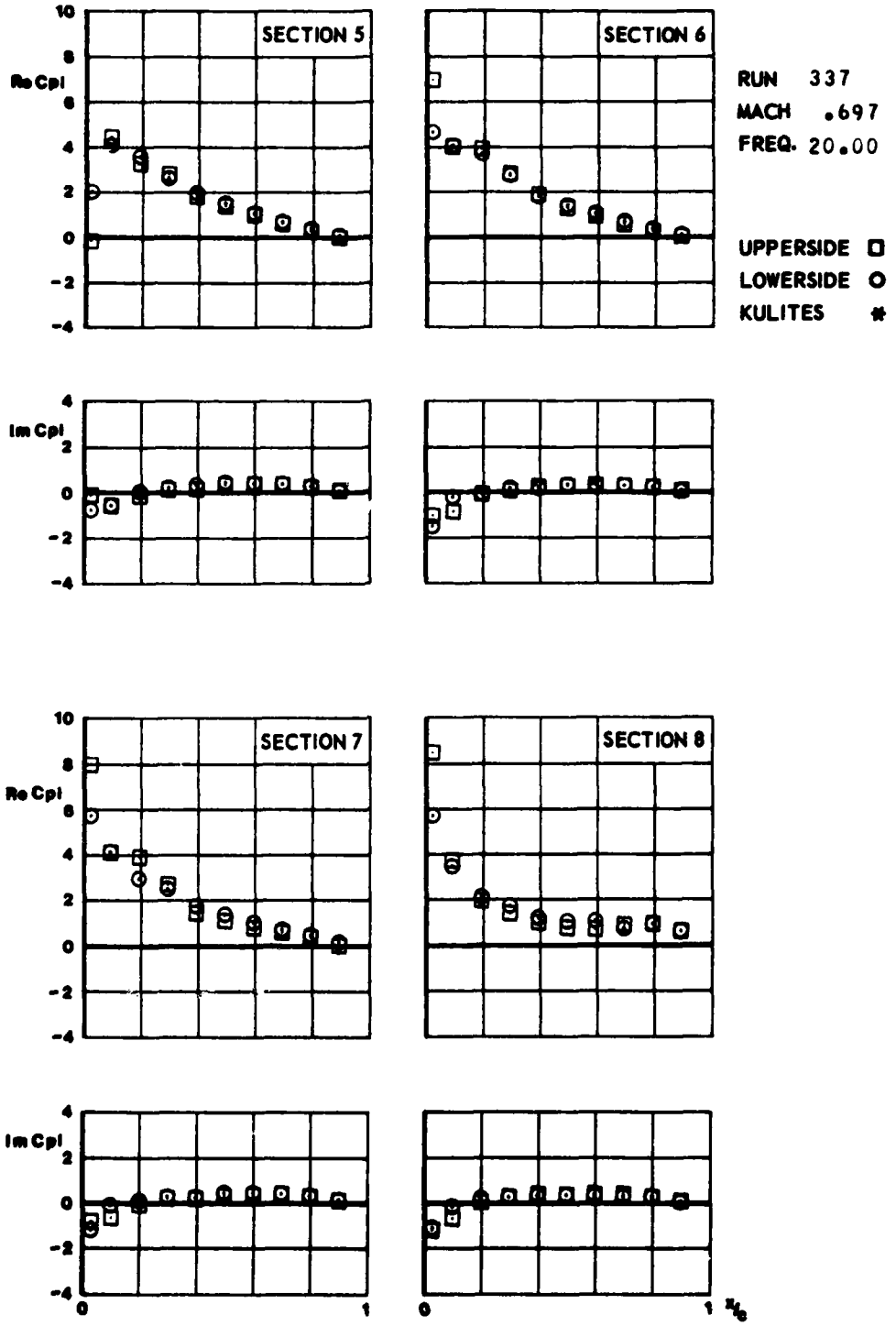

CONF. 4 (WING + TIPLAUNCHER + COMPLETE MISSILE)

FIG.
III.C.38.a

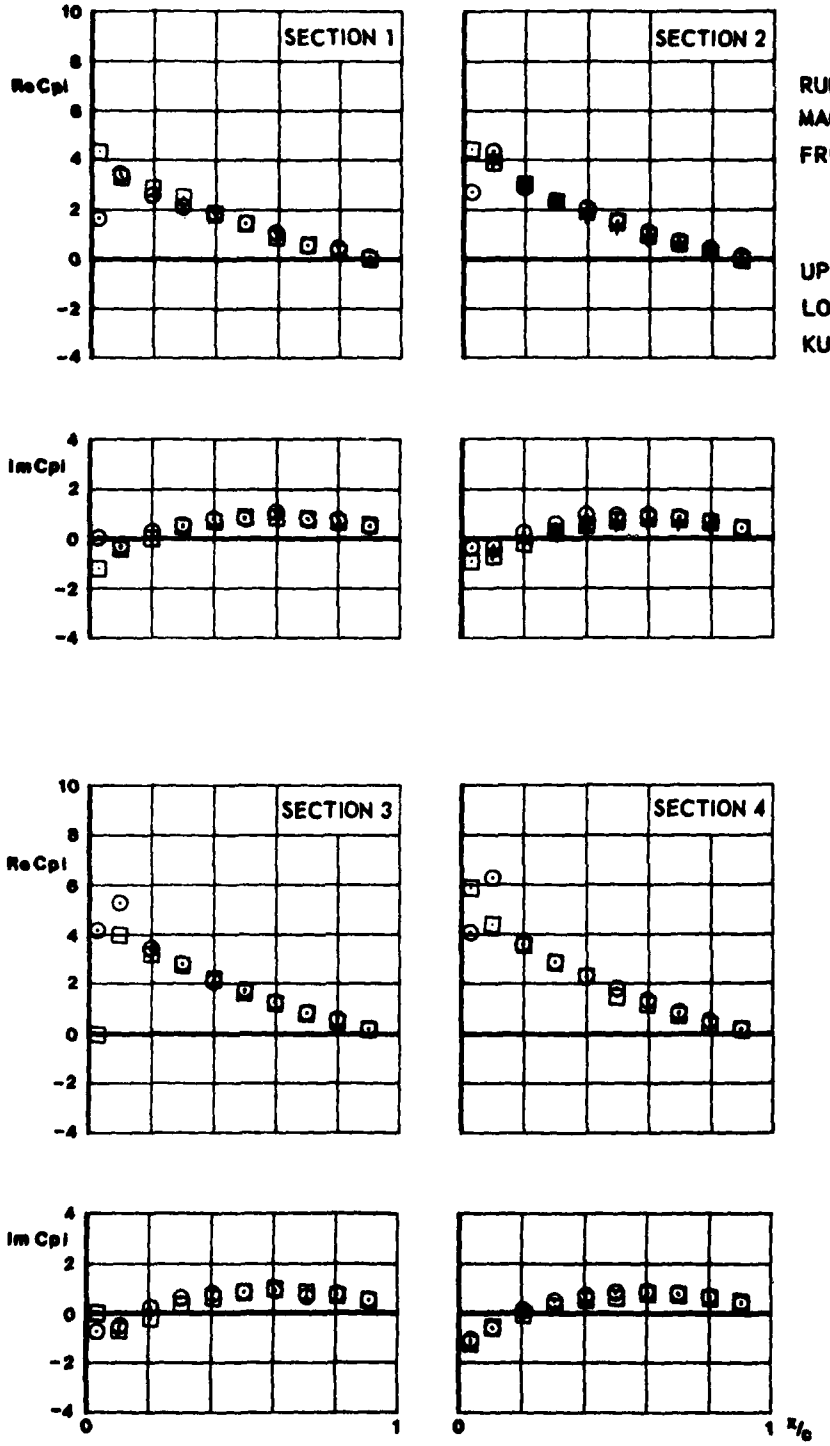

CONF.4 (WING + TIPLAUNCHER + COMPLETE MISSILE)

FIG.
III.C.38.6

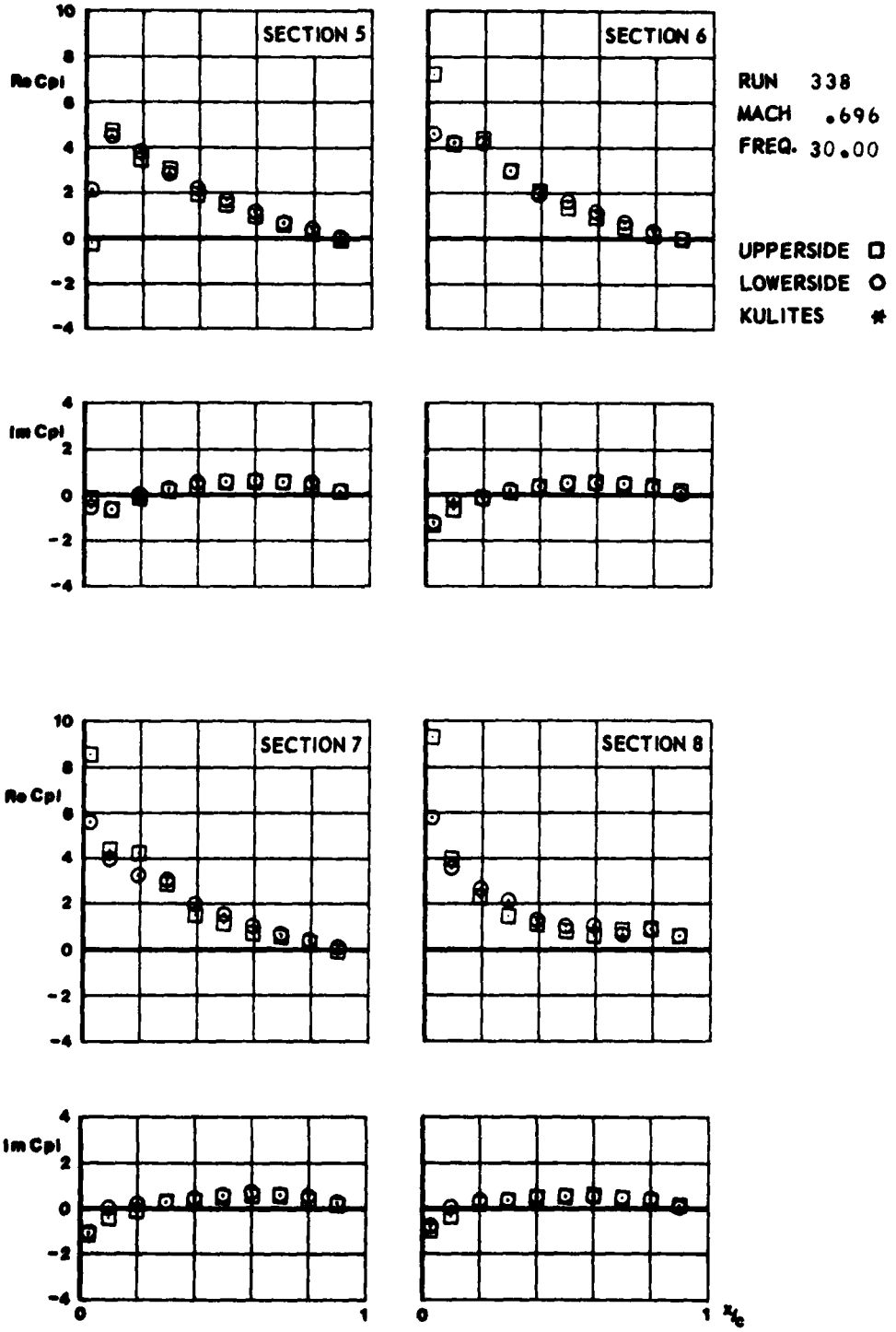

CONF. 4 (WING + TIPLAUNCHER + COMPLETE MISSILE)

FIG.
III.C.39.a

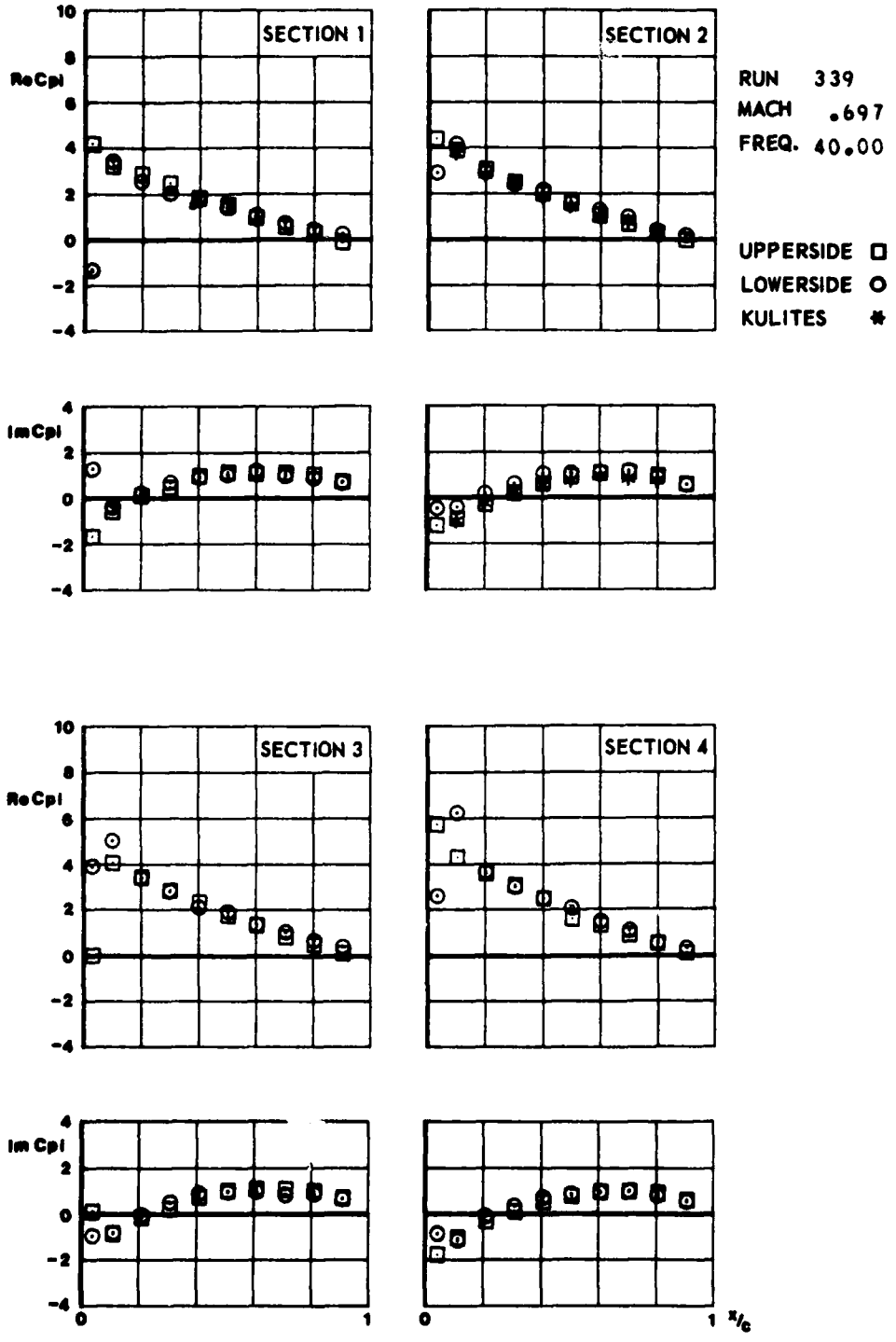

CONF.4 (WING + TIPLAUNCHER + COMPLETE MISSILE)

FIG.
III.C.39.b

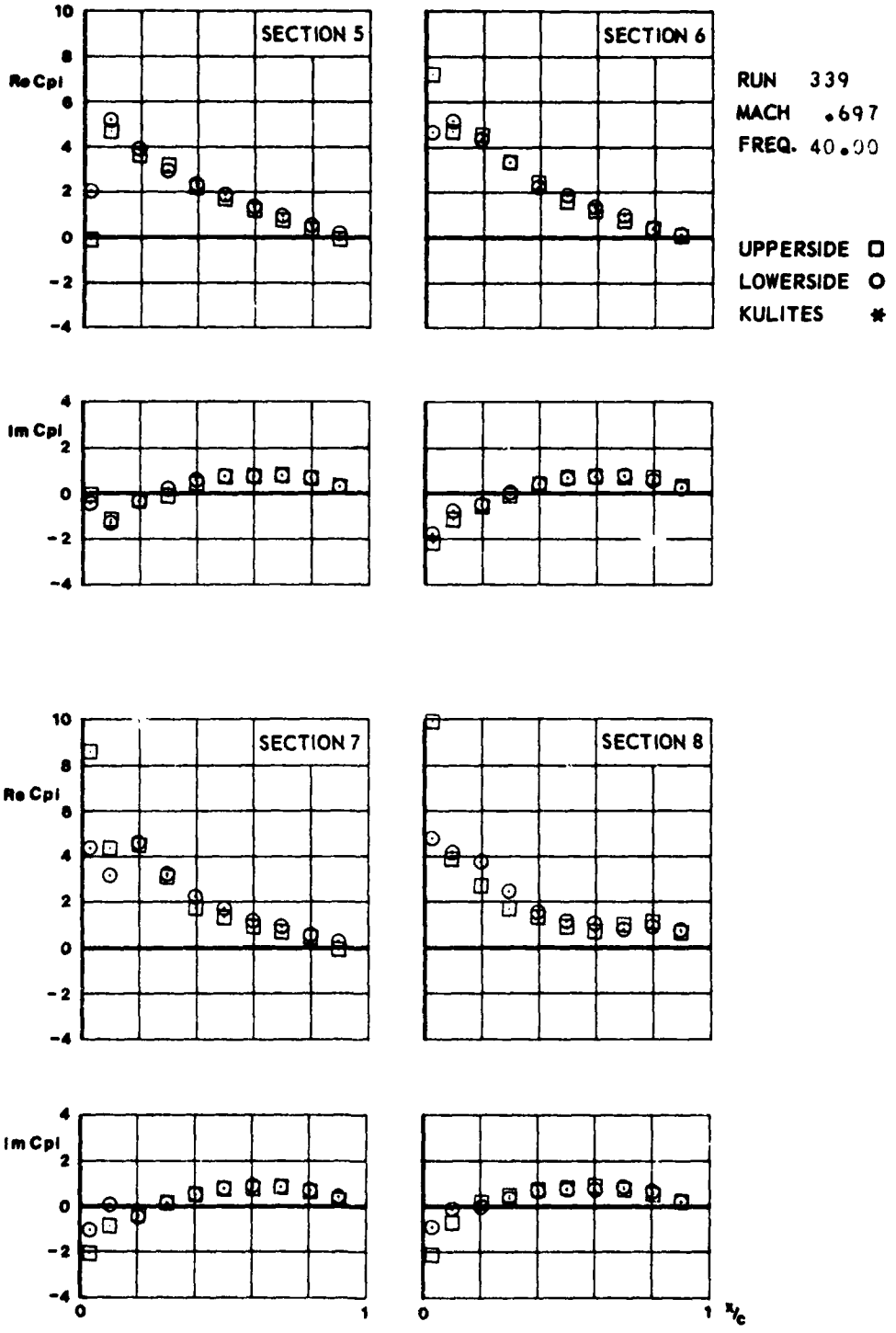

CONF. 4 (WING + TIPLAUNCHER + COMPLETE MISSILE)

FIG.
III.C.4.2a

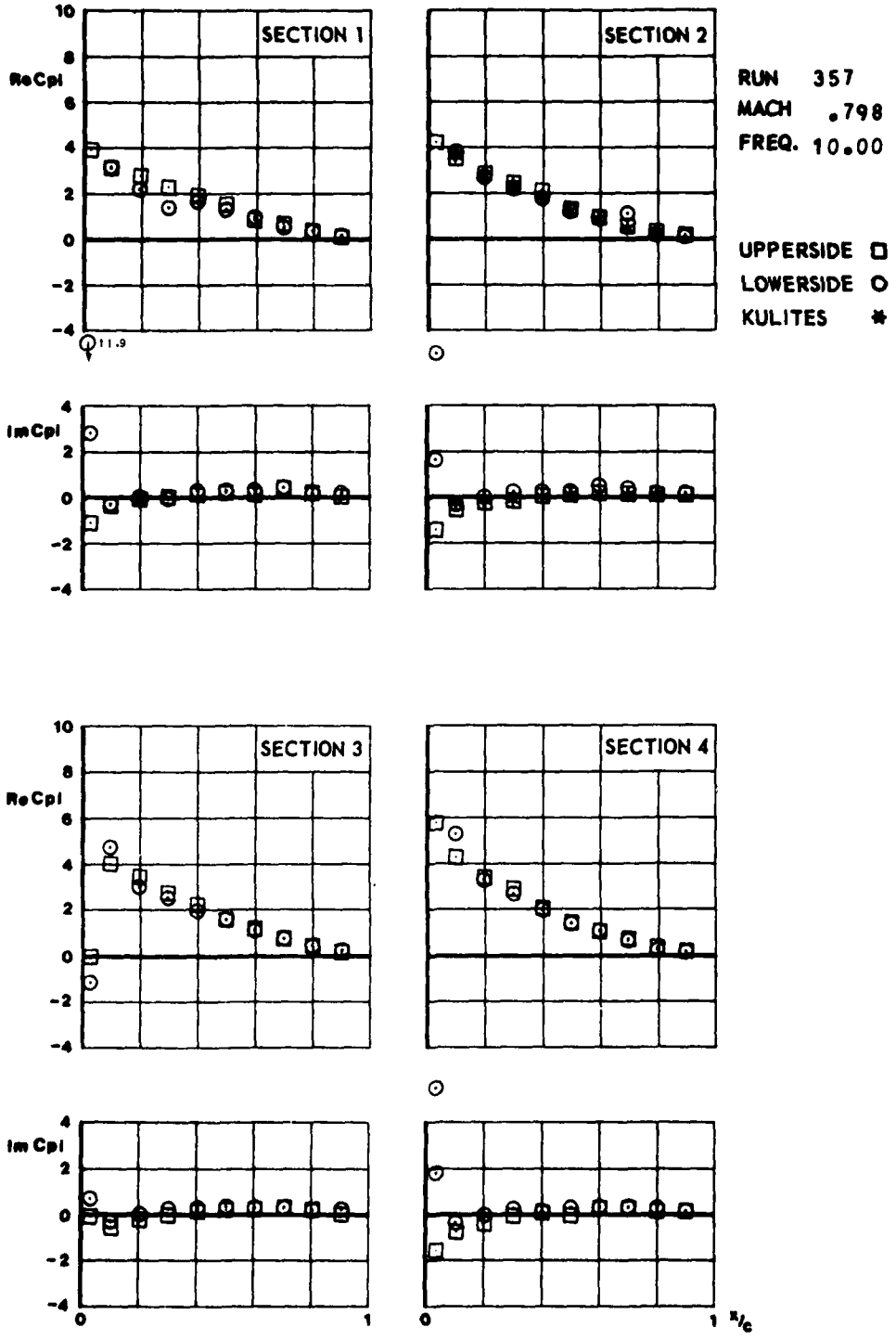

CONF.4 (WING + TIPLAUNCHER + COMPLETE MISSILE)

FIG.
III.C.40.b

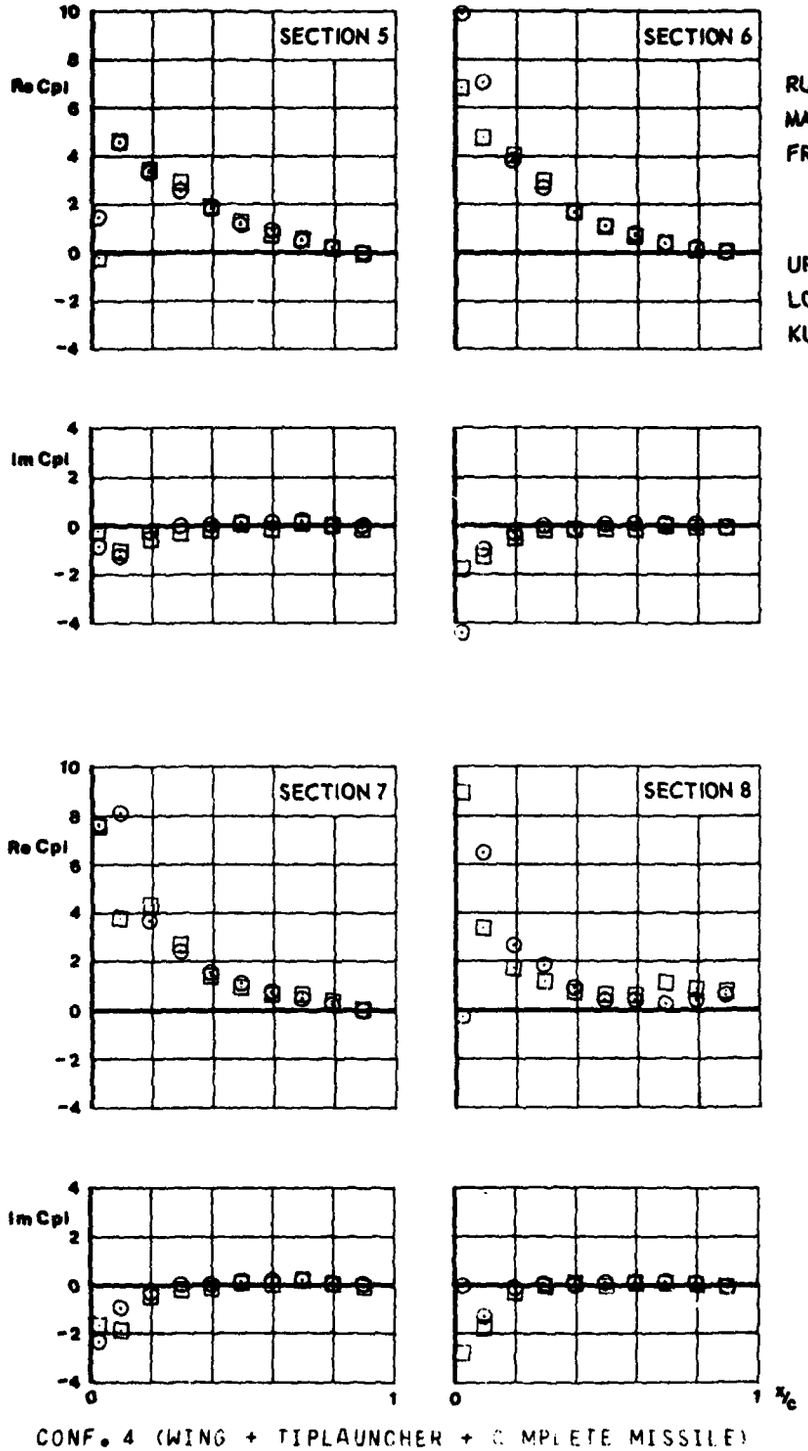

CONF. 4 (WING + TIPLAUNCHER + COMPLETE MISSILE)

FIG.
III.C.41.a.

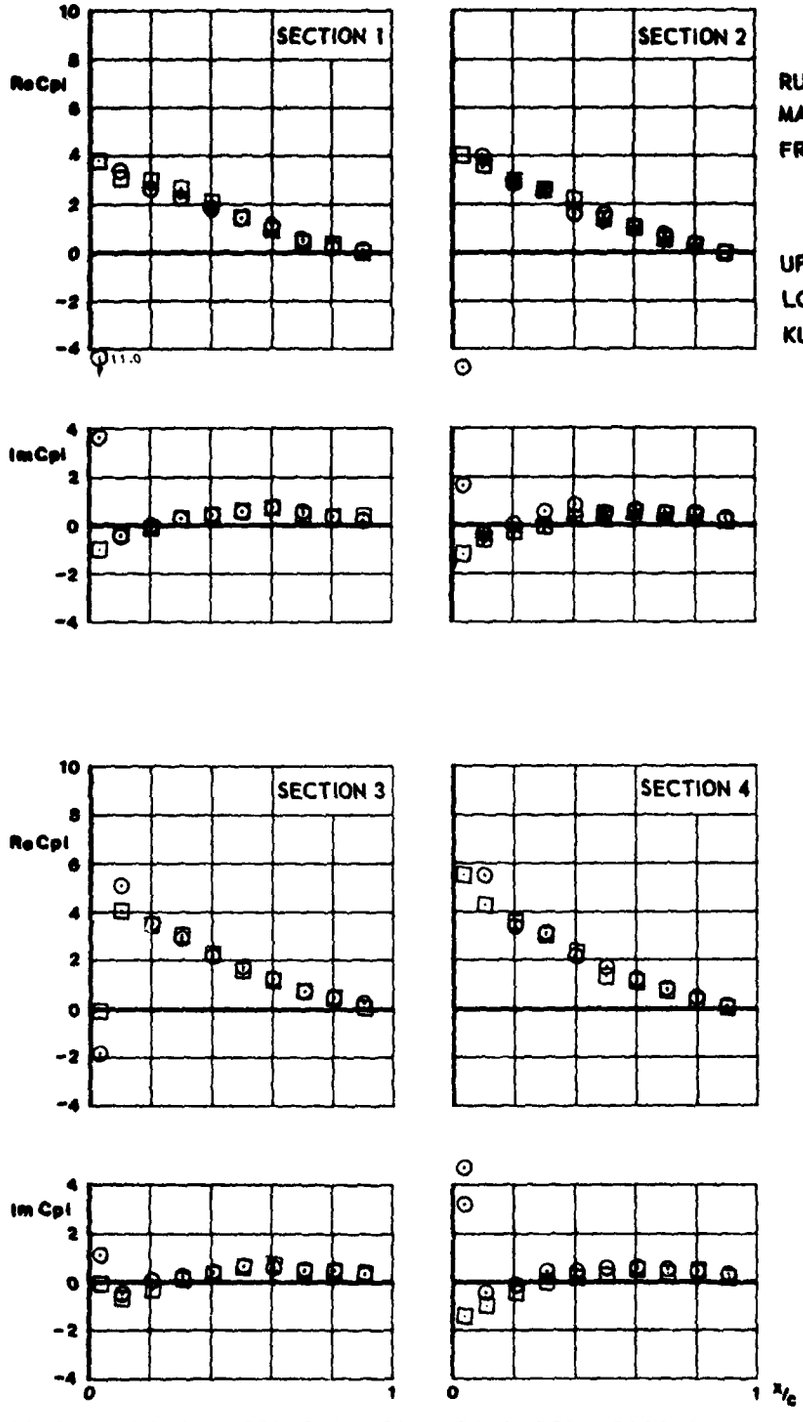

CONF.4 (WING + TIPLAUNCHER + COMPLETE MISSILE)

FIG.
III.C.41.b

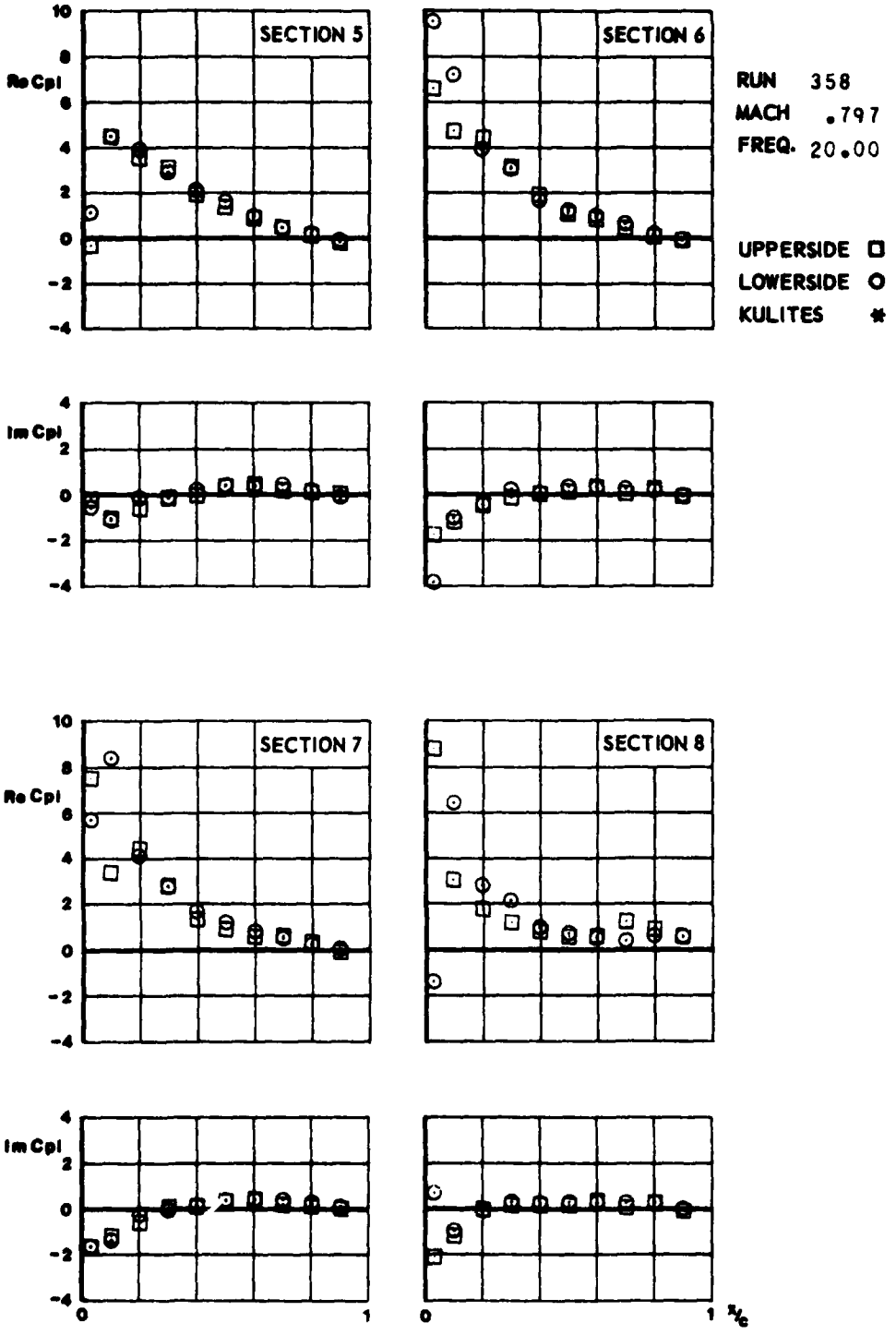

CONF. 4 (WING + TIPLAUNCHER + COMPLETE MISSILE)

FIG.
III.C.42.a

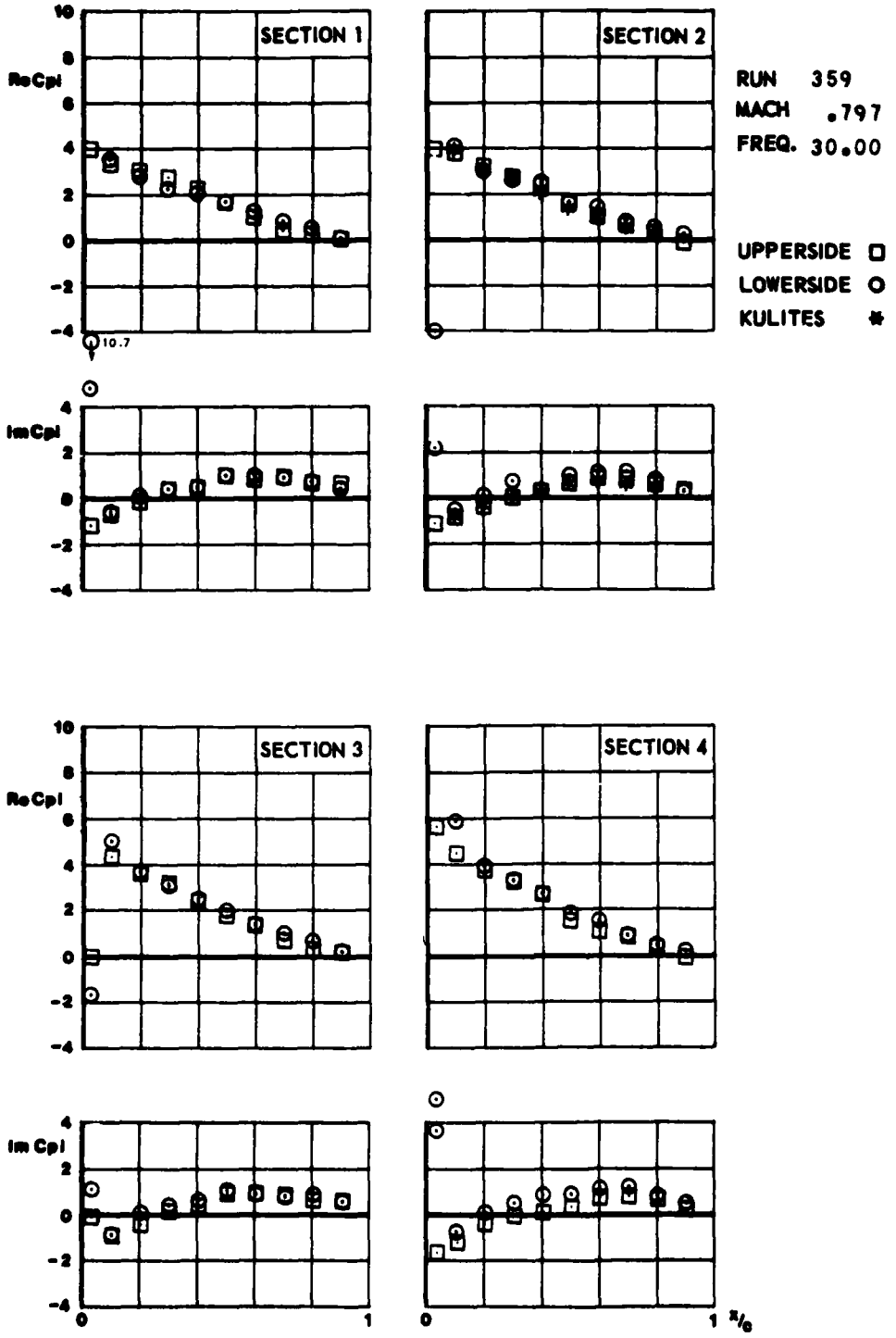

CONF.4 (WING + TIPLAUNCHER + COMPLETE MISSILE)

FIG.
III.C.42.b

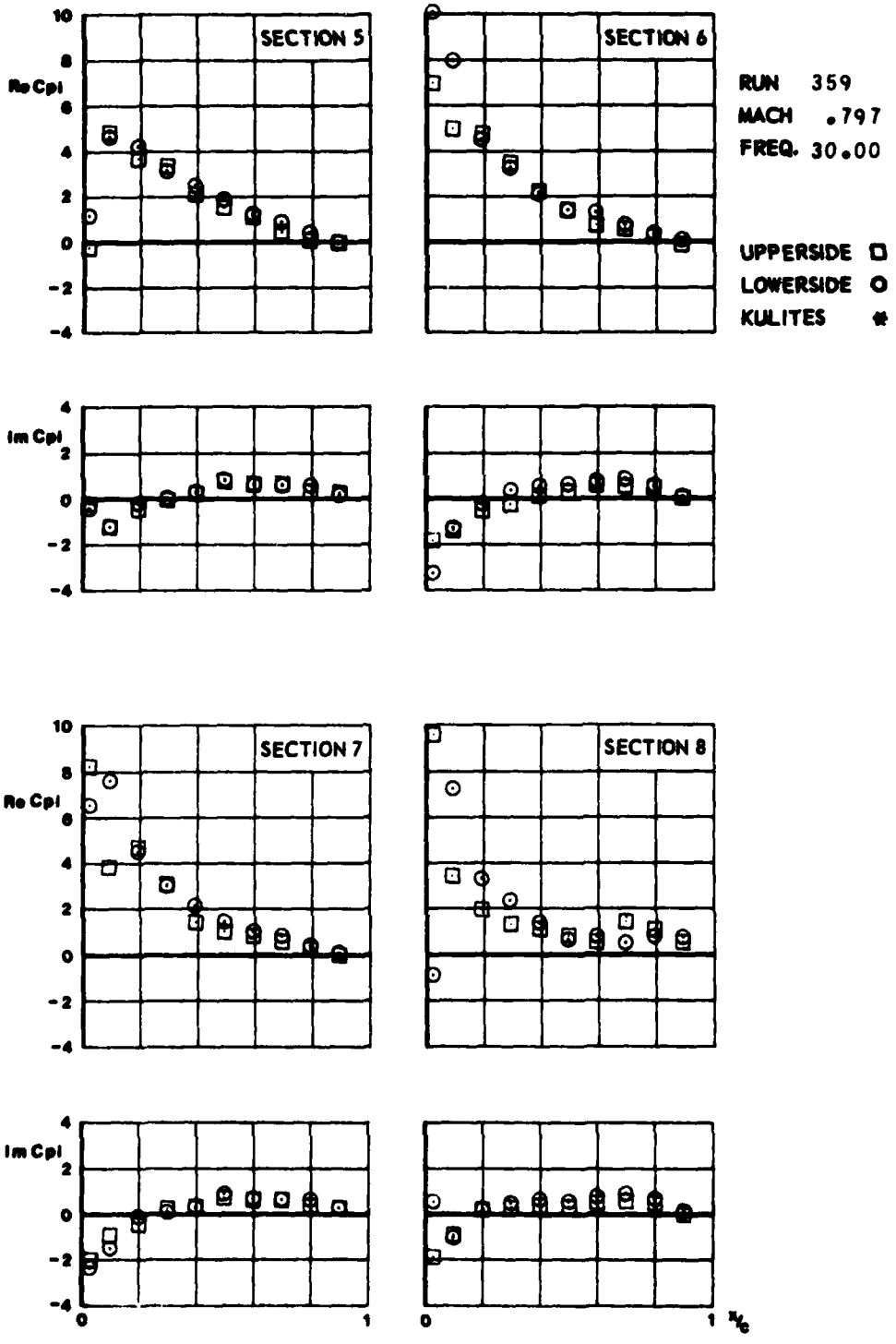

CONF. 4 (WING + TIPLAUNCHER + COMPLETE MISSILE)

FIG.
III.C.43.a

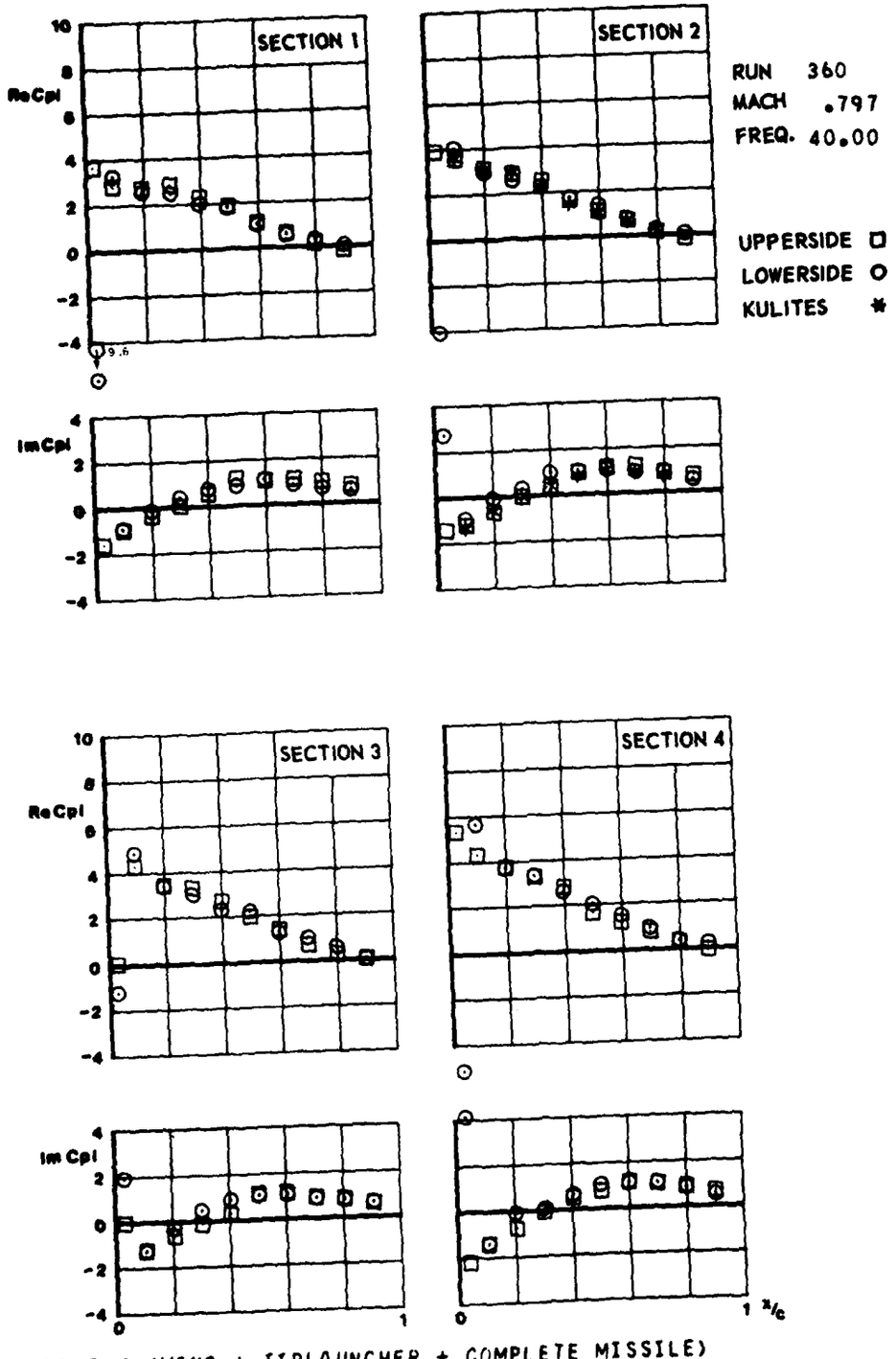

CONF.4 (WING + TIPLAUNCHER + COMPLETE MISSILE)

FIG.
III.C.43.b

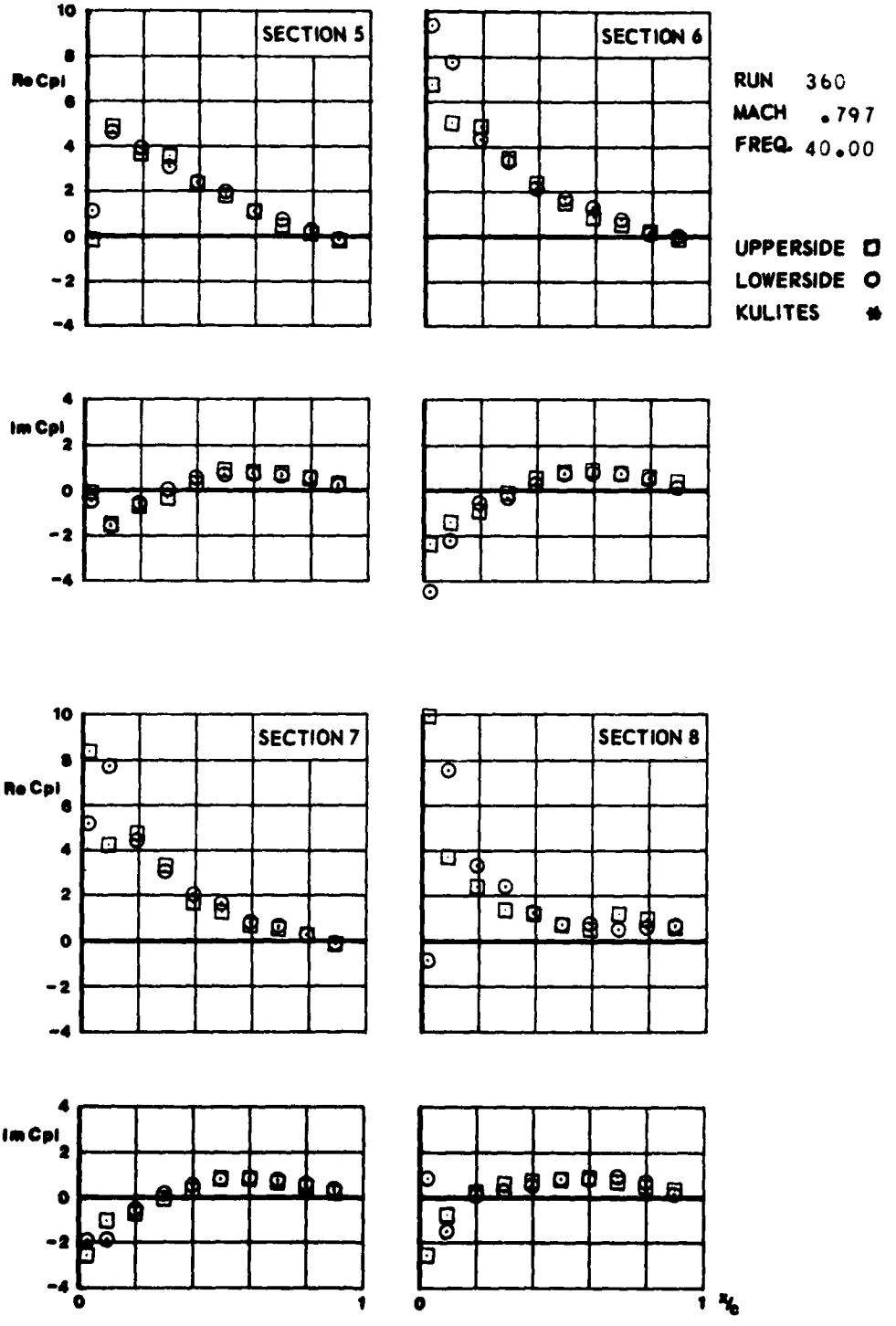

CONF. 4 (WING + TIPLAUNCHER + COMPLETE MISSILE)

FIG.
III.C.44.a

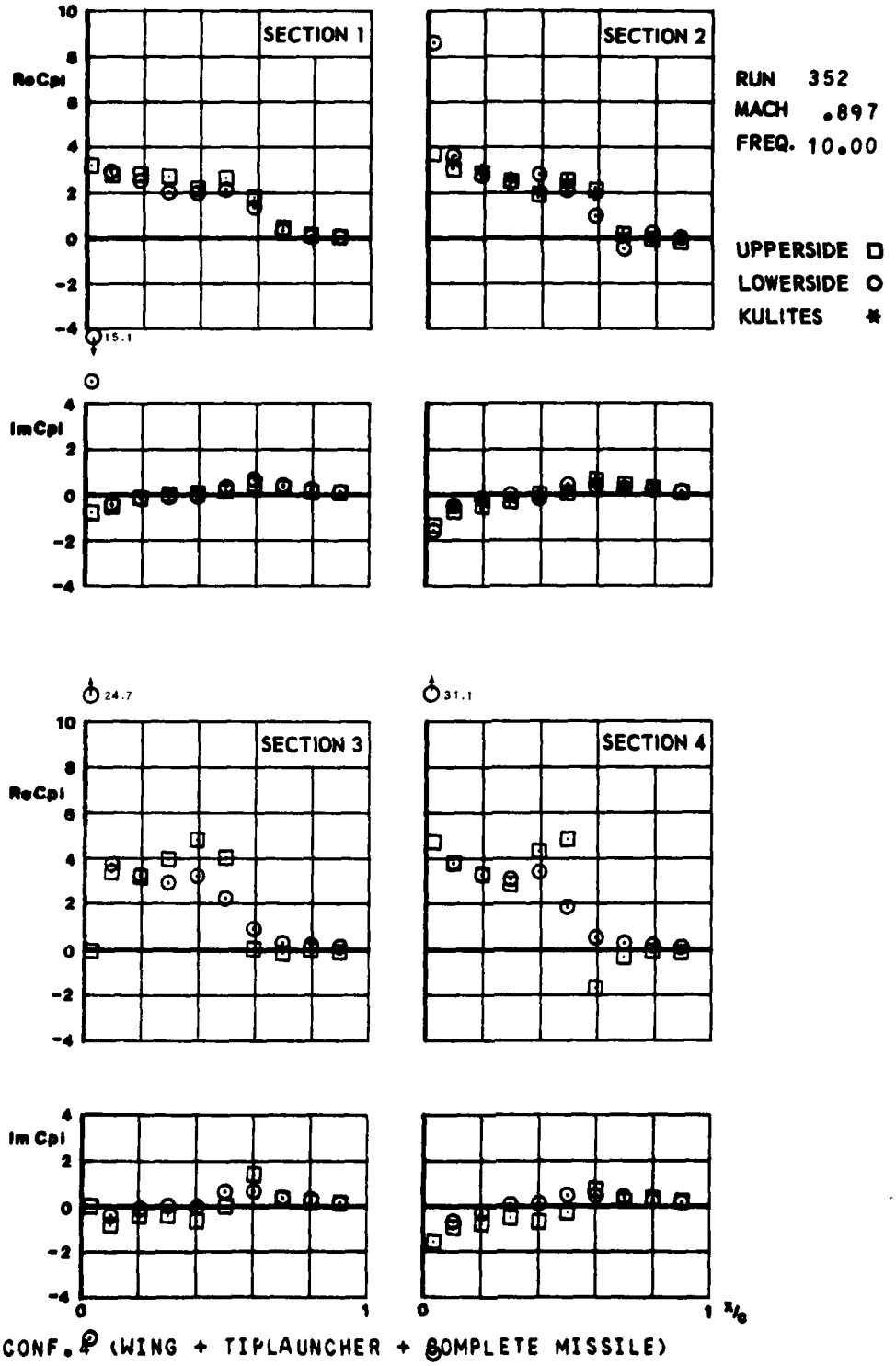

CONF. 2 (WING + TIPLAUNCHER + COMPLETE MISSILE)

FIG.
III.C.44.b

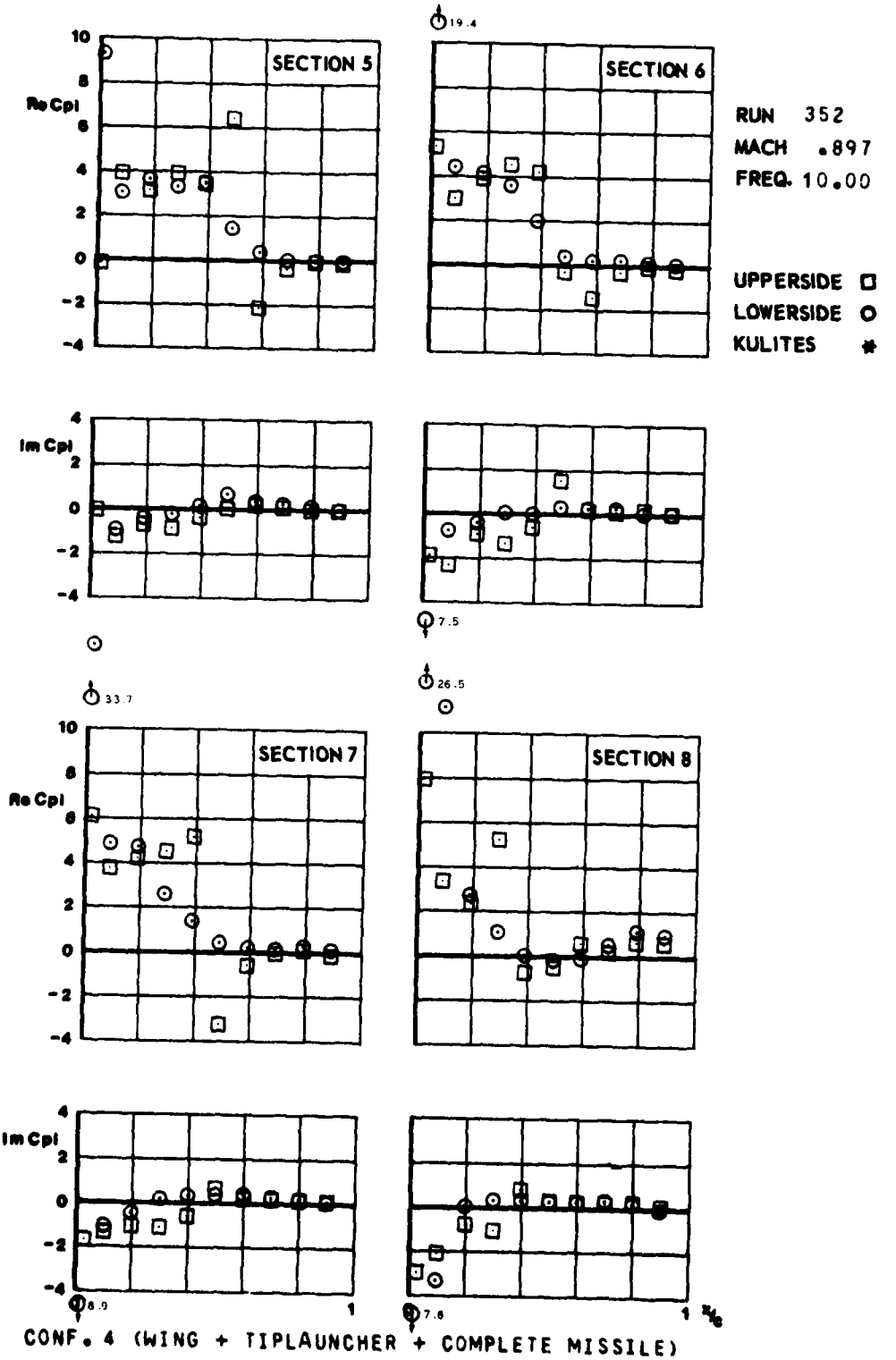

CONF. 4 (WING + TIPLAUNCHER + COMPLETE MISSILE)

FIG.
III.C.45.a

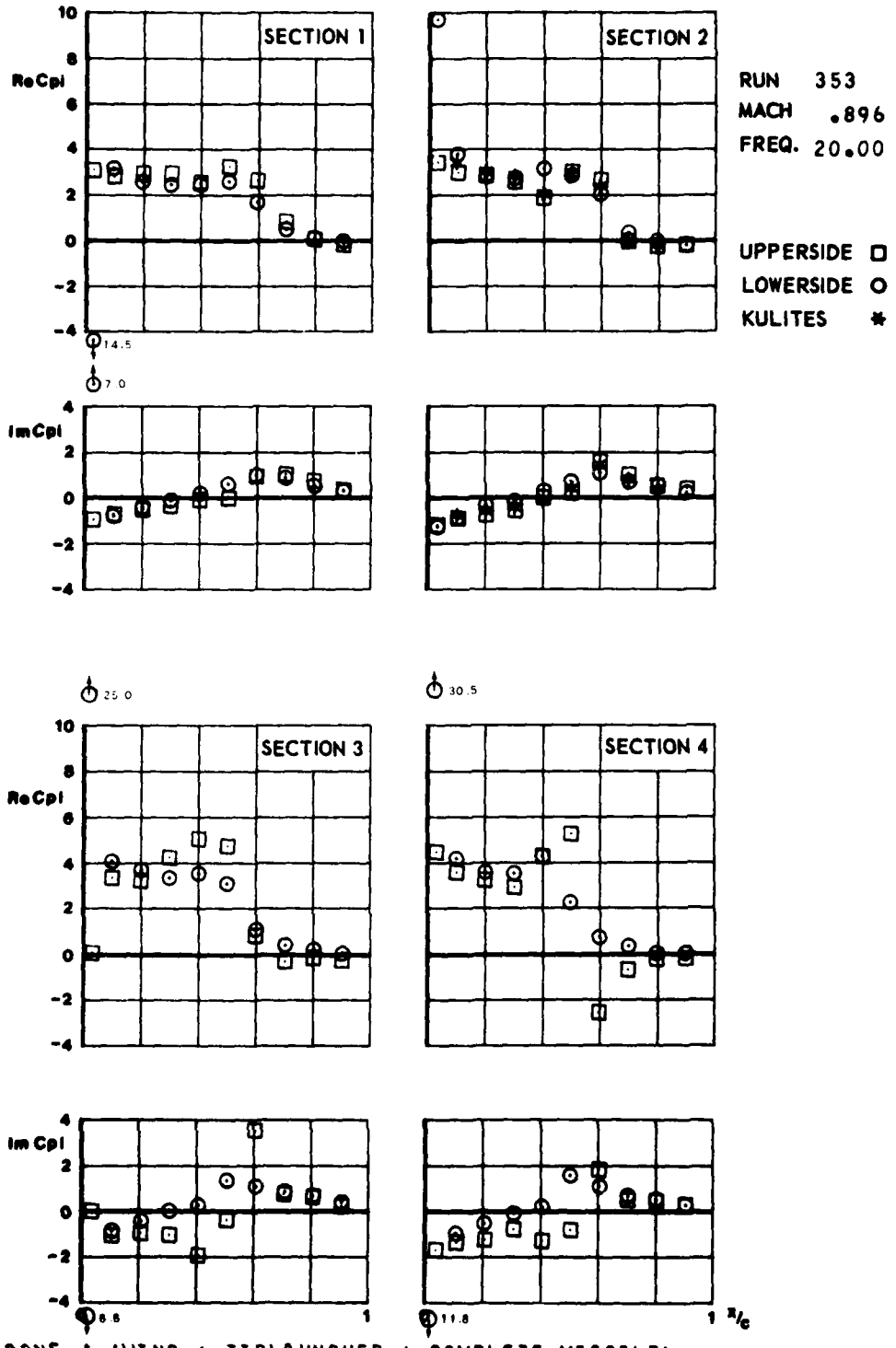

CONF.4 (WING + TIPLAUNCHER + COMPLETE MISSILE)

FIG.
III.C.45.6

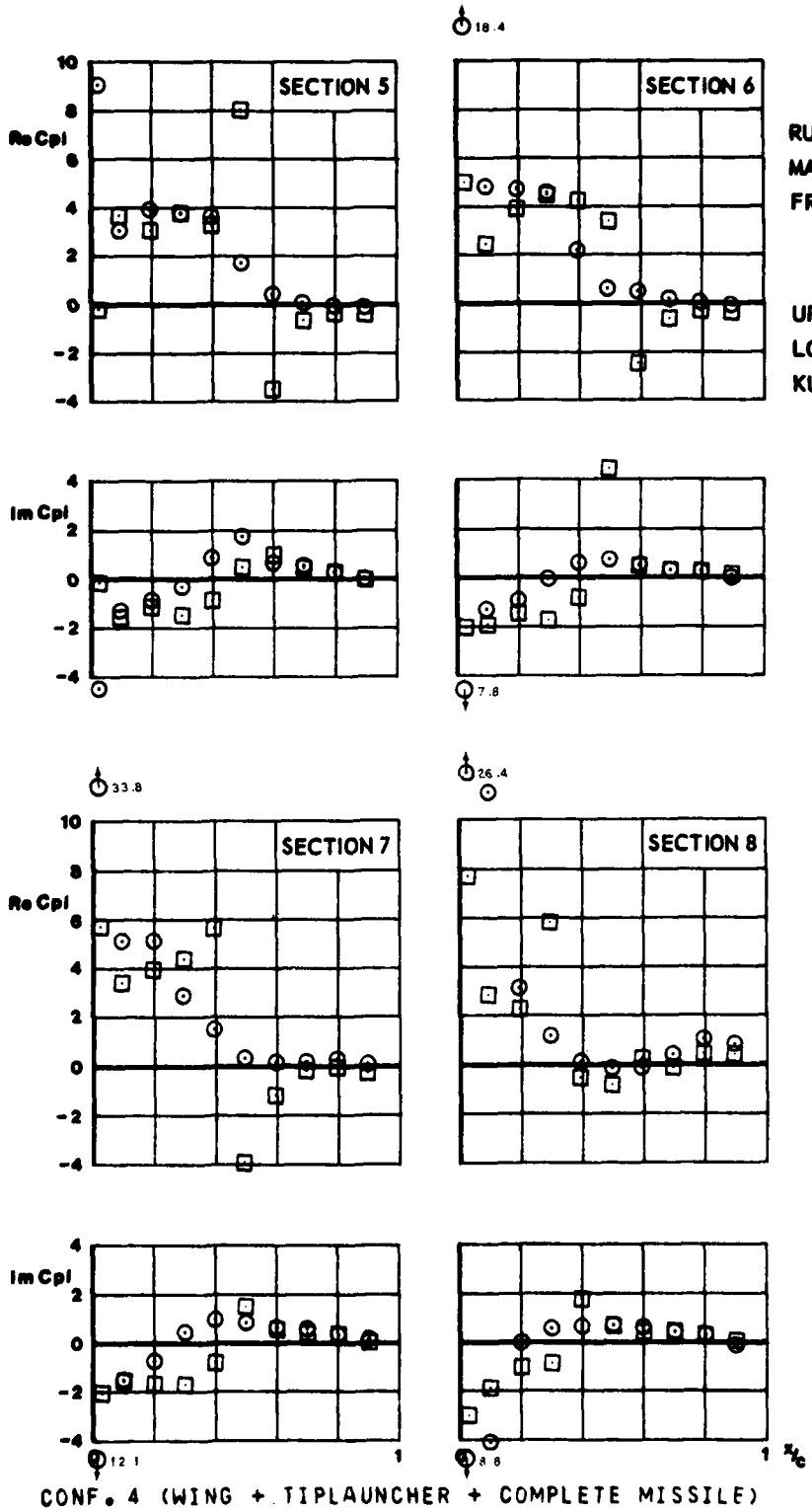

CONF. 4 (WING + TIPLAUNCHER + COMPLETE MISSILE)

FIG.
III.C.46.a

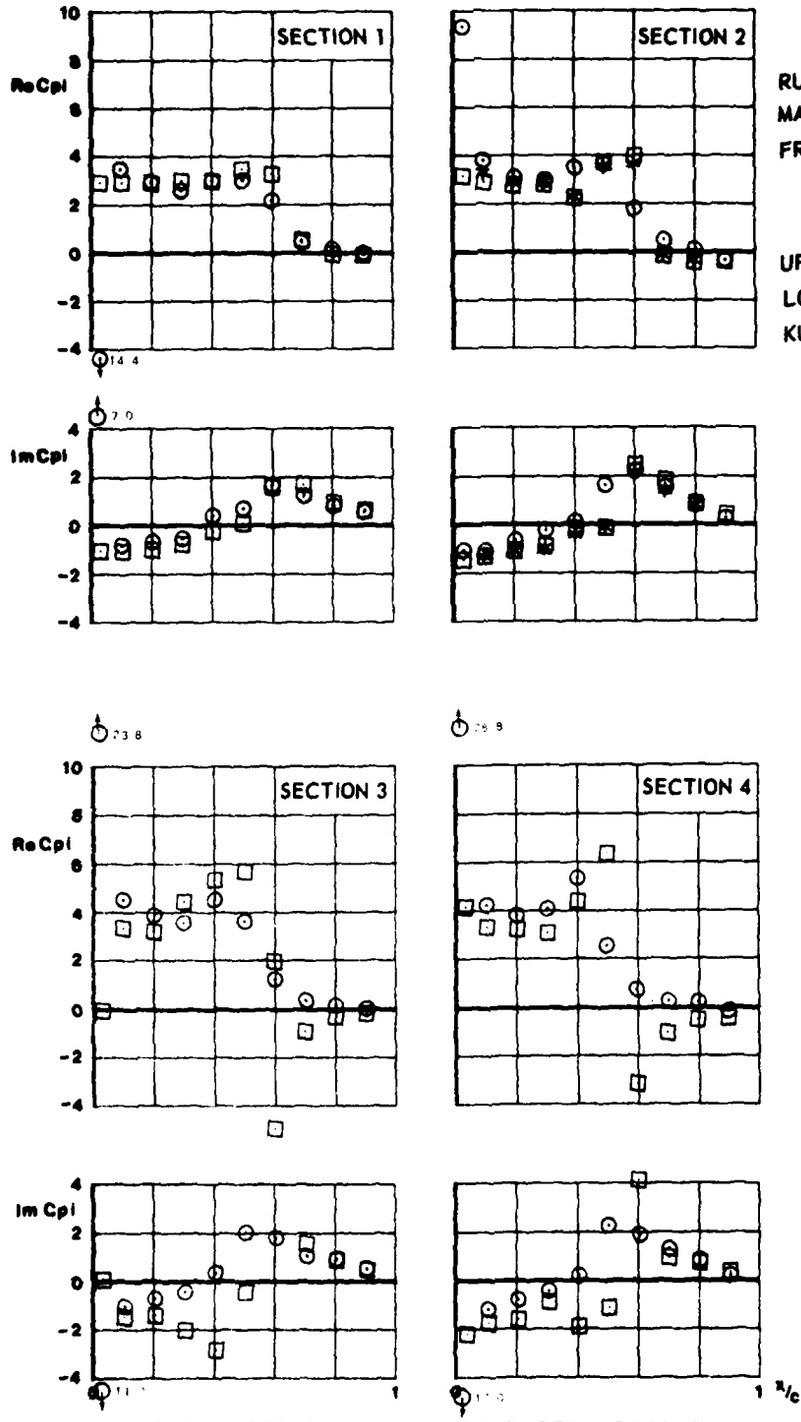

CONF.4 (WING + TIPLAUNCHER + COMPLETE MISSILE)

FIG.
III.C.46.b

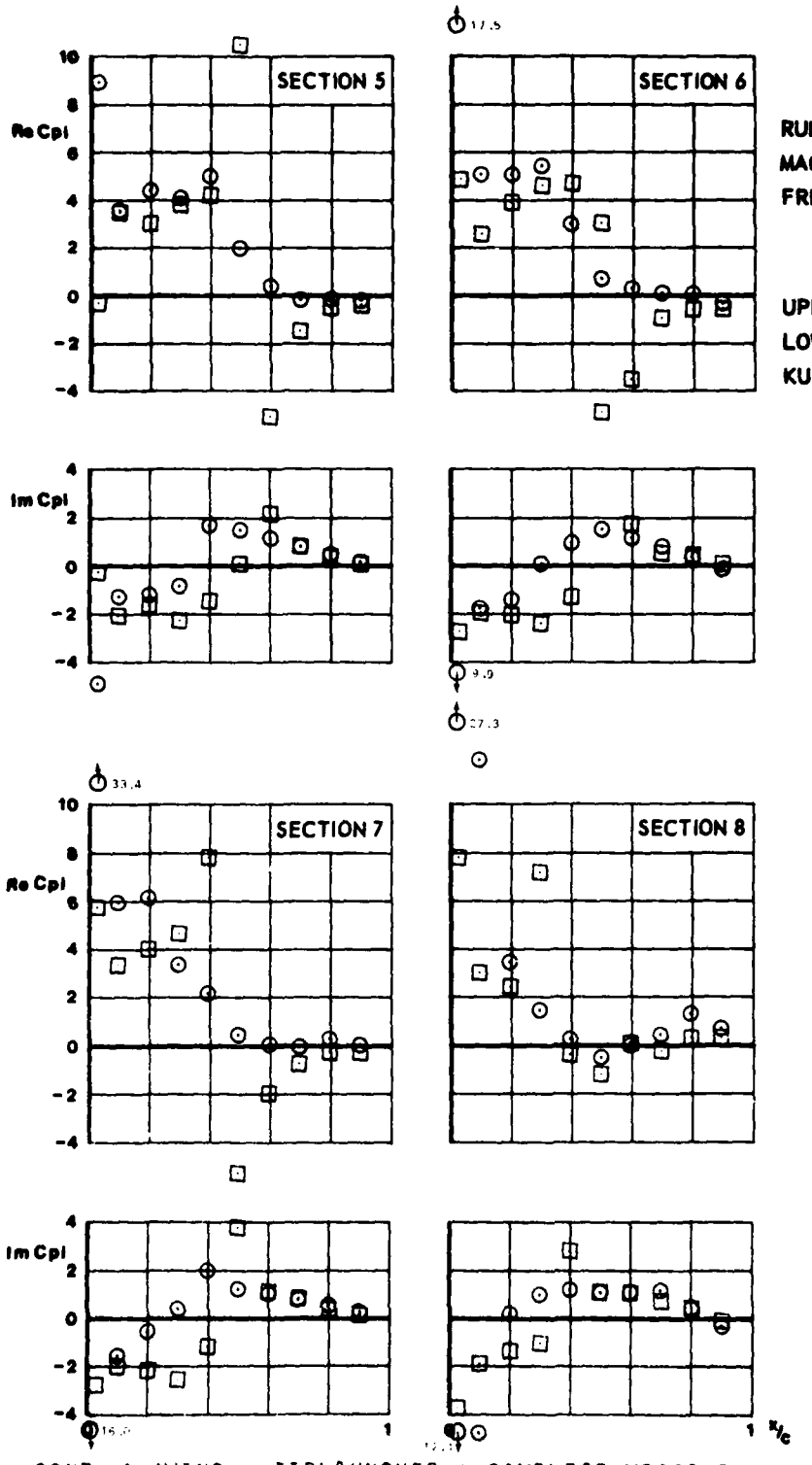

CONF. 4 (WING + TIPLAUNCHER + COMPLETE MISSILE)

FIG.
III.C.47.a

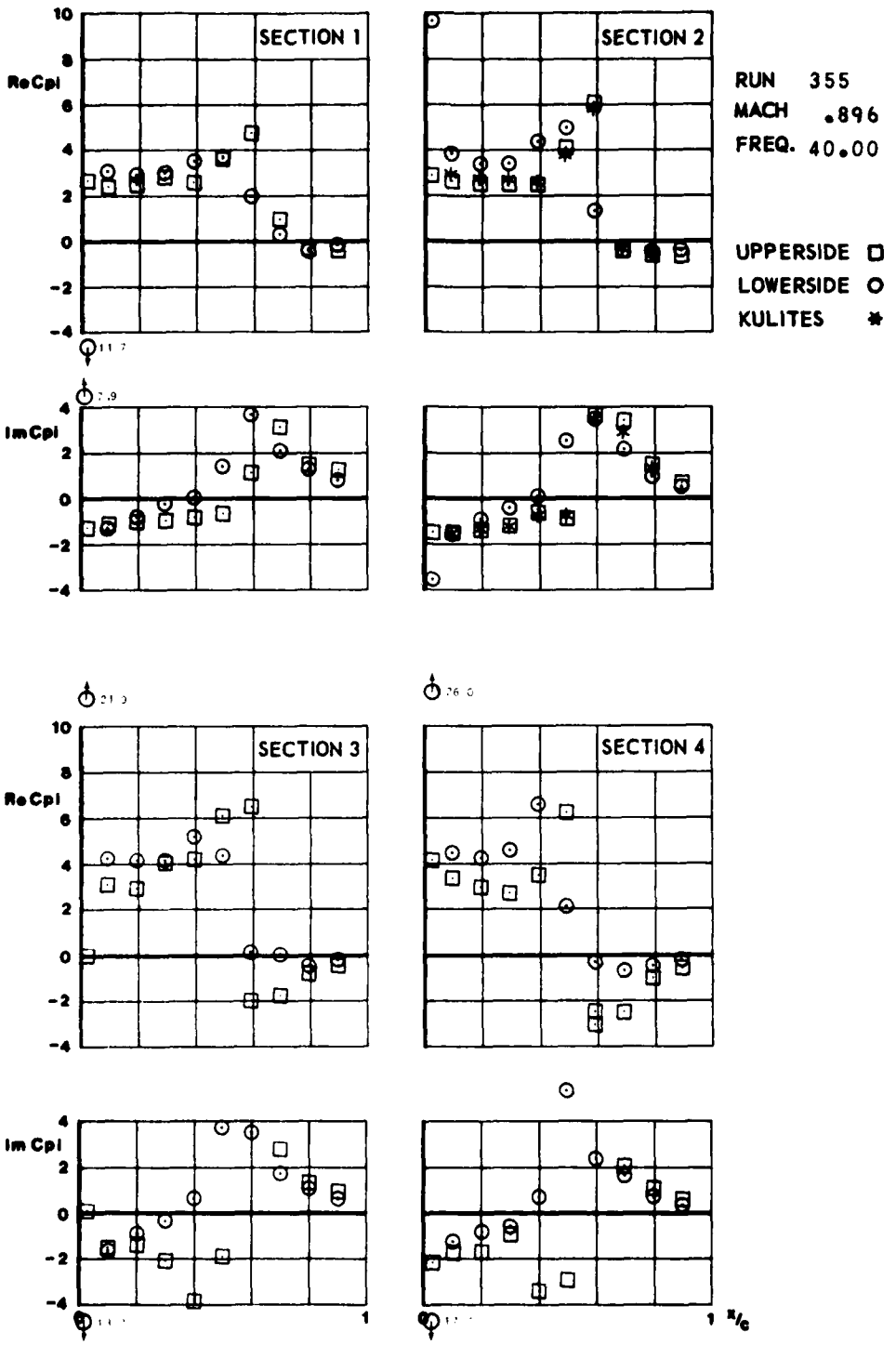

CONF.4 (WING + TIPLAUNCHER + COMPLETE MISSILE)

FIG.
III.C.47.b

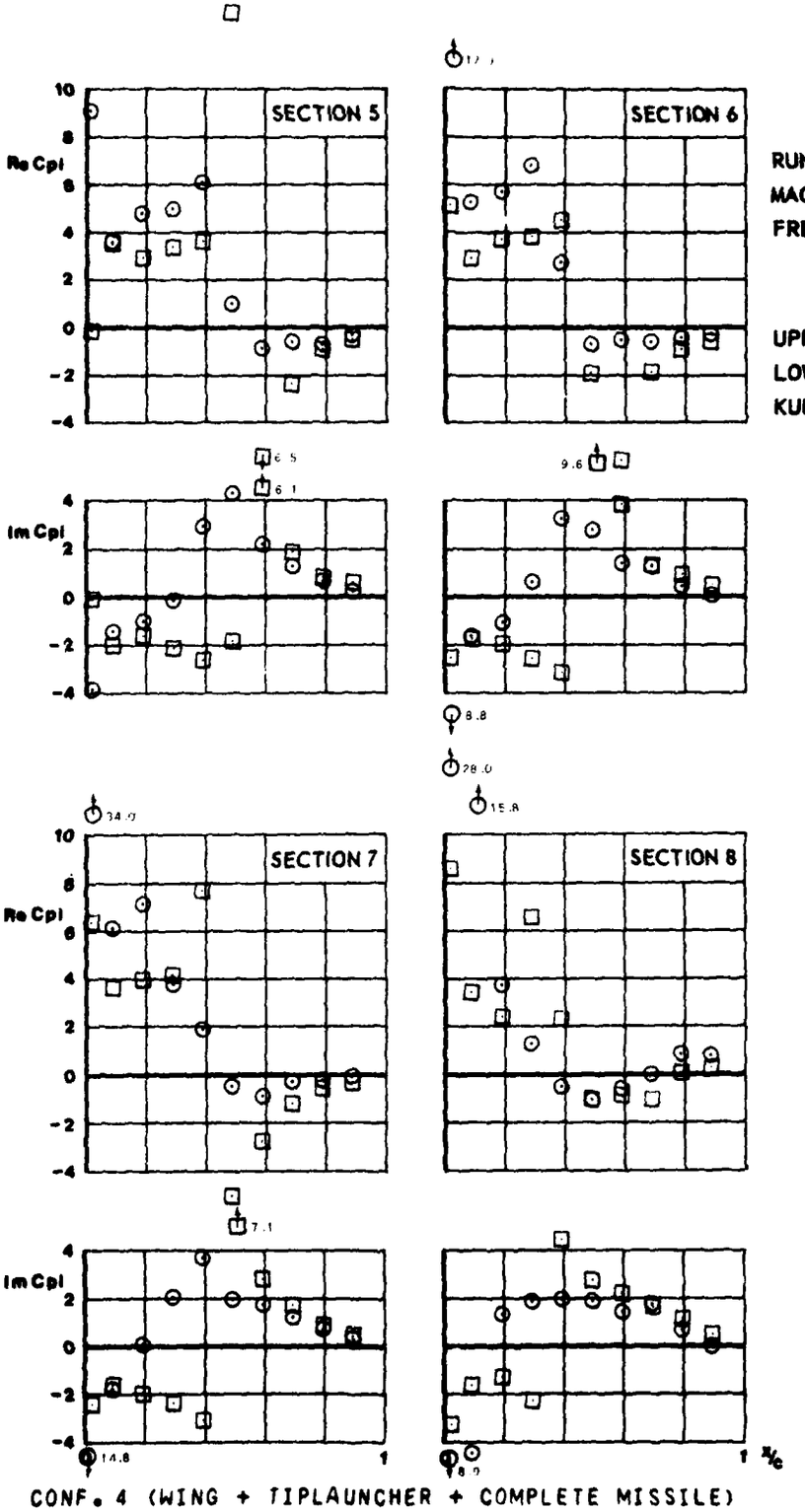

CONF. 4 (WING + TIPLAUNCHER + COMPLETE MISSILE)

FIG.
III.C.49.a

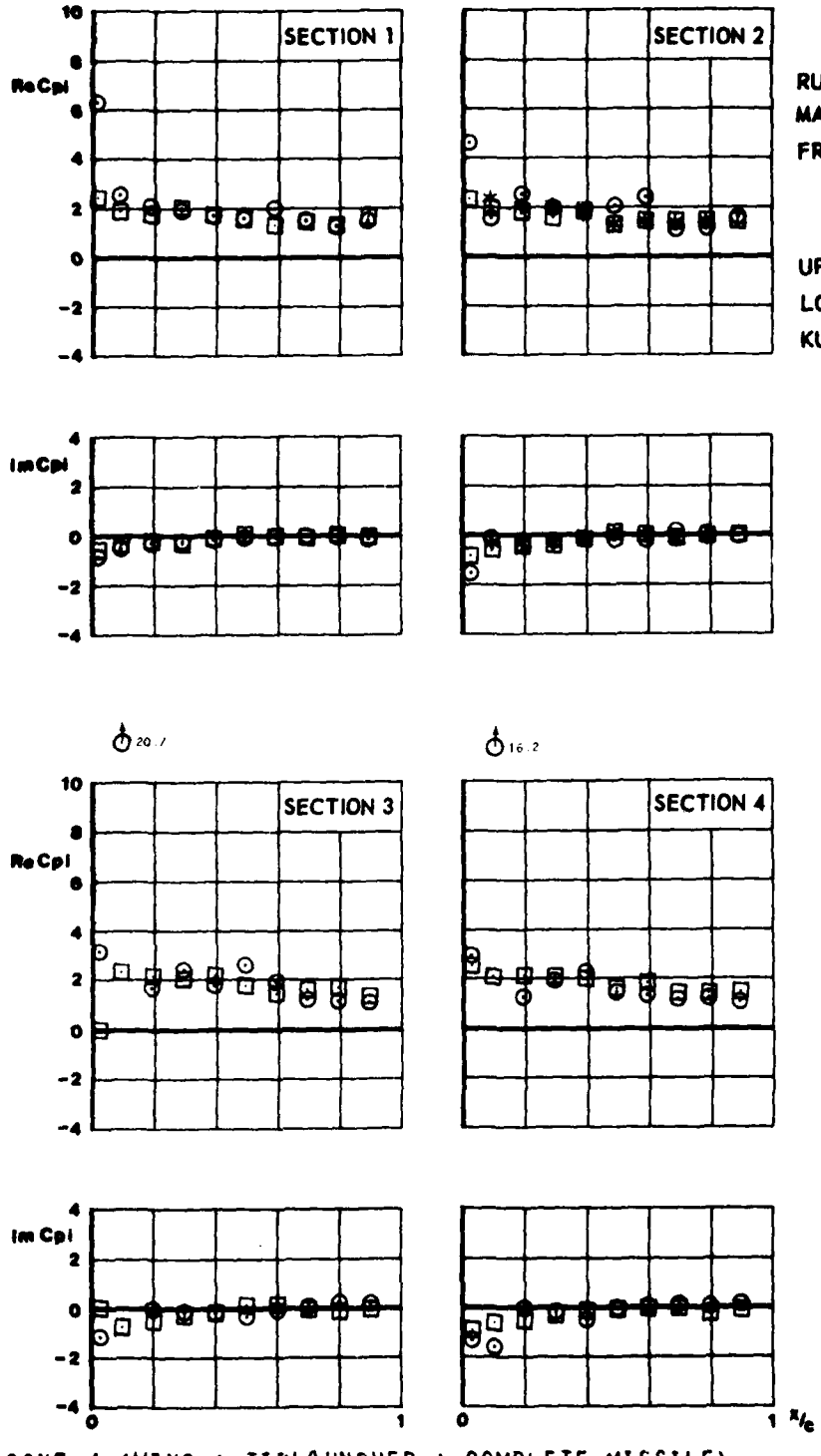

CONF.4 (WING + TIPLAUNCHER + COMPLETE MISSILE)

FIG.
III.C.4B.6

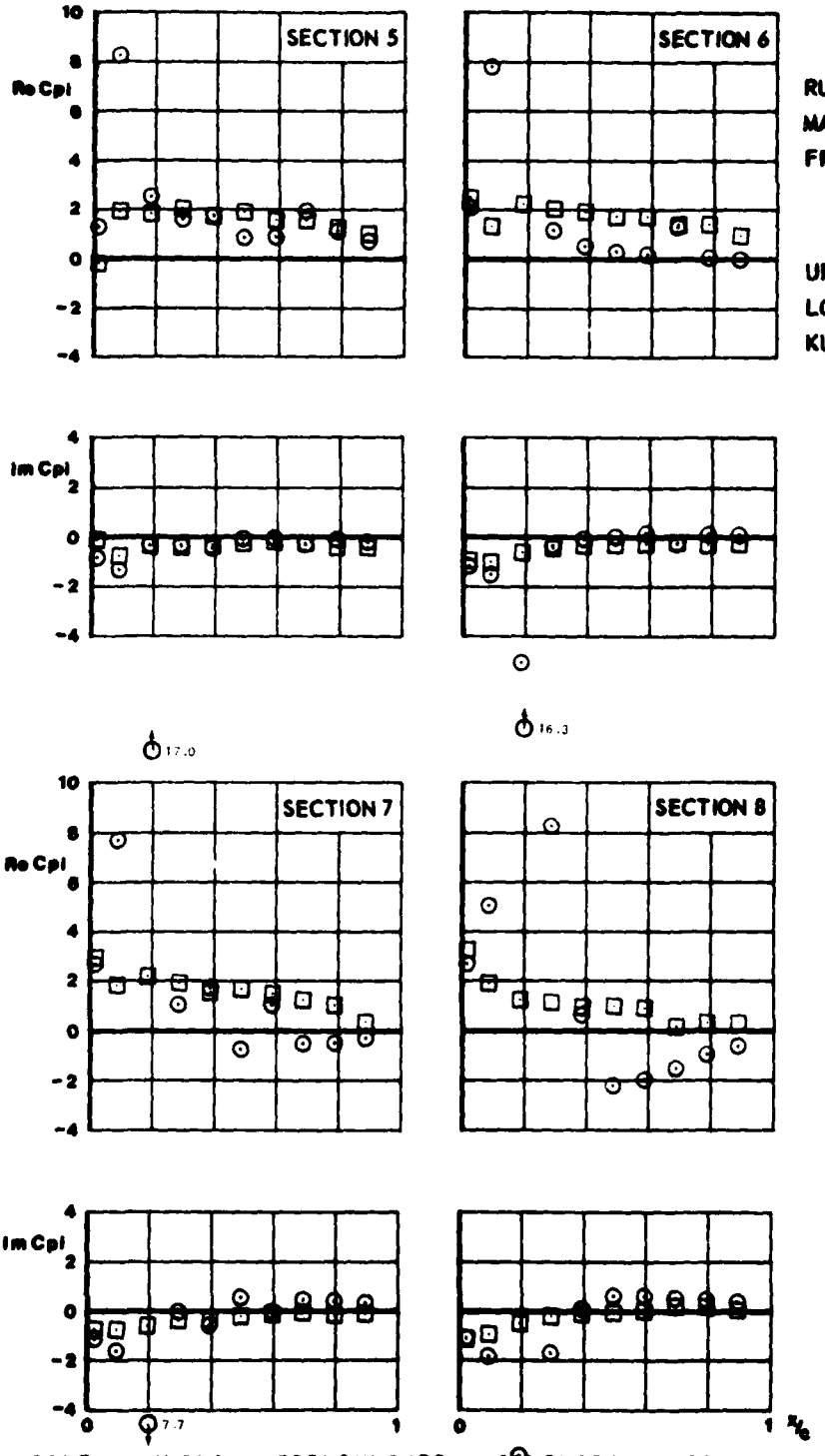

CONF. 4 (WING + TIPLAUNCHER + COMPLETE MISSILE)

FIG.
III.C.49.a

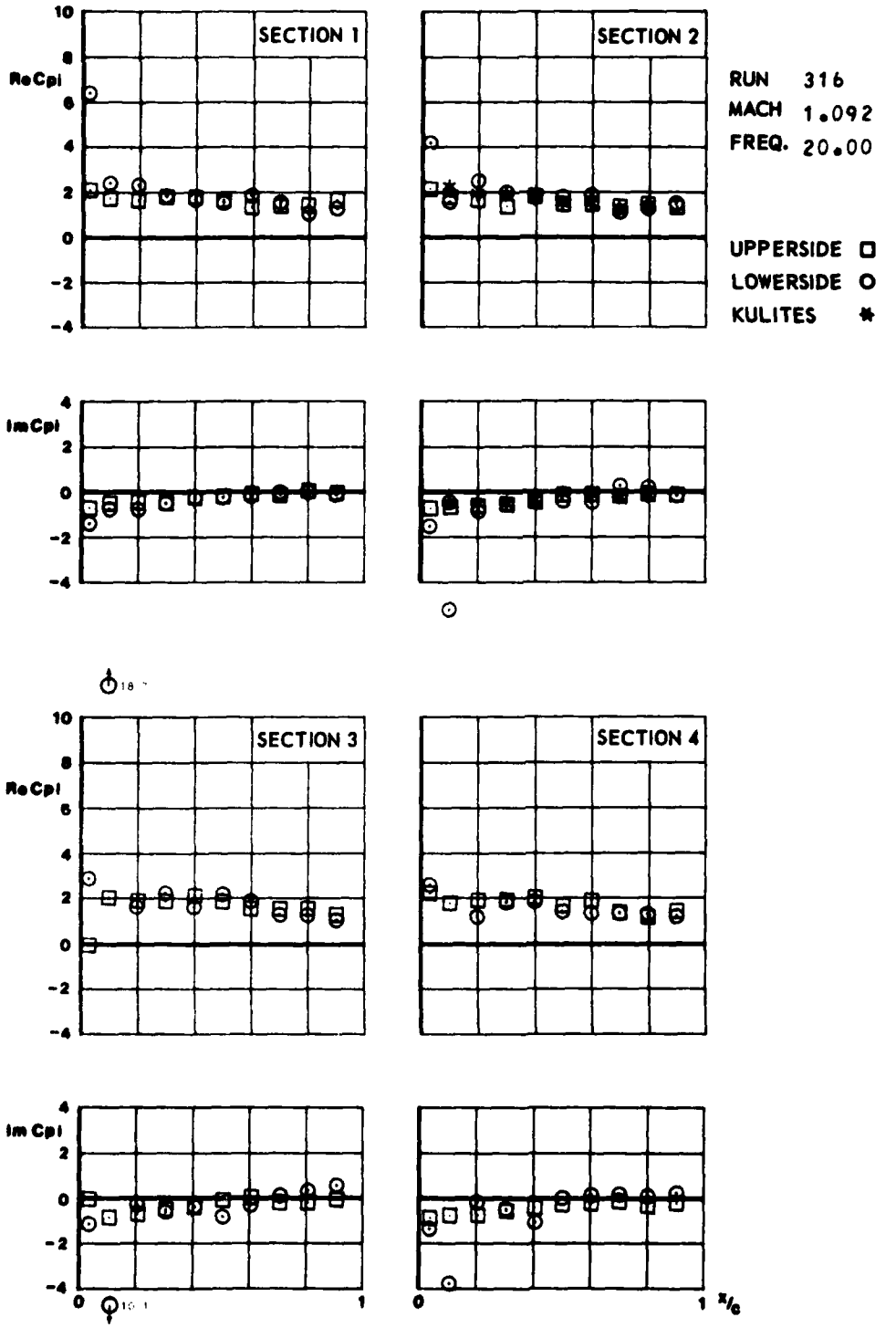

CONF.4 (WING + TIPLAUNCHER + COMPLETE MISSILE)

FIG.
III.C.49.6

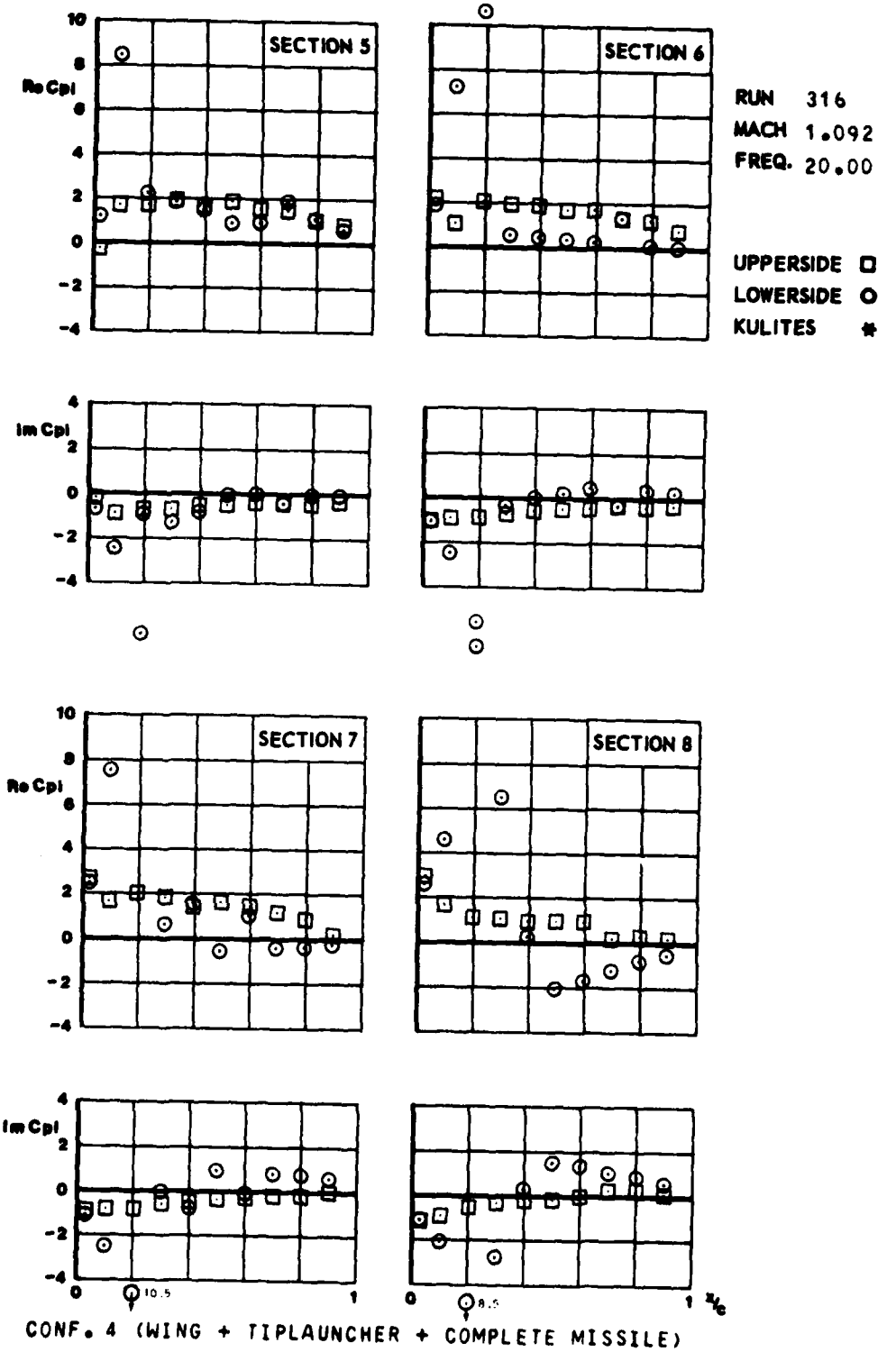

CONF. 4 (WING + TIPLAUNCHER + COMPLETE MISSILE)

FIG.
III.C.50.a

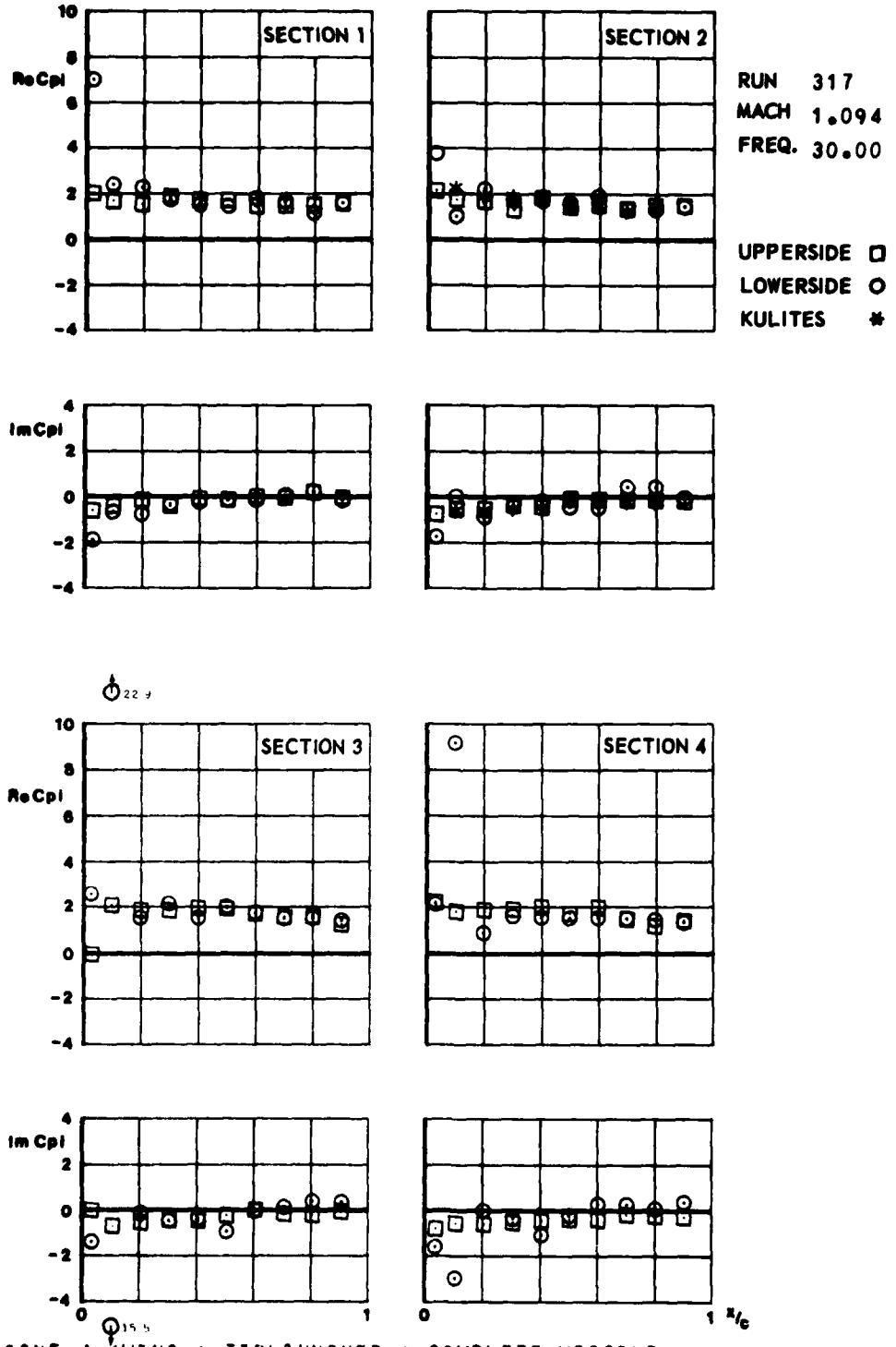

CONF.4 (WING + TIPLAUNCHER + COMPLETE MISSILE)

FIG.
III.C.5a.6

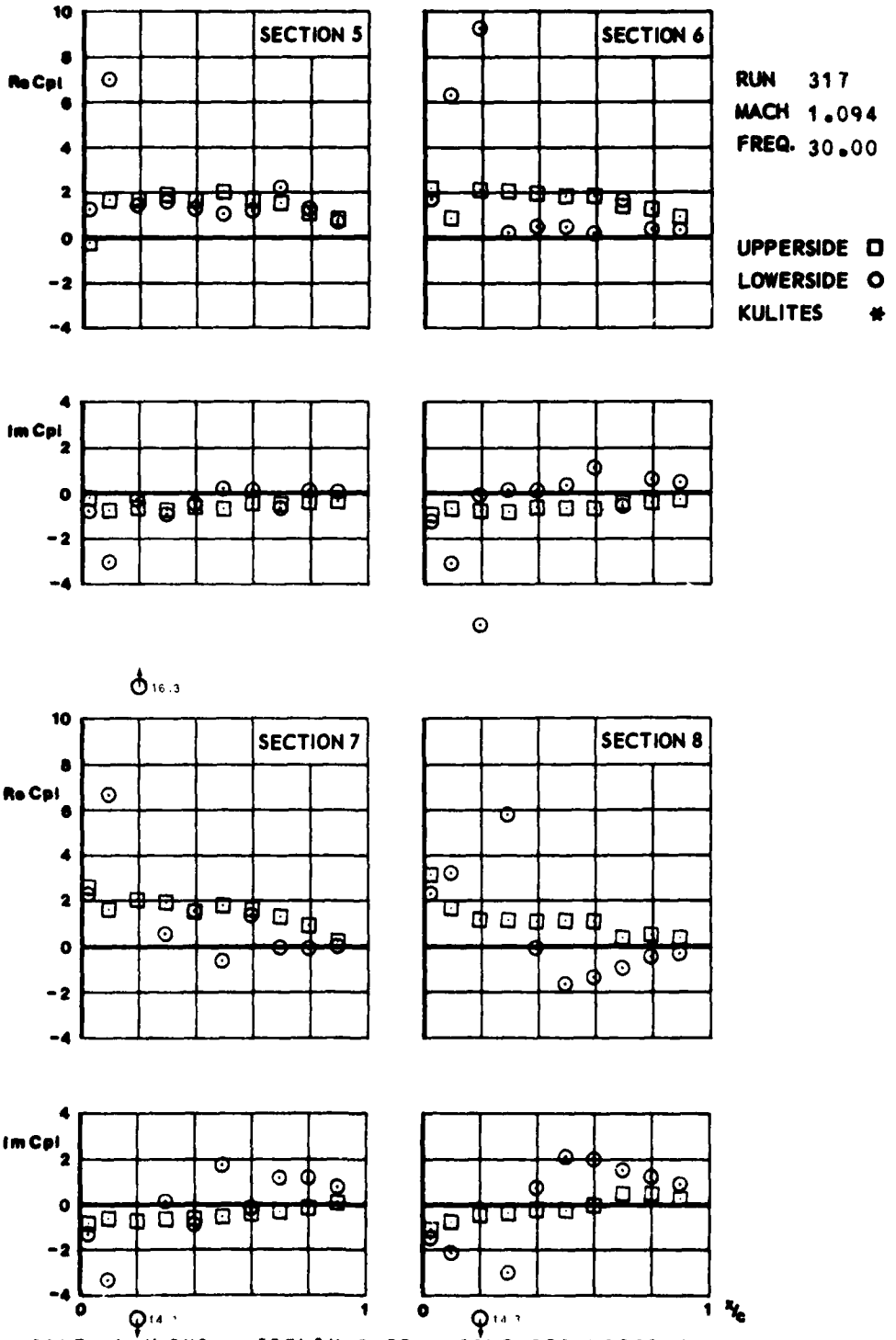

CONF. 4 (WING + TIPLAUNCHER + COMPLETE MISSILE)

FIG.
III.C.51.a

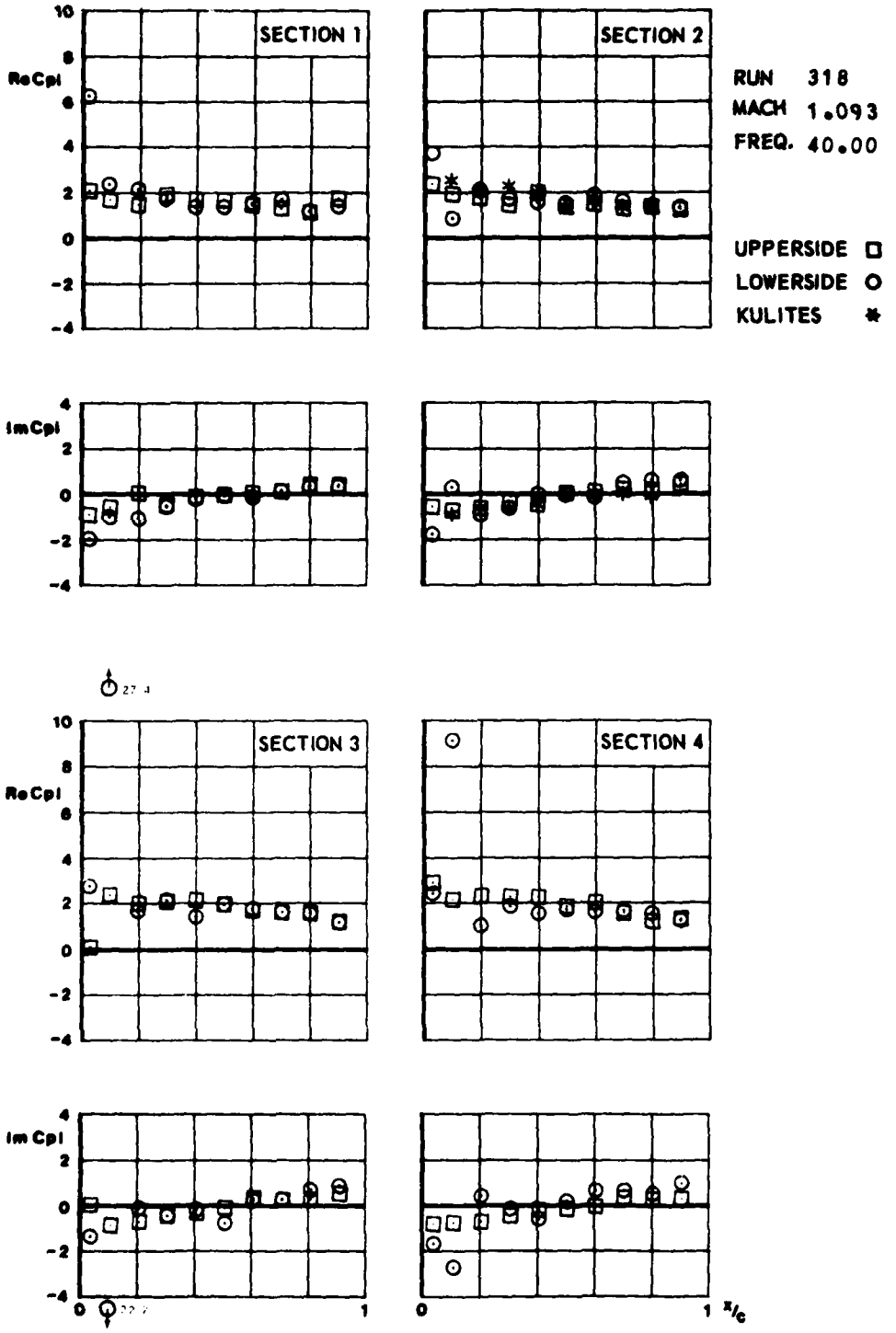

CONF.4 (WING + TIPLAUNCHER + COMPLETE MISSILE)

FIG.
III.C.51.b

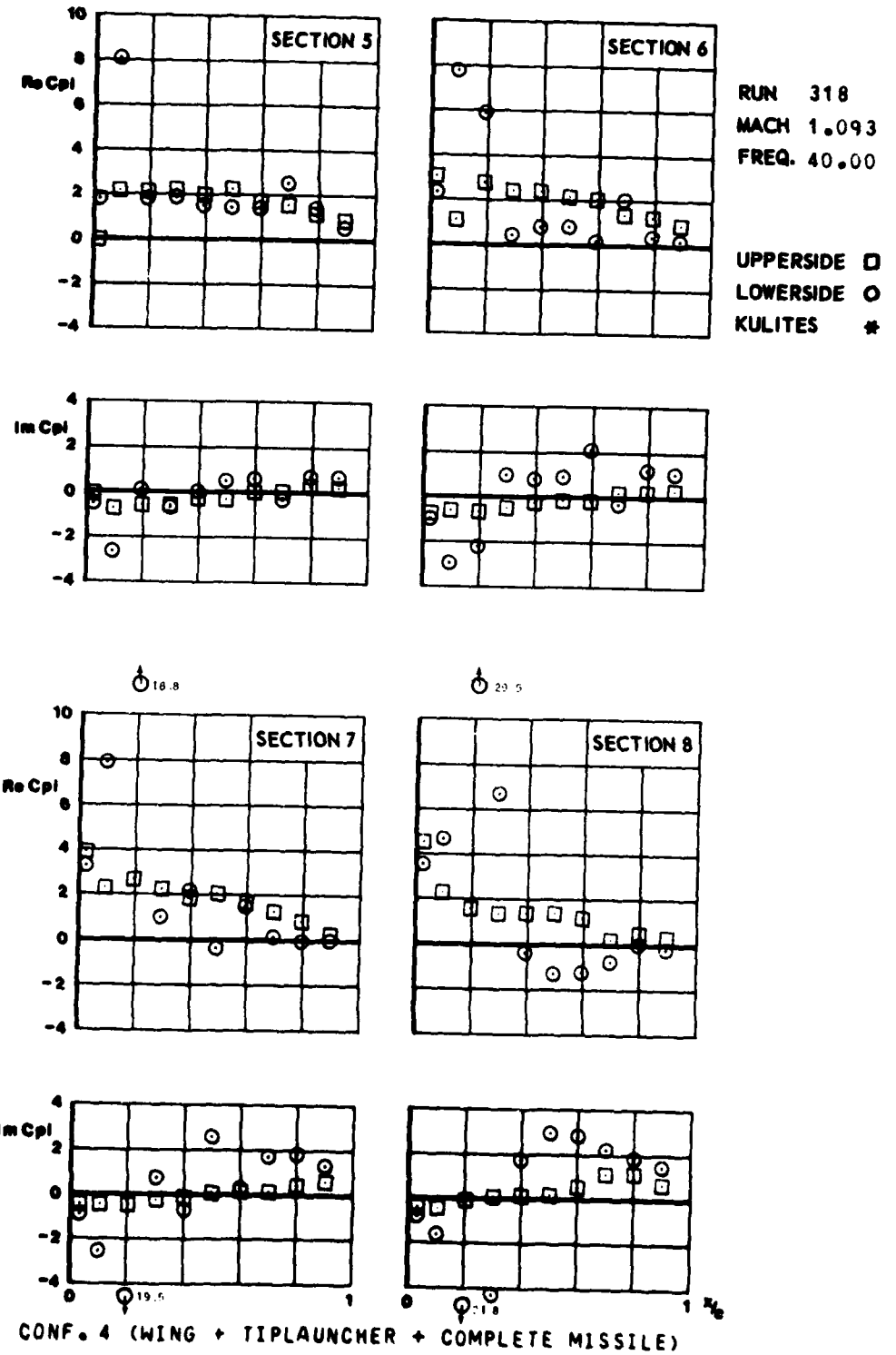

CONF. 4 (WING + TIPLAUNCHER + COMPLETE MISSILE)

FIG.
III.C.52.a

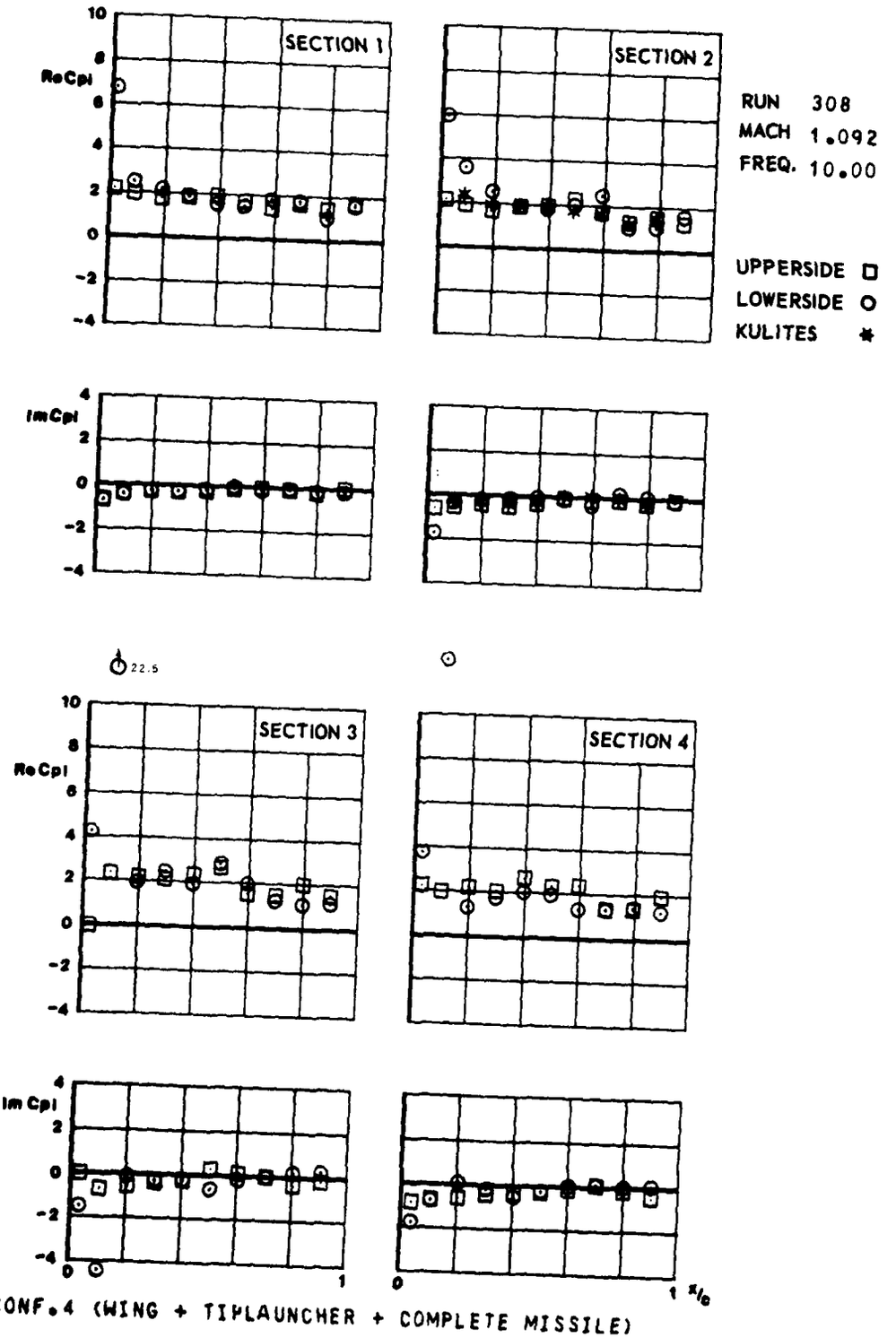

CONF.4 (WING + TIPLAUNCHER + COMPLETE MISSILE)

FIG.
III.C.52.6

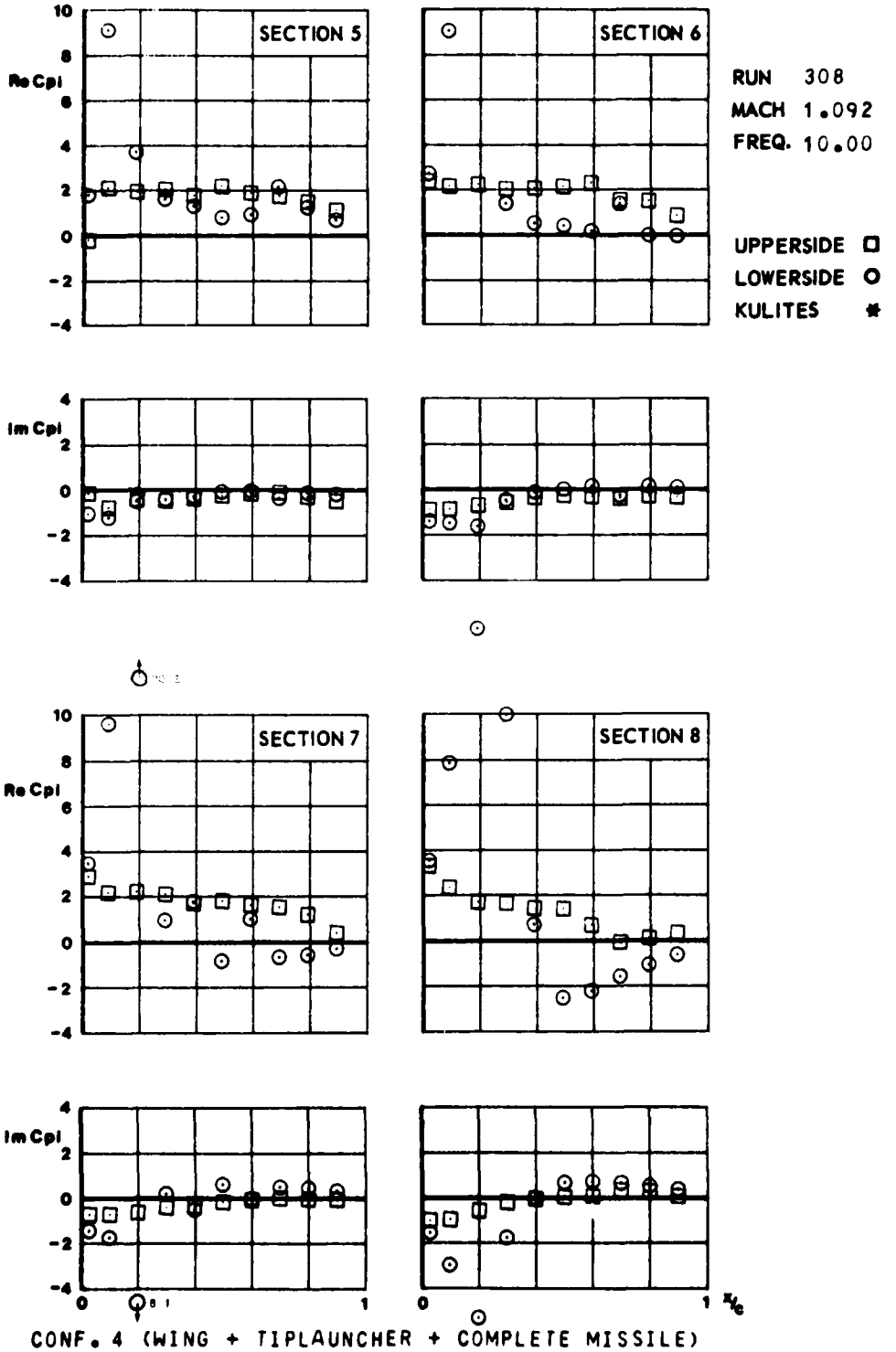

CONF. 4 (WING + TIPLAUNCHER + COMPLETE MISSILE)

FIG.
III.C.53.a

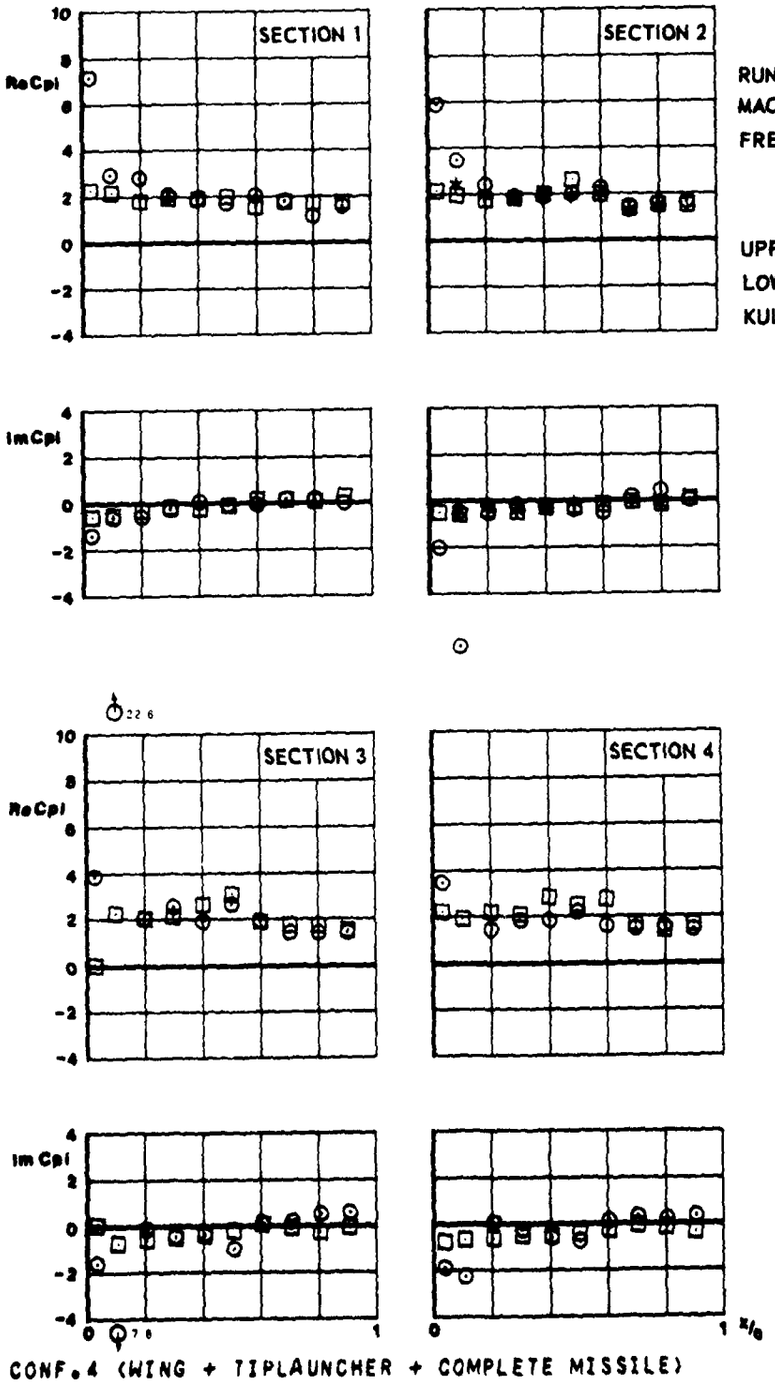

CONF.4 (WING + TIPLAUNCHER + COMPLETE MISSILE)

FIG.
III.C.53.b

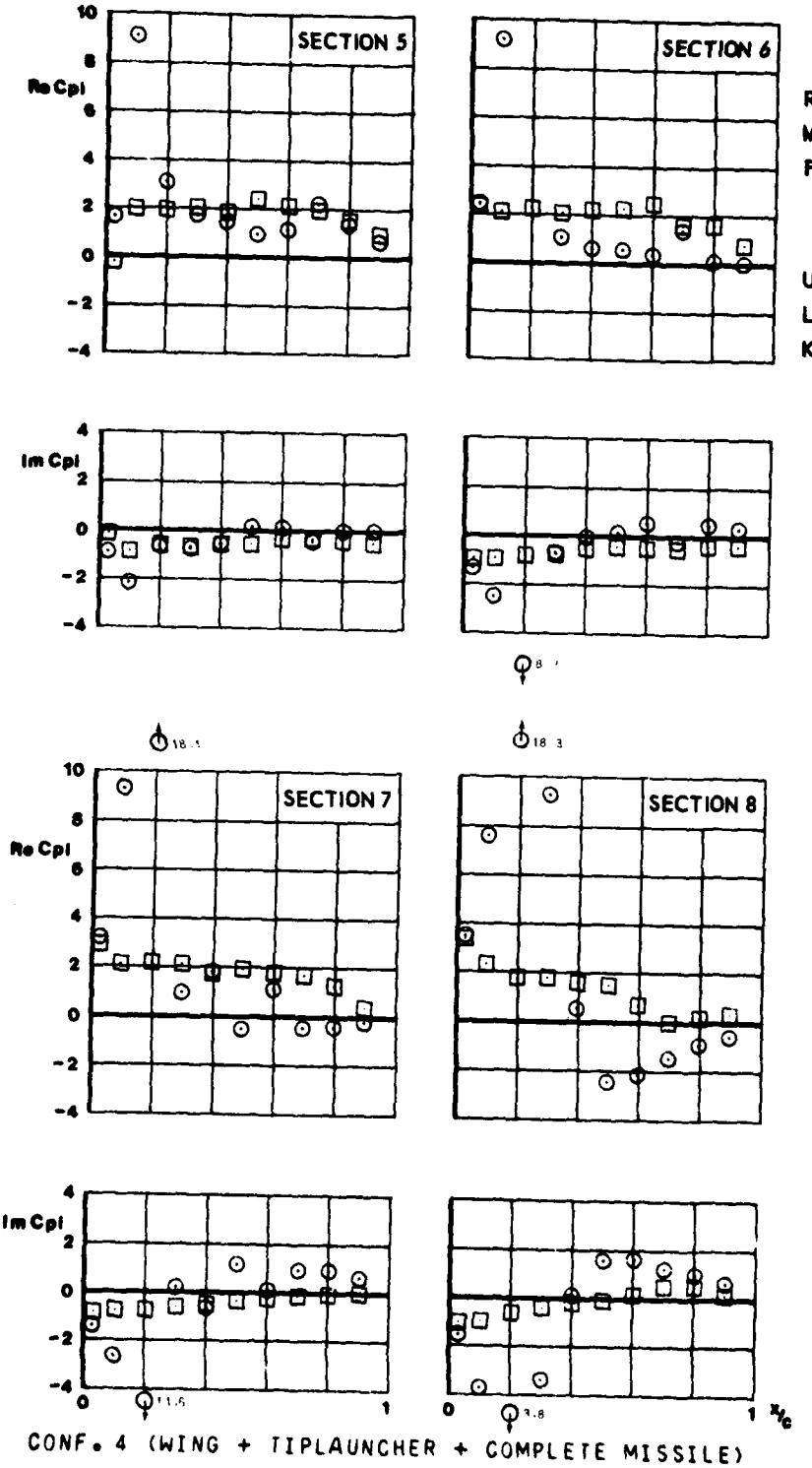

CONF. 4 (WING + TIPLAUNCHER + COMPLETE MISSILE)

FIG.
III.C.54.a

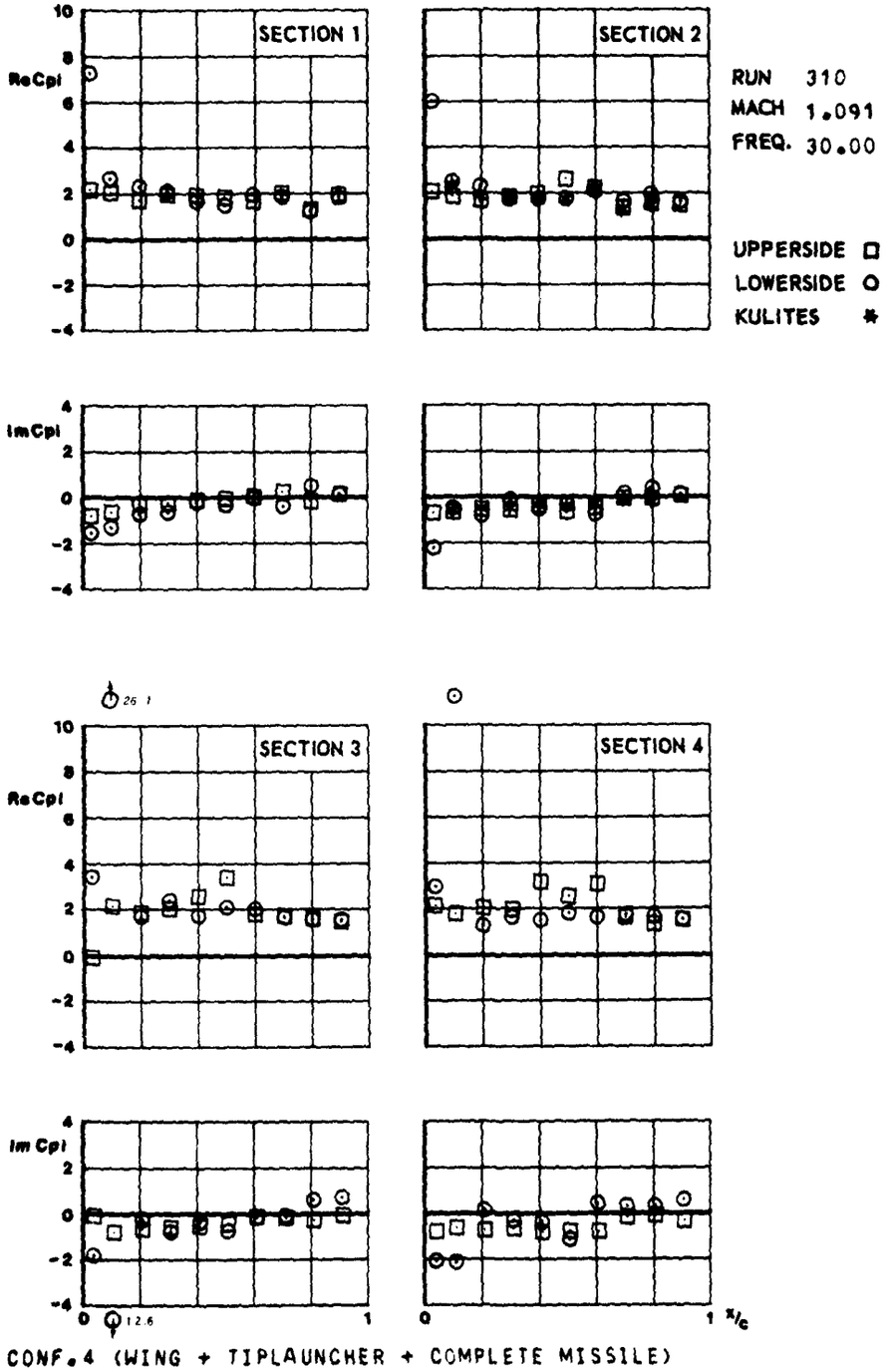

CONF.4 (WING + TIPLAUNCHER + COMPLETE MISSILE)

FIG.
III.C.54.b

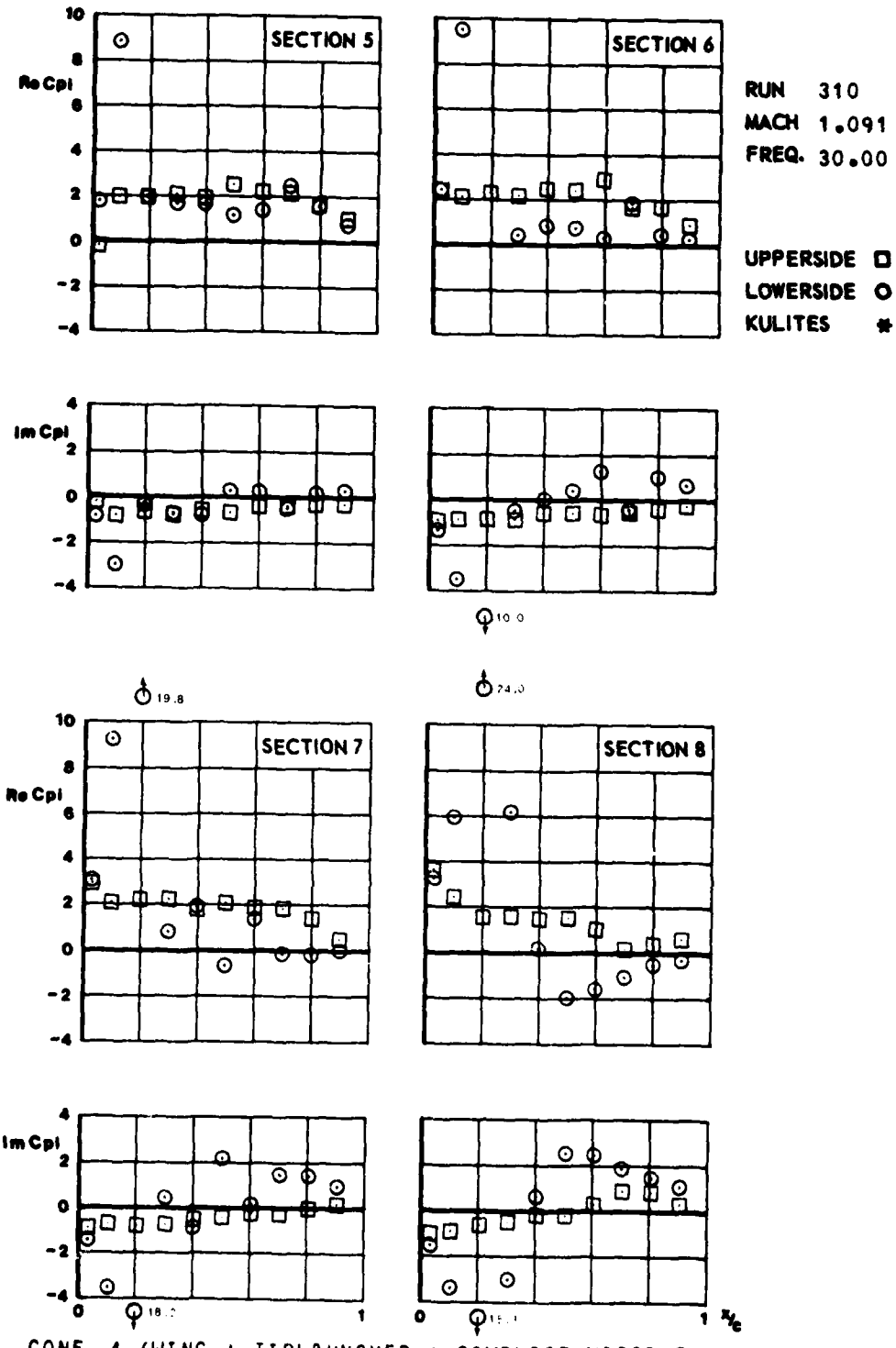

CONF. 4 (WING + TIPLAUNCHER + COMPLETE MISSILE)

FIG.
III.C.55.a

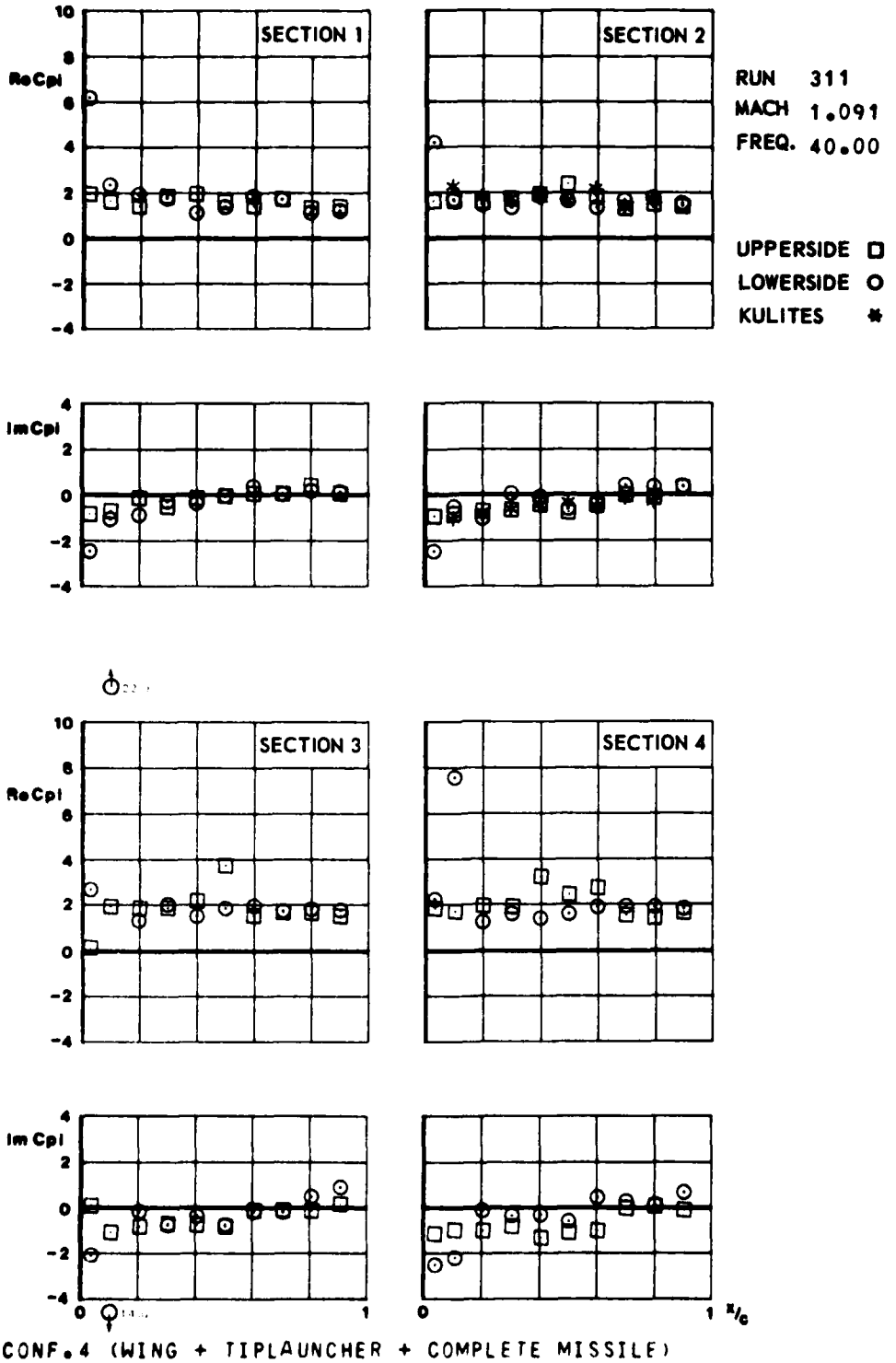

CONF.4 (WING + TIPLAUNCHER + COMPLETE MISSILE)

FIG.
III.C.55b

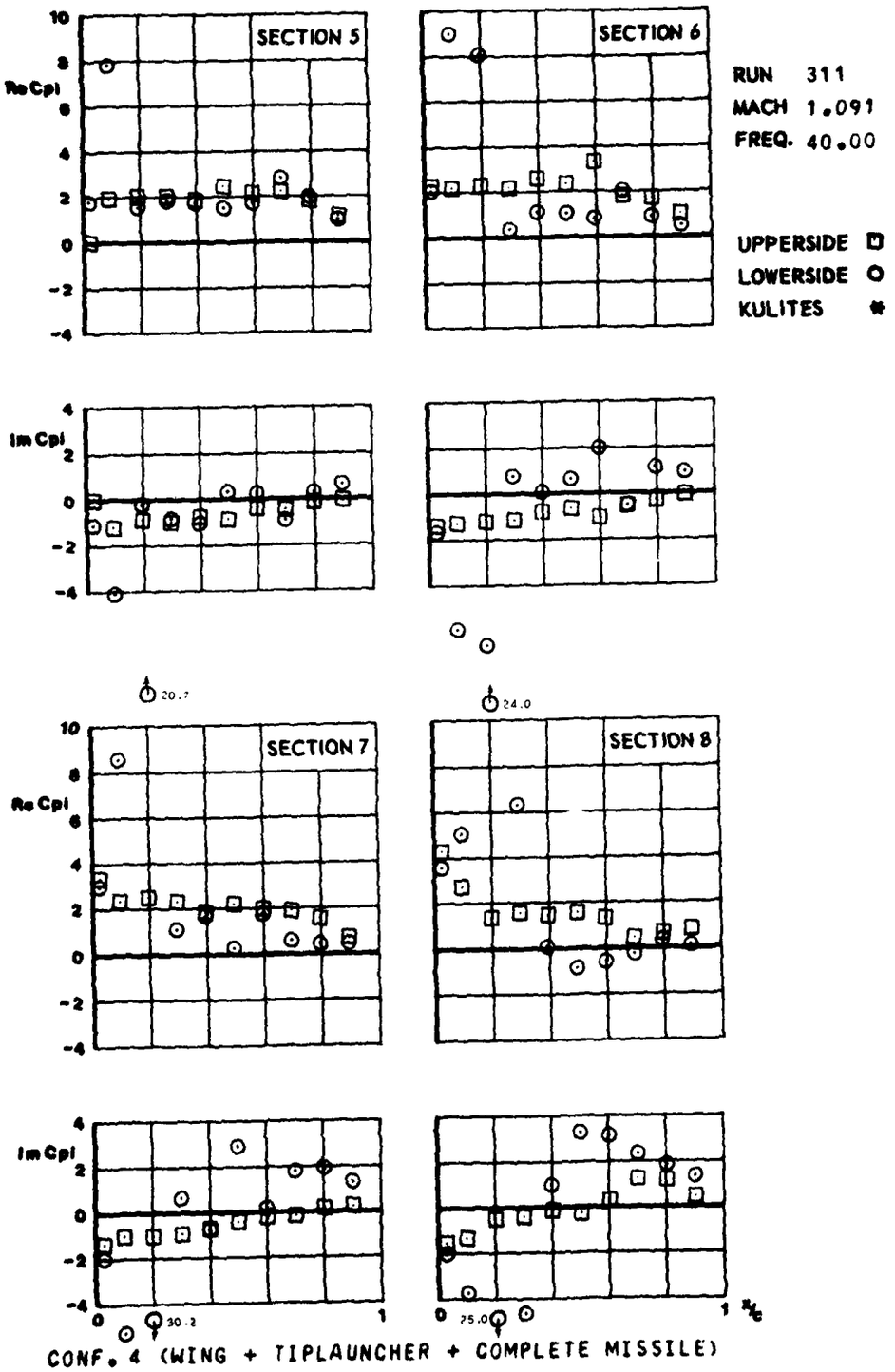

CONF. 4 (WING + TIPLAUNCHER + COMPLETE MISSILE)

FIG.
III.C.56.a

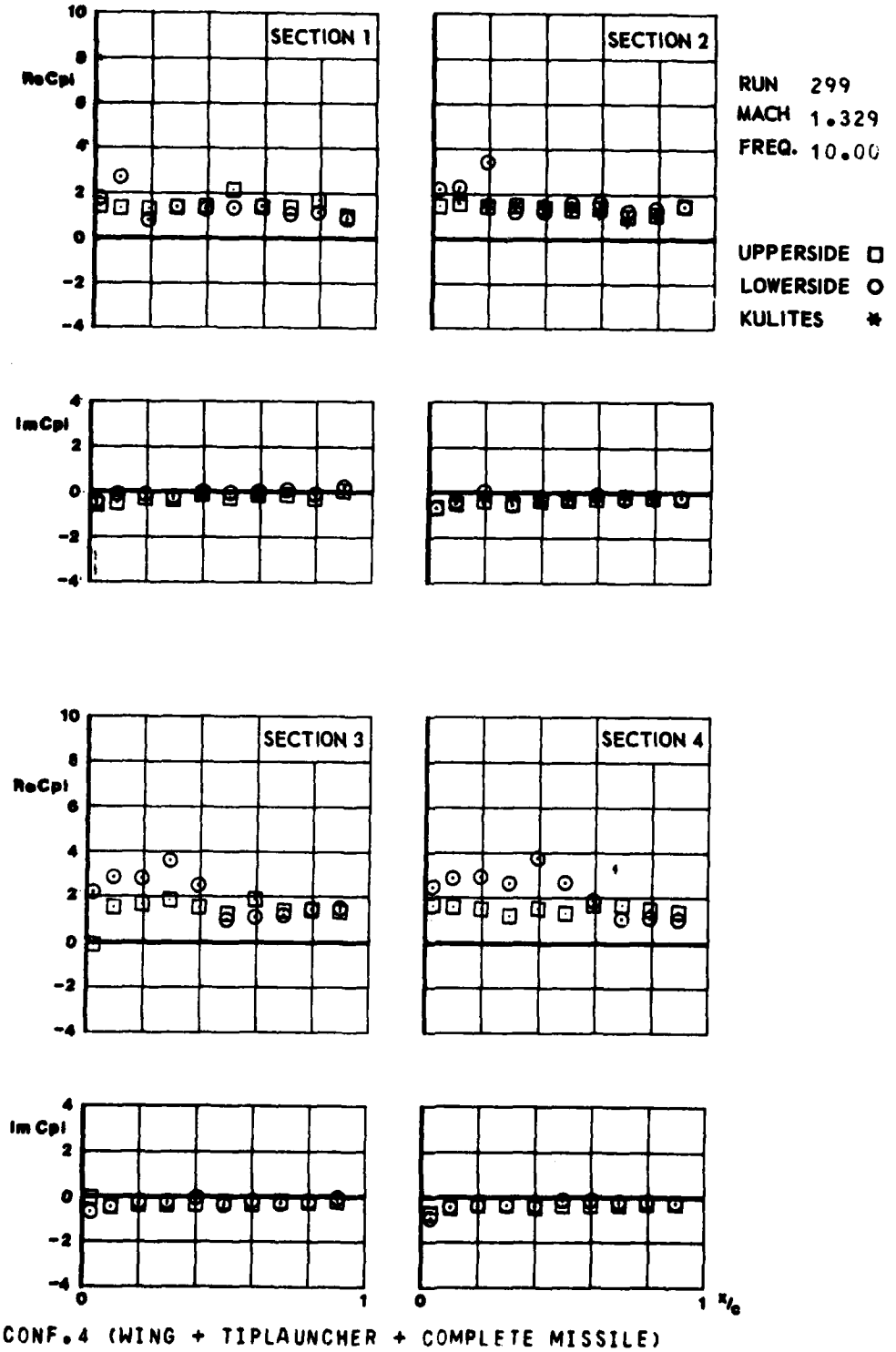

CONF.4 (WING + TIPLAUNCHER + COMPLETE MISSILE)

FIG.
III.C.56.6

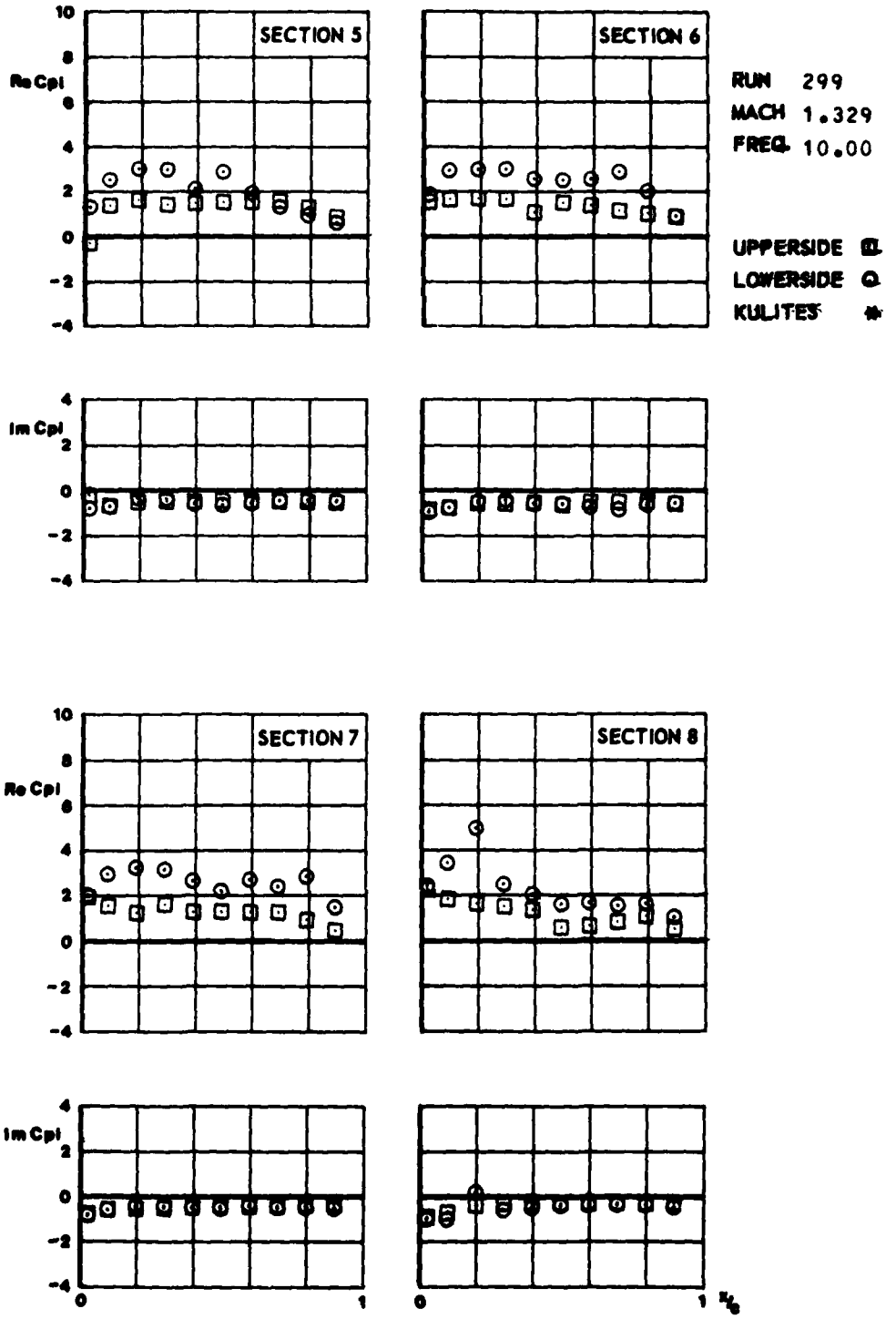

CONF. 4 (WING + TIPLAUNCHER + COMPLETE MISSILE)

FIG.
III.C.57.a

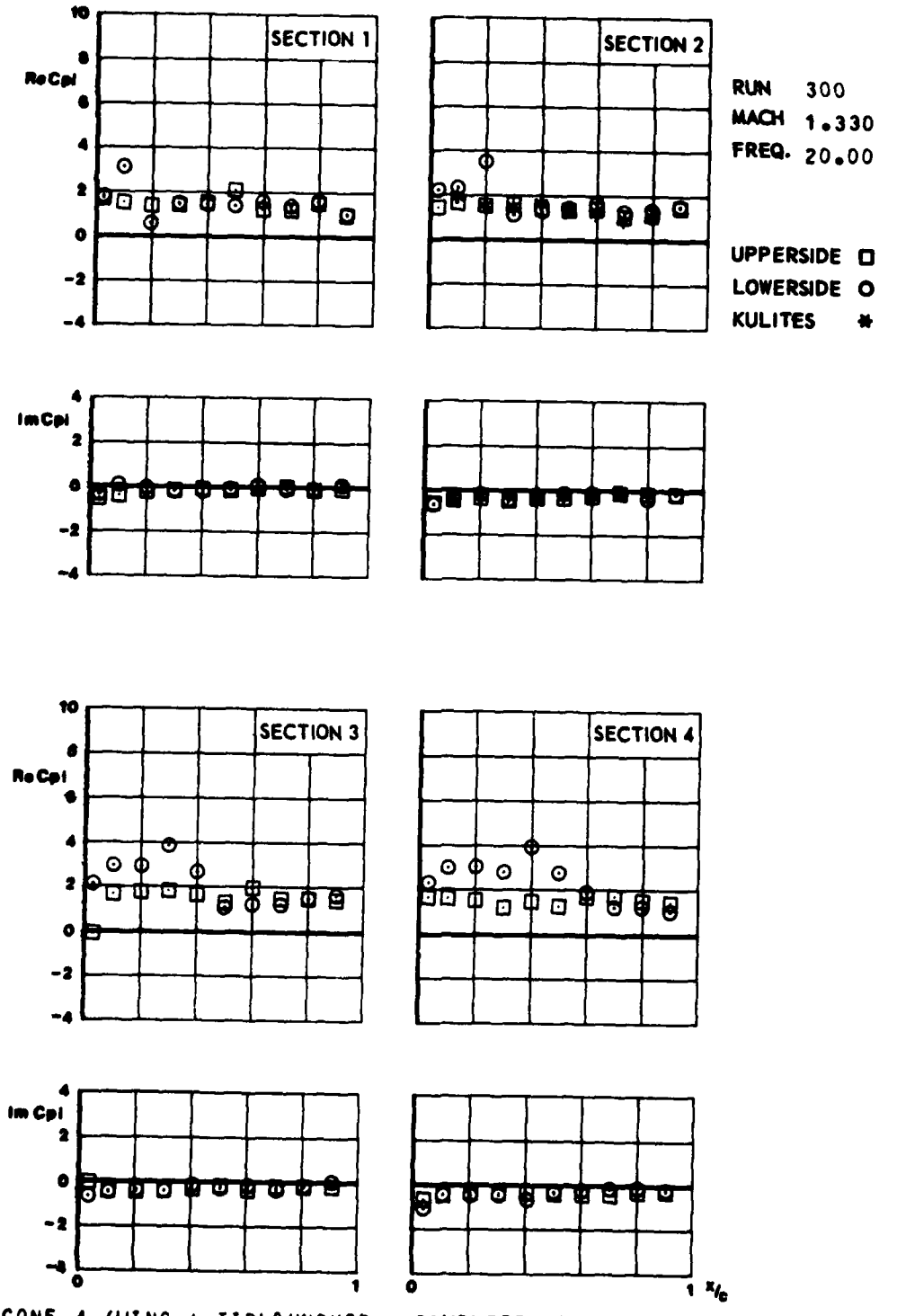

CONF.4 (WING + TIPLAUNCHER + COMPLETE MISSILE)

FIG.
III.C.57.b

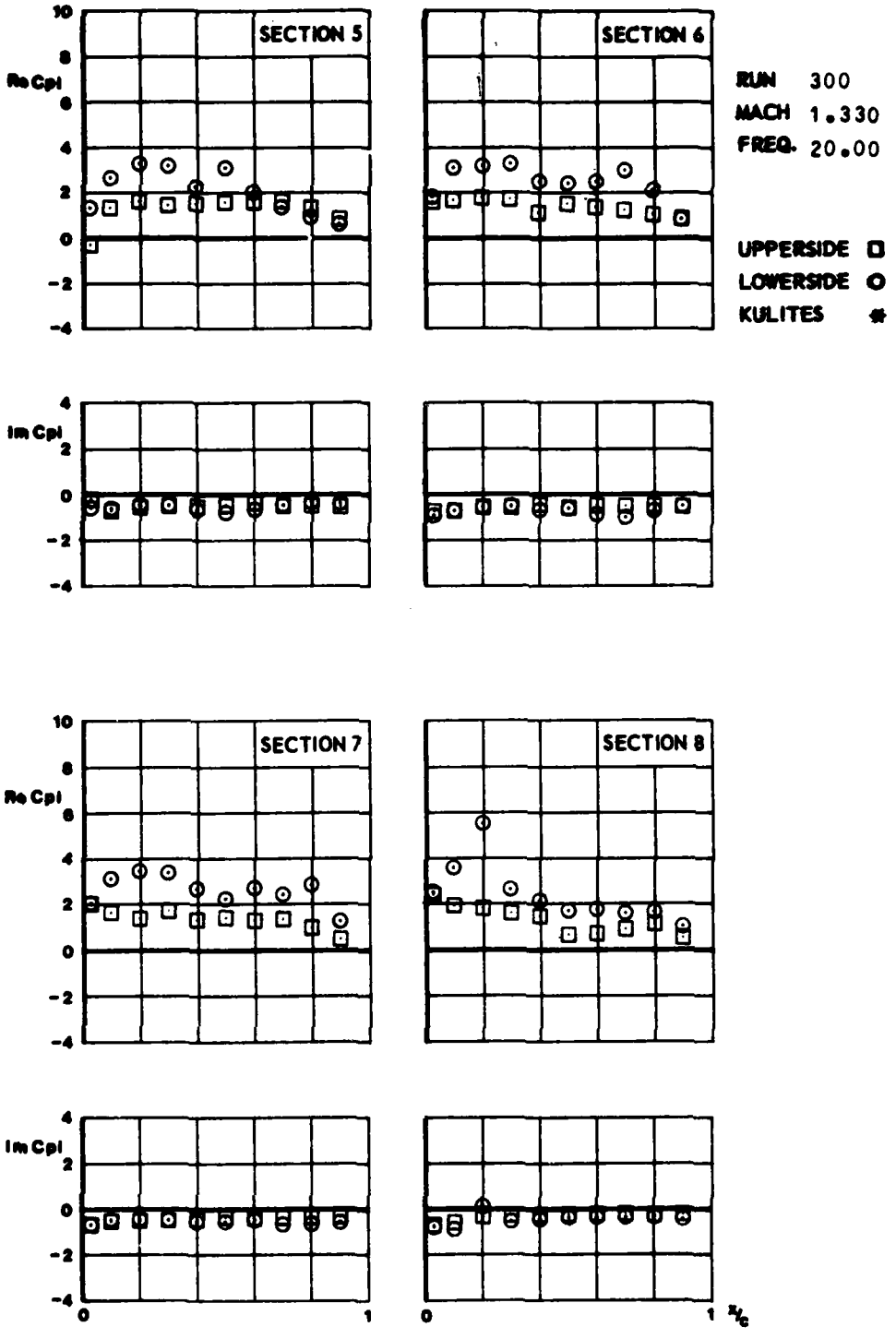

CONF. 4 (WING + TIPLAUNCHER + COMPLETE MISSILE)

FIG.
III.C.58.a

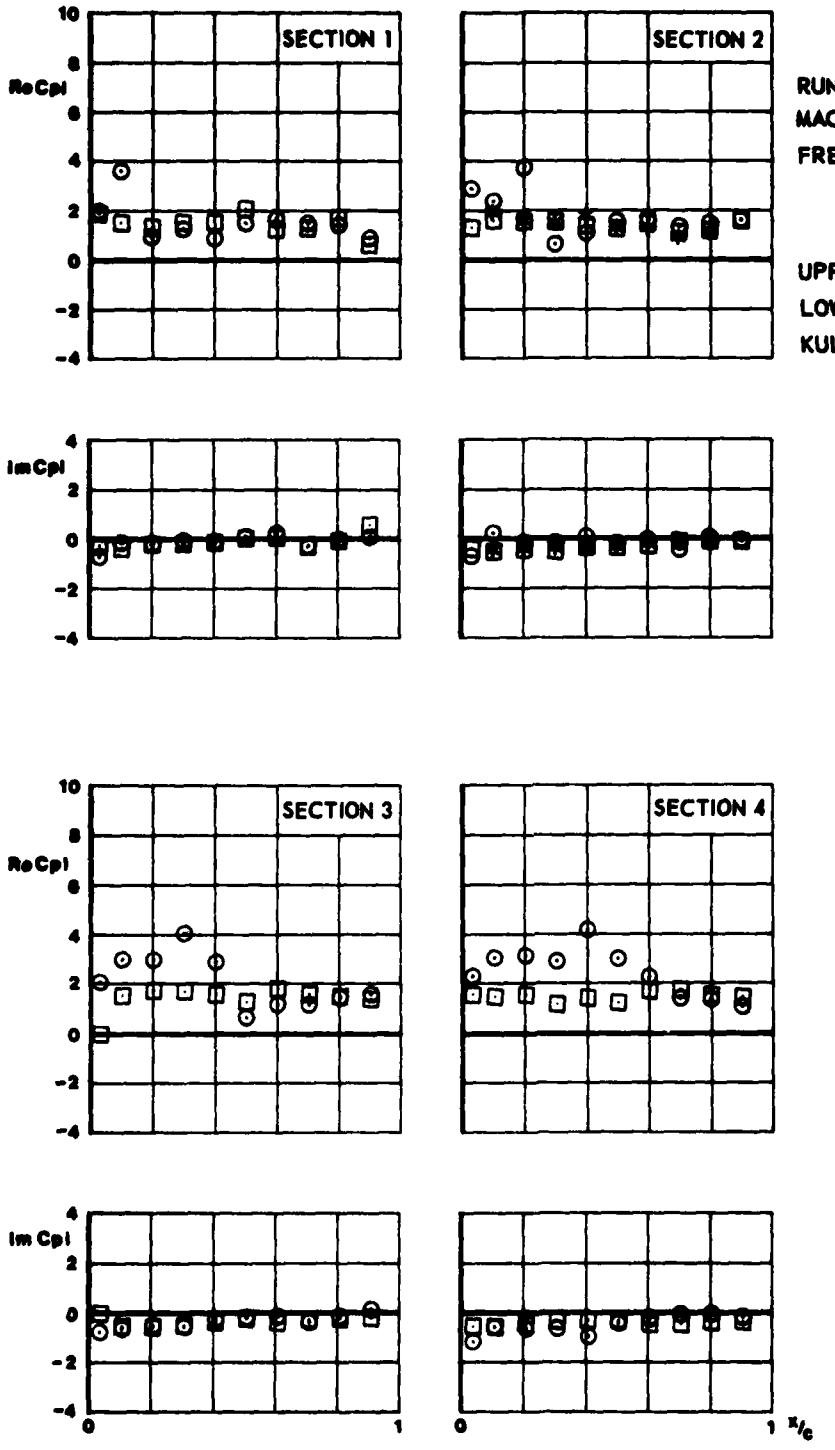

CONF.4 (WING + TIPLAUNCHER + COMPLETE MISSILE)

FIG.
III.C.52.6

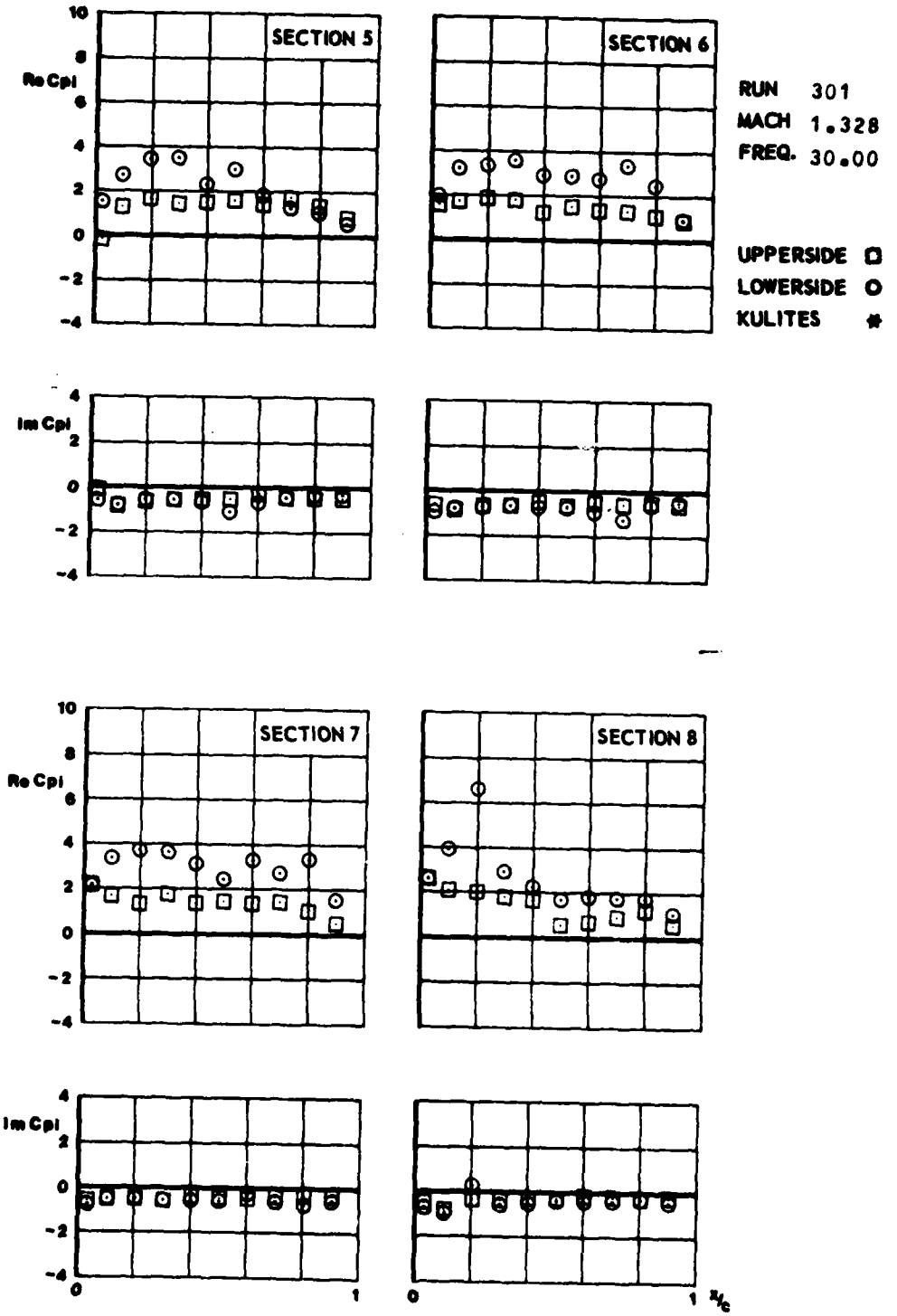

CONF. 4 (WING + TIPLAUNCHER + COMPLETE MISSILE)

FIG.
III.C.52a

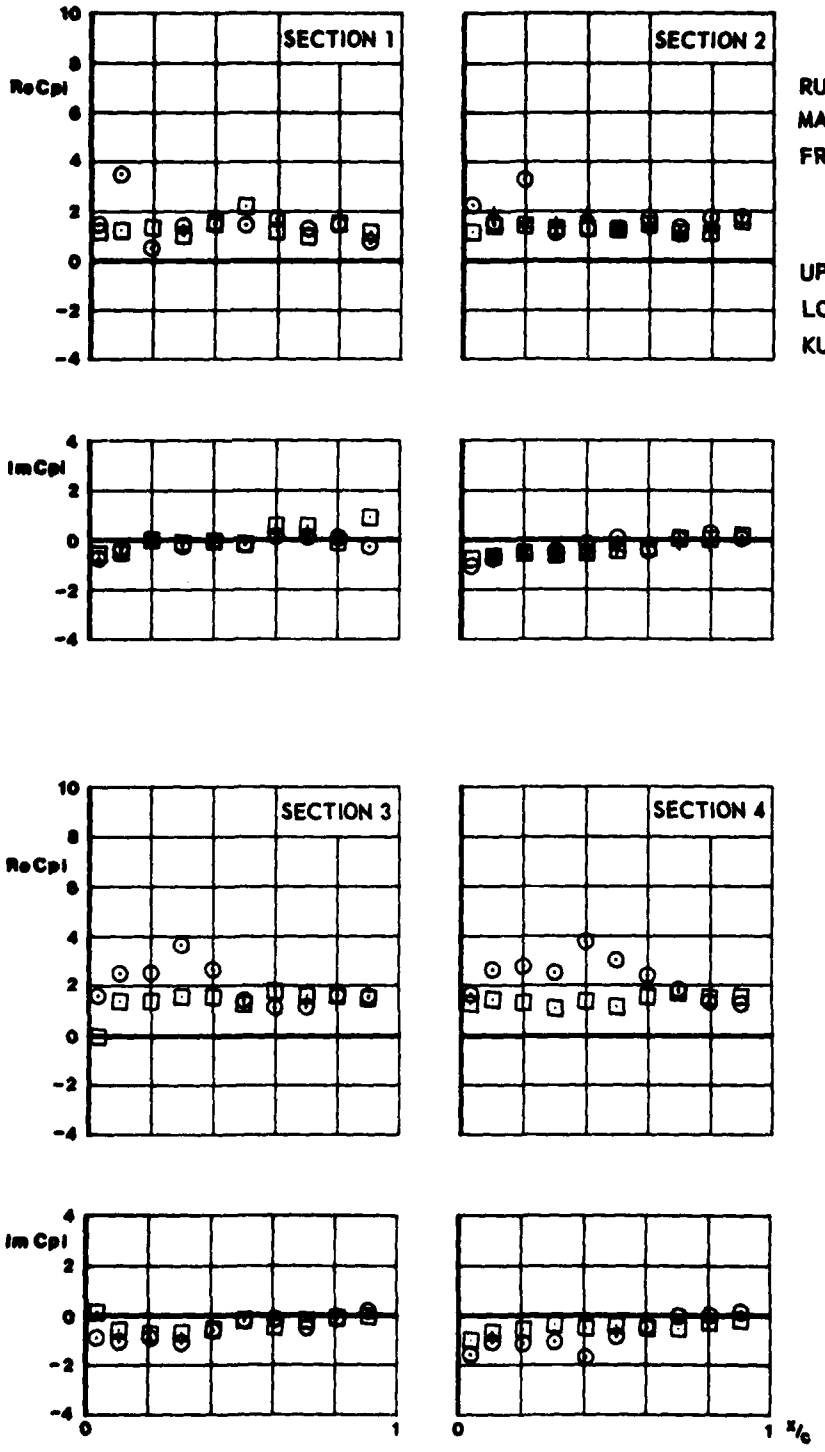

CONF. 4 (WING + TIPLAUNCHER + COMPLETE MISSILE)

FIG.
III.C.59.b

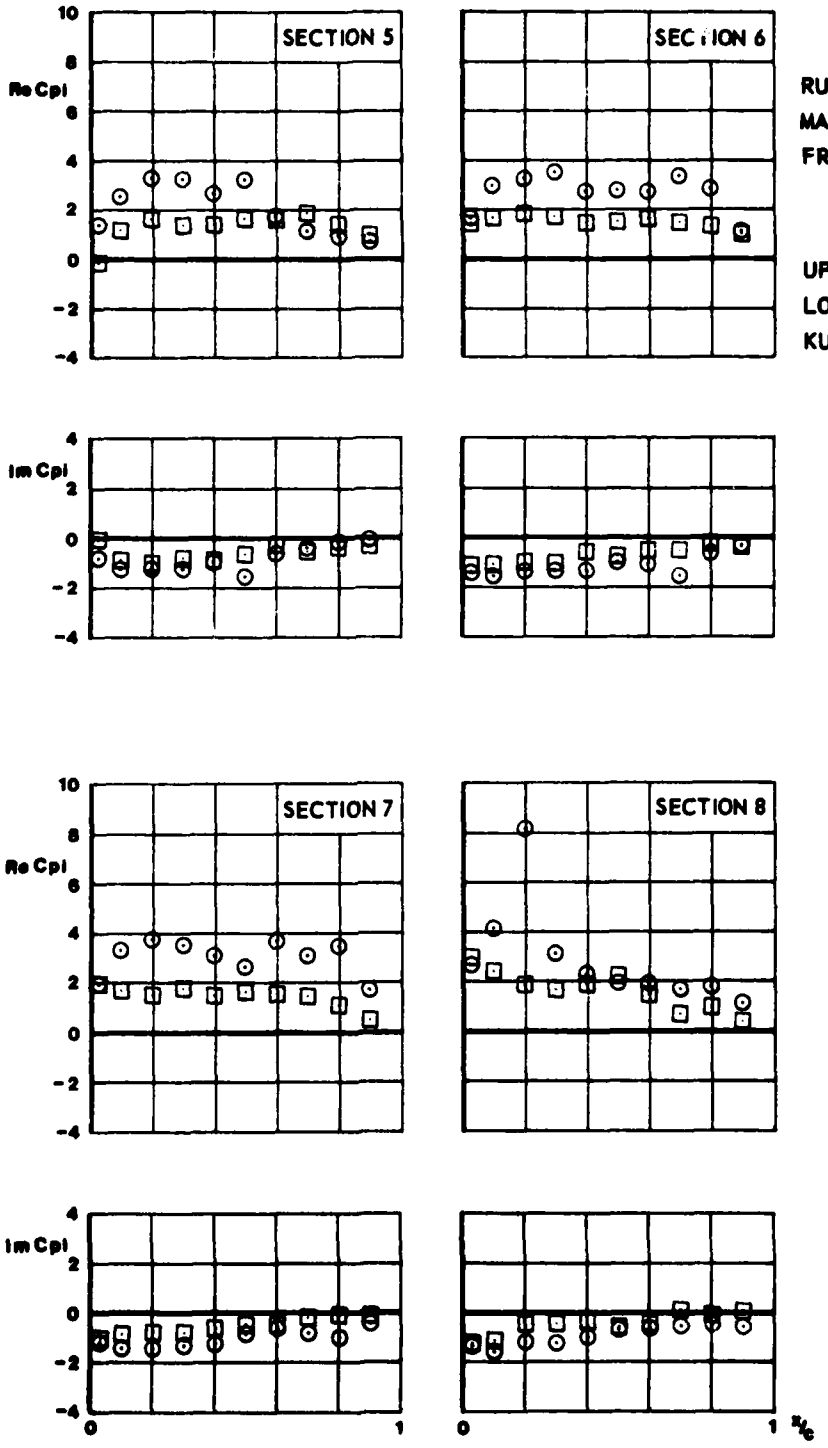

CONF. 4 (WING + TIPLAUNCHER + COMPLETE MISSILE)

APPENDIX III.D

Steady and Unsteady Store Loads

Steady :

Conf. No.	Configuration	Fig. No.
1	W + TL	III.D.1a
2	W + TL + MB	III.D.1b
3	W + TL + MB + AW	III.D.2
4	W + TL + MB + AW + CF	III.D.3

Unsteady :

Conf. No.	Configuration	F (Hz)	Fig. No.
1	W + TL	20	III.D.4
2	W + TL + MB	20	III.D.5
3	W + TL + MB + AW	20	III.D.6
4	W + TL + MB + AW + CF	10	III.D.7
4	W + TL + MB + AW + CF	20	III.D.8
4	W + TL + MB + AW + CF	30	III.D.9

W = Wing

TL = Tiplauncher

MB = Missile Body

AW = Aft Wings

CF = Canard Fins

ⓐ TIPLAUNCHER (CONF. 1)

STEADY NORMAL FORCE

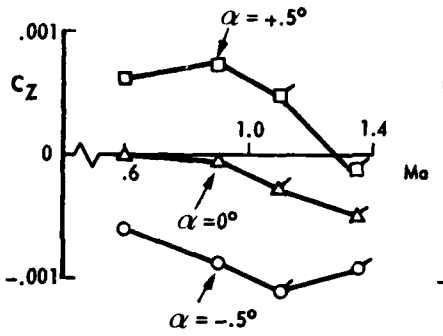

STEADY PITCHING MOMENT

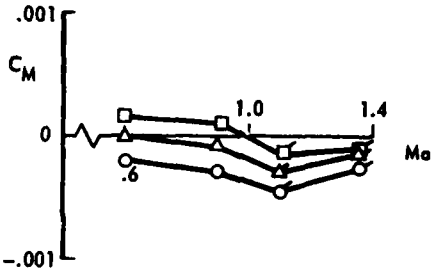

ⓑ TIPLAUNCHER + MISSILE BODY (CONF. 2)

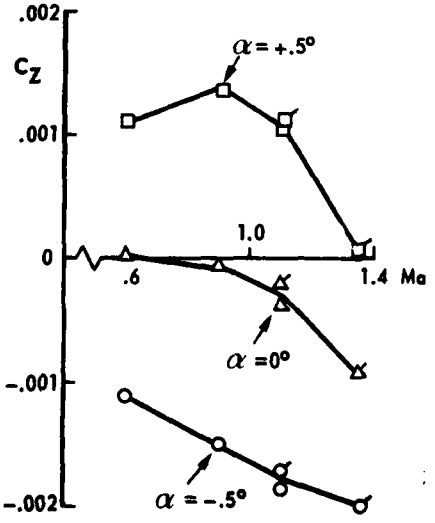

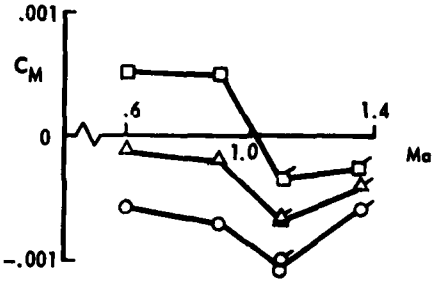

○ □ △ $P_0 = 1.0 \times 10^5$ Pa
○ □ △ $P_0 = 0.7 \times 10^5$ Pa

TIPLAUNCHER + MISSILE BODY
+ AFT WINGS (CONF. 3)

STEADY NORMAL FORCE

STEADY PITCHING MOMENT

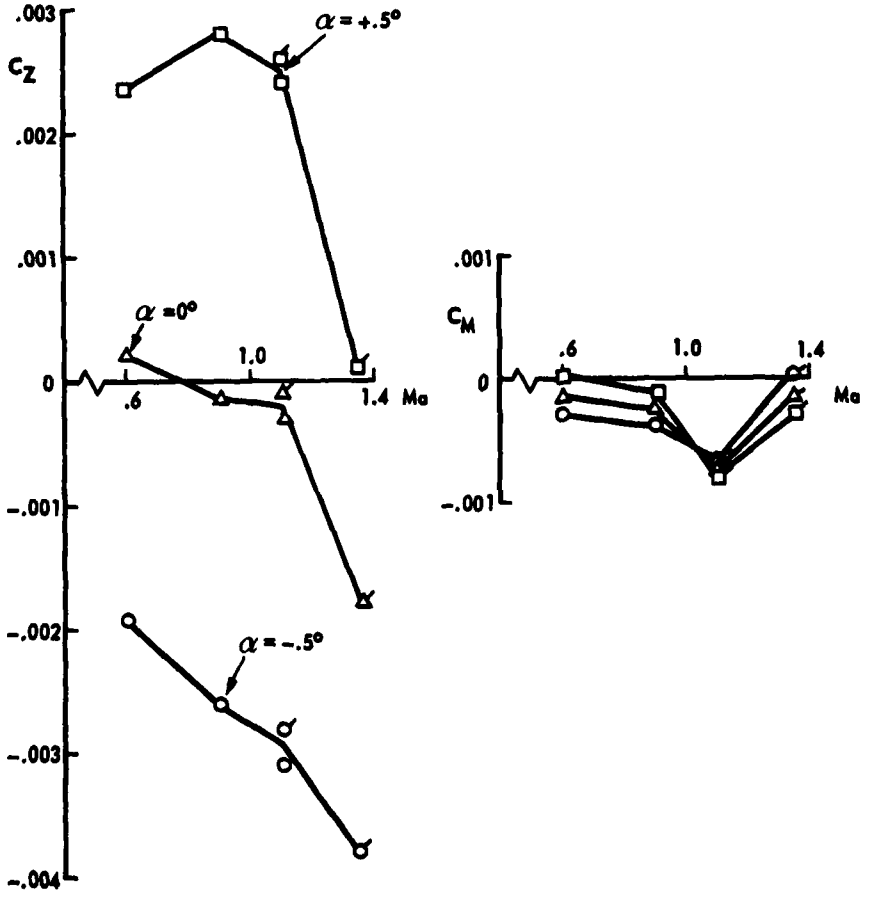

TIPLAUNCHER + COMPLETE MISSILE (CONF. 4)

STEADY NORMAL FORCE

STEADY PITCHING MOMENT

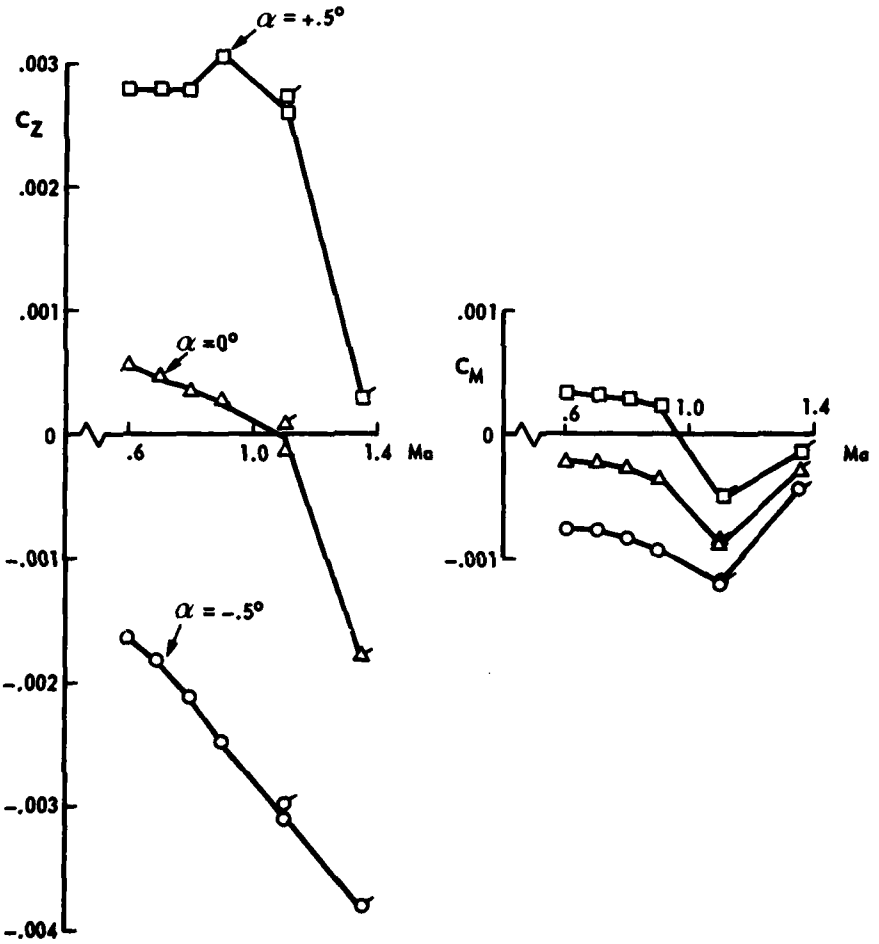

○ □ △ $P_0 = 1.0 \times 10^5$ Pa

○ □ △ $P_0 = 0.7 \times 10^5$ Pa

TIPLAUNCHER (CONF. 1)
F = 20 Hz

UNSTEADY NORMAL FORCE

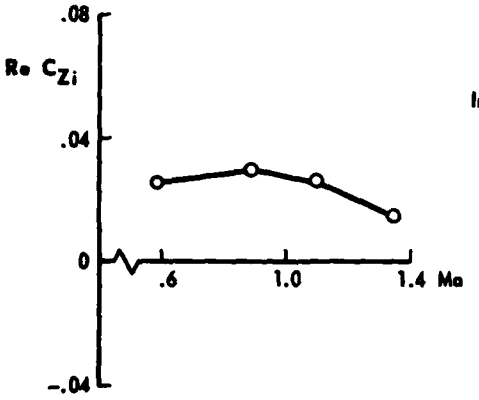

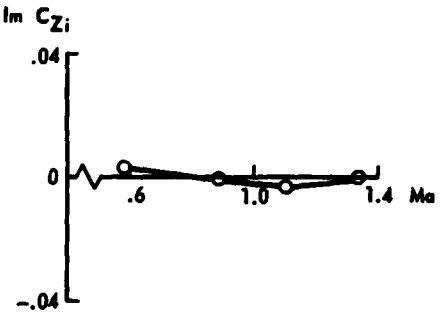

UNSTEADY PITCHING MOMENT

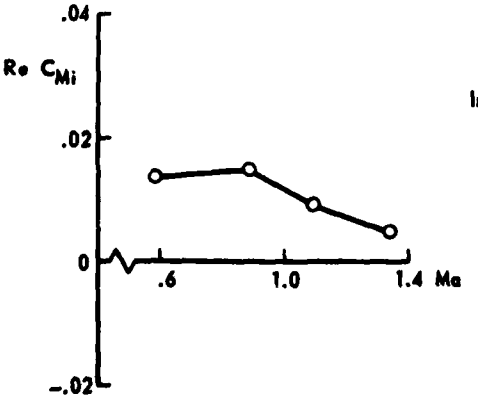

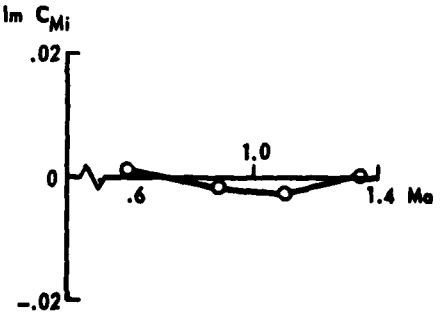

TIPLAUNCHER + MISSILE BODY
(CONF. 2) F = 20 Hz

UNSTEADY NORMAL FORCE

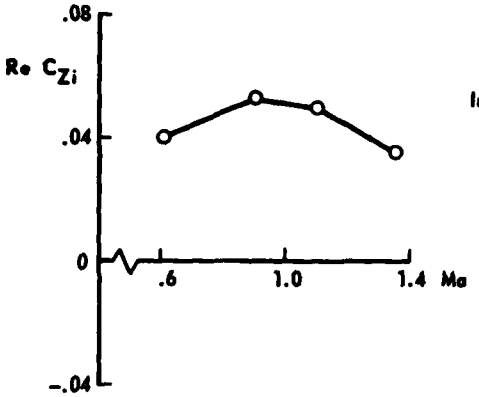

UNSTEADY PITCHING MOMENT

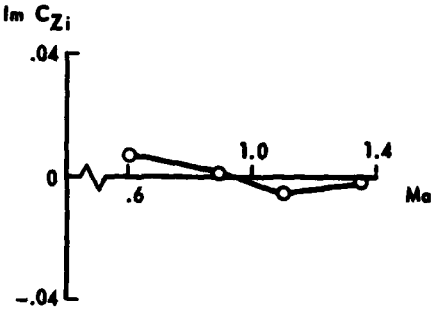

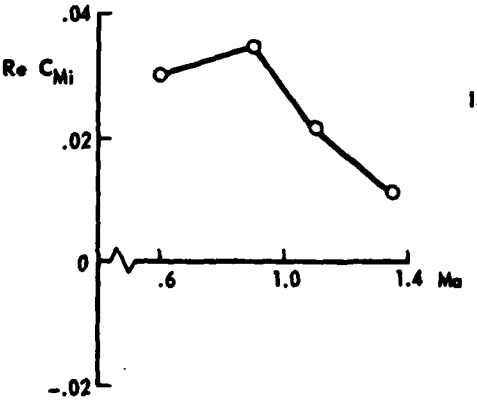

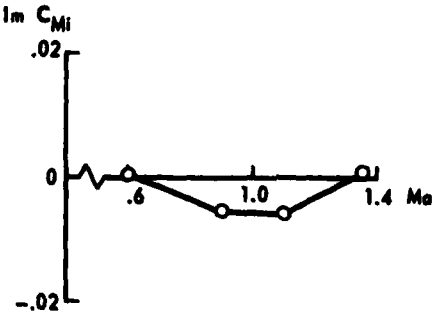

TIPLAUNCHER + MISSILE BODY
+ AFT WINGS (CONF. 3)
F = 20 Hz

UNSTEADY NORMAL FORCE

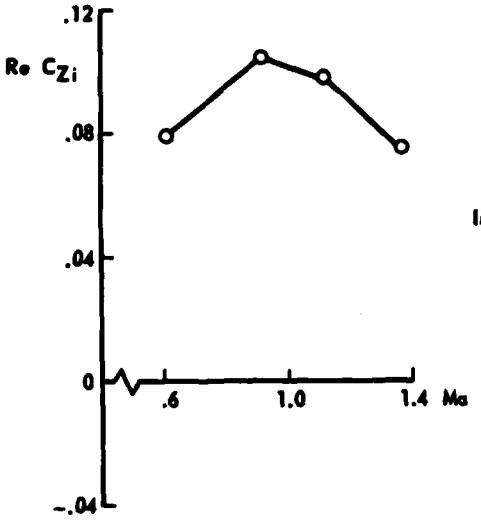

UNSTEADY PITCHING MOMENT

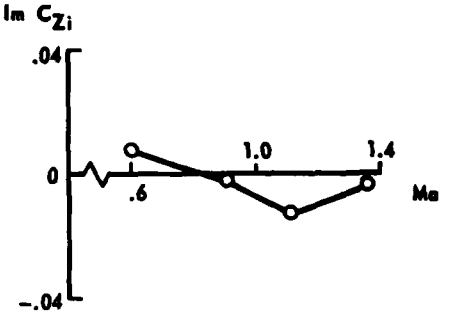

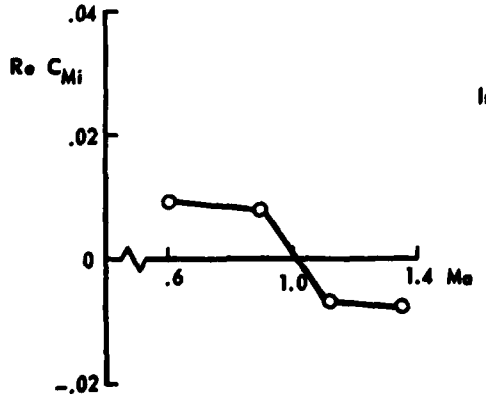

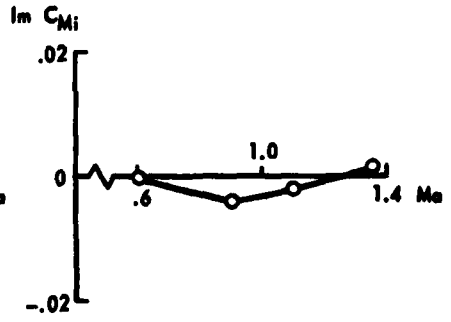

TIPLAUNCHER +
COMPLETE MISSILE (CONF. 4)
F = 10 Hz

UNSTEADY NORMAL FORCE

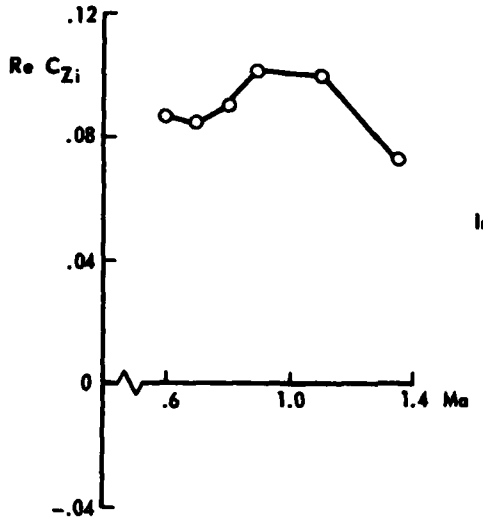

UNSTEADY PITCHING MOMENT

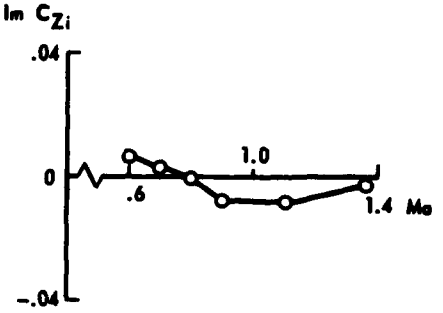

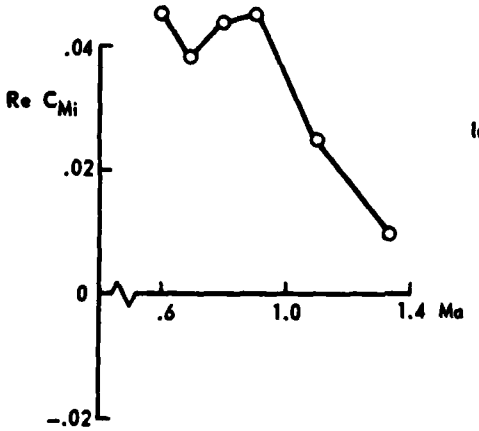

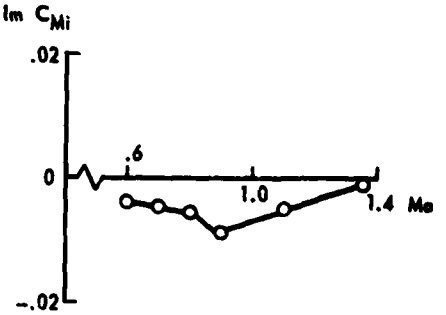

TIPLAUNCHER +
COMPLETE MISSILE (CONF. 4)
F = 20 Hz

△ RUN NO. : 344

UNSTEADY NORMAL FORCE

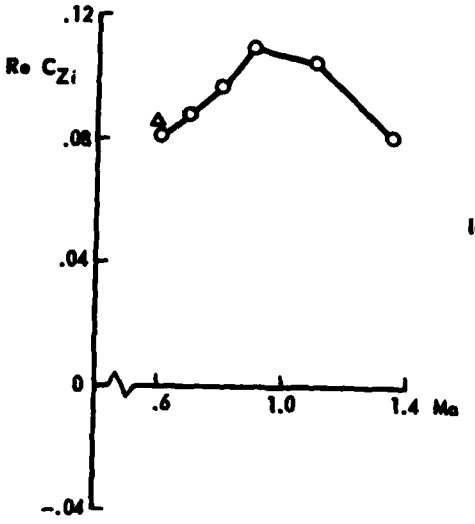

UNSTEADY PITCHING MOMENT

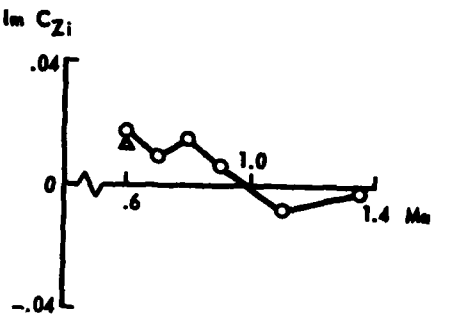

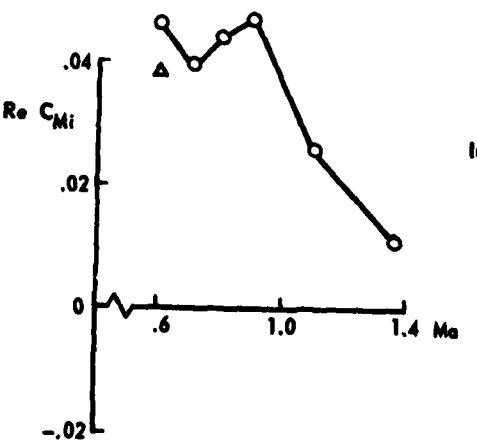

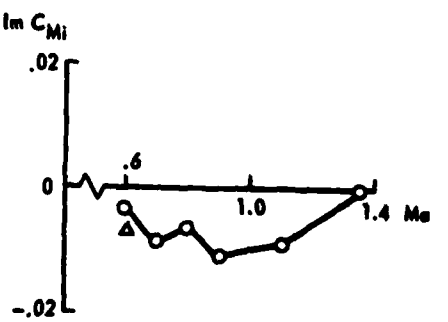

TIPLAUNCHER +
COMPLETE MISSILE (CONF.4)
F = 30 Hz

UNSTEADY NORMAL FORCE

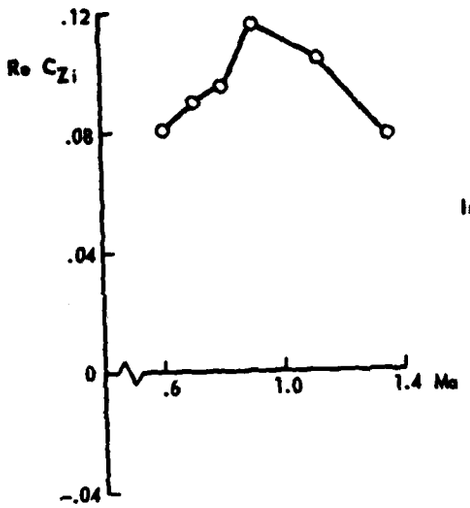

UNSTEADY PITCHING MOMENT

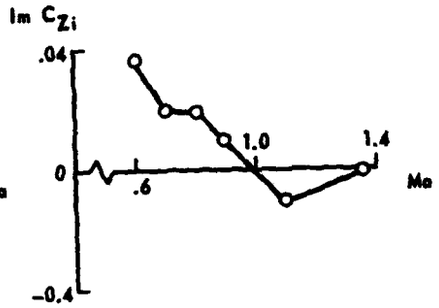

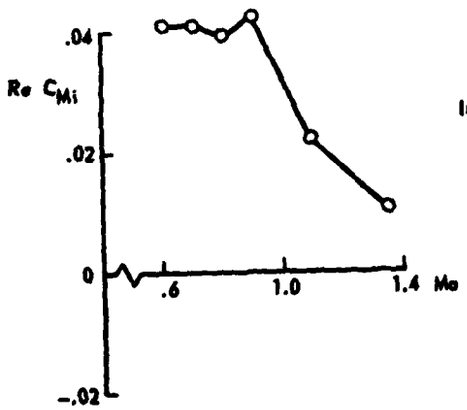

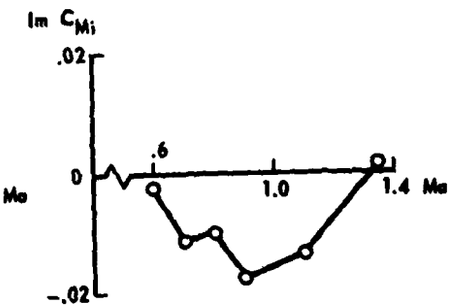

*U.S.Government Printing Office: 1979 — 657-002/90